



UNIVERSITÀ DEGLI STUDI DI MILANO  
DEPARTMENT OF CHEMISTRY  
DOCTORATE SCHOOL OF CHEMICAL SCIENCES  
AND TECHNOLOGIES  
PhD COURSE IN CHEMICAL SCIENCES, XXVIII CYCLE

# Reductions catalyzed by first-row transition metals

**Piotr Gajewski**

R10357

CHIM/06 Organic Chemistry

*Tutor:* Prof. Dr. Cesare Gennari

*Academic Co-Tutor:* Prof. Dr. Johannes de Vries (Leibniz Institute for Catalysis)

*Industrial Co-Tutor:* Dr. Laurent Lefort (DSM Ahead R&D)

Milan, 2016



The present work was lead by: Prof. Dr. Cesare Gennari, Prof. Dr. Johannes de Vries,  
Dr. Luca Pignataro and Dr. Laurent Lefort

Doctoral Final Oral Examination: 7<sup>th</sup> March 2016

Examination Committee:

Chairperson:	Prof. Dr. Maurizio Benaglia Università degli Studi di Milano
Second Member:	Prof. Dr. Luca Bernardi Università di Bologna
Third Member:	Prof. Dr. Umberto Piarulli Università dell'Insubria



*Gold is for the mistress – silver for the maid –  
Copper for the craftsman cunning at his trade.*

*"Good!" said the Baron, sitting in his hall,  
"But Iron – Cold Iron – is master of them all."*

Rudyard Kipling, *Cold Iron* poem (1910)



## Table of contents

<b>1</b>	<b>General introduction .....</b>	<b>1</b>
1.1	Catalysis.....	1
1.2	Homogeneous asymmetric hydrogenations .....	2
1.3	Advantages and limitations of asymmetric hydrogenations .....	4
1.4	Iron .....	6
1.5	Aim of the thesis .....	8
<b>2</b>	<b>Iron catalyzed hydrogenations: state of the art.....</b>	<b>9</b>
2.1	General difficulties related to the development of new iron catalysts .....	9
2.2	Multidentate ligands.....	9
2.2.1	Cooperative and redox non-innocent ligands.....	10
2.3	Hydrogenation of alkenes and alkynes.....	11
2.3.1	Iron carbonyls .....	11
2.3.2	Biomimetic complexes.....	11
2.3.3	Multidentate <i>P</i> -ligand complexes .....	12
2.3.4	<i>P,N,P</i> - and <i>N,N,N,N</i> -ligand complexes .....	13
2.3.5	(Cyclopentadienyl)iron complex .....	14
2.3.6	Bis(iminopyridine) complexes .....	15
2.3.7	Iron nanoparticles.....	17
2.4	Hydrogenation of ketones and imines.....	18
2.4.1	Iron carbonyl <i>in situ</i> systems.....	18
2.4.2	<i>P,N,N,P</i> -complexes.....	18
2.4.3	Macrocyclic complexes.....	21
2.4.4	<i>P,N,P</i> -pincer complexes.....	24
2.4.5	Multidentate <i>N</i> - and <i>P</i> -ligand complexes.....	25
2.4.6	Isonitrile complex.....	26
2.4.7	(Cyclopentadionene)iron complexes .....	27
2.4.7.1	Reduction of aldehydes, ketones and imines.....	27
2.4.7.2	Asymmetric reductions.....	29
2.4.7.3	Amination of aldehydes, ketones and alcohols.....	31

2.4.7.4	Other applications of iron cyclopentadienone complexes .....	33
2.5	Hydrogenation of other carbonyl compounds.....	33
2.5.1	Hydrogenation of sodium carbonate and carbon dioxide.....	33
2.5.2	Ester hydrogenation .....	35
2.6	Summary of iron catalyzed reductions.....	36
<b>3</b>	<b>Iron complexes with <i>N,N,N,N</i>-ligands.....</b>	<b>39</b>
3.1	Tetradentate <i>N</i> -ligands to stabilise Fe(II) metal center .....	39
3.2	Iron complexes for C-H oxidation .....	40
3.3	Chiral tetradentate <i>N</i> -ligand complexes.....	40
3.4	Achiral tetradentate <i>N</i> -ligand complexes.....	45
3.5	Introduction of CO ligands on tetradentate <i>N</i> -ligand complexes .....	47
3.6	Concluding remarks .....	48
3.7	Experimental section .....	50
<b>4</b>	<b>Iron complexes with isonitrile ligands .....</b>	<b>59</b>
4.1	Isonitrile complexes.....	59
4.2	Novel complexes featuring bis(isonitrile) ligand.....	59
4.3	Tetra(isonitrile) complexes.....	63
4.4	Second generation of tetra(isonitrile) complexes .....	65
4.4.1	Possible improvements to the second generation isonitrile complexes .....	67
4.5	Summary of the isonitrile complexes .....	68
4.6	Experimental section .....	70
<b>5</b>	<b>Chiral (cyclopentadienone)iron complexes .....</b>	<b>79</b>
5.1	( <i>R</i> )-BINOL derived complexes .....	79
5.2	Towards a new family of chiral cyclopentadienone(iron) complexes.....	83
5.3	Conditions screening .....	86
5.4	Synthesis of a library of new chiral pre-catalysts.....	88
5.5	Catalytic test with new chiral cyclopentadienone(iron) complexes .....	96
5.6	Substrate screening with the best complex.....	97
5.7	Variation of the 2,5-substituents of the cyclopentadienone ring.....	98
5.8	Cyclopentadienone(iron) complexes bearing chiral 2,5-substituents .....	101



5.9	Complexes derived from chiral diamines .....	103
5.10	Summary of chiral (cyclopentadienone)iron complexes .....	105
5.11	Experimental section .....	106
<b>6</b>	<b>New application of cyclopentadienone(iron) complexes..</b>	<b>125</b>
6.1	Ester hydrogenation with (cyclopentadienone)iron complex.....	125
6.2	Conditions screening .....	127
6.3	Substrate screening .....	129
6.4	Tentative mechanism of ester hydrogenation .....	130
6.5	Summary .....	131
6.6	Experimental section .....	132
<b>7</b>	<b>Conclusions and perspectives.....</b>	<b>135</b>
<b>8</b>	<b>List of publications.....</b>	<b>138</b>
<b>9</b>	<b>Acknowledgments .....</b>	<b>139</b>
<b>10</b>	<b>Bibliography.....</b>	<b>140</b>

The work reported in this thesis has been carried out between the University of Milan (IT), for 18 months, and the DSM Ahead R&D (NL), for 18 months more, within the Marie Skłodowska Curie EID-ITN Network "REDUCTO" (contract PITN-GA-2012-316371). During the months spent at the DSM Ahead R&D I was also involved in projects aiming at the development of new chiral, tandem hydrogenation and transfer-hydrogenation reactions with Grubbs methathesis catalysts, and asymmetric hydrogenation of 2- and 3-substituted pyridines.



# 1 General introduction

## 1.1 Catalysis

The term "catalysis" was introduced by Berzelius in 1836,<sup>1</sup> although mankind used catalytic processes for thousands of years without knowing its principles, i.e. for fermentation of the alcohol but also to produce sulphuric acid. The word "catalysis" originates from Greek and it means "to untie" or "to pick up". By definition catalysis "is increasing in the rate of a chemical reaction due to the participation of an additional substance - a catalyst". Catalyst itself is not consumed or modified during a chemical process and catalytic transformations occur faster and require less activation energy than non-catalytic processes. Moreover, using different catalysts, not only one, but a variety of different products can be obtained from the same substrate.

Catalysis is fundamental for chemistry and has enormous importance, both in academia and industry. Hundreds of commercially available catalyst are accessible for chemists all around the world. Catalysts allow to lower the cost and to save energy and materials, increasing selectivities and yields. They are a key factor for development of sustainable organic synthesis and as so, they are one of the pillar of the Green Chemistry.<sup>2</sup> Without them, synthesis of various complex molecules would not be feasible.<sup>3</sup> No doubt catalysis has a tremendous economic impact. According to the American Chemical Society, over 95% of all chemical products are obtained using at least one catalytic transformation.<sup>4</sup>

Catalysis can be divided into two subdisciplines - homogenous and heterogeneous. Homogenous catalysis involves one or more reactions where reactants and catalyst are in the same phase. There is a huge variety of molecules that can be used as homogenous catalysts. Organic molecules, organometallic complexes, acids, bases, enzymes and salts can be used as catalysts. Homogenous catalysis relies on well-defined active sites (typically one site per molecule of catalyst) which facilitates a rational design to obtain specific catalytic performances. Mild experimental conditions are typically required and such problems as limited stability, recycling, handling and high cost often limit their industrial applications.



## Chapter 1

Heterogeneous catalysts operate in different phases than other reactants. Typically, they are solid and they work in contact with a gas or liquid phase. Owing to this feature, they can be readily separated from reactants, and their stability is much higher compared to homogenous catalysts. This makes them easy-to-recycle and thus perfect for large-scale processes. Indeed, the industrial manufacturing of commodity chemicals mostly relies on heterogeneous catalysts. Still, they bring many variables and potential problems, such as limited tolerance towards functional groups, dependence of reproducibility and selectivity on various parameters, as well as difficulty in investigating the reaction mechanism. Still, small to medium scale manufacture processes, especially for fine chemicals (like active pharmaceutical ingredients - API), relies mostly on homogenous catalysis. In particular, homogeneous catalysis is largely dominant in the field of enantioselective catalysis.

### 1.2 Homogeneous asymmetric hydrogenations

Stereospecific synthesis is widely utilized by nature and chiral natural compounds surround us everywhere. All natural amino acids are chiral and have the L-form and only D-sugars can be metabolized by living organisms. Chirality of enzymes and receptors is a consequence of being build from chiral amino acids.<sup>5</sup> Also nucleic acids exhibit chirality, as sugar building blocks present in their sugar-phosphate skeleton are chiral as well. Moreover, many hormones and pheromones possess asymmetric carbon atoms in their structures. This is why stereochemistry plays a crucial role in synthesis of new drugs or agrochemicals. Enantiopure compounds have to precisely fit to the active sites of enzymes. It is also common that two enantiomers of the same molecule can manifest completely different properties. In the case of fragrances or flavor additives, they can just smell or taste differently. In the case of drugs, one enantiomer can have a therapeutic use while second can be highly toxic or even possess strong teratogenic properties. Most known and infamous example of such a drug is Thalidomide, which led to birth of thousands disabled children in 1950's. This fact led to an increasing need for enantiopure chiral molecules, particularly in the field of pharmaceutical intermediates, witnessed by the fact that in 1992, the US's Food and Drug Administration (FDA) introduced a new policy for the production of new stereoisomeric drugs, where the use of single enantiomers was recommended.<sup>6</sup> Since then, a rapid growth of new registered compounds existing as single enantiomers (rather than mixtures of them) was observed and defined the future trend for drugs development. Numerous methodologies were developed to meet the need for synthesizing single isomers of API.<sup>7</sup>

Asymmetric hydrogenation (AH) has been one of the first enantioselective catalytic transformation developed and is particularly suitable for large-scale applications due its operational simplicity and atom economy. It is not a well known fact, that the first catalytic homogenous hydrogenation was not based on a noble metal but on copper.<sup>8</sup>

The most commonly accepted date for the birth of homogeneous reduction is 1966, when Wilkinson found  $\text{RhCl}(\text{PPh}_3)_3$  as an effective catalyst for hydrogenation of alkenes.<sup>9</sup> Then the idea of replacing the triphenylphosphine from this catalyst with a chiral ligand led to the first examples of AH. Research in this direction began in the late 1960's with the work on rhodium complexes of chiral monodentate phosphines, carried out by the groups of Knowles<sup>10</sup> and Horner.<sup>11</sup> Although the early efforts were rewarded with only modest enantiomeric excesses, the initial values were gradually increased by careful design of the ligands. From the beginning of this research it was clear that the choice of proper ligands for a given metal center is essential to obtain a high level of catalytic activity and stereoselectivity for the desired transformation. It is worth mentioning, that just 100 years earlier Pauster, precursor of the asymmetric chemistry, declined the possibility that the chiral organic synthesis would be ever possible.<sup>12</sup>

In 1972 Kagan reported DIOP,<sup>13</sup> the first example of chiral bidentate phosphorus ligand for Rh-catalyzed asymmetric hydrogenation, and few years later Knowles designed DIPAMP,<sup>14</sup> a chiral diphosphine with  $C_2$  symmetry (Figure 1.1). The latter, combined with a rhodium source, formed a catalytic system able to hydrogenate  $\alpha$ -dehydroamino acids. This catalytic system was exploited for the large-scale production of L-dopa, i.e. (*S*)-3,4-dihydroxyphenylalanine, used as a drug for Parkinson's disease. After these fundamental contributions by Knowles and Kagan, hundreds of chiral bidentate *P*-ligands for AH were developed in the following 30 years. Among them, BINAP<sup>15</sup> (Figure 1.1) gained the inventor Noyori the Noble Prize in 2001,<sup>16</sup> which he shared with Knowles<sup>17</sup> and Sharpless.<sup>18</sup> BINAP is employed in a variety of Ru(II) complexes for the AH of olefins and ketones.<sup>19</sup> As there was a high need for cheap methods to prepare  $\beta$ -hydroxy esters for drugs (i.e. statins for lowering the cholesterol), this was a major occasion for the industry to consider asymmetric hydrogenation as an useful methodology.

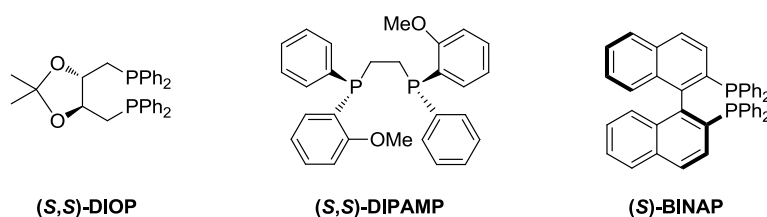


Figure 1.1 Milestones in homogeneous asymmetric hydrogenation: bidentate *P*-ligands developed by Kagan, Knowles and Noyori.

Given such brilliant achievements, for a long time the structural rigidity typical of bidentate systems was considered essential for an effective transmission of the stereochemical information in asymmetric catalysis. This situation changed 15 years ago, when noble metal complexes with new (and easy to make) chiral monodentate *P*-ligands (phosponites, phosphites and phosphoramidites) were used to catalyze the hydrogenation of pro-chiral olefins, in some cases even outperforming bidentate ligands.<sup>20</sup> The combinatorial potential of monodentate ligands became evident with the

## Chapter 1

studies on hetero- and homocombinations, autonomously published by Reetz<sup>21</sup> and Feringa, de Vries *et al.*<sup>22</sup> They proved that a binary combination of two different monodentate ligands ( $L^a$  and  $L^b$ ) can lead to a higher activity and enantioselectivity, compared to complex of each single ligand separately. When employing two monodentate ligands  $L^a$  and  $L^b$ , it was inevitable to obtain a mixture of the three species  $[ML^aL^b]$  (heterocomplex),  $[ML^aL^a]$  and  $[ML^bL^b]$  (homocomplexes), which were decreasing the overall activity and results. With the aim to improve the selectivity for the formation of heterocomplexes over the homocomplexes, the so-called "supramolecular" ligands were developed.<sup>23</sup> These ligands, besides the donor atom (usually phosphorous) used to coordinate the metal, possess a further functional group capable of non-covalent interactions either with another complementarily functionalized ligand or with the substrate. This reduces degrees of freedom in the respective metal coordination complexes and leads to more pre-organized systems, where a better capacity of controlling the metal-catalyzed reaction can be achieved.

### 1.3 Advantages and limitations of asymmetric hydrogenations

Enantioselective catalysis is in principle the most efficient strategy for the synthesis of enantiopure molecules (Figure 1.2) and enantioselective hydrogenation of pro-stereogenic carbon double bonds (with carbon, oxygen or nitrogen) undoubtedly is one of its most well-developed applications.

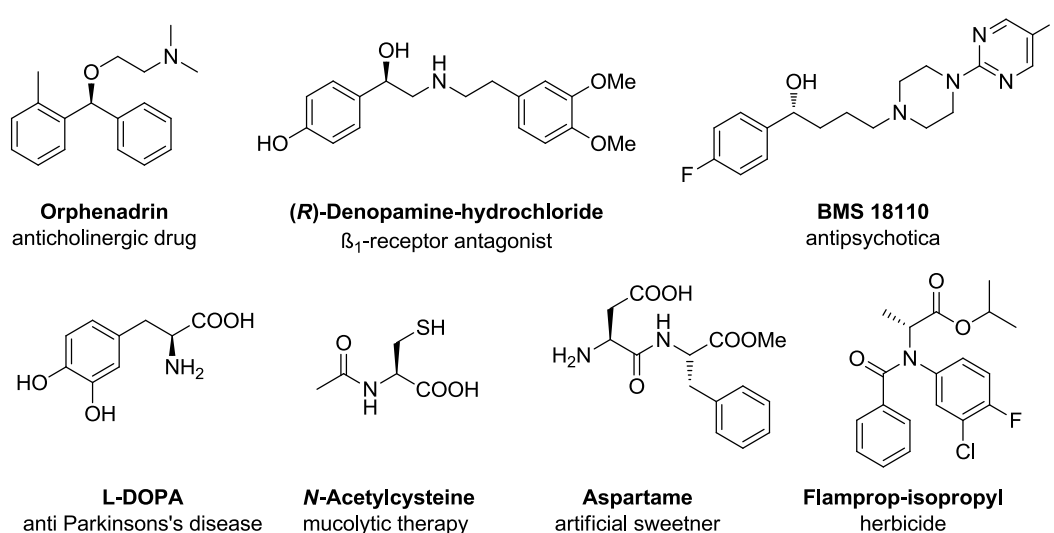


Figure 1.2 Selected pharmaceuticals accessible by asymmetric hydrogenation of double bonds.<sup>24</sup>

There is a long list of factors that make catalytic asymmetric hydrogenation a valuable method both on the laboratory and the industrial scale, such as:

- ✓ hydrogenation is a 100% atom-efficient methodology, with a very broad scope as well as a good chemoselectivity;
- ✓ high conversions (and enantiomeric excesses) can be obtained without harsh, dangerous and energy-consuming conditions;



- ✓ with thousands developed methods, there is a high level of expertise in the field which increases the chance of solving specific problems;
- ✓ scale-up of the process (when economically convenient) is straightforward as the process technology is well known.<sup>25</sup>

Enantioselective transfer hydrogenation for the reduction of ketones, imines and conjugated C=C double bonds, also gained a prominent position in recent years, even if its exploitation in the chemical industry still remains behind the one of asymmetric hydrogenation with molecular hydrogen. In this methodology, organic molecules are used as an equivalent for H<sub>2</sub> - isopropanol and formic acid/triethylamine being by far the most used sources of hydrogen.<sup>26</sup>

During last 50 years various catalysts based on transition metals were developed. In particular, catalytic systems based on noble metals like palladium, iridium, ruthenium and rhodium turned out to be very effective for a broad range of chemical transformations. Nevertheless, in spite of the immense academic efforts in the field of AH, the amount of implemented processes is rather limited and is below 20.<sup>27</sup> In spite of all advances in the technology, a vast number of chiral pharma intermediates are still prepared via traditional resolution of diastereomeric salts. This lack of AH processes can be explained by various reasons:

- a) time-to-market pressure doesn't give enough time to optimize or to develop a new catalytic methods;
- b) high cost of the catalysts (both the metal and the ligand) coupled to the relatively low turnover numbers that can be achieved in most cases makes the technology too expensive;
- c) limited availability of noble metals, as long-term supply for the chemical process could exceed their occurrence in nature;
- d) technology works fine on a limited number of benchmark substrates, however the catalyst is often too slow on real pharma intermediates (this is often caused by the presence of nitrogen-containing substituents that can bind to the catalyst);
- e) toxicity problems, since even trace amounts of toxic metals are often not allowed to occur in the final products.

These limitations concern also other industry sectors (like agro-chemistry, food industry or cosmetic sector) which require the usage of enantiopure compounds.

Replacing precious metals with cheap first-row transition metals would be a major breakthrough, with an enormous scientific and industrial impact. A comparison of prices of noble metals with base metals, shows that the latter are at least 1000 times cheaper. To clearly visualize that and compare the cost of noble metals expressed in price per gram, base metals costs have to be shown in price per one kilogram (Figure 1.3).<sup>28</sup> For this reason, catalysis with inexpensive transition metals is an area undergoing rapid growth.<sup>29</sup>

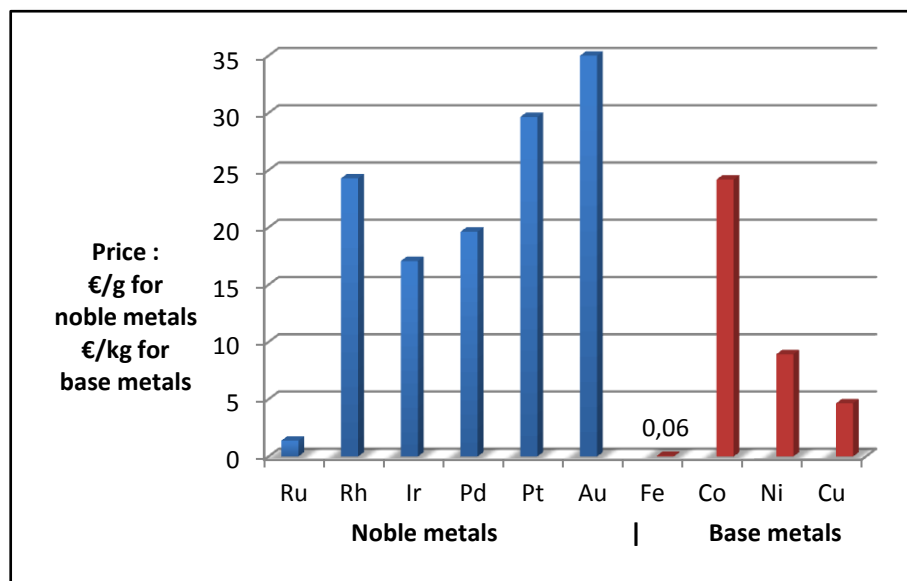


Figure 1.3 Prices of noble and base metals.

## 1.4 Iron

Global efforts in sustainability, coupled with high prices of noble metals, have recently inspired a flurry of activity in iron catalysis.<sup>30</sup> Iron is a fundamental element of our planet. It is the second most common metal after aluminum and it is accountable for one third of the Earth's mass. People have known and used iron since nearly 3200 years ago and it always played a crucial role in humans' world. Iron is essential in biology as iron-proteins are present within all living organisms, from bacteria's to humans. The red color of our blood is caused by an iron-containing protein - hemoglobin - without which blood would not be able to transport oxygen in our bodies. Iron is a vital part of human's history and culture. It is truly surrounding our lives without being even noticed by us. Nevertheless, most of all, iron means chemistry. It is not a well known fact by most of the people, but over 80% of nitrogen in our bodies is originated from the Haber-Bosh process of synthesizing ammonia using iron catalyst.

*Ferrum* is a first row transition metal element with an electronic configuration of  $[\text{Ar}]4s^03d^8$ . We hardly ever find iron as a pure metal, as it readily oxidizes in the presence of oxygen and moisture. As so, the most stable compounds have the oxidation state +2 or +3, but as a group 8 element, iron can exist in a wide range of oxidation states, from -2 up to +6. In low oxidation states it may act as an iron-centered nucleophile and catalyze reactions such as nucleophilic substitutions, additions to carboxylic substrates, cycloisomerization and others.<sup>31</sup> In its most common oxidation states (+2 and +3), iron has a tendency to engage in single electron transfer reactions, and for this reason it has found wide application as a catalyst for oxidation processes.<sup>24</sup> By contrast, many Fe-complexes have little propensity to participate in two-electron processes which are typical of many precious metal catalyzed reactions starting from hydrogenation. For this



reason, until recent years iron has been scarcely exploited for classical reactions following the oxidative addition/reductive elimination pathway.

From a practical point of view, studies devoted to investigate the use of iron in chemical industry processes would meet a urgent need for environmentally friendly and economically affordable synthetic methodologies. High-added value compounds such as chiral alcohols, amines, esters and amino acids would become accessible by reduction of parent olefins, ketones and imines at an economic and environmental cost much lower than that involved by noble metal-based processes. Iron can be considered as one of the least toxic transition metals and it is widely present in biological systems.<sup>32</sup> For this reason, its use in catalysis implicates less toxicity problems than the use of other transition metals: limits for residual iron traces are hundreds times greater when compared to noble metals.<sup>33</sup> From a merely scientific perspective, research on iron catalysis would disclose new prospects and give exciting insights in the relatively underdeveloped field of iron-catalysis, where new catalytic systems and patterns are to be devised and studied. Given those facts, many scientists have recently devoted their research activity to develop an efficient iron catalyst. When performing SCOPUS® search for "iron, catalysis" phrase an increased trend in recent 15 years is clearly seen (Figure 1.4). So, as proclaimed by Bolm in 2009,<sup>34</sup> has a new Iron Age begun?

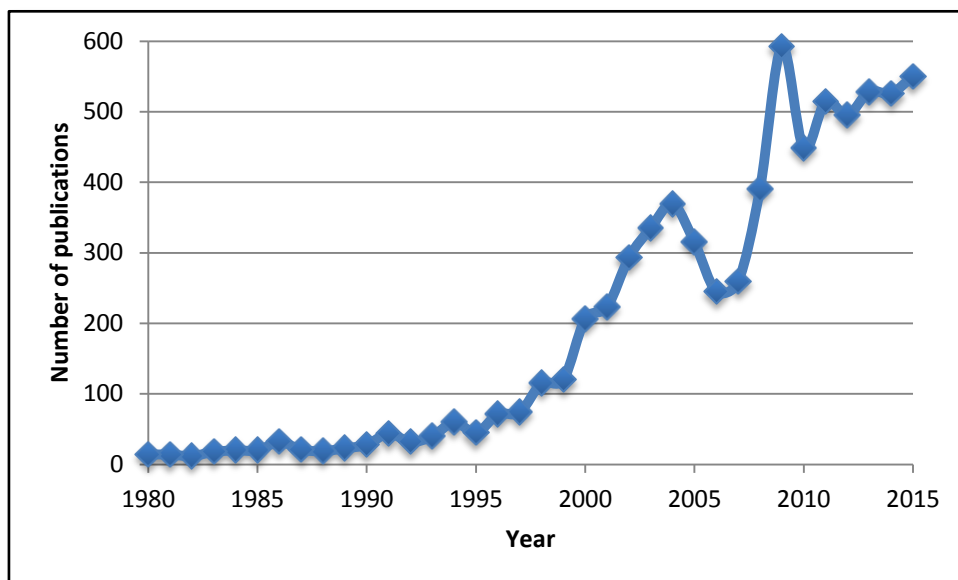


Figure 1.4 Number of iron catalysis-related publications over the last 35 years.

On the other hand, the Fe-based catalytic reductions reported so far suffer from serious limitations, such as difficult synthesis/lack of robustness of the catalyst, moderate activity/(enantio)selectivity, high cost/poor atom economy of the catalyzed process. These limitations need to be overcome, in order for Fe-catalysis to become of practical utility for the industrial production of fine chemicals.

## 1.5 Aim of the thesis

The aim of the research carried out during my PhD was to develop new iron catalysts for hydrogenation of various unsaturated compounds (like olefins or ketones) that could possibly satisfy the following requirements:

- a) high efficiency (conversion and enantioselectivity);
- a) simple preparation of the ligands/complexes from commercially available materials;
- b) reasonable stability of the catalysts or pre-catalysts to air and moisture;
- c) affordable cost of reagents and good atom economy of the catalytic process.

We were trying to base our studies on existing catalytic systems and develop them further to meet our expectations. In course of our research, we have investigated mostly three classes of iron complexes, namely:

- a) iron *N,N,N,N*-ligand based complexes for the hydrogenation of olefins and ketones (described in Chapter 3);
- b) iron isonitrile complexes for the asymmetric transfer hydrogenation of ketones (described in Chapter 4);
- c) (cyclopentadienone)iron complexes for the asymmetric hydrogenation of ketones (described in Chapter 5).

We tried also to find new possible applications of existing iron catalytic systems, which resulted in finding new iron catalysts for ester hydrogenation (described in Chapter 6).

## 2 Iron catalyzed hydrogenations: state of the art

### 2.1 General difficulties related to the development of new iron catalysts

Iron catalysis, as the first-row transition metal catalysis in general, presents unique features which usually are not encountered with traditional precious metal compounds. To mimic noble metals, one-electron redox changes must be suppressed and two-electron redox interplay (e.g.  $\text{Fe}^0/\text{Fe}^{\text{II}}$ ) facilitated. Harnessing radical chemistry, contending with multiple oxidation states and coping with paramagnetic compounds are all potential obstacles when entering the field of iron chemistry.<sup>35</sup>

Furthermore, most of  $\text{Fe}(\text{II})$ -complexes are paramagnetic due to the small energy gap ( $\Delta_0$ ) between the  $t_{2g}$  and the  $e_g$  orbitals (see Figure 2.1), and therefore NMR spectroscopy is scarcely useful for their characterization, which mostly relies on mass spectrometry and X-ray diffraction.

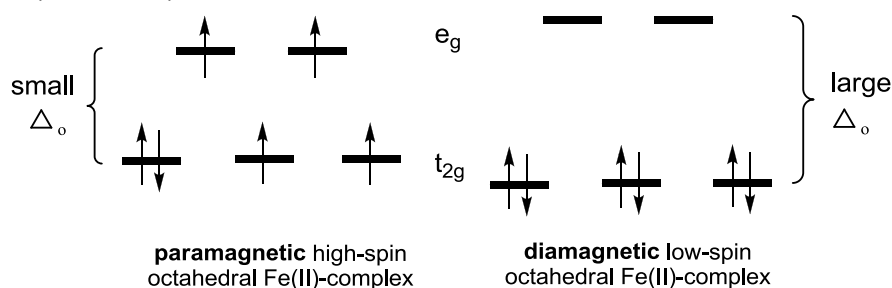


Figure 2.1 MO diagrams for octahedral crystal field: distribution of six valence electrons in high-spin and low-spin  $\text{Fe}(\text{II})$ -complexes.

### 2.2 Multidentate ligands

Interactions between ligands and metals are defining the properties of metal complexes. Use of tri- and tetradentate ligands is a widely exploited way to stabilize the metal centre. They can bear phosphorus and/or nitrogen donors such as porphyrins or diimidodiphosphines. Besides stabilizing the active metal centre, these structures can be easily tuned for specific stability and selectivity needs.<sup>36</sup> Nevertheless, in most chemical catalyzed transformations, their structure is not affected by the course of the reaction, so they just act as "spectators" and the main reactivity is occurring at the metal centre. Then, in order to improve the catalytic properties of the complexes, the typical approach is to modify the ligand by changing its steric and electronic properties.

### 2.2.1 Cooperative and redox non-innocent ligands

One of the main difficulties to use first-row transition metals is their electronic structure, different from that of noble metals. As already mentioned in Paragraph 1.4, precious metals easily undergo two-electron redox changes (e.g., Rh<sup>I</sup>/Rh<sup>III</sup>, Ir<sup>I</sup>/Ir<sup>III</sup>, Pd<sup>0</sup>/Pd<sup>II</sup>) that can be used to promote bond breaking or making. On the contrary, typical base metals are more prone to one-electron redox changes. This tendency is a challenge, both for reactivity control as well as stabilizing and maintaining the catalytic functions of complex.

To tackle these undesired electron properties, recent advances brought new type of "reactive" ligands that can play much more significant roles in bond-making and bond-breaking processes.<sup>37</sup> The main idea behind those new ligands is their synergistic cooperation with the metal, which can facilitate the catalytic transformation. In principle they can be divided into two categories, redox non-innocent or cooperative ligands, but often they can exhibit properties from both categories.

In redox non-innocent (redox active) ligands, it is ambiguous to determine the oxidation state, both the metal and the ligand parts of a complex. To do so, usually set of spectroscopic studies have to be performed, like: Raman or electron paramagnetic resonance (EPR), X-ray absorption (XAS), UV-vis or Mössbauer spectroscopy. The "non-innocent" term, was introduced by Jørgensen in 1966.<sup>38</sup> By delocalizing part of electronic density of the complexes, they become a kind of "electronic reservoir" during the reaction and catalytic process. As such, they can allow multi-electron transformations for metals, for which this kind of transformations are unfavorable. They can also initiate and control radical-type transformations. Additionally to the metal, they can become a place where a redox process can also occur. As a result, new "redox isomers" can form, which should not be confused with resonance structures, and can exhibit a variety of different properties and reactivities.

Cooperative (or chemically non-innocent) ligands are "participating directly in bond-activation reaction and undergo reversible chemical transformations".<sup>39</sup> The metal part of the complex, although it can (but does not have to) poses an intrinsic reactivity, its main role is to act as a binding site and bring reactants together. In that way, the metal and the ligand acts cooperatively in a synergistic way and their interactions triggers a chemical transformation.

Non-innocence should not be identified strictly with a particular group of ligands. It is rather a state, which can be attributed to any ligand under the right conditions. Observed innocence behavior of ligand in a metal complex, does not guarantee that it will act the same with different metal or under different conditions. Only detailed spectroscopic investigations can confirm non-innocent structure of the ligand in the specific transformation.

## 2.3 Hydrogenation of alkenes and alkynes

### 2.3.1 Iron carbonyls

The first iron complex - iron pentacarbonyl was discovered in 1891 independently by Berthelot<sup>40</sup> and Mond.<sup>41</sup> Together with its related homoleptic iron clusters (Figure 2.2), it was used in the initial efforts for iron-catalyzed hydrogenations.<sup>42</sup> Carbon monoxide ligands served as strong field ligands, capable of stabilizing low spin electronic structures of iron(0).

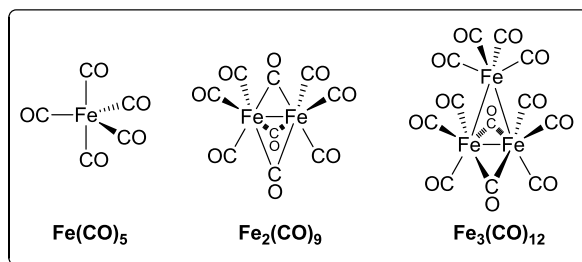
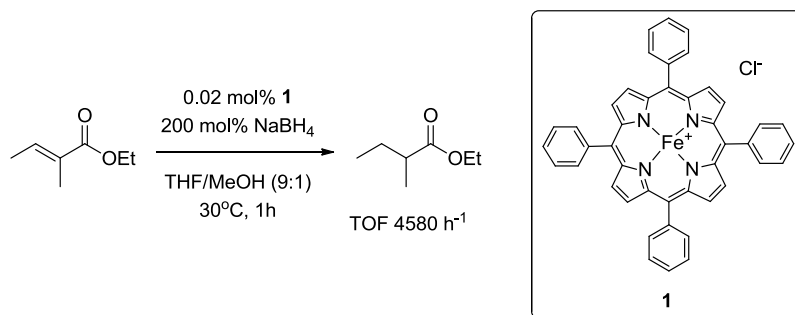


Figure 2.2 Homoleptic ironcarbonyl complexes.

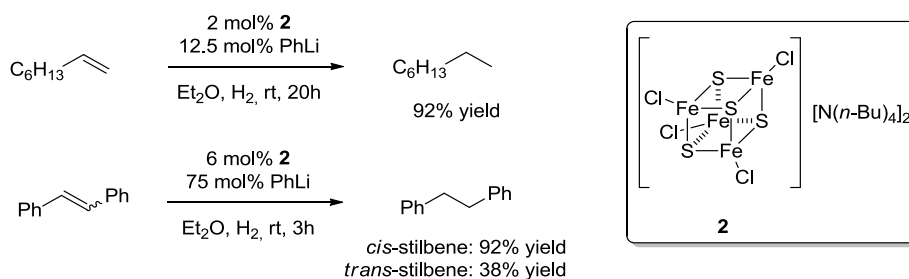
$\text{Fe}(\text{CO})_5$  was used by Frankle *et al.* to hydrogenate methyl linoleate and methyl linolenate to get monoenoic fatty esters.<sup>43</sup> Noyori and co-workers were among next researchers who used iron pentacarbonyl to obtain saturated ketones from  $\alpha,\beta$ -unsaturated ketones with very good yields.<sup>44</sup> Wrighton and co-workers found that the activity of  $\text{Fe}(\text{CO})_5$  under ambient conditions is improved upon constant UV irradiation, although only low yields were obtained with narrow variety of alkene substrates.<sup>45</sup> The mechanism of the hydrogenation was studied by Grant and co-workers.<sup>46</sup> The active species in the hydrogenation was found to be  $\text{Fe}(\text{CO})_3$ , with a vacant site for coordination, which is formed from  $\text{Fe}(\text{CO})_5$  upon heating or photoirradiation. This activation pathway (with temperatures  $>150^\circ\text{C}$  or upon constant UV-irradiation) is a drawback which prevents the potential practical use of those type  $\text{Fe}^0$  carbonyl complexes.

### 2.3.2 Biomimetic complexes

Several biomimetic catalysts were proposed by researchers who took inspiration from natural iron-complexes. Kano and co-workers used Fe-porphyrines together with  $\text{NaBH}_4$  as a hydride source to radically hydrogenate styrene, getting TOFs up to  $81 \text{ h}^{-1}$ .<sup>47</sup> A similar approach was later presented by Sakaki *et al.* with porphyrine **1** to hydrogenate  $\alpha,\beta$ -unsaturated esters with a high turnover frequencies (TOFs) up to  $4850 \text{ h}^{-1}$  (Scheme 2.1).<sup>48</sup> Studies revealed that besides a hydride from  $\text{NaBH}_4$ , a proton transferred from methanol was involved in the hydrogenation.

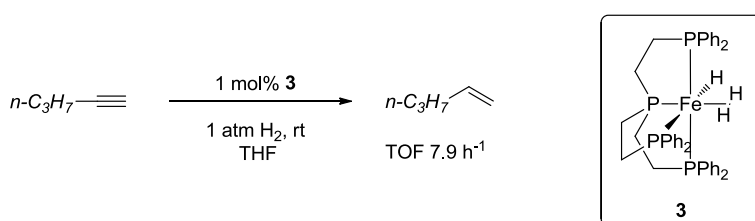
Scheme 2.1 Reduction of  $\alpha,\beta$ -unsaturated ester catalyzed by iron porphyrin **1**.

Inspired by iron-sulfur clusters present in the active sites of hydrogenase enzymes, a deeper biomimetic approach was reported by Inoue *et al.*<sup>49</sup> Using Fe<sub>4</sub>S<sub>4</sub> cluster **2** activated by PhLi, it was possible to hydrogenate 1-octene and stilbene with very good yields, although reported catalyst **2** was more active with (*Z*)-alkenes (Scheme 2.2).

Scheme 2.2 Reduction of olefins using bio-inspired iron cluster catalyst **2**.

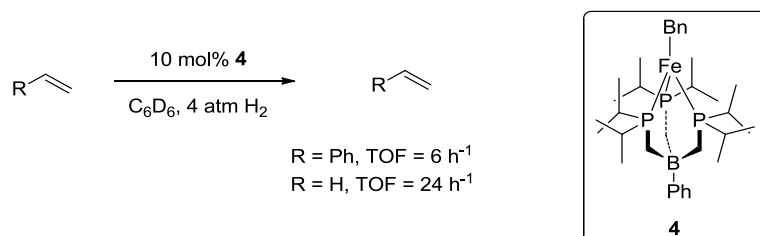
### 2.3.3 Multidentate *P*-ligand complexes

The first catalyst able to hydrogenate alkyne bond was a multidentate *P*-complex **3** developed by Bianchini and co-workers in 1992.<sup>50</sup> This catalyst was able to promote the reduction of terminal alkynes to corresponding alkenes at room temperature, under atmospheric pressure of H<sub>2</sub> (Scheme 2.3). The complex **3** is an example of a cooperative involvement of the ligand during the transformation, as it can leave a free coordination site for the incoming substrate by unfastening one terminal phosphine arm. The bulkier alkynes substituents were, the lower conversions were obtained, but the reaction always proceeded with a full selectivity of reducing alkynes to alkenes. It was postulated that crucial insertion of olefin to iron hydride was not occurring in order to get fully saturated products.

Scheme 2.3 Selective reduction of pent-1-yne using multidentate *P*-complex **3**.

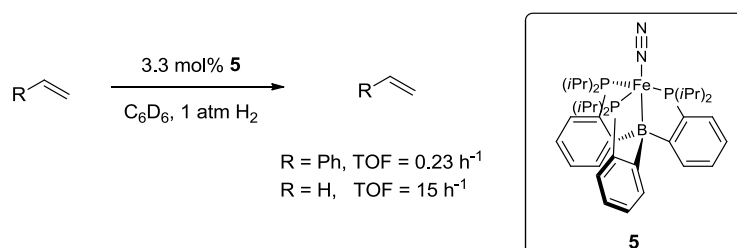
## Iron catalyzed hydrogenations: state of the art

A more recent example of polydentate phosphine complex **4** was reported by Peters and Daida in 2004 (Scheme 2.4).<sup>51</sup> Hydrogenation of alkenes required high catalyst loading (10 mol%), while alkynes were undergoing undesired side reactions, such as reductive dimerisation or polymerization. Peters proposed that the hydrogenation with catalyst **4** occurs with an unusual Fe<sup>II</sup>/Fe<sup>IV</sup> catalytic cycle, together with reversible dissociation of the ligand from the iron centre, in a similar way described by Bianchini.<sup>53</sup>



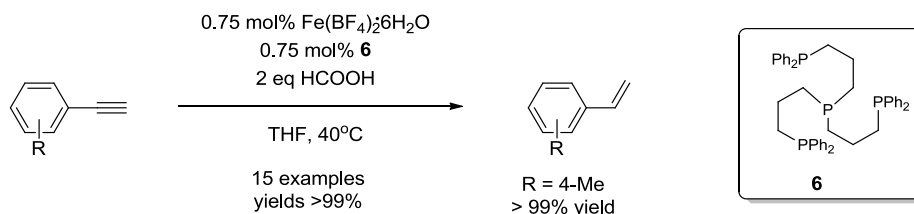
Scheme 2.4 Hydrogenation of olefins using by polydentate phosphine catalyst **4**.

The Peters' group continued their efforts to hydrogenate ethene and styrene, but new ferraboratrane complex **5** (Scheme 2.5) allowed to achieve only low TOFs (up 15 h<sup>-1</sup>).<sup>52</sup> Despite these not encouraging results, a detailed mechanistic studies about the transformation were performed which revealed that a boron atom can act as a hydride carrier being accompanied by reversible iron-boron bond cleavage.



Scheme 2.5 Hydrogenation of olefins using by ferraboratrane catalyst **5**.

A selective transformation of alkynes to alkenes by the means of transfer hydrogenation was reported by Beller and co-workers in 2012.<sup>53</sup> *In situ* formed catalyst from Fe(BF<sub>4</sub>)<sub>2</sub>·6H<sub>2</sub>O and a tetraphos ligand **6**, together with formic acid as hydrogen source gave nearly quantitative yields for a series of aromatic alkynes (Scheme 2.6).



Scheme 2.6 Selective hydrogenation of alkynes to alkenes using Fe(BF<sub>4</sub>)<sub>2</sub>·6H<sub>2</sub>O/tetraphos ligand **6** complex.

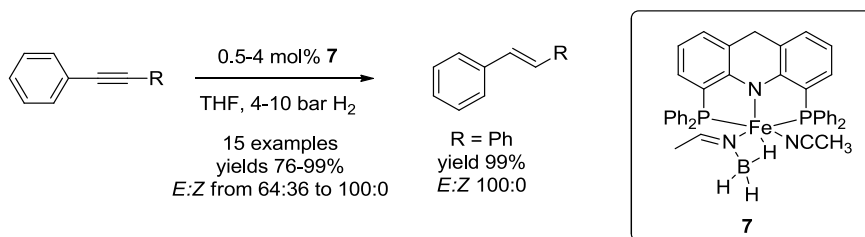
### 2.3.4 P,N,P- and N,N,N,N-ligand complexes

In 2013 Milstein and co-workers reported acridine-based P,N,P-iron pincer complex **7** for hydrogenation of alkynes to alkenes with high yields and excellent *E*-selectivity (Scheme 2.7).<sup>54</sup> This reaction did not required addition of base. Moreover



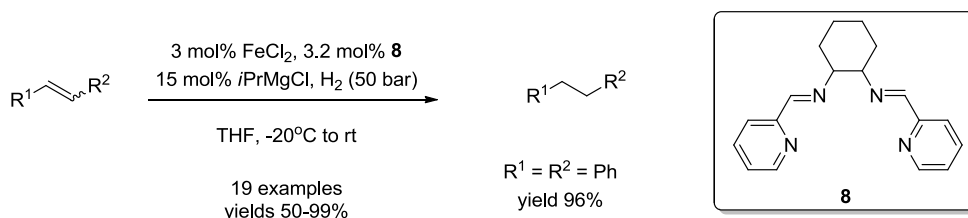
## Chapter 2

many functional groups like carbonyl, nitrile or halogen substituents were not affected by the course of the hydrogenation.



Scheme 2.7 Selective hydrogenation of alkynes using Milstein acridine-based *PNP*-iron pincer complex **7**.

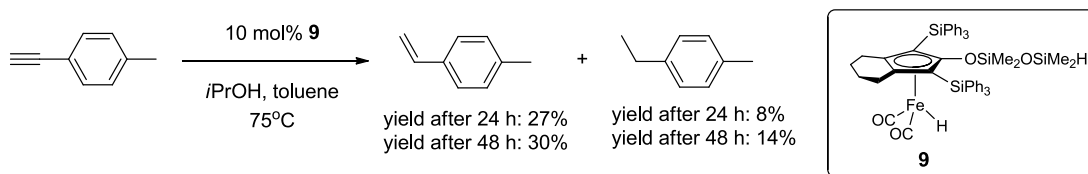
The group of Thomas employed *in situ* formed complex from a tetradentate iminopyridine ligand **8** with FeCl<sub>2</sub>, which was subsequently reduced with an organometallic coupling reagent (*i*PrMgCl) to form active, low valent catalyst. This allowed to avoid to work with a highly air- and moisture sensitive low valent iron species. Thomas and co-workers were able to hydrogenate a broad range of mono-substituted, 1,1- and 1,2-substituted aryl- and alkyl-substituted alkenes (Scheme 2.8).<sup>55</sup>



Scheme 2.8 Hydrogenation of alkenes with *in situ* obtained tetradentate *N,N,N,N*-iron complex.

### 2.3.5 (Cyclopentadienyl)iron complex

In 2014, a very interesting example of transfer hydrogenation of alkynes with isopropanol was reported by Nakazawa and co-workers.<sup>56</sup> They used a (hydrido)iron complex **9** with Si-H functionalized cyclopentadienyl ligand to achieve conversion of alkynes to alkenes and alkanes, although only partial and in a non-selective manner (Scheme 2.9). The obtained results were not spectacular, but they were the first reported example of iron complex involved in a transfer hydrogenation reaction from isopropanol to an alkyne or an alkene. Interesting mechanistic studies were performed, according to which, the hydrogen atoms were transferred first by hydrometalation, followed by reductive elimination. A more detailed description of (cyclopentadienyl)iron complexes will be discussed in the Paragraph 2.4.7.

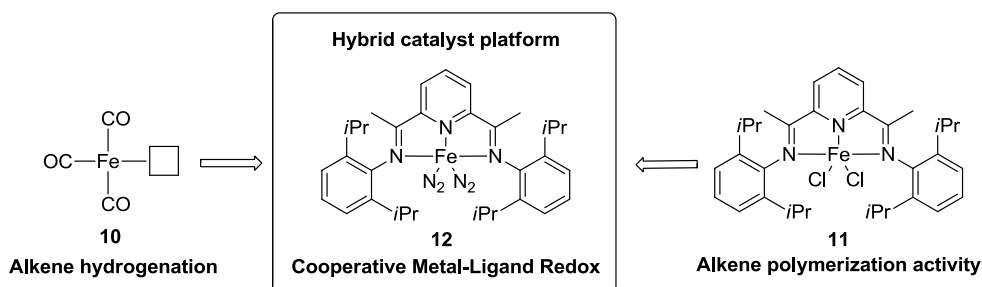


Scheme 2.9 Alkyne transfer hydrogenation with (hydrido)iron complex **9**.

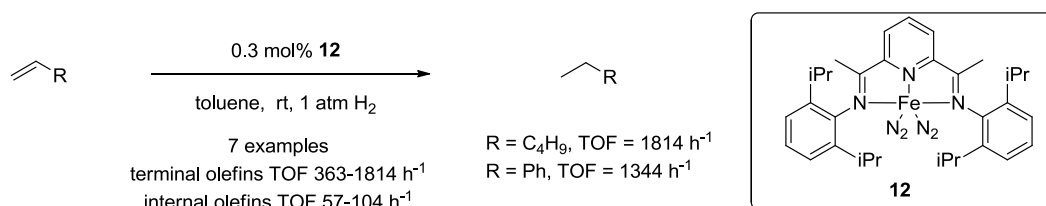


## 2.3.6 Bis(iminopyridine) complexes

The most important group of iron catalysts for alkene reduction was introduced by group of Chirik in 2004.<sup>57</sup> The design of a new iron catalyst **12** stemmed from combining previous observations of active carbonyl compounds for alkene hydrogenation (Figure 2.2) together with a polymerization catalysts **11** made by Gibson and Brookhart.<sup>58</sup> As it was confirmed that **10** ( $\text{Fe}(\text{CO})_3$  with a vacant site) is the active species in hydrogenation of olefins promoted by iron carbonyls,<sup>46</sup> Chirik postulated that a similar reduced bis(iminopyridine) [PDI] bis(dinitrogen) iron complex **12** would be isolobal to it (Figure 2.3). Moreover, PDI ligand was straightforward to synthesize and easy-to-tune.<sup>59</sup> In contrast to the homoleptic iron carbonyl compounds, it provided the opportunity to synthesize a library of new catalysts by tuning both steric and electronic properties.

Figure 2.3 Concept for a new iron catalyst **12**.

The first generation catalyst **12** exhibited an excellent activity in the hydrogenation of olefins. An unprecedented activity for a base metal was obtained, with TOF of  $1814 \text{ h}^{-1}$  for reducing 1-hexene at room temperature and under 1 atm  $\text{H}_2$  (Scheme 2.10). This result exceeded the efficiency of many classical noble metal catalysts like Pd/C, Wilkinon's  $(\text{Ph}_3\text{P})_3\text{RhCl}$  and Crabtree's  $[(\text{COD})\text{Ir}(\text{PCy}_3)\text{Py}]\text{PF}_6$ , under identical conditions. Internal alkenes required prolonged reaction times in comparison to terminal olefins.

Scheme 2.10 Olefin hydrogenation with catalyst **12**.

An additional catalyst's feature was the possibility of conducting solvent-free, neat reactions. The system was not affected by various functional groups like amines, esters, ketones or ethers.<sup>60</sup> Albeit the catalyst was undergoing decomposition with  $\alpha,\beta$ -unsaturated ketones, it was able to achieve TOFs up to  $240 \text{ h}^{-1}$  in the hydrogenation of  $\alpha,\beta$ -unsaturated esters to corresponding saturated esters. The steric optimization of ligand allowed to improve the activity of the catalyst **13** (Figure 2.4), but a more

remarkable effect was obtained upon introduction of electron donating substituents like  $\text{NMe}_2$  at the 4-position of the pyridine ring (complex **14**). Also dinuclear catalyst **15** revealed excellent catalytic activity.

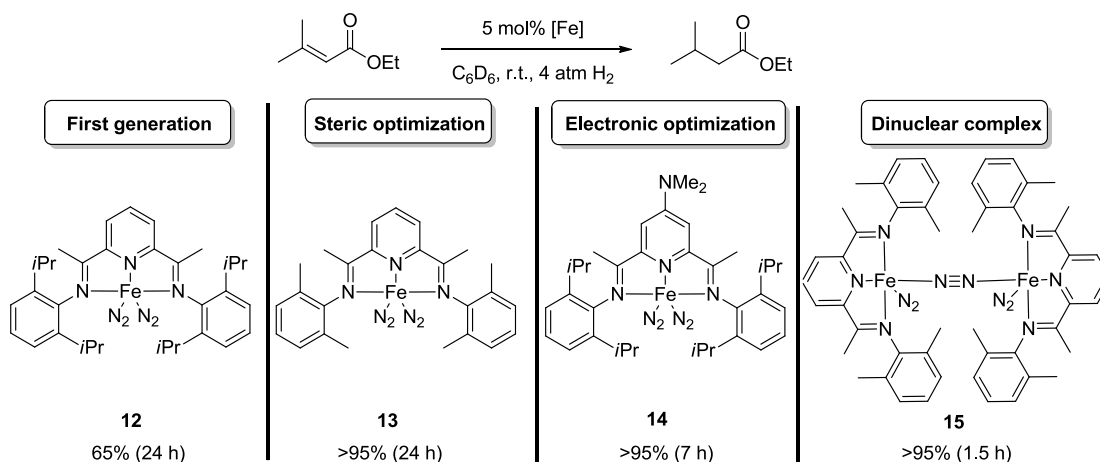


Figure 2.4 Ligand optimization effects on hydrogenation of ethyl 3-methylbut-2-enoate.

A combination of spectroscopic techniques and density functional theory (DFT) calculations revealed that in these formally  $\text{Fe}^0$  compounds (with neutral ligands), iron had actually oxidation state +2 and the metal had transferred two electrons to the bis(imino)pyridine ligand (Figure 2.5).<sup>61</sup> The latter is supposed to act as a redox-active ligand in the course of the catalytic cycle, as it changes its charge state and behave as a redox non-innocent ligand (see Paragraph 2.2.1).

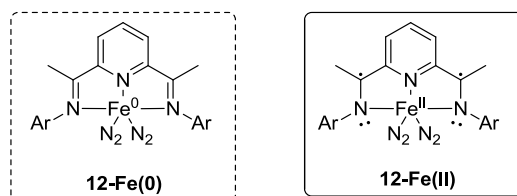


Figure 2.5 Incorrect  $\text{Fe}(\text{0})$  and correct  $\text{Fe}(\text{II})$  structures of complex **12**.

The Chirik's group evaluated replacement of the imino functionalities present in reported iron complexes with phosphino groups (Figure 2.6).<sup>62</sup> The catalyst **16** had a different coordination model, as hydrogen atom replaced one of nitrogen ligands. Nevertheless, it did not lead to the increased activity. A lower TOF of  $325 \text{ h}^{-1}$  was achieved in the hydrogenation of 1-hexene under the same conditions as in Scheme 2.10.

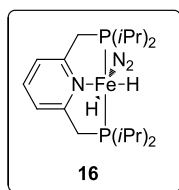


Figure 2.6 Iron-aminodiphosphine complex **16**.

Following research on different imino functionalities, new iron  $\alpha$ -diimine complexes were obtained (Figure 2.7).<sup>63</sup> As the dinitrogen-substituted complexes were

unstable, ligands like alkynes, alkenes (**17**) or dialkenes (**18**) were introduced to stabilize the structure. However, using conditions similar to those previously reported for **12** (Scheme 2.10), only relatively low TOFs ( $90 \text{ h}^{-1}$ ) were achieved by both of them in the hydrogenation of 1-hexene.

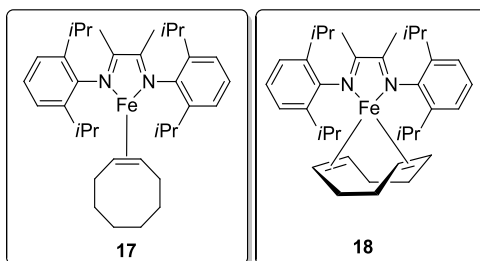


Figure 2.7  $\alpha$ -Diimine iron alkene complexes **17** and **18**.

Despite the significant achievements made by Chirik's group, their catalysts suffer from serious practical limitations which preclude their industrial application. They are highly air-sensitive, hence their synthesis and manipulation must take place under rigorously dry conditions, inside the glovebox, under argon atmosphere.

### 2.3.7 Iron nanoparticles

Homogenous reduction of alkenes and alkynes is not limited to iron carbonyls or multidantete ligand complexes. Unlike the above mentioned authors, de Vries and co-workers, reported a non-ligand approach using iron nanoparticles (NPs).<sup>64</sup> Fe-NPs were prepared by reducing  $\text{FeCl}_3$  with  $\text{EtMgCl}$  in THF, basing on methodology described by Bedford.<sup>65</sup> A quick and quantitative conversion was obtained with *cis*-1,2 and 1,1-disubstituted alkenes. A lower reduction rate was observed with 1,2-*trans*-disubstituted and cyclic *cis*-alkenes. 1-octyne was hydrogenated with TOF  $118 \text{ h}^{-1}$ . Generally, the hydrogenation of tri- and tetrasubstituted alkenes with the Fe-NPs was unsuccessful. Also the presence of OH groups in substrates had the retardation effect on the rate of reaction. Fe-NPs were found to be rather stable, and were successfully applied in continuous hydrogenation of norbornene.

Similar iron nanoparticles were also found to be catalytically active, when supported on a graphene. They were utilized for hydrogenation reactions with various cyclic and terminal olefins.<sup>66</sup> The main advantage of this system was an efficient removal of the nanoparticles by simple magnetic decantation and re-using them without any significant loss in the activity.

To induce a high *Z*-selectivity in alkene hydrogenation using Fe-NPs, Wangelin, and co-workers used them in a biphasic heptane/ionic liquid system.<sup>67</sup> The nitrile function was essential for achieving high *Z*-selectivity and it could be introduced either as a substituent in the ionic liquid or as an acetonitrile additive. It was also possible to easily remove the iron nanoparticles, as the ionic liquid prevented from their aggregation, enabling to decant them and being re-used without any loss of activity.

## Chapter 2

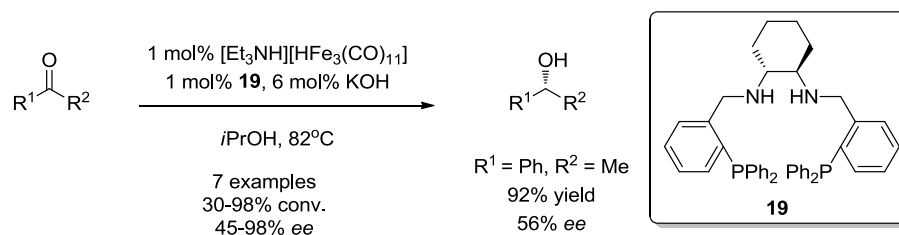
Ultra small Fe-NPs were obtained by Beller and co-workers from the decomposition of  $\{\text{Fe}[\text{N}(\text{SiMe}_3)_2]\}_2$  under hydrogen.<sup>68</sup> These NPs promoted the hydrogenation of terminal alkenes and alkynes, as well as cyclic alkenes, but were ineffective for non-cyclic internal alkenes and internal alkynes.

### 2.4 Hydrogenation of ketones and imines

#### 2.4.1 Iron carbonyl *in situ* systems

Noble metals remained the only option for the catalytic hydrogenation of carbonyl compounds until 1980s, when Markó and co-workers reported the use of  $\text{Fe}(\text{CO})_5$  together with triethylamine to hydrogenate various ketones and aldehydes to the corresponding alcohol products.<sup>69</sup>

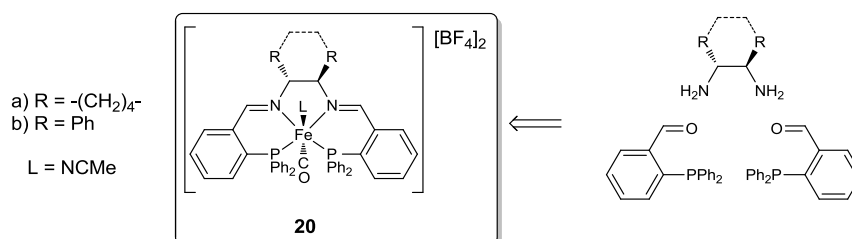
More recently, in 2004 Gao and co-workers used Markó's catalytic system together with a chiral ligand **19** for an asymmetric transfer hydrogenation (ATH) with isopropanol as a hydrogen source (Scheme 2.11).<sup>70</sup> This system revealed good to very high conversions with moderate to good enantiomeric excesses. The highest *ee* values (up to 98% *ee*) were obtained for sterically crowded ketones.



Scheme 2.11 Asymmetric transfer hydrogenation of ketones using catalytic system with ligand **19**.

#### 2.4.2 *P,N,N,P*-complexes

The Gao's system (Scheme 2.11) was an inspiration for Morris and co-workers. In 2008, they synthesized a well-defined iron diiminophosphine complexes **20a-b**.<sup>71</sup> The mentioned catalysts were prepared by the condensation of commercially available diamines and phosphinealdehyde (Scheme 2.12). It was expected that due to hydrogenation reaction course, the imine donors in synthesized complexes would be reduced to amines.

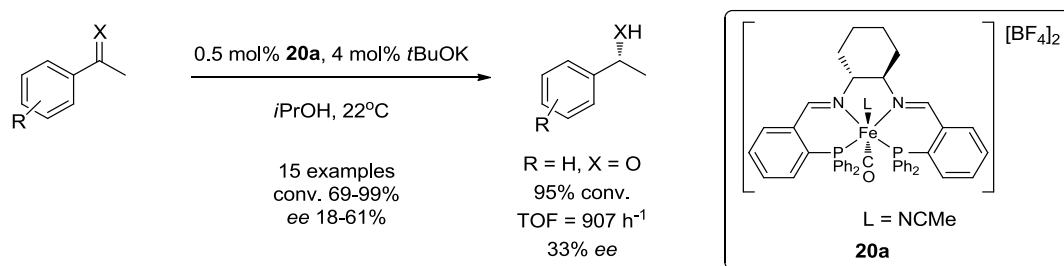


Scheme 2.12 First generation diiminophosphine complexes **20**.

Complex **20a** was employed for the ATH of a range of ketones and imines using



isopropanol and allowed to obtain high conversions, but only modest enantioselectivities (Scheme 2.13). TOFs up to  $907 \text{ h}^{-1}$  were reported, which were comparable with those of the ruthenium catalyst developed up to that moment.



Scheme 2.13 ATH of ketones and imines using complex **20a**.

Further research led to an unexpected results. Morris discovered that the active species in the reaction were actually iron nanoparticles formed from complexes **20**.<sup>72</sup> This was the first reported example of use of Fe-NPs to promote enantioselective transformations. According to the authors, the flexible six-membered chelate rings were responsible for the occurring formation of Fe-NPs. Under reducing conditions, they allowed ligand dissociation to form active Fe-NPs. To prevent this phenomenon, Morris and co-workers developed the second generation "FeATHer" complexes **21a-d**, featuring five-membered rings, obtained from the condensation of an enantiopure diamine and dialkyl- or diarylphosphinoacetaldehydes (Figure 2.8).<sup>73</sup>

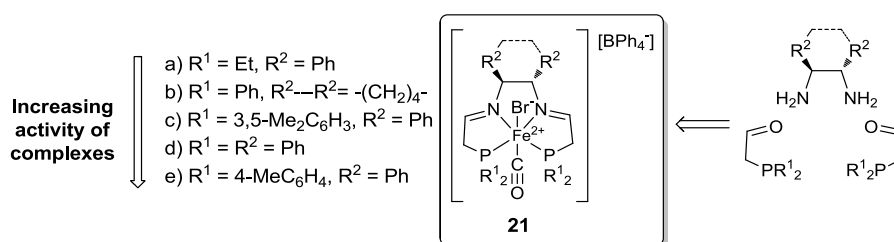
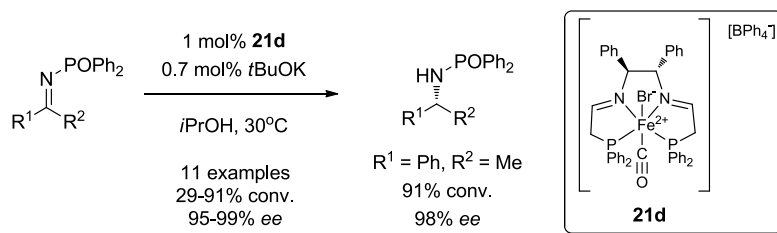


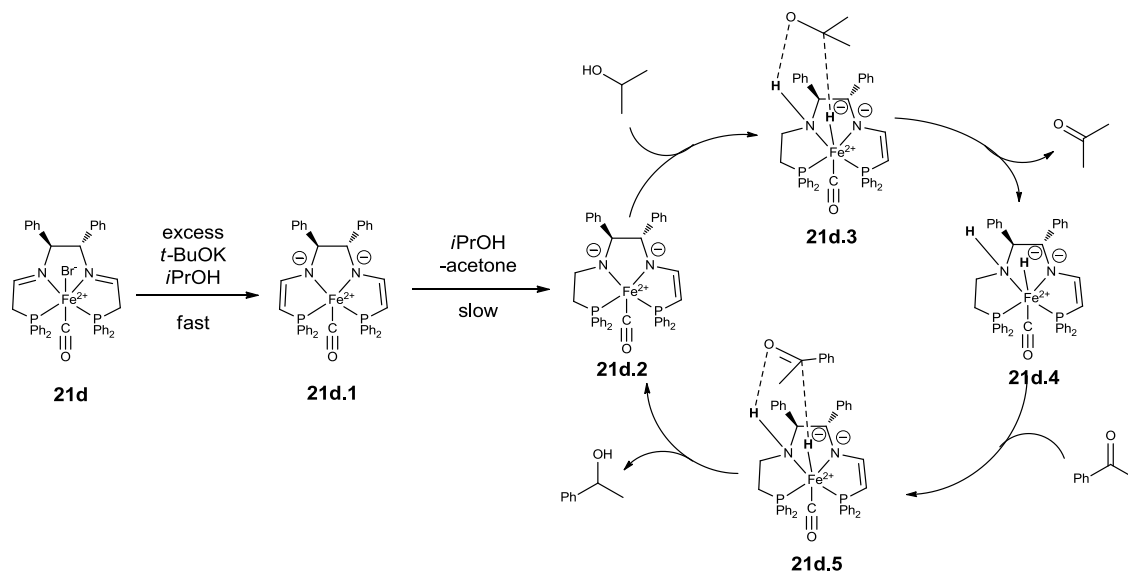
Figure 2.8 Examples of 2<sup>nd</sup> generation of "FeATHer" precatalysts **21**.

The maximum TOF obtained by the second generation catalysts in the ATH of ketones (under similar conditions presented on Scheme 2.13) reached  $30\,000 \text{ h}^{-1}$ , together with high enantiomeric excesses (up to 90%). Along many investigated structural changes in his second generation catalysts, crucial for activity appeared to be the substituent on phosphorus. It had to be moderate size and have moderate donor ability, otherwise complexes were catalytically inactive.<sup>74</sup>

Complex **21d** proved to be also an active catalyst for ATH of variety of prochiral ketimines bearing diphenylphosphino group at the nitrogen (Scheme 2.14). High conversions (up to 91%) with excellent *ee* (95-99%) were reported.

Scheme 2.14 ATH of diphenylphosphinoyl ketoimine using 2<sup>nd</sup> generation "FeATHer" complex **21d**.

Further mechanistic studies on this complex revealed that before the actual catalysis starts, the ligand gets modified twice (Scheme 2.15).<sup>75</sup> The first step of activation is deprotonation of **21d** using a strong base in order to form bis-anionic bis-enamide complex **21d.1**. In the second activation step occurs a slow addition of a proton and a hydride from isopropanol to one of the enamide groups, forming **21d.2**. This "one-side" hydrogenated monoanionic amido-enamido complex is the active iron complex in the ATH. Remarkably, further studies of Morris' group confirmed that a "both-sides" hydrogenated complex is a totally non-active catalyst.<sup>76</sup> In the course of the catalytic cycle the *P,N,N,P*-ligand **21d.2** picks up a proton and a hydride from isopropanol (**21d.3** → **4**) to deliver them to the substrate (**21d.5**). The hydride transfer from iron to the carbonyl group of acetophenone proceeds according to an outer-sphere pathway, with no substrate coordinated to the metal, and proton transfer from the amino group of the ligand to the carbonyl oxygen. As the diiminodiphosphino ligand actively participates in the mechanism of C=O reduction by mediating the proton transfer, this is the perfect example of redox non-innocent ligand. The described outer-sphere mechanism, closely resembles the one described by Noyori for Ru(II).<sup>77</sup>

Scheme 2.15 Proposed mechanism of activation of the 2<sup>nd</sup> generation of "FeATHer" complex **21d**.

Following the lead of importance of unsymmetrical ligands, the third generation catalysts **22** (obtained by condensation of enantiopure *P-NH-NH*<sub>2</sub> diamine and dialkyl- or diaryl-phosphinoacetaldehydes) meant to involve all of the iron complex rapidly into the

hydrogenation (Figure 2.9).<sup>78</sup>

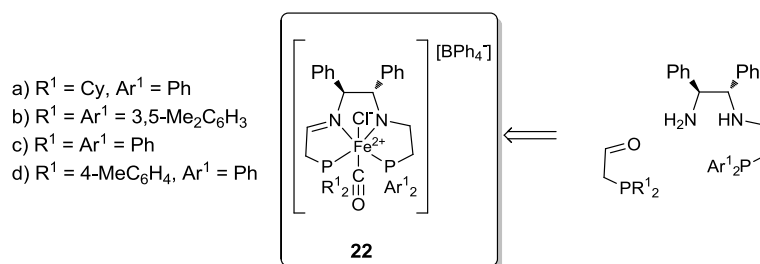
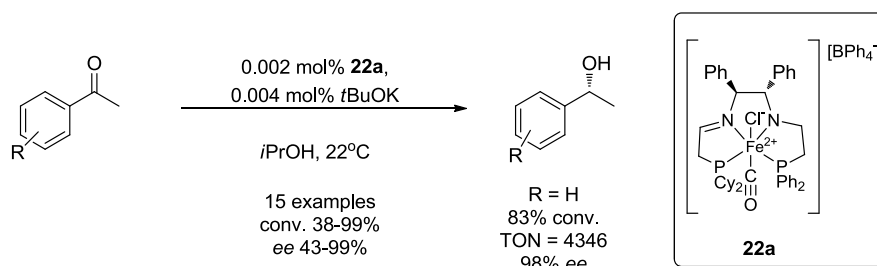


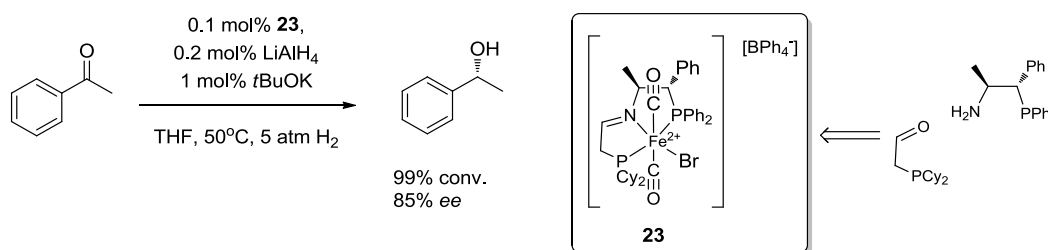
Figure 2.9 Examples of 3<sup>rd</sup> generation of "FeATHer" precatalysts **22**.

As expected, treatment of new complexes with excess of base, allowed to directly convert them to catalytically active unsymmetrical amide-enamide catalyst. The obtained catalysts were very active for the ATH of a huge range of ketones and ketoimines, achieving TOF up to  $150 \text{ s}^{-1}$  and 99% *ee* (Scheme 2.16). Moreover, an easy synthesis of the pre-catalyst allowed to optimize its structure for certain substrates.



Scheme 2.16 ATH of ketones using 3<sup>rd</sup> generation "FeATHer" complex **22a**.

The Morris' group continued their research towards a new catalyst for the asymmetric hydrogenation using molecular hydrogen, instead of transfer hydrogenation with isopropanol.<sup>79</sup> The new complex **23** prepared by the condensation of enantiopure *P*- $\text{NH}_2$  amine and dicyclohexylphosphinoacetaldehyde (Scheme 2.17) was activated with  $\text{LiAlH}_4$  and alcohol to obtain active *P,NH,P* catalyst for reducing ketones and imines. TOFs up to  $1980 \text{ h}^{-1}$  with *ee* up to 85% were obtained, but the structure of the active catalyst is still not clear.



Scheme 2.17 4<sup>th</sup> generation precatalyst **23** for AH of ketones and imines.

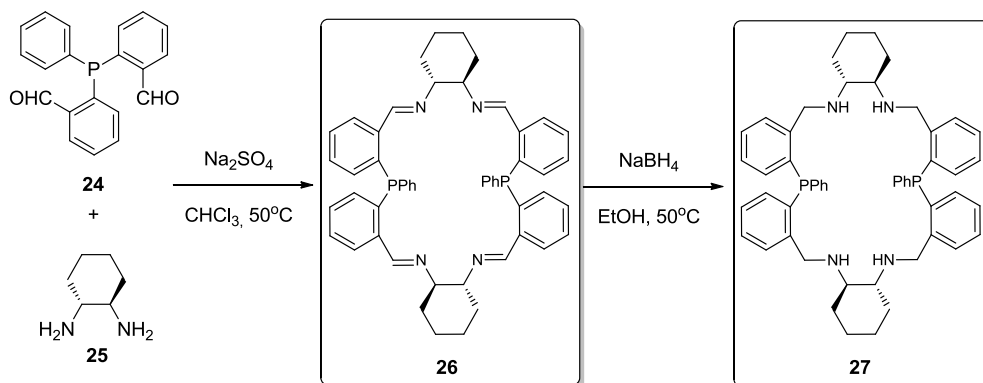
### 2.4.3 Macrocyclic complexes

Gao and co-workers performed further studies on diamino- and diiminodiphospine ligands to turn them into macrocyclic structures.<sup>80</sup> They described a condensation of bis(*o*-formylphenyl)-phenylphosphane **24** and (*R,R*)-cyclohexane-1,2-



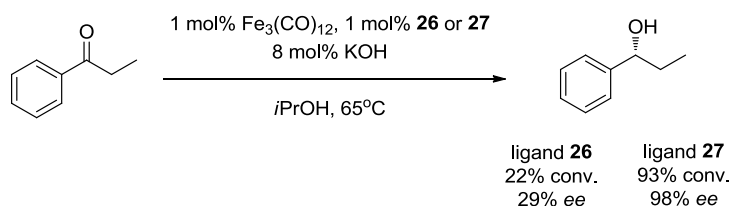
## Chapter 2

diamine **25** which led to a 22-membered diiminodiphosphine macrocycle **26** (Scheme 2.18). It was followed by a reduction of **26** with  $\text{NaBH}_4$ , which yielded corresponding diaminodiphosphine ligand **27**.



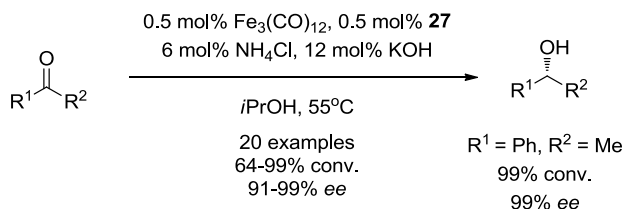
Scheme 2.18 Synthesis of chiral macrocyclic ligands **26** and **27**.

New macrocycles, together with  $\text{Fe}_3(\text{CO})_{12}$ , were compared in ATH of propiophenone (Scheme 2.19). The diiminodiphosphine ligand **27** appeared to be much more active than diiminodiphosphine macrocycle **26**. By contrast, use of different iron sources (like iron(0)  $\text{Fe}_2(\text{CO})_9$ , iron(II)  $\text{FeCl}_2$  or iron(III)  $\text{FeCl}_3$ ) gave almost no activity in the reaction with both ligands.



Scheme 2.19 ATH of propiophenone catalyzed by iron complexes with chiral macrocycles **26** and **27**.

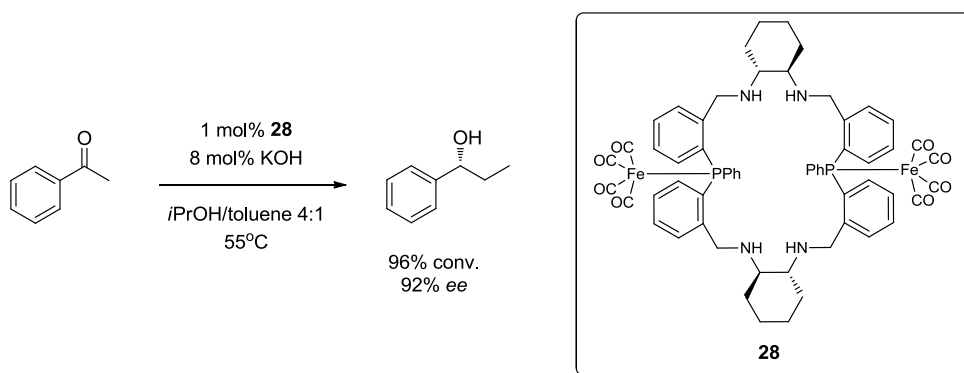
Gao and co-workers found that the use of ammonium salts is promoting the reaction, although its role remained unknown. The substrate screening revealed high activity of the catalytic system for a broad range of aromatic and heteroaromatic ketones (Scheme 2.20).



Scheme 2.20 ATH of ketones catalyzed by iron complex with chiral macrocycle **27**.

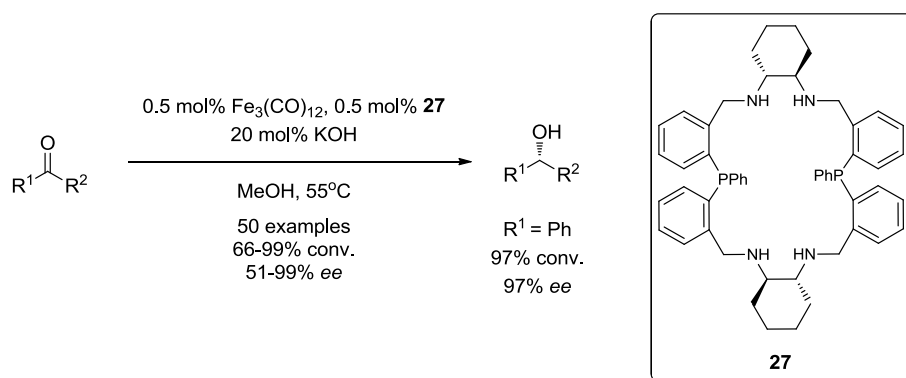
To gain more knowledge about possible interactions between iron and the macrocycle, Gao and co-workers synthesized iron catalyst **28**, but it possessed lower catalytic activity than catalytic system formed *in situ* (Scheme 2.21). In fact, this could suggest that **28** is not the active species in the ATH of ketones.





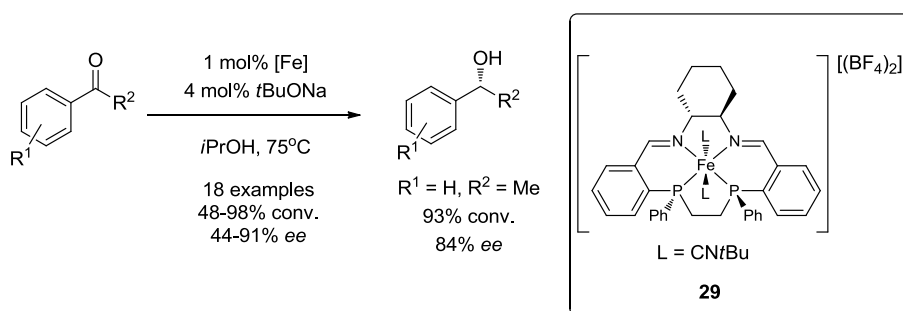
Scheme 2.21 ATH of acetophenone catalyzed by chiral P<sub>2</sub>N<sub>4</sub>-Fe(0) complex **28**.

Subsequent work of Gao's group showed also the high activity of chiral macrocycle **27** in the AH of aromatic and heteroaromatic ketones (Scheme 2.22).<sup>81</sup> Preliminary studies on the hydrogenation's mechanism suggest formation of chiral macrocycle-modified iron nanoparticles which could be the active species.



Scheme 2.22 AH of ketones using macrocyclic ligand **27**.

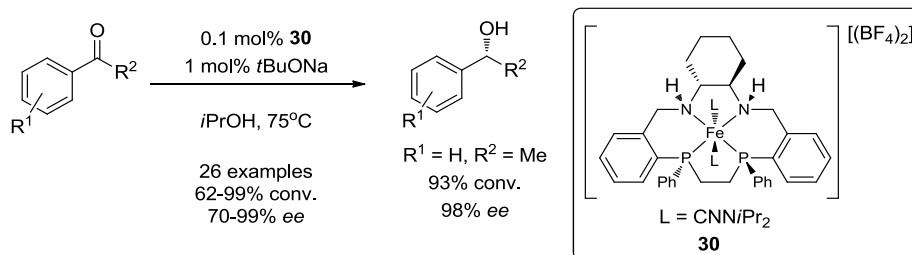
Recently Mezzetti and co-workers developed new chiral C<sub>2</sub>-symmetric P<sub>2</sub>N<sub>2</sub>-macrocyclic ligands and their iron(II) isolated complexes.<sup>82,83</sup> Chiral P<sub>2</sub>N<sub>2</sub>-iron(II) complex **29** revealed very good activity in ATH, both in terms of conversion and enantioselectivity (Scheme 2.23).<sup>84</sup>



Scheme 2.23 ATH with chiral P<sub>2</sub>N<sub>2</sub>-iron(II) complex **29**.

Replacing diimino macrocycle, with diamino analogue, led to even higher activity in ATH of ketones (Scheme 2.24).<sup>85</sup> Excellent results in terms of yields (up to 98%) and enantioselectivities (up to 91% ee) were obtained with ketones, enones and imines, albeit using only 0.1 mol% of catalyst. In both of presented classes of complexes, iron's

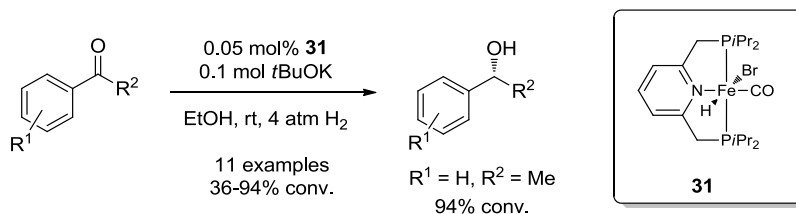
isonitrile ligands, turned out to affect both the enantioselectivity and the activity of the catalyst.



Scheme 2.24 ATH with chiral  $P_2(NH)_2$ -iron(II) complex **30**.

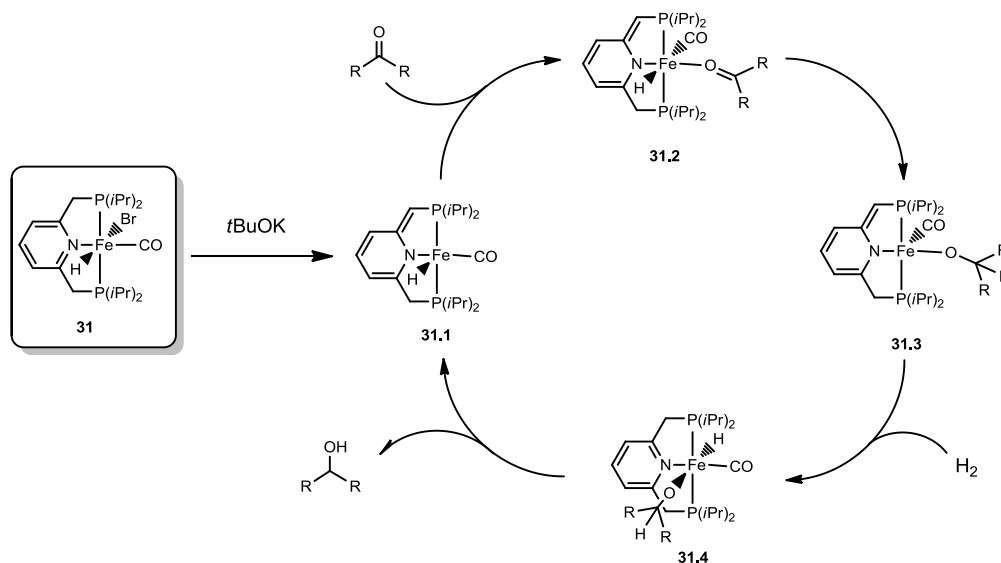
#### 2.4.4 $P,N,P$ -pincer complexes

In 2011 Milstein and co-workers reported the use of (hydrido)iron(II) pincer  $P,N,P$ -complex **31** in ATH of ketones, achieving high turnover numbers (TONs) – up to 1880.<sup>86</sup> Despite using only 0.05 mol% catalyst loading, the reaction proceeded under room temperature (Scheme 2.25).



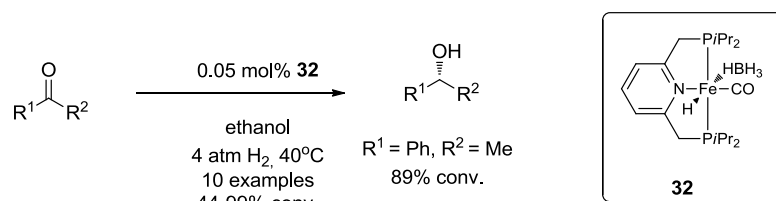
Scheme 2.25 ATH with iron(II) pincer complex **31**.

A possible reaction mechanism for ketone hydrogenation (Scheme 2.26), features hydride transfer from activated catalyst **31.1** to the coordinated substrate (**31.2** → **31.3**), according to an inner-sphere pathway. Remarkably, in this mechanism the pyridine ring of the tridentate ligand plays a key role flipping between the aromatic (**31.4**) and the dearomatized form (**31.1**), thus acting as a redox non-innocent ligand.



Scheme 2.26 Possible reaction mechanism for ketone hydrogenation using complex **31**.

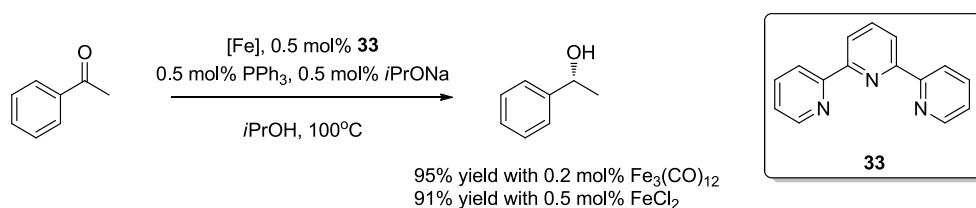
Using the second-generation iron pincer catalyst **32** featuring a borohydride ligand, the same research group was able to achieve comparable TONs as the first generation, without any addition of base required (Scheme 2.27).<sup>87</sup>



Scheme 2.27 Base-free ATH with iron(II) pincer complex **32**.

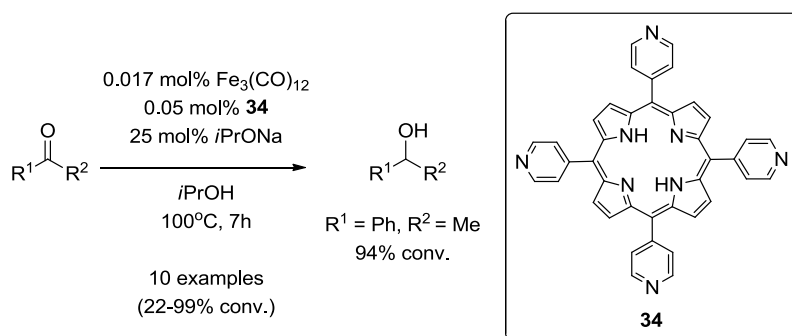
#### 2.4.5 Multidentate *N*- and *P*-ligand complexes

Beller and co-workers worked also on ATH of ketones.<sup>88</sup> The employed catalytic system combined Fe<sub>3</sub>(CO)<sub>12</sub> or FeCl<sub>2</sub>, the ligand **33** and PPh<sub>3</sub>, in isopropanol as hydrogen donor (Scheme 2.28). The reaction outcome was strongly dependent on the choice of base, but when *i*PrONa or *t*BuONa were used, corresponding alcohols were obtained with high yields, regardless applied iron source employed.



Scheme 2.28 ATH with a terpy ligand **33**.

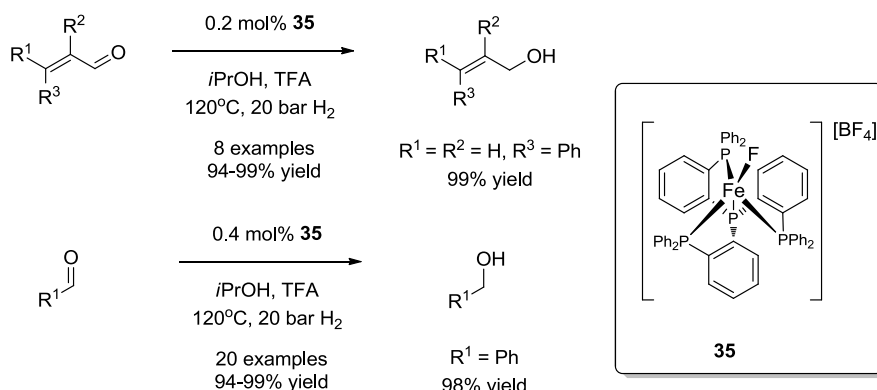
Beller's group also pursued a biomimetic approach, using *in situ* generated iron porphyrines instead of iron triphenylphosphine systems (Scheme 2.29).<sup>89</sup> This system was less base-dependent and allowed to obtain excellent conversion in the transfer hydrogenation of ketones with isopropanol, again independent on the applied iron source.



Scheme 2.29 ATH with a *in situ* generated iron porphyrine from **34**.

A well-defined iron(II) tetradentate phosphine complex **35** was employed by Beller and co-workers for the selective hydrogenation of  $\alpha,\beta$ -unsaturated aldehydes.<sup>90</sup> Excellent yields of allylic alcohols were obtained from corresponding allylic aldehydes, as well as alcohols from aromatic, heteroaromatic or alkyl aldehydes (Scheme 2.30). This complex

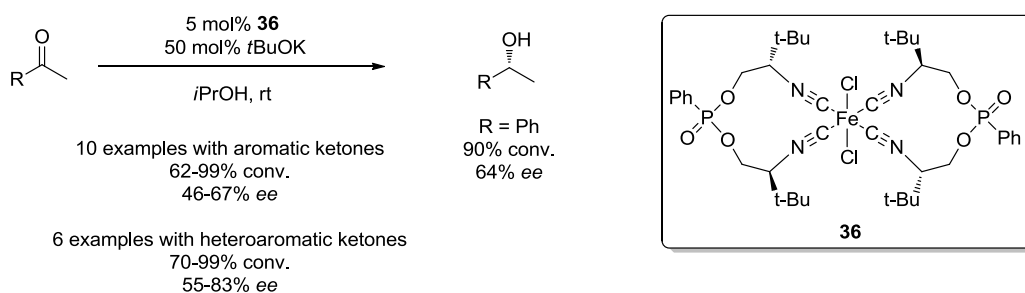
could leave a free coordination site for the incoming substrate by unfastening one terminal phosphine arm, as proposed by Bianchini *et al.* for the related iron-catalyzed hydrogenation of alkynes.<sup>50</sup>



Scheme 2.30. ATH with an iron(II) tetradentate phosphine complex **35**.

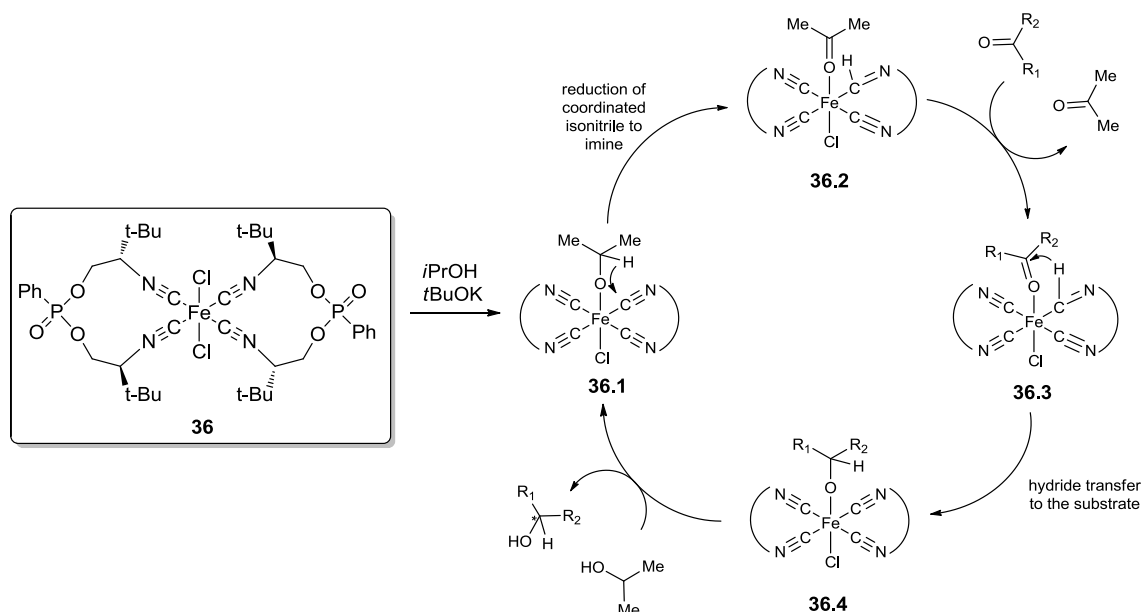
#### 2.4.6 Isonitrile complex

In 2010 Reiser and co-workers reported a chiral bis(isonitrile)iron(II) complexes **36** for the ATH of aromatic and heteroaromatic ketones.<sup>91</sup> The transformation proceeded under mild conditions but although obtaining very good conversions, only modest enantioselectivities could be achieved (up to 67% *ee*).



Scheme 2.31 ATH with a chiral bis(isonitrile)iron(II) complex **36**

For this transfer hydrogenation, a Meerwein-Ponndorf-Verley-type mechanism was proposed (Scheme 2.32). After activation of **36** with *t*BuOK, isopropanol is being coordinated to iron (**36.1**) and the catalytic cycle follows with reduction of coordinated isonitrile ligand to an imine (**36.2**). Formed acetone is being removed and the reaction follows an inner-sphere pathway, with substrate coordination at the Fe<sup>II</sup> centre (**36.3**). Remarkably, the formation of an iron hydride does not take place. Rather, the imine with a hydride absorbed from isopropanol, transfers it to the substrate (**36.4**). Therefore, in this case the ligand shows a clearly non-innocent behavior owing to the peculiar properties of the isonitrile group. Catalytic cycle is closed by displacing the newly reduced carbonyl with a fresh isopropanol from the reaction solution.

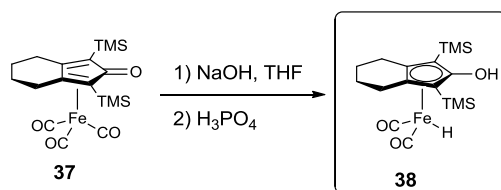


Scheme 2.32 Meerwein-Ponndorf-Verley mechanism for ATH with bis(isonitrile)iron(II) complex **36**.

## 2.4.7 (Cyclopentadienone)iron complexes

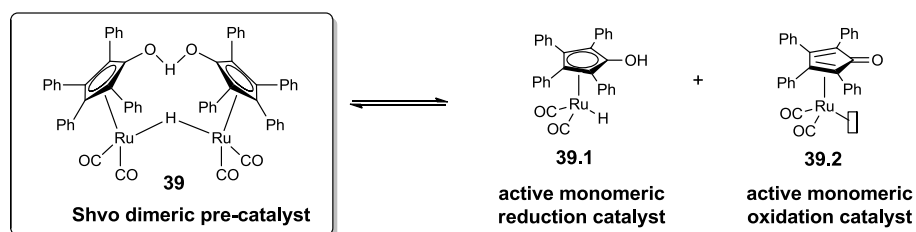
### 2.4.7.1 Reduction of aldehydes, ketones and imines

(Cyclopentadienone)iron complexes were firstly reported by Reppe and Vetter in 1953.<sup>92</sup> They are easy to synthesize and to purify (they are stable to flash chromatography over silica). Moreover their structure can be easily tuned. For a long time, despite their unique structural features they were not highly investigated - they were regarded as "scientific curiosities". It took over 40 years until they were studied with more attention by Knölker<sup>93</sup> and Pearson.<sup>94</sup> In 1999, Knölker and co-workers synthesized and isolated the first (hydrocyclopentadienyl)iron complex **38** (now known as the Knölker catalyst) from the bench-stable (cyclopentadienone)iron complex **37** using a Hieber-base reaction (Scheme 2.33).<sup>95</sup>

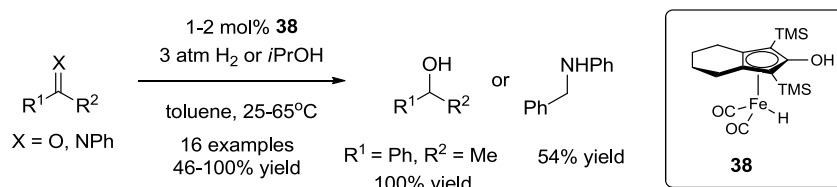


Scheme 2.33 Obtaining iron hydrocyclopentadienyl complex **38** by a Hieber-base reaction from **37**.

Still, as the main focus of the research was to obtain the metal-free cyclopentadienone ligand, the potential use of hydride **38** in catalysis remained unseen until 2007. In this year Casey and Guan<sup>96</sup> reported that complex **38** possesses similar properties to structurally related Shvo catalyst, which was known since 1985 (Scheme 2.34).<sup>97</sup>

Scheme 2.34 Shvo dimeric pre-catalyst **39** and its active structures **39.1** and **39.2**.

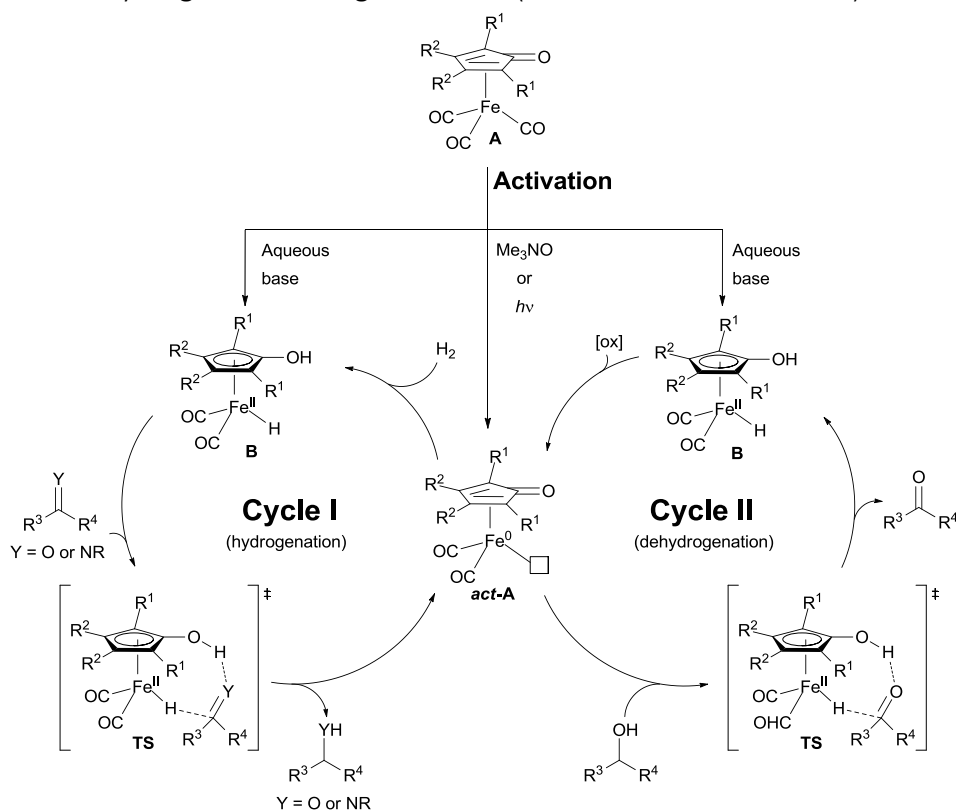
Casey and Guan demonstrated that the hydride **38** is a highly efficient catalyst for the chemoselective hydrogenation of aldehydes, ketones and imines under mild conditions (Scheme 2.35). A large number of groups, such as isolated carbon-carbon double or triple bonds, halides, nitro groups or epoxides, were perfectly tolerated under the described conditions. Further computational studies performed by Sun and co-workers confirmed that catalyst **38** is not able to hydrogenate olefins and alkynes under relatively low temperatures.<sup>98</sup> Hydride **38** was also proved to work under transfer-hydrogenation conditions.

Scheme 2.35 Hydrogenation and transfer hydrogenation using (hydrocyclopentadienyl)iron complex **38**.

The main drawback of the active hydride **38**, was its sensitivity to air and light, which makes the glove-box necessary to handle it. Later contributions by other researchers demonstrated that it is possible to use bench-stable (cyclopentadienone)iron pre-catalysts such as **37** and to activate them *in situ* (Scheme 2.36, top part - Activation). The first method is based on the selective mono-decoordination of one of the CO ligands with oxidative cleavage using Me<sub>3</sub>NO.<sup>99</sup> The same effect can be also obtained by UV radiation.<sup>100</sup> Obtained complex **act-A** can be considered as a frustrated Lewis pair and as such, under hydrogen, is able to split H<sub>2</sub> and form the active hydride **B**. The hydride itself, can be also generated by *in situ* Hieber reaction of (cyclopentadienone)iron **A** with aqueous bases.<sup>101</sup>

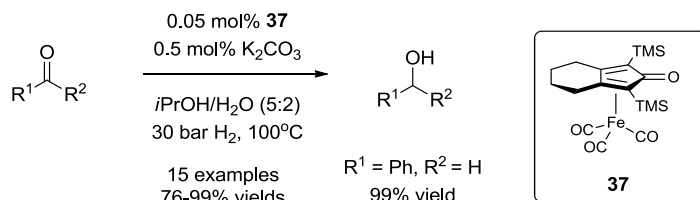
The mechanism of the transformation with this non-innocent ligand has been carefully studied.<sup>102</sup> As in the Shvo's ruthenium catalyst, the ligand is able to shuttle between the cyclopentadienone **act-A** and hydroxycyclopentadienyl **B** form, enabling an uncharacteristic catalytic cycle involving Fe(0) and iron Fe(II) (Scheme 2.36, Cycle I). The active species **act-A** splits hydrogen and then catalyzes the reduction of carbonyl compounds according to a concerted outer-sphere mechanism, in which the OH group of the ligand allows transient substrate's activation by hydrogen-bonding. Moreover, hydride **B** is acting under the same mechanism (Scheme 2.36, Cycle II) is also able to catalyze dehydrogenation of alcohols to carbonyl compounds in an Oppenauer-type

oxidation and "hydrogen-borrowing" reactions (like amination of alcohols).



Scheme 2.36 Catalytic pathways of i) hydrogenation of C=O and C=N double bonds (Cycle I), and ii) Oppenauer-type alcohol oxidation (Cycle II) catalyzed by cyclopentadienone complexes **act-A**.

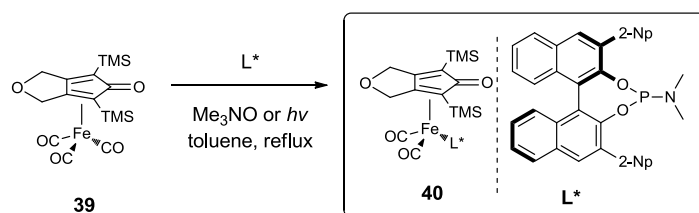
After optimizing the conditions for ketone hydrogenation, Beller and co-workers obtained TON up to 3800 using pre-catalyst **37** (Scheme 2.37).<sup>103</sup>



Scheme 2.37 Hydrogenation of ketones using bench-stable **37**.

### 2.4.7.2 Asymmetric reductions

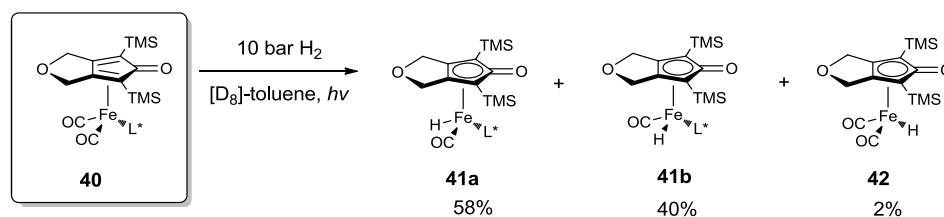
Attempts to perform enantioselective reductions using Knölker-type catalysts were made by the groups of Berkessel<sup>104</sup> and Wills.<sup>105</sup> Berkessel and co-workers replaced one of CO ligands from **39** with a chiral phosphoramidite ligand under UV irradiation or using  $Me_3NO$  (Scheme 2.38).



Scheme 2.38 Introducing a chiral ligand to the (cyclopentadienone)iron complex **38**.

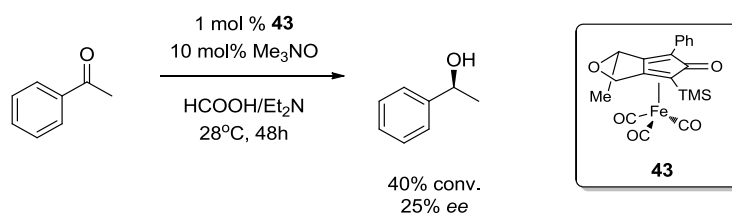
## Chapter 2

Using this chiral pre-catalyst **40**, acetophenone was hydrogenated with only 31% *ee*. Moreover, hydrogenation required constant UV radiation to cleave the second CO ligand and to form active hydride species. To investigate the reason of a low enantioselectivity, NMR studies were performed. They revealed that upon hydrogenation, two iron hydride diastereoisomers **41a** and **41b** are formed at the newly generated iron-stereocenter in ratio 1:0.7 (Scheme 2.39). This occurred because of the non-selective dissociation of CO from the pre-catalytic complex **40** and explains the low enantioselectivity of the reaction. Moreover, upon hydrogenation, a partial removal of the chiral ligand occurred and gave 2% of the achiral, but most likely highly active hydride complex **42**.



Scheme 2.39 Formation of diastereoisomers upon hydrogenation of **40**.

Wills and co-workers presented a different approach to solve the chirality problem.<sup>105</sup> Instead of replacing a CO with a chiral ligand, they decided to use a chiral cyclopentadienyl ligand by insertion of a remote chiral centre in addition to the planar symmetry of a (cyclopentadienone)iron complex, thus obtaining pre-catalyst **43** (Scheme 2.40). Performing the ATH of acetophenone in the presence of **43** with formic acid/triethylamine as a hydrogen source, only up to 25% *ee* was achieved. This poor enantiocontrol was independent on the metal employed, as the corresponding ruthenium chiral catalyst was able to achieve only 21% *ee*.

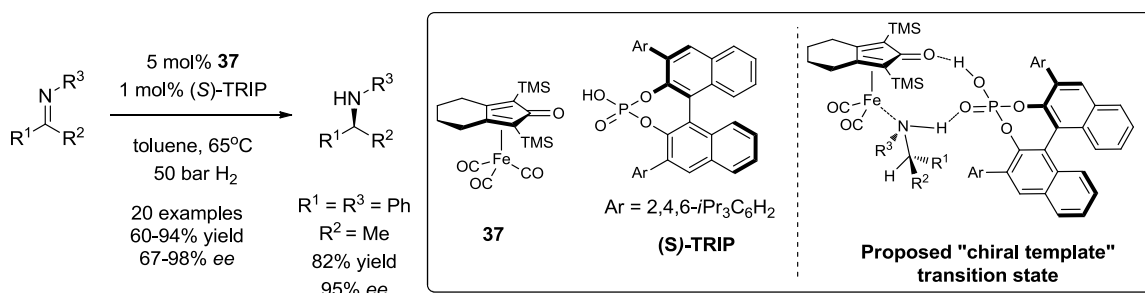


Scheme 2.40 ATH of acetophenone using chiral (cyclopentadienone)iron complex.

Beller and co-workers developed a methodology for the asymmetric hydrogenation of *N*-aryl ketoimines based on the use of the achiral pre-catalyst **37** in combination with a chiral phosphoric acid - (*S*)-TRIP.<sup>106</sup> For this reaction, the authors proposed a mechanism in which the Brønsted acid acts as a “chiral template” forming hydrogen bonds simultaneously with the substrate and with the catalyst (Scheme 2.41). A large number of different *N*-aryl ketoimines were hydrogenated with high yields and excellent *ee*. In a subsequent paper, Beller and co-workers used also this system to hydrogenate variety of quinoxalines to tetrahydroquinoxalines and 2H-1,4-benzoxazines to dihydro-2H-benzoxazines, again with high yields and excellent *ee*.<sup>107</sup> In other

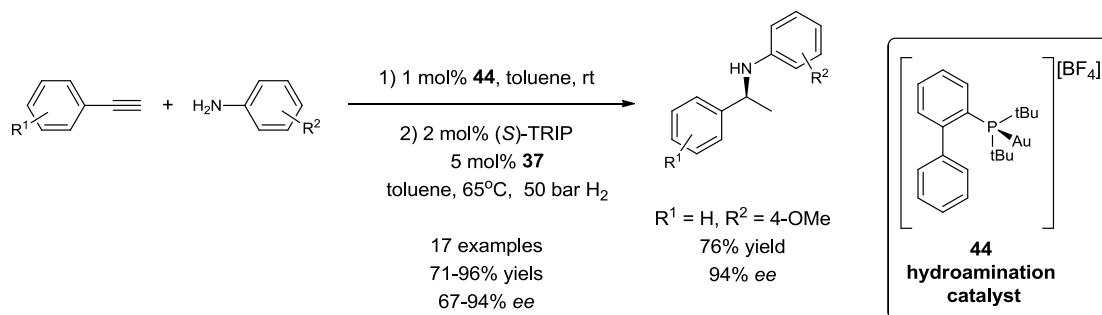


publication, Beller and co-workers used this methodology also for asymmetric reductive amination of ketones with anilines, once more with high yields and excellent *ee*.<sup>108</sup>



Scheme 2.41 Hydrogenation of imines using iron pre-catalyst **37** and (S)-TRIP.

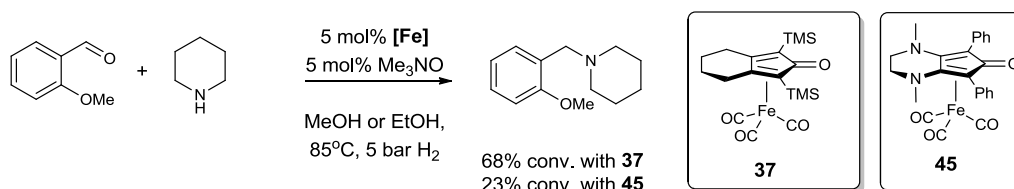
The above-mentioned methodology was employed in a combinatorial multi step, one-pot hydroamination of alkynes followed by enantioselective hydrogenation (Scheme 2.42).<sup>109</sup> The first step was catalyzed by gold(I) complex **44**, followed by hydrogenation carried out using **37** with a chiral Brønsted acid. Once more, high yields and enantioselectivities were obtained.



Scheme 2.42 One-pot enantioselective reductive hydroamination using **44**, **37** and (S)-TRIP.

### 2.4.7.3 Amination of aldehydes, ketones and alcohols

The cyclopentadienone complex **37** was also applied for reductive amination by the group of Renaud.<sup>110</sup> This transformation was efficient for variety of primary or secondary amines and worked with both ketones and aldehydes. In a subsequent article, Renaud and co-workers reported that more electron-rich (cyclopentadienone)iron complex **45** was more effective for the reductive amination of aromatic aldehydes (Scheme 2.43).<sup>111</sup>

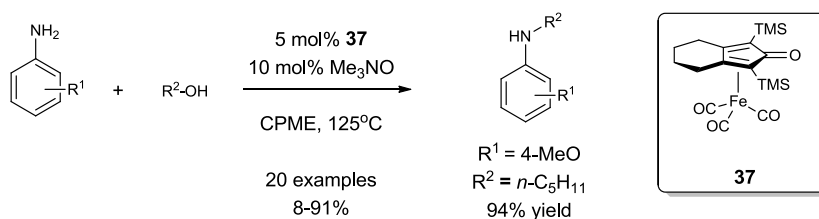


Scheme 2.43 Reductive amination using complexes **37** and **45**.

Feringa and Barta exploited further possibilities of amine functionalization using (cyclopentadienone)iron complex **37**. They performed simple and direct *N*-alkylation of amines with alcohols using a hydrogen-borrowing process.<sup>112</sup> A variety of primary

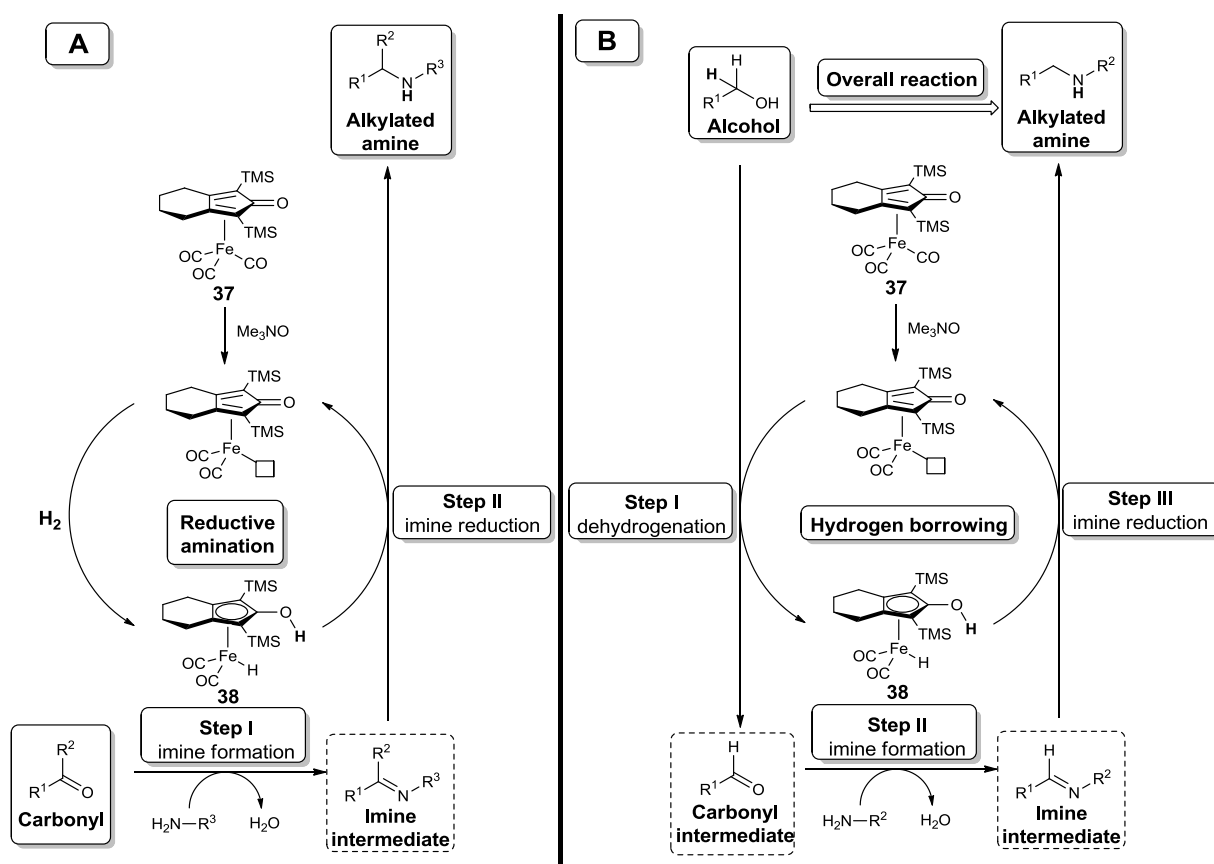


alcohols and amines were coupled with good yields.



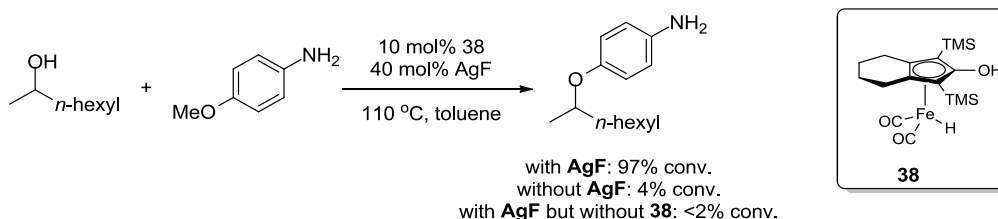
Scheme 2.44 *N*-alkylation of amines with alcohols using complex **37**.

In comparison to reductive amination by Renaud (Scheme 2.43 and Scheme 2.45A), alcohol substrates were acting as a hydrogen source in this process (Scheme 2.45B), making it much easier to perform. Drawback of this hydrogen borrowing process, was its ineffectiveness with other than primary alcohols.



Scheme 2.45 Comparison of: A) reductive amination and B) hydrogen borrowing methodologies to obtain alkylated amines.

Very recently, the hydrogen borrowing strategy was greatly improved by Zhao and co-workers.<sup>113</sup> Using iron hydride **38**, the active form of the pre-catalyst **37**, together with a Lewis acid (finding AgF as the most efficient), they managed to perform amination of not only of primary alcohols, but secondary as well (Scheme 2.46). Mechanism of this transformation proceeded via hydrogen borrowing from alcohol (as so, use of an enantiopure alcohol leads to racemate product). The exact nature of the Lewis acid was not determined. Most likely AgF assisted in the imine formation step and activated it towards reduction by iron hydride **38**.



Scheme 2.46 Lewis acid supported amination of secondary alcohol using catalyst **38**.

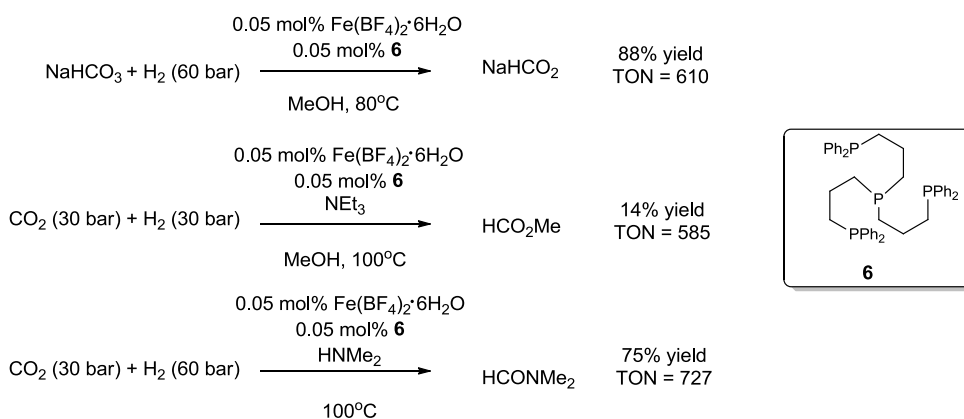
#### 2.4.7.4 Other applications of iron cyclopentadienone complexes

In Paragraph 2.3.5, an alkyne transferhydrogenation with (hydrido)iron complex **10** is described. Also in the following Paragraph 2.5.1, use of (cyclopentadienone)iron complexes **37** and **45** in the hydrogenation of sodium bicarbonate is presented.

## 2.5 Hydrogenation of other carbonyl compounds

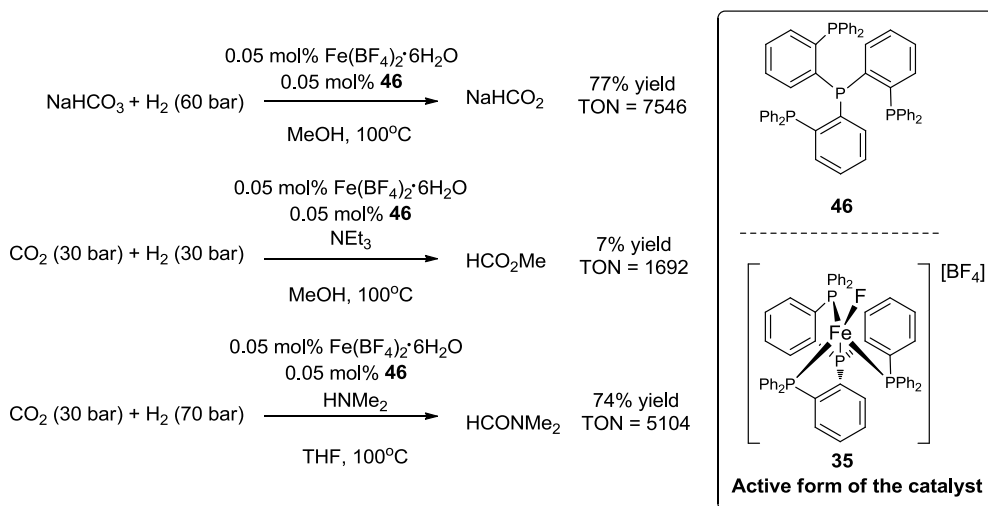
### 2.5.1 Hydrogenation of sodium carbonate and carbon dioxide

The first hydrogenation of carbon dioxide and sodium bicarbonate using an iron catalyst, was described by Beller and co-workers in 2010 (Scheme 2.47).<sup>114</sup> They used catalyst formed *in situ* from  $\text{Fe}(\text{BF}_4)_2 \cdot 6\text{H}_2\text{O}$  and the tetraphos ligand **6** (similar catalytic system was used in later studies in the selective transfer hydrogenation of alkynes to alkenes, Paragraph 2.3.3). Obtained results were very promising for the use of iron catalyst in this new field.

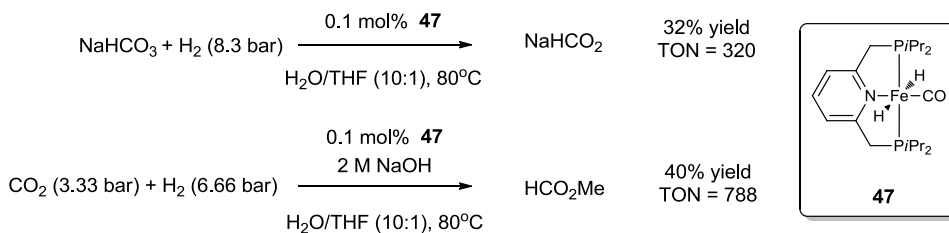


Scheme 2.47 Hydrogenation of sodium bicarbonate and carbon dioxide using tetraphos ligand **6**.

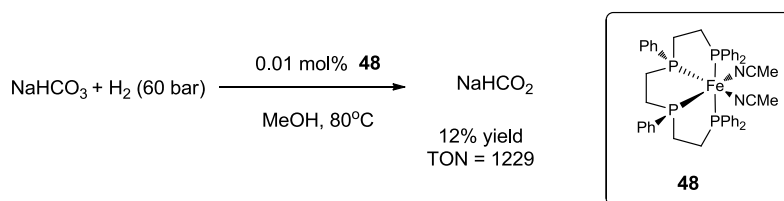
In the follow-up research, they exploited analogous *in situ* formed catalytic system with ligand **46**, used also later (as well-defined **35**) in aldehyde hydrogenation (already described in Paragraph 2.4.5). A huge improvement in the catalyst activity was observed (Scheme 2.48).<sup>115</sup> Sodium bicarbonate was hydrogenated with excellent TONs exceeding 7500. Carbon dioxide was reduced to methyl formate in the presence of methanol and triethylamine (as a base) with TONs reaching almost 1700. When hydrogenation was carried out in the presence of a secondary amine, DMF was obtained with TONs up to 5100.

Scheme 2.48 Hydrogenation of sodium bicarbonate and carbon dioxide using tetraphos ligand **44**.

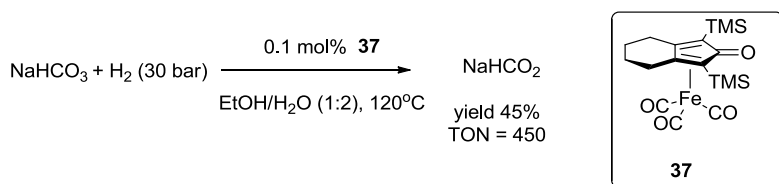
A new iron pincer complex **47** was used by Milstein and co-workers for the hydrogenation of bicarbonate and  $\text{CO}_2$ .<sup>116</sup> Hydrogenation of  $\text{CO}_2$  was effective with TONs up to 788, but the hydrogenation of sodium bicarbonate led only to moderate yields (Scheme 2.49).

Scheme 2.49 Hydrogenation of sodium bicarbonate and carbon dioxide using pincer complex **47**.

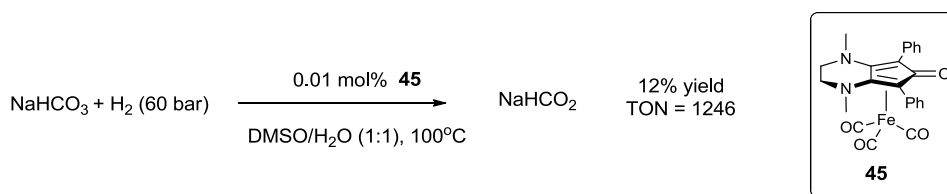
Gonsalvi and co-workers used a tetraphos iron(II) catalyst **48** to hydrogenate sodium bicarbonate with very good TONs up to 1229 (Scheme 2.50).<sup>117</sup>

Scheme 2.50 Hydrogenation of sodium bicarbonate using catalyst **48**.

Recently Zhou and co-workers proved that the (cyclopentadienone)iron complex **37** can be also applied for hydrogenation of sodium bicarbonate with a good TONs up to 450 (Scheme 2.51).<sup>118</sup> Attempts to hydrogenate carbon dioxide were unsuccessful.

Scheme 2.51 Hydrogenation of sodium bicarbonate using iron complex **37**.

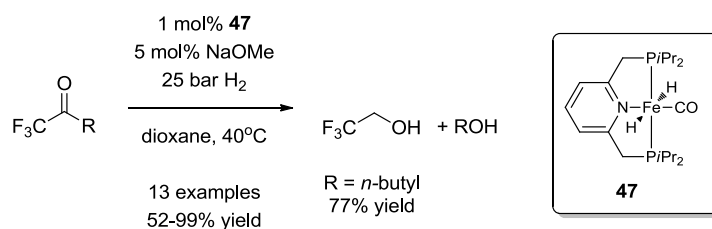
In a recent work of Renaud and co-workers used previously described for reductive amination (see Paragraph 2.4.7.3), a diamino-related iron complex **45** which led to hydrogenations of sodium bicarbonate with TONs up to 1246 (Scheme 2.52).<sup>111</sup>



Scheme 2.52 Hydrogenation of sodium bicarbonate using (cyclopentadienone)iron complex **45**.

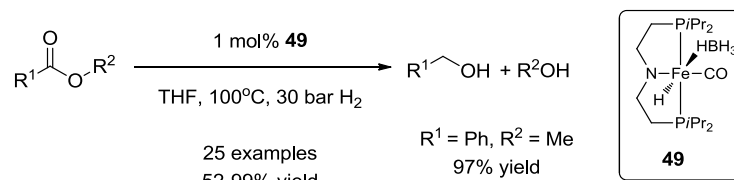
### 2.5.2 Ester hydrogenation

In 2014 Milstein observed that the *P,N,P*-ligand complex **47**, previously reported for the hydrogenation of carbon dioxide, was active in the hydrogenation of esters (Scheme 2.53).<sup>119</sup> This was the first example of iron catalyst able to catalyze this transformation, although it was able to hydrogenate only activated trifluoroacetic esters to trifluoroethanol and as so, it presented no practical applications.



Scheme 2.53 Hydrogenation of activated esters using catalyst **47**.

Iron catalyzed hydrogenation of non-activated esters was described subsequently by groups of Beller<sup>120</sup> and Guan/Fairweather.<sup>121</sup> Inspired by osmium-catalysts for hydrogenation of esters,<sup>122</sup> they found independently that a *P,N,P*-pincer (hydrido-borohydride)iron complex **49** was able to hydrogenate esters under base-free conditions and with excellent yields (Scheme 2.54). Fully saturated alcohols were obtained from corresponding  $\alpha,\beta$ -unsaturated esters. This catalyst was also active with fatty esters under neat conditions.



Scheme 2.54 Hydrogenation of esters using catalyst **49**.

The presented catalysts **47** and **49** clearly opened a new chapter in the ester hydrogenation, proving that it can be accomplished using complexes with a cheap and abundant metal such as iron. Yet, in order for these catalysts to become really suitable for the industrial use, their catalytic activity still has to be improved, and the pincer ligands ideally should be replaced with less expensive and easy-to-handle ones.

## 2.6 Summary of iron catalyzed reductions

In recent years, the iron catalyzed reductions were progressing really fast. In this chapter nearly 40 well-defined catalysts were described, from which the majority was reported just in recent 10 years. Selection of most important contributions and most important iron based catalytic systems is presented on Figure 2.10.

Undoubtedly the biggest contribution to the olefin reduction was brought by Chirik and co-workers (**14**) and up to now there are no examples of more active catalysts for carbon-carbon double bond reduction. Also no asymmetric hydrogenation was reported with any olefin. In alkyne reduction the best results were reported by Beller and co-workers (**6**) and Milstein and co-workers (**8**). Their systems provided good activity and selectivity, but a good catalyst for reduction of alkynes to fully unsaturated alkanes is still missing.

The biggest variety of catalyst is offered for the reductions of C=O bond. Many structurally different catalysts were proved to be effective in this field: *P,N,N,P*-ligands (**22a**), macrocyclic  $P_2N_4$ - (**27**) or  $P_2N_2$ -ligands (**30**), pincer *P,N,P*-ligands (**33**), *P,P,P,P*-ligands (**35**), isonitrile (**36**) or cyclopentadienyl (**38**). Nearly all of the reported ligands are acting as chemically or redox non-innocent, proving that this is the best option to stabilize low valent iron species. In recent year, field of iron catalyzed reductions was expanded to hydrogenation of esters thanks to the *P,N,P*-catalysts **45** and **49**, first developed by Milstein and co-workers and second reported independently by Beller and co-workers and Guan/Fairweather and co-workers.

Still, almost all of the catalysts reported so far, suffer of at least one serious limitation among the following: difficult synthesis, lack of robustness and moderate activity/enantioselectivity. In particular, it should be pointed out that Fe-based reduction catalysts are often difficult to handle due to air- and moisture-sensitivity. As a consequence, the usage of a glovebox is commonplace for synthesis and manipulation of many iron catalysts, and in some cases even for the setup of hydrogenation tests.<sup>107</sup> These drawbacks need to be overcome in order for iron catalysis to become of practical utility for the industrial manufacturing of fine chemicals.

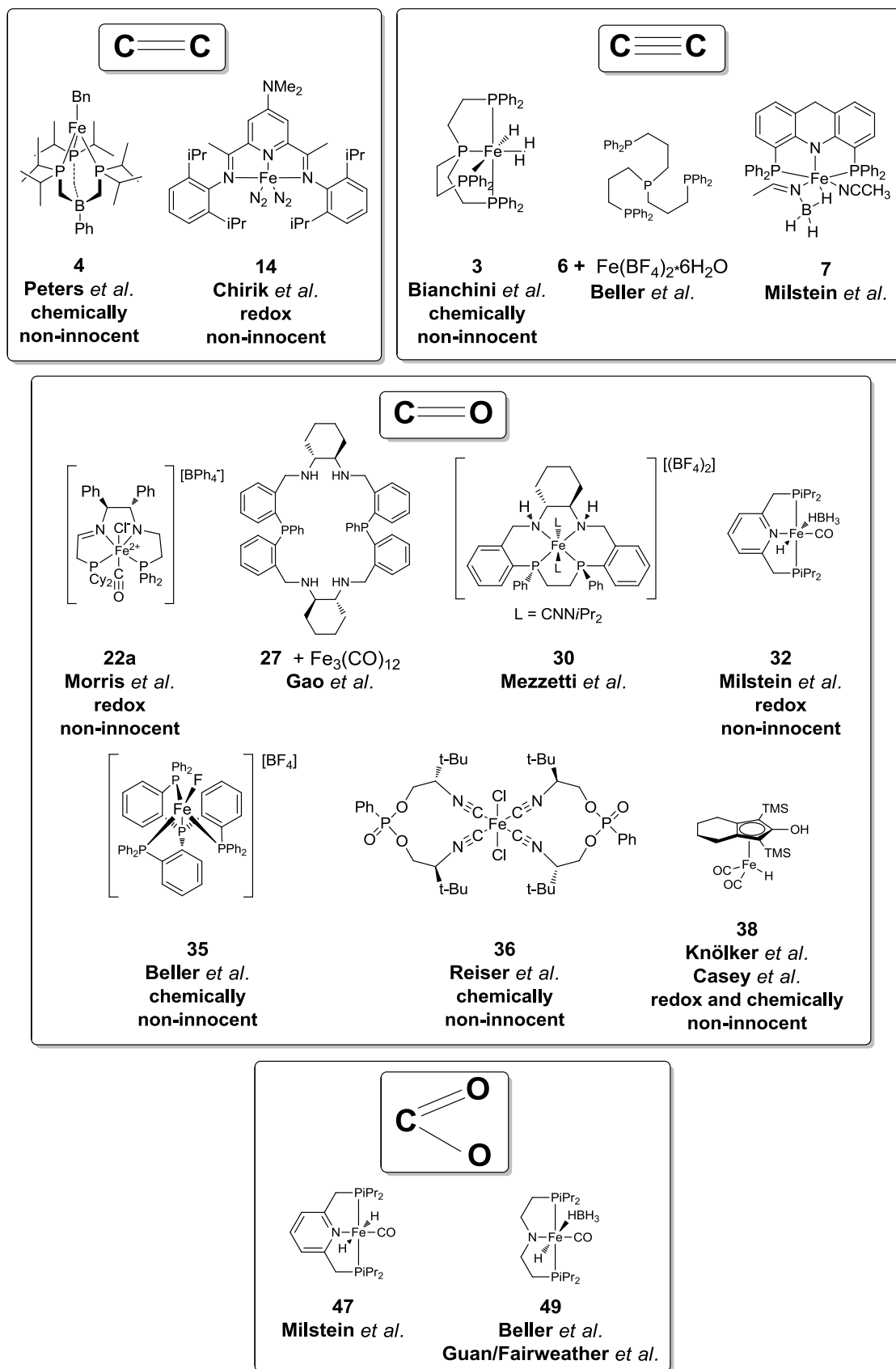


Figure 2.10 Selection of the most important and effective iron based systems for reductions of olefins, alkynes, ketones and esters.





## 3 Iron complexes with *N,N,N,N*-ligands

### 3.1 Tetradentate *N*-ligands to stabilise Fe(II) metal center

Our initial studies, particularly focused attention on Fe(II) complexes, as the oxidation state +2:

- is the most stable oxidation state of iron under moderately reducing conditions;
- is compatible with the presence of the coordinated hydride required for some kinds of hydrogenation mechanisms;
- in principle, can allow two-electron redox processes with  $\text{Fe}^0/\text{Fe}^{\text{II}}$  or  $\text{Fe}^{\text{II}}/\text{Fe}^{\text{IV}}$  interplay as well as mechanisms with participation of “non-innocent” ligands.

On the other hand, Fe(II) is very prone to oxidation to Fe(III), and therefore it usually needs to be handled under extra-dry and oxygen-free conditions. The best way to stabilize the reactive Fe(II) metal centre is the use of polydentate ligands, which provide the desired stabilization by means of kinetic (steric) and thermodynamic (entropic) effects. In particular tetradentate nitrogen-ligands were appealing, since:

- N*-donors are expected to efficiently stabilize the relatively hard Fe(II);
- compared to *P*-ligands, which are also extensively used in iron catalysis, they are easier to prepare and more stable.

In fact, *P*-ligands are themselves often prone to oxidation, especially in the case of electron-rich phosphines. Indeed, tetradentate *N*-ligands considerably stabilize the  $\text{Fe}^{2+}$  cation, forming robust Fe(II) complexes having two coordination sites available for catalysis (Figure 3.1).<sup>123</sup> According to the geometry of the chelating ligand, the two ancillary ligands X and Y may occupy cis- or trans- coordination sites.

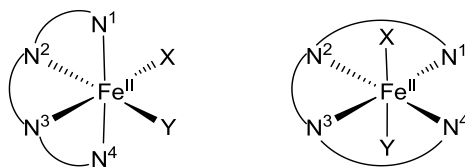


Figure 3.1 Octahedral Fe(II)-complexes featuring *N,N,N,N*-ligands.

### 3.2 Iron complexes for C-H oxidation

In recent decades, mononuclear tetradentate Fe(II) complexes for C-H oxidation were studied very carefully.<sup>124</sup> Besides many metalloporphyrin catalysts, which are mimicking the reactivity of cytochrome P450, a variety of other tetradentate ligands were developed (Figure 3.2).

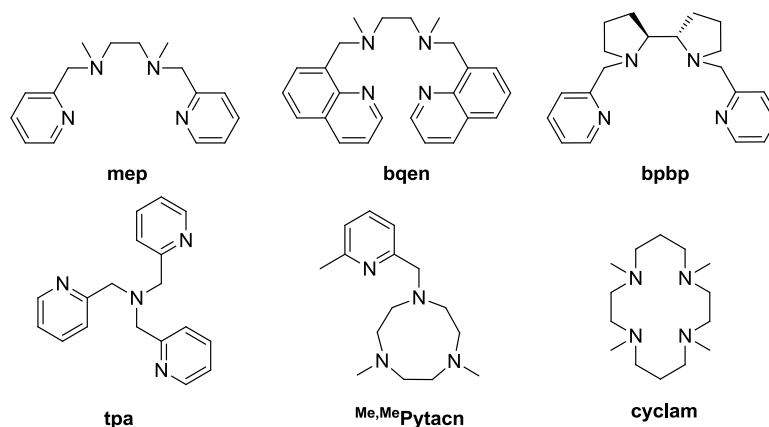
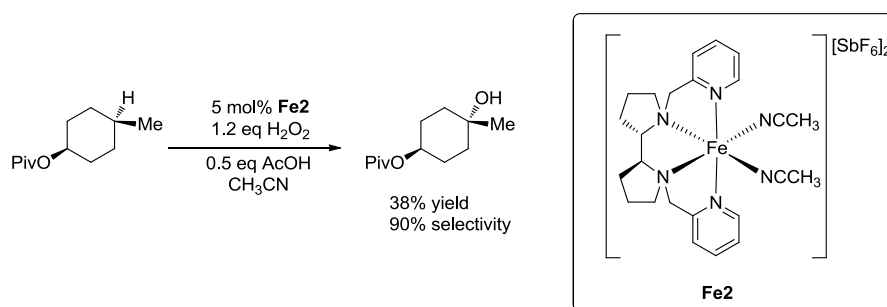


Figure 3.2 Examples of relevant tetradentate *N,N,N,N*-ligands used to prepare mononuclear iron(II) complexes for alkane oxidations.<sup>125</sup>

Compared to porphyrins, tetradentate *N,N,N,N*-ligands usually require multi-step synthesis and offer lower stability to harsh oxidation conditions, but still, they are more appealing for the industry as cheaper and easier to prepare on a large scale. To be stable and useful in oxidation chemistry, these strong field tetradentate ligands have to be rigid and low reactive. As these principle requirements were in line with our assumption to use tetradentate *N*-ligands to stabilize Fe(II) for hydrogenation purposes, we decided to take inspiration directly from them.

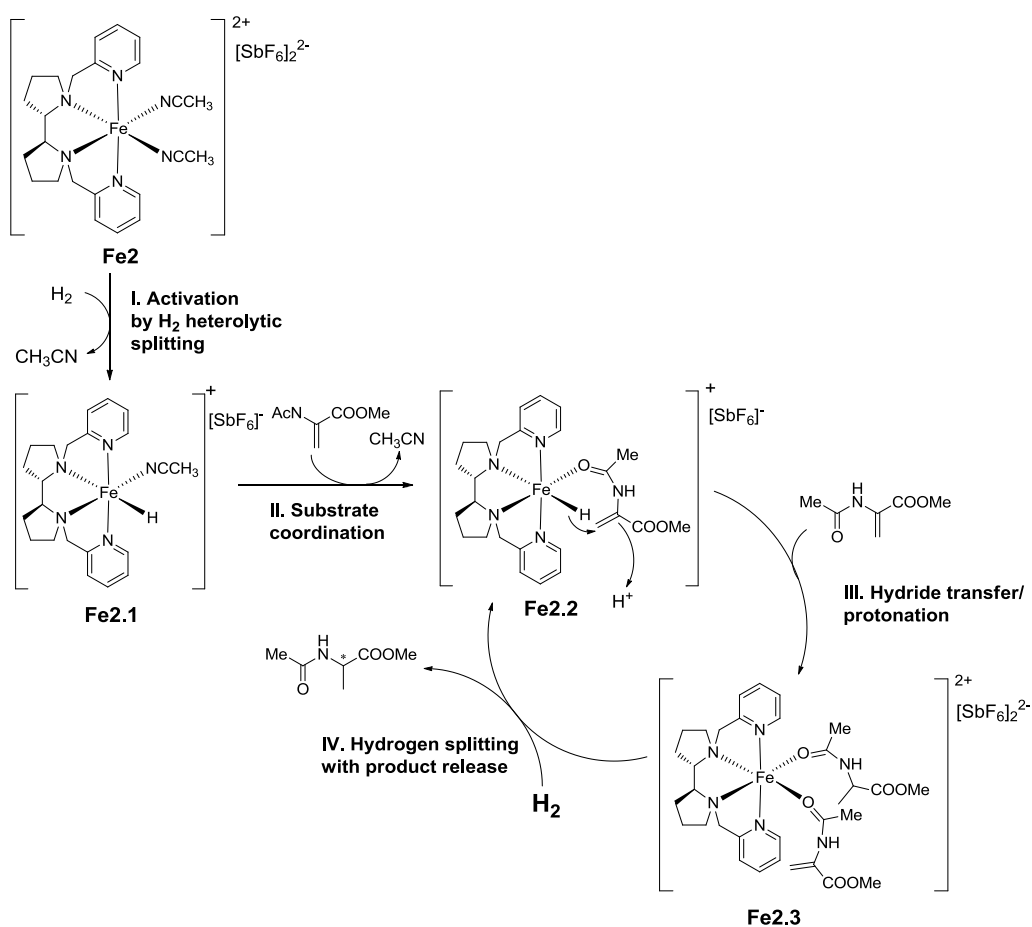
### 3.3 Chiral tetradentate *N*-ligand complexes

As a starting point for the development of new iron catalysts, the chiral octahedral Fe(II) complex **Fe2** (Scheme 3.1) developed by White and Chen<sup>126</sup> was chosen by virtue of its stability to air and moisture, easy preparation and modular structure, facilitating possible modifications. X-ray crystallographic analysis revealed that the chiral bipyrrolidine scaffold functionalized with two pyridine rings, constitutes a tetradentate *N*-ligand which leaves two *cis* coordination sites for the iron centre.<sup>127</sup>



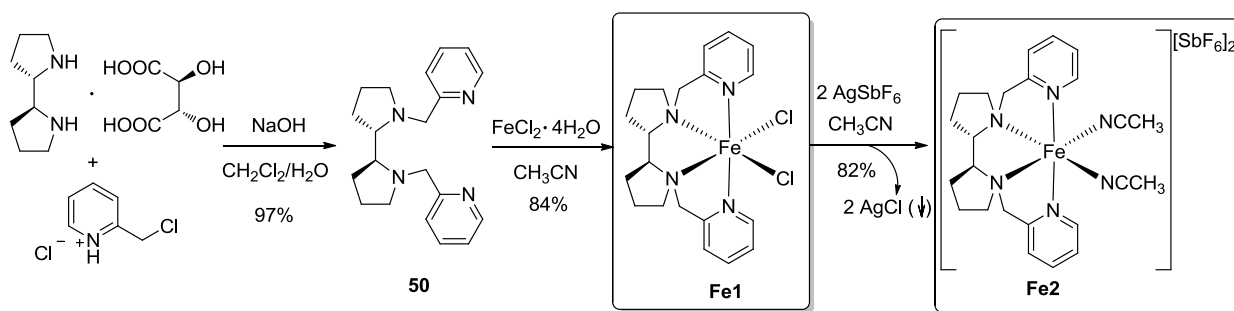
Scheme 3.1 Aliphatic C-H oxidation by catalyst **Fe2**.

Whereas White and co-workers applied **Fe2** for the oxidation of aliphatic C-H bonds, our aim was to test it in the enantioselective hydrogenation of activated olefins (i.e. possessing a donor atom close to the C=C bond). In this mechanistic speculation, iron would promote the reduction, while retaining its +2 oxidation state (Scheme 3.2). The critical step would be the formation of the Fe(II) hydride complex **Fe2.1** by heterolytic splitting of H<sub>2</sub> (step I). The substrate would be then expected to coordinate via the lonely electron pair on its donor atom (**Fe2.2**), rather than via the π-orbital of the C=C bond, since Fe(II) prefers relatively hard ligands. At this point, hydride transfer to the terminal olefinic carbon atom and protonation of the internal one were supposed to take place (**Fe2.3**). Eventually, H<sub>2</sub> splitting with concomitant release of the reduced product would close the catalytic cycle.

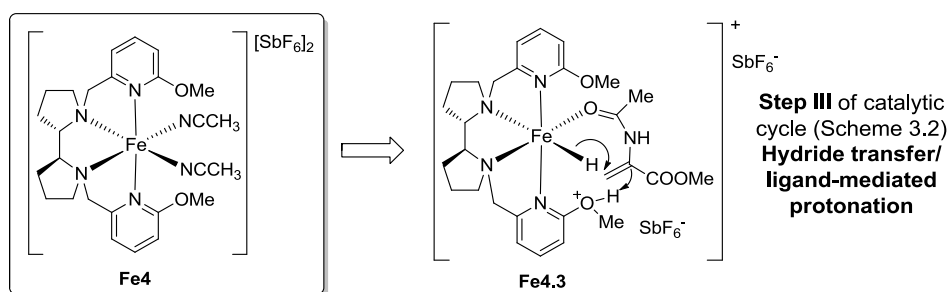


Scheme 3.2 Proposed catalytic cycle for olefin reduction promoted by complex **Fe2**.

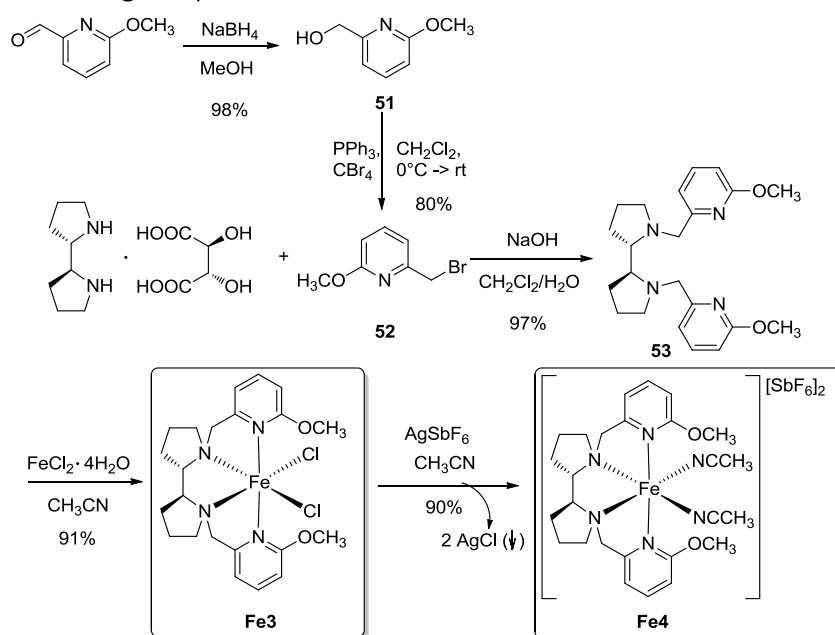
The tetradentate ligand **50** was synthesized via S<sub>N</sub>2 reaction between (*S,S*)-2,2'-bipyrrolidine and 2-picolyl chloride in a biphasic solvent system (Scheme 3.3). Subsequent reaction of **50** with iron(II) chloride tetrahydrate in acetonitrile gave the bench-stable neutral complex **Fe1**. The latter was then treated with silver hexafluoroantimonate to remove the chloride ligands by precipitation of AgCl, obtaining the dicationic complex **Fe2**.

Scheme 3.3 Synthesis of complexes **Fe1** and **Fe2**.

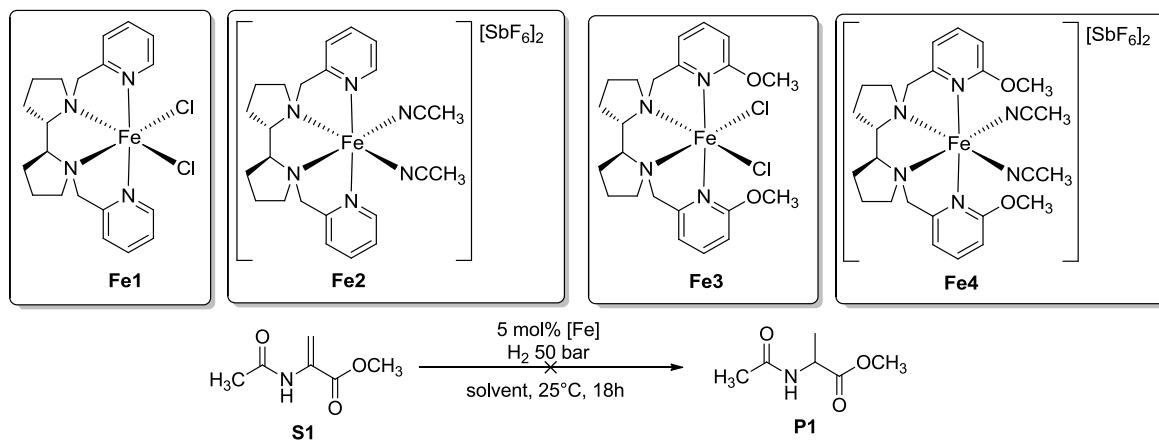
On the basis of the mechanistic hypothesis shown at (Scheme 3.2), it was decided to endow the ligand with a functional group capable of mediating the proton transfer (Figure 3.3). Our plan was to introduce methoxy groups in the *ortho* position of the pyridine rings of **Fe2**.

Figure 3.3 Modified complex **Fe4** bearing two methoxy groups in the *ortho* position of the pyridine rings.

The straightforward synthetic pathway to complex **Fe2** was easily modified to prepare complex **Fe4** (Scheme 3.4). 6-methoxy-2-picolylbromide **52** was obtained by Appel reaction from 6-methoxypicolinalcohol **51**, synthesized by reducing 6-methoxypicolinaldehyde. Following previously described steps, complexes **Fe3** and **Fe4** was obtained with a good yield.

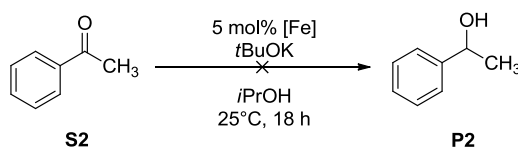
Scheme 3.4 Synthesis of complexes **Fe3** and **Fe4**.

All four iron complexes (**Fe1-4**) were tested in the hydrogenation of the benchmark substrate methyl 2-acetamidoacrylate (**S1**) under the conditions reported in Scheme 3.5.

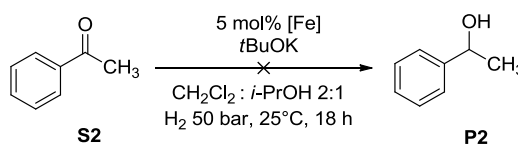


Scheme 3.5 Attempts to hydrogenate **S1** using complexes **Fe1-4**.

Reactions were performed in toluene, acetonitrile, dichloromethane, methanol and tetrahydrofuran. No sign of conversion was observed in any of them. Neither prolonged reaction times nor higher temperatures (50 °C) led to any conversion. Complexes were tested also in the transfer (Scheme 3.6) and pressure (Scheme 3.7) hydrogenations of acetophenone (**S2**), but they resulted inactive as well.

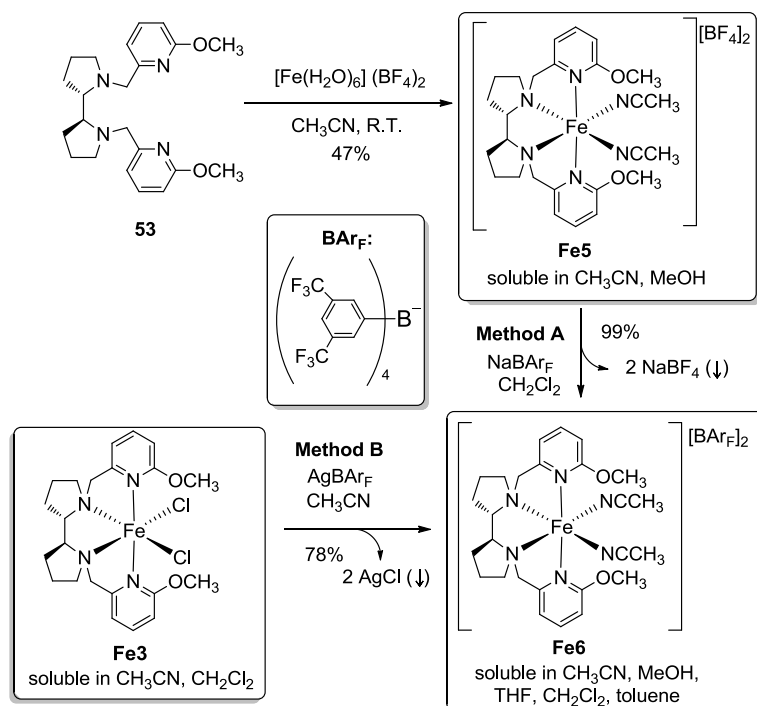


Scheme 3.6 Attempts to transfer hydrogenate **S2** using complexes **Fe1-4**.



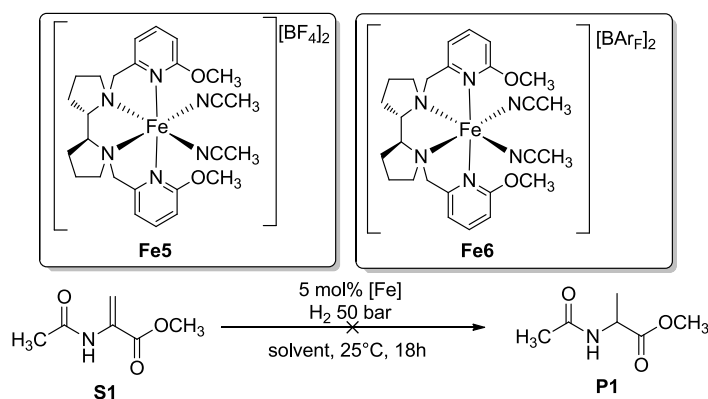
Scheme 3.7 Attempts to hydrogenate **S2** using complexes **Fe1-4**.

In order to rule out the possibility that the observed lack of reactivity was derived from the scarce solubility of the complexes **Fe1-4** in some of the solvents used for the preliminary tests, new complexes with more lipophilic counter ions were prepared (Scheme 3.8). Instead of hexafluoroantimonate, the newly synthesized complexes **Fe5** and **Fe6** beared, respectively, tetrafluoroborate and tetrakis[3,5-bis(trifluoromethyl)phenyl]-borate (shortly indicated as  $\text{BAr}_f$ ).<sup>128</sup> Such highly lipophilic counterion greatly improves the solubility of organometallic complexes in several organic solvents, including nonpolar ones such as toluene.

Scheme 3.8 Synthesis of more soluble complexes **Fe5** and **Fe6**.

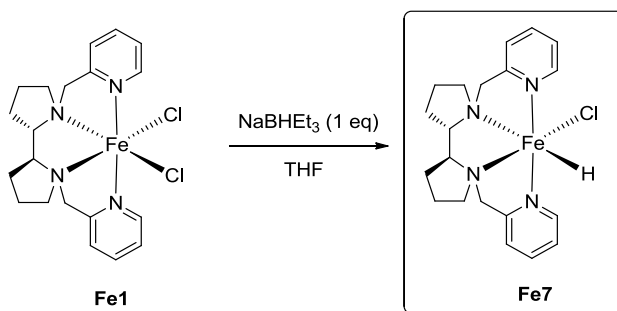
Complex **Fe5** was prepared by combining ligand **54** with the iron(II) tetrafluoroborate hexahydrate, whereas synthesis of complex **Fe6** was attempted according to two different methods. Method A involved treatment of **Fe5** with  $\text{NaBAR}_F$  in DCM which caused the precipitation of sodium tetrafluoroborate, while the desired complex remained in solution. In method B, addition of freshly prepared  $\text{AgBAR}_F$  to a solution of the dichloride complex **Fe3** in ACN caused  $\text{AgCl}$  precipitation while complex **Fe6** remained in solution. In this method a stoichiometric amount of  $\text{NaBAR}_F$  did not succeed in removing both chloride ligands because of the better solubility of  $\text{NaCl}$  in ACN compared to  $\text{AgCl}$ . Thus, for the method B to be effective in ACN, the use of pure  $\text{AgBAR}_F$  salt instead of  $\text{NaBAR}_F$  was crucial.

Once synthesized, complexes **Fe5** and **Fe6** were tested in the hydrogenation of methyl 2-acetamidoacrylate (Scheme 3.9) using solvents in which catalyst **Fe4** was insoluble (toluene, THF, DCM), but still no conversion was observed.

Scheme 3.9 Attempts to hydrogenate **S1** using complexes **Fe5-6**.

The negative results obtained with this family of complexes clearly indicated that the hypothetic catalytic cycle (Scheme 3.2) did not take place. It is likely that, in the first activation step, the heterolytic splitting of the hydrogen molecule does not occur and no Fe-H species forms under the hydrogenation conditions.

However, following another approach,<sup>129</sup> it was possible to install a hydride ligand on *N,N,N,N*-ligand complex **Fe1** (Scheme 3.10). Unfortunately, the obtained deep purple complex **Fe7** turned out to be very air-sensitive and unstable, and shortly become brown after minimal contact with air and as so, it was not possible to use it in catalytic tests.



Scheme 3.10 Synthesis of iron hydride complex **Fe7**.

### 3.4 Achiral tetradentate *N*-ligand complexes

Another family of *N,N,N,N*-ligand complexes, inspired by *P,N,N,P*-ligands developed by Morris and co-workers<sup>71</sup> were designed specifically to be employed in ketone reduction (Figure 3.4). The simple achiral complexes **Fe8-9** (Scheme 3.11) were expected to work in a similar fashion, according to an outer-sphere mechanism (with no substrate coordination to the metal centre) already described by Noyori for Ru(II).<sup>77</sup> This mechanism involves the reduction of C=O double bond via transfer of a hydride from the metal centre and of a proton from a -NH group on the ligand. As such, it requires the presence of at least one primary or secondary amino group coordinated to the metal. This functional group can also be generated *in situ* by reduction of an imine, as in the case of Morris' complexes (see Paragraph 2.4.2 and Scheme 2.15 for a detailed discussion of the catalytic cycle).

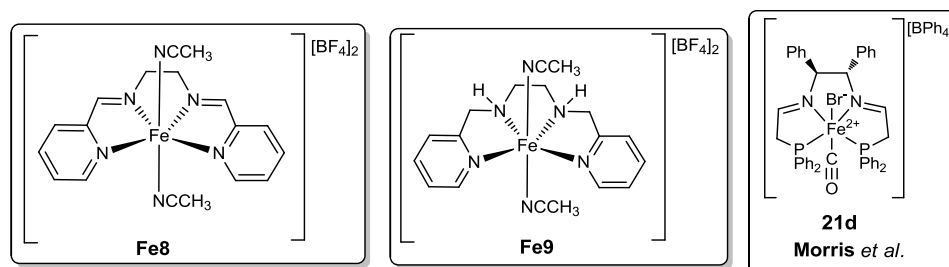
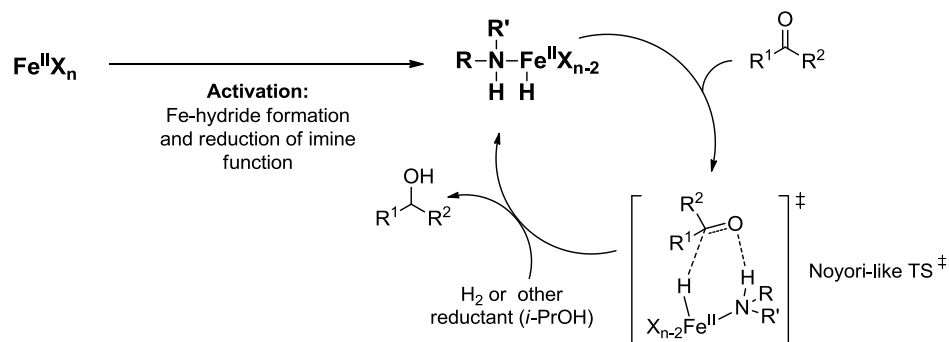
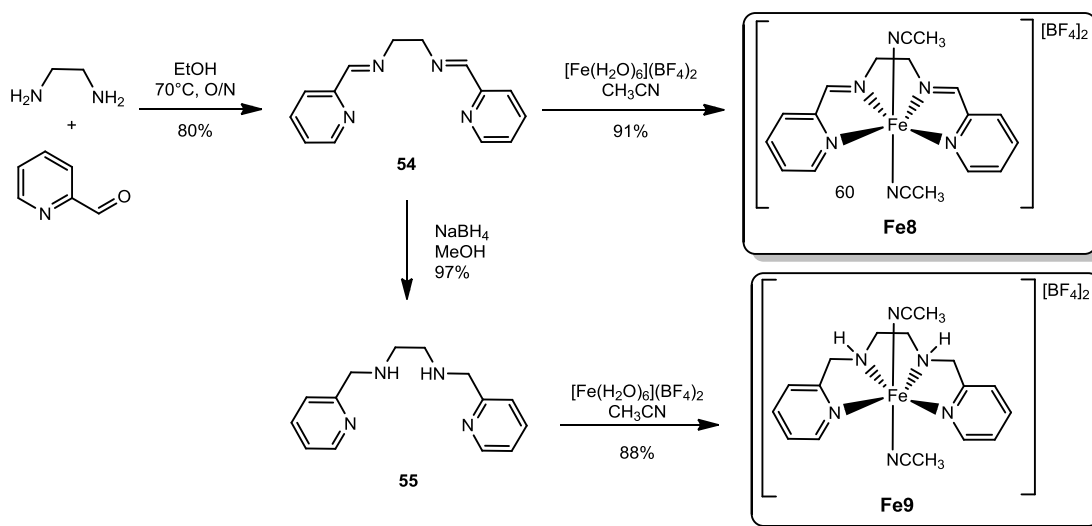


Figure 3.4 New achiral *N,N,N,N*-ligand complexes inspired by complex **21d**.



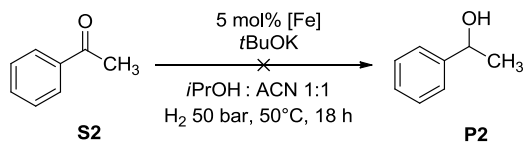
Scheme 3.11 Achiral *N,N,N,N*-ligand complexes and proposed Noyori-like catalytic cycle for C=O hydrogenation and transfer hydrogenation

The synthesis of complexes **Fe8** and **Fe9**, did not pose any particular problem (Scheme 3.12). The diimine ligand **54** was prepared by condensation between ethylenediamine and 2-pyridinecarboxaldehyde and then reduced with  $\text{NaBH}_4$  to give the saturated analogue **55**. Both **54** and **55** were treated with iron tetrafluoroborate hexahydrate in acetonitrile, yielding complexes **Fe8** and **Fe9** respectively.



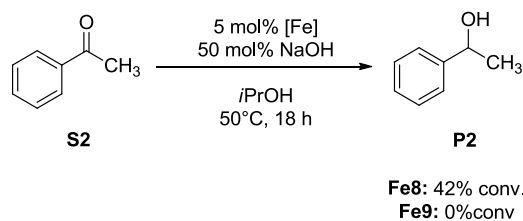
Scheme 3.12 Synthesis of achiral *N,N,N,N*-ligand complexes **Fe8-9**.

Complexes **Fe8** and **Fe9** were tested as catalysts both in the pressure (Scheme 3.13) and transfer hydrogenation (Scheme 3.14) of acetophenone.

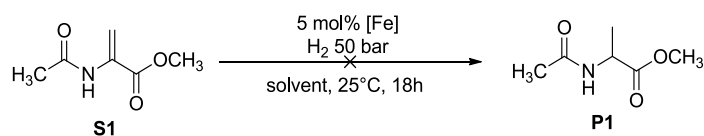


Scheme 3.13 Attempts to hydrogenate **S2** using complexes **Fe8-9**.



Scheme 3.14 Attempts to transfer hydrogenate **S2** using complexes **Fe8-9**.

These *N*-based Morris-like complexes, unlike the original *P,N,N,P*-ones, showed no catalytic activity for the pressure hydrogenation of acetophenone. Under transfer hydrogenation conditions only diimine complex **Fe8** achieved 42% conversion of **S2**. Complexes **Fe8-9** were also inactive in olefin hydrogenation of **S1** (Scheme 3.15).

Scheme 3.15 Attempts to hydrogenate **S1** using complexes **Fe8-9**.

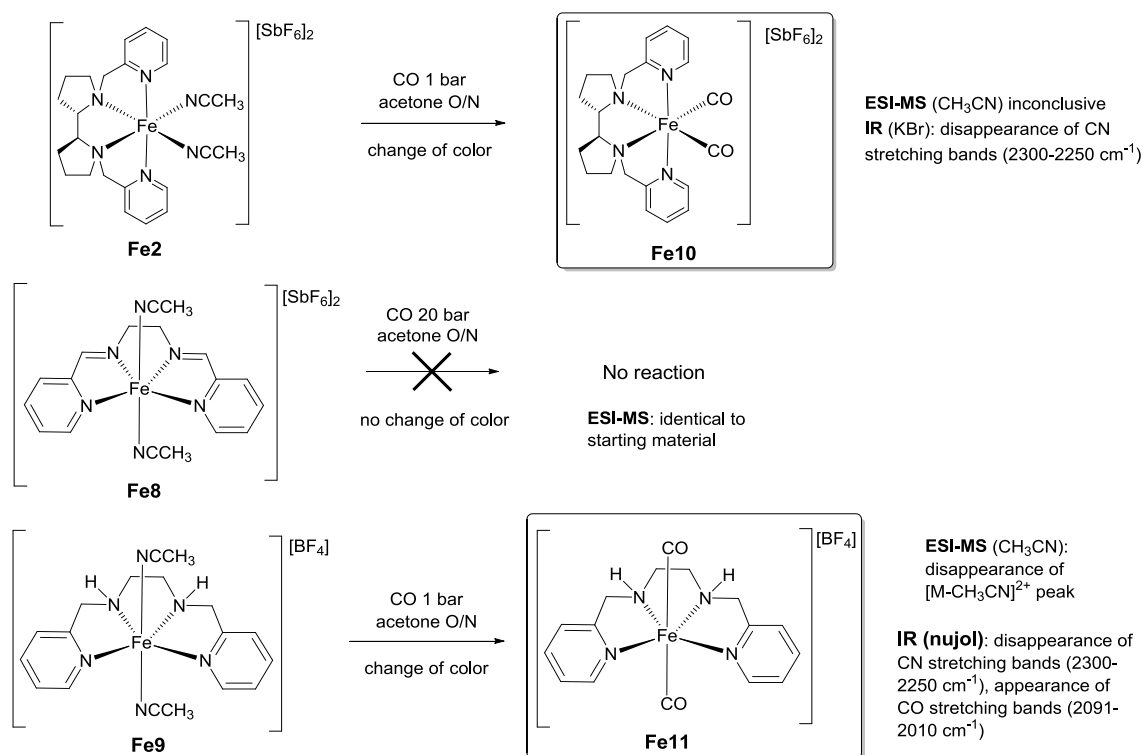
### 3.5 Introduction of CO ligands on tetradentate *N*-ligand complexes

In the attempt to improve the catalytic activity of these two families of tetradentate *N*-ligand complexes (**Fe1-9**), it was decided to endow them with a CO ligand. The latter is present as an ancillary ligand in several of the catalysts for hydrogenation of ketones, aldehydes and imines.

Carbon monoxide acts as  $\sigma$ -donor through its HOMO, which is mainly localized on the carbon atom and can thus be roughly identified with the lone pair present on C. The CO ligand is also a strong  $\pi$ -acceptor: in the so-called back-donation process, electron density is released from filled d-orbitals of electron-rich, low oxidation state metals (such as  $\text{Fe}^0$  and  $\text{Fe}^{\text{II}}$ ) into the empty  $\pi^*$  molecular orbital of CO (LUMO). Owing to this stabilizing capability, the presence of a CO ligand may be beneficial to catalytic cycles where  $\text{Fe}(0)$ - and/or  $\text{Fe}(\text{II})$ -species are involved.

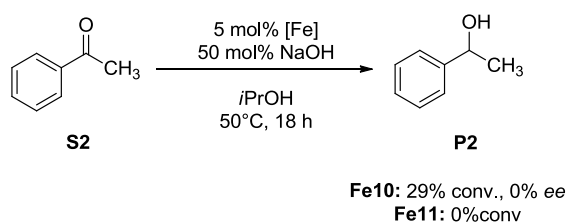
As shown in Scheme 3.16, complexes **Fe2**, **Fe8** and **Fe9** were treated with gaseous carbon monoxide, in order to exchange the coordinated acetonitrile with CO. Despite inconclusive ESI-MS for **Fe10**, a disappearance of CN stretching bands ( $2300\text{--}2250\text{ cm}^{-1}$ ) was observed and could mean successful CO insertion. No reaction was observed with **Fe8** (even with 20 bar of CO). Complex **Fe11**, as confirmed by ESI-MS and IR, was successfully obtained.

## Chapter 3



Scheme 3.16 Introduction of CO ligands to N,N,N,N-ligand complexes.

With the newly synthesized complexes **Fe10** and **Fe11**, the reduction of C=C and C=O double bonds on the benchmark substrates **S1** and **S2** was investigated. Both of them appeared to be inactive in hydrogenation (using conditions from Scheme 3.13 and Scheme 3.15), whereas **Fe10** gave 29% conversion in transfer hydrogenation of **S2** (with no *ee* - Scheme 3.17). Although this result was not groundbreaking, it proved importance of strong  $\pi$ -acceptor ligands for iron catalysts, as parent complex **Fe2** was not active at all in any of the investigated transformations.



Scheme 3.17 Attempts to transfer hydrogenate **S2** using complexes **Fe10-11**.

### 3.6 Concluding remarks

The negative results obtained with synthesized *N,N,N,N*-ligand complexes in the hydrogenation of C=C and C=O double bonds indicate that *N*-based tetradentate ligands (Figure 3.5), despite being an effective option for stabilizing the Fe(II) metal centre, are not particularly good candidates for promoting Fe-catalyzed reductions. In addition to the *N*-based tetradentate ligand, they require strong  $\pi$ -acceptors like CO, to stabilize the low valent iron species produced in the course of the reaction.



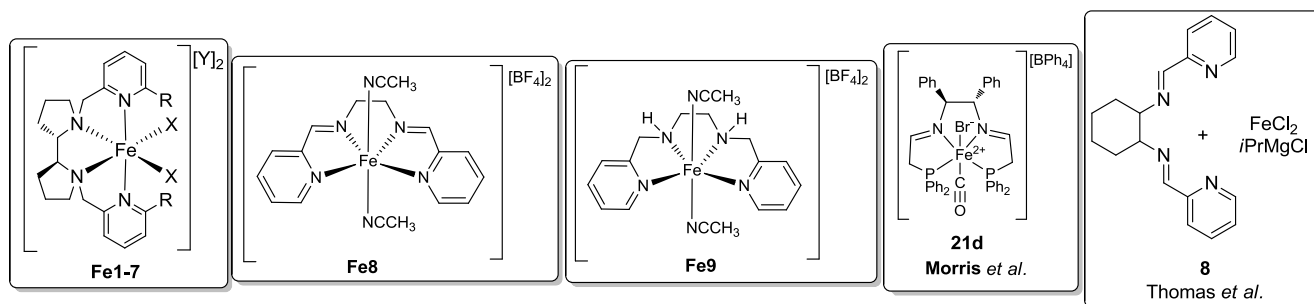


Figure 3.5 Tetradentate *N*-ligands complexes synthesized in this work of thesis in comparison with Morris' *P,N,N,P*-complex **21d** and Thomas' catalytic system based on ligand **8**.

The structural analogy of the achiral *N,N,N,N*-complexes **Fe8** and **Fe9** with Morris' *P,N,N,P*-complex **21** on one side and the striking difference in terms of catalytic activity on the other, suggest that the stereoelectronic nature of *N*- and *P*-ligands is a decisive factor. The two more relevant stereoelectronic differences between *N*-ligands and phosphines (which are extensively used in Fe-catalysed reductions) concern the hardness and the capability of accepting  $\pi$ -backdonation from metals in low oxidation states. Compared to phosphines, amines are harder, as the small, electronegative nitrogen atom is less easily polarizable than phosphorus. Moreover, *N*-ligands are weaker  $\pi$ -acceptors. A possible solution to this problem was later (i.e., after we gave up our tests with this family of catalysts) proposed by Thomas and co-workers, as they used Grignard compounds to activate *in situ* formed iron(II) complex from ligand **8**.<sup>55</sup> As reported in Paragraph 2.3.4, they managed to hydrogenate variety of olefins with a catalytic system generated *in situ*. Our efforts to form a well-defined hydride catalyst from complex **Fe7** (Scheme 3.10) were unsuccessful, as we did not have access to a glovebox, necessary to handle such sensitive compounds.

In conclusion, it appears that the presence of strong  $\pi$ -acceptor ligands is crucial for the relatively electron-rich Fe(0)- and/or Fe(II)-species to be catalytically active in reduction mechanisms. This inference is supported by the fact that almost all of the iron complexes that catalyze the hydrogenation of multiple C-X bonds (X = C, O) possess at least two *P*-ligands. The exceptions are represented by catalysts **14**, **36** and **38** (Figure 2.10), which work according to mechanisms where the chelating ligand acts as a “non-innocent” ligand, rather than as a simple bystander. Furthermore, it is noteworthy that complexes **38** and **36**, despite having no *P*-ligands, bear other strong  $\pi$ -acceptor ligands, namely CO and isonitrile.

### 3.7 Experimental section

#### General remarks

All reactions were carried out in flame-dried glassware with magnetic stirring under nitrogen atmosphere, unless otherwise stated. Synthesis of complexes was performed under argon using standard Schlenk-techniques.

The solvents for reactions were distilled over the following drying agents and transferred under nitrogen: CH<sub>2</sub>Cl<sub>2</sub> (CaH<sub>2</sub>), MeOH (CaH<sub>2</sub>), CH<sub>3</sub>CN (CaH<sub>2</sub>), THF (Na), dioxane (Na), toluene (Na), hexane (Na), Et<sub>3</sub>N (CaH<sub>2</sub>). Acetophenone and *i*-PrOH were distilled on CaH<sub>2</sub> (a small amount of PPh<sub>3</sub> was added when distilling isopropanol) and stored over molecular sieves. Et<sub>2</sub>O and DMF were purchased in bottles with crown cap, over molecular sieves, and stored under nitrogen. The commercially available starting products [3,5-bis(trifluoromethyl)bromobenzene, (*S,S*)-2,2'-bipyrrrolidine D-tartrate trihydrate, 6-methoxy-2-pyridinecarboxaldehyde, 2-pyridine carboxaldehyde, 2,2'-bis(bromomethyl)-1,1'-biphenyl, 2-fluoronitrobenzene, (*R*)-binaphthol] were used as received.

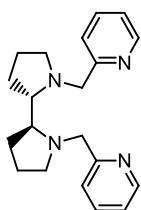
The reactions were monitored by analytical thin-layer chromatography (TLC) using silica gel 60 F<sub>254</sub> pre-coated glass plates (0.25 mm thickness). Visualisation was accomplished by irradiation with a UV lamp and/or staining with a potassium permanganate alkaline solution, a ninydrine solution or a ceric ammonium molybdate solution. Flash column chromatography was performed using silica gel (60 Å, particle size 40-64 μm) as stationary phase, following the procedure by Still and co-workers.<sup>130</sup> Gas chromatography was performed by a GC instrument equipped with a flame ionization detector, using the chiral capillary column MEGADEX DACTBSβ, diacetyl-*t*-butylsilyl-β-cyclodextrin.

Proton NMR spectra were recorded on a spectrometer operating at 400.13 MHz. Proton chemical shifts are reported in ppm (δ) relative to tetramethylsilane (TMS) with the solvent resonance employed as the internal standard (CDCl<sub>3</sub>, δ = 7.26 ppm; CD<sub>2</sub>Cl<sub>2</sub>, δ = 5.32 ppm; (CD<sub>3</sub>)<sub>2</sub>SO, δ = 2.50 ppm; CD<sub>3</sub>OD, δ = 3.33 ppm; CD<sub>3</sub>CN, δ = 1.94 ppm). The following abbreviations are used to describe spin multiplicity: s = singlet, d = doublet, t = triplet, q = quartet, m = multiplet, br = broad signal. The coupling constant values are given in Hz. <sup>13</sup>C-NMR spectra were recorded on a 400 MHz spectrometer operating at 100.56 MHz, with complete proton decoupling. Carbon chemical shifts are reported in ppm (δ) relative to TMS with the respective solvent resonance as the internal standard (CDCl<sub>3</sub>, δ = 77.23 ppm; CD<sub>2</sub>Cl<sub>2</sub>, δ = 54.00 ppm; (CD<sub>3</sub>)<sub>2</sub>SO, δ = 39.51 ppm; CD<sub>3</sub>OD, δ = 49.05; CD<sub>3</sub>CN, δ = 118.26 ppm).

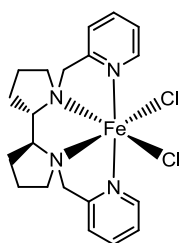
High resolution mass spectra (HRMS) were performed on a Fourier Transform Ion Cyclotron Resonance (FT-ICR) Mass Spectrometer APEX II & Xmass software (Bruker Daltonics) – 4.7 T Magnet (Magnex) equipped with ESI source, available at CIGA (Centro Interdipartimentale Grandi Apparecchiature) c/o Università degli Studi di Milano. Low resolution mass spectra (MS) were acquired either on a Thermo-Finnigan LCQ Advantage mass spectrometer (ESI ion source) or on a VG Autospec M246 spectrometer (FAB ion source).

Elemental analyses were performed on a Perkin Elmer Series II CHNS/O Analyzer 2000.

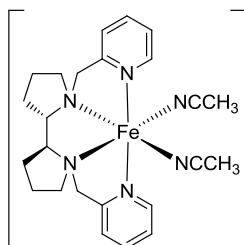
Infrared spectra were recorded on a standard FT/IR spectrometer.

**(2*S*,2'*S*')-1,1'-Bis(pyridin-2-ylmethyl)-2,2'-bipyrrolidine<sup>126</sup> (*S,S*-PDP) **50****

NaOH (0.74 g, 18.4 mmol, 6.4 eq) and 2-(chloromethyl)pyridine hydrochloride (1.04 g, 6.3 mmol, 2.2 eq) were added in sequence to a stirred suspension of (*S,S*)-2,2'-bipyrrolidine D-tartrate trihydrate (1.00 g, 2.87 mmol, 1 eq) in 12 mL H<sub>2</sub>O/CH<sub>2</sub>Cl<sub>2</sub> 1:1. The obtained mixture was stirred overnight at RT, then diluted with 1M NaOH and extracted with CH<sub>2</sub>Cl<sub>2</sub> (3x). The combined organic phases were dried with Na<sub>2</sub>SO<sub>4</sub> and concentrated in vacuo to give a sticky oil. The crude was purified by FCC (CH<sub>2</sub>Cl<sub>2</sub>/MeOH/aqueous NH<sub>3</sub> 33% 95:5:2). The collected fractions were combined, diluted with CH<sub>2</sub>Cl<sub>2</sub>, washed with 1M NaOH (2x) and dried with Na<sub>2</sub>SO<sub>4</sub>. Evaporation of solvents afforded the product as a colorless oil in 97% yield. <sup>1</sup>H NMR (400 MHz, CDCl<sub>3</sub>): δ 8.52 (d, *J* = 4.2 Hz, 2H), δ 7.61 (td, *J* = 7.6, 1.7 Hz, 2H), δ 7.42 (d, *J* = 7.8 Hz, 2H), δ 7.12 (dd, *J* = 7.0, 5.2 Hz, 2H), δ 4.21 (d, *J* = 14.0 Hz, 2H), δ 3.53 (d, *J* = 14.4 Hz, 2H), δ 3.02 (m, 2H), δ 2.83 (m, 2H), δ 2.26 (q, *J* = 8.6 Hz, 2H), δ 1.91-1.68 (m, 8H).

**[FeCl<sub>2</sub>(*S,S*-PDP)]<sup>126</sup> **Fe1****

Under Ar, FeCl<sub>2</sub>·4H<sub>2</sub>O (554 mg, 2.79 mmol, 1 eq) was added to a stirred solution of ligand **50** (899 mg, 2.79 mmol, 1 eq) in 16 mL CH<sub>3</sub>CN. Upon addition, immediate precipitation of a dark orange solid was observed. The reaction mixture was stirred overnight at RT, then Et<sub>2</sub>O was added to aid precipitation. The solvent was decanted off via syringe. The precipitate was washed two more times with Et<sub>2</sub>O, until the decanted solvent was colorless. The orange solid was dried in a tarred Schlenk tube under N<sub>2</sub> stream for 2 hours, then under high vacuum. Yield: 84%. ESI-MS in CH<sub>3</sub>CN: [M-Cl]<sup>+</sup> *m/z* 413.3. Elemental analysis: calculated C 53,48%, H 5,83%, N 12,47%; found C 53,14%, H 5,95%, N 12,45%.

**[Fe(CH<sub>3</sub>CN)<sub>2</sub>(*S,S*-PDP)](SbF<sub>6</sub>)<sup>126</sup> **Fe2****

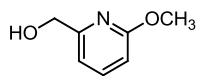
Under Ar, silver hexafluoroantimonate (98%, 937 mg, 2.67 mmol, 2 eq) was added to a stirred suspension of **Fe1** (600 mg, 1.34 mmol, 1 eq) in 17 mL CH<sub>3</sub>CN. The mixture became purple and an off-white solid precipitated. The flask was covered with aluminum foils to protect the silver salts from light and the mixture was stirred overnight at RT. Silver chloride was filtered off under Ar and the filtrate was evaporated under high vacuum. The purple residue was re-dissolved in CH<sub>3</sub>CN, filtered through a 0.2 μm Acrodisc<sup>®</sup> LC PVDV syringe filter and concentrated. The filtration/evaporation procedure was repeated two more times to ensure no silver salts remains. The last time the filtrate was evaporated under N<sub>2</sub> stream and then under high vacuum, obtaining **Fe2** as a dark purple solid in 82% yield. The complex could be crystallized as follows. Under Ar, 356 mg **Fe2** were dissolved in 4 mL CH<sub>3</sub>CN, then 12.5 mL Et<sub>2</sub>O were added. After 4 days at -30 °C, some purple rod-shaped crystals were present. Solvents were decanted off and the solid was washed with Et<sub>2</sub>O (3x). The purple crystals were dried under high vacuum for 2 hours (252 mg). Crystallization yield: 69%. <sup>1</sup>H NMR (400 MHz, CD<sub>3</sub>CN): δ 43.8 (br s, 2 H), 17.8 (br s, 1H), δ 17.4-16.5 (br s, 4H), δ 16.1 (br s, 2H), δ 10.8 (br s, 2H), δ 9.7 (br s, 2H), δ 9.0-8.3 (br s, 4H), δ 4.5 (br s, 2H), δ 3.5 (br s, 2H), δ 2.4-1.9 (br s, 8 H), δ 0.1 (br s, 2H). ESI-MS in CH<sub>3</sub>CN: [M-CH<sub>3</sub>CN]<sup>2+</sup> *m/z* 209.5, [M-2CH<sub>3</sub>CN+F]<sup>+</sup> *m/z* 397.4, [M-2CH<sub>3</sub>CN+SbF<sub>6</sub>]<sup>+</sup> *m/z* 613.0; [SbF<sub>6</sub>]<sup>-</sup> *m/z* 235.2. IR (Nujol):



## Chapter 3

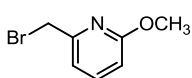
2308.37  $\text{cm}^{-1}$ , 2273.66  $\text{cm}^{-1}$  (weak,  $\text{CH}_3\text{C}\equiv\text{N}$  stretching).

### 2-(Hydroxymethyl)-6-methoxypyridine **51**



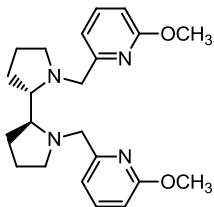
$\text{NaBH}_4$  (96%, 0.85 g, 21.6 mmol, 2.9 eq) was added portion wise to a stirred solution of 6-methoxy-2-pyridinecarboxaldehyde (97%, 1.04 g, 7.37 mmol, 1 eq) in 20 mL MeOH kept at 0 °C. The reaction mixture was stirred at RT for 3 hours, then distilled  $\text{H}_2\text{O}$  was added and MeOH was evaporated. The aqueous layer was extracted with  $\text{CH}_2\text{Cl}_2$  (3x), the collected organic phases were washed with brine, dried with  $\text{Na}_2\text{SO}_4$  and filtered. Evaporation of solvents afforded a pale yellow liquid which was used in the following step without further purification. Yield: 98%.  $^1\text{H}$  NMR (400 MHz,  $\text{CDCl}_3$ ):  $\delta$  7.51 (t,  $J = 7.7$  Hz, 1H),  $\delta$  6.80 (d,  $J = 7.2$  Hz, 1H),  $\delta$  6.59 (d,  $J = 8.2$  Hz, 1H),  $\delta$  4.64 (s, 2H),  $\delta$  3.89 (s, 3H),  $\delta$  3.65 (br s, 1H).

### 2-(Bromomethyl)-6-methoxypyridine **52**



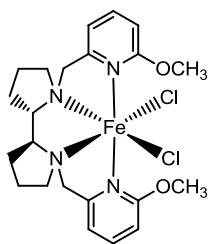
$\text{CBr}_4$  (99%, 3.61 g, 10.8 mmol, 1.5 eq) and  $\text{PPh}_3$  (2.83 g, 10.8 mmol, 1.5 eq) were added in sequence to a stirred solution of **51** (1.00 g, 7.18 mmol, 1 eq) in 18 mL  $\text{CH}_2\text{Cl}_2$  kept at 0 °C. Upon addition of the triphenylphosphine the solution became purple/brown. The reaction mixture was allowed to warm up at RT and was stirred for 2 hours, after which period a whitish precipitate was present. Solvents were evaporated to give a brown oil, which was purified by FCC (hexane/AcOEt 98:2). **52** was obtained as a colourless oil in 80% yield.  $^1\text{H}$  NMR (400 MHz,  $\text{CDCl}_3$ ):  $\delta$  7.56 (t,  $J = 7.8$  Hz, 1H),  $\delta$  7.00 (d,  $J = 7.2$  Hz, 1H),  $\delta$  6.67 (d,  $J = 8.4$  Hz, 1H),  $\delta$  4.48 (s, 2H),  $\delta$  3.96 (s, 3H).

### (2*S*,2'*S*)-1,1'-Bis((6-methoxypyridin-2-yl)methyl)-2,2'-bipyrrolidine (*S,S*-PDP-OMe) **53**



$\text{NaOH}$  (512 mg, 12.8 mmol, 5.0 eq) and 2-(bromomethyl)-6-methoxypyridine **52** (1137 mg, 5.6 mmol, 2.2 eq, dissolved in 9 mL  $\text{CH}_2\text{Cl}_2$ ) were added in sequence to a stirred suspension of (*S,S*)-2,2'-bipyrrolidine D-tartrate trihydrate (890 mg, 2.6 mmol, 1.0 eq) in 9 mL  $\text{H}_2\text{O}$ . The obtained biphasic mixture was stirred overnight at RT, then diluted with 1M  $\text{NaOH}$  and extracted with  $\text{CH}_2\text{Cl}_2$  (3x). The combined organic phases were dried with  $\text{Na}_2\text{SO}_4$ , filtered and concentrated in vacuo to obtain a sticky yellow oil. The crude was purified by FCC ( $\text{CH}_2\text{Cl}_2/\text{MeOH}/\text{aqueous NH}_3$  33% 97:3:2). The collected fractions were combined, diluted with  $\text{CH}_2\text{Cl}_2$ , washed with 1M  $\text{NaOH}$  (2x) and dried with  $\text{Na}_2\text{SO}_4$ . Evaporation of solvents afforded the product as a pale yellow oil in 97% yield.  $^1\text{H}$  NMR (400 MHz,  $\text{CDCl}_3$ ):  $\delta$  7.51 (t,  $J = 7.6$  Hz, 2H),  $\delta$  6.98 (d,  $J = 7.2$  Hz, 2H),  $\delta$  6.57 (d,  $J = 8.0$  Hz, 2H),  $\delta$  4.14 (d,  $J = 14.4$  Hz, 2H),  $\delta$  3.91 (s, 6H),  $\delta$  3.45 (d,  $J = 14.4$  Hz, 2H),  $\delta$  3.10 (m, 2H),  $\delta$  2.87 (br s, 2H),  $\delta$  2.29 (m, 2H),  $\delta$  1.90-1.68 (m, 8H).  $^{13}\text{C}$  NMR (100 MHz,  $\text{CDCl}_3$ ):  $\delta$  163.49, 158.25, 138.83, 115.27, 108.14, 65.23, 60.54, 55.34, 53.35, 26.16, 23.74.

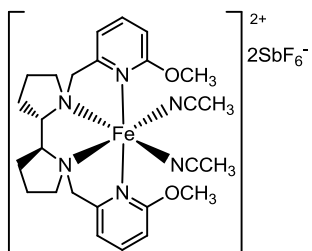
### $[\text{FeCl}_2(\text{S,S-PDP-OMe})] \text{Fe}_3$



Under Ar,  $\text{FeCl}_2 \cdot 4\text{H}_2\text{O}$  (273 mg, 1.37 mmol, 1 eq) was added to a stirred solution of ligand **53** (525 mg, 1.37 mmol, 1 eq) in 8 mL  $\text{CH}_3\text{CN}$ . The yellowish, slightly turbid solution was stirred overnight at RT. 10 mL  $\text{Et}_2\text{O}$  were added and a sticky brown solid precipitated. Solvents were decanted off and the residue was dried under high vacuum, then dissolved in  $\text{CH}_2\text{Cl}_2$ . Addition of pentane caused precipitation of a brown solid again. The solvents were

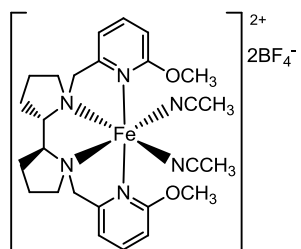
decanted off and the solid was dried under high vacuum, giving **Fe3** in 91% yield. ESI-MS in CH<sub>3</sub>CN: [M-Cl]<sup>+</sup> m/z 473.2, [ligand+H]<sup>+</sup> m/z 383.4.

**[Fe(CH<sub>3</sub>CN)<sub>2</sub>(S,S-PDP-OMe)](SbF<sub>6</sub>)<sub>2</sub> Fe4**



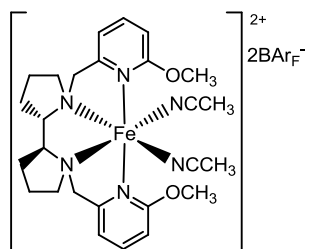
Under Ar, silver hexafluoroantimonate (98%, 207 mg, 0.59 mmol, 2eq) was added to a stirred thick brown solution of **Fe3** (150 mg, 0.29 mmol, 1 eq) in 5 mL CH<sub>3</sub>CN. The reaction mixture became beige and a white precipitate formed. The flask was covered with aluminum foils and the mixture was stirred overnight at RT. On the next day silver chloride was filtered off under Ar and the clear brown filtrate was evaporated to dryness. The residue was re-dissolved in CH<sub>3</sub>CN, filtered through a 0.2 μm Acrodisc<sup>®</sup> LC PVDV syringe filter and concentrated. The filtration/evaporation procedure was repeated two more times to ensure no silver salts remains. The last time the filtrate was evaporated under N<sub>2</sub> stream and then under high vacuum, obtaining a brilliant brown solid in 90% yield. <sup>1</sup>H NMR (400 MHz, CD<sub>3</sub>CN): δ 8.02 (t, *J* = 7.4 Hz, 2H), δ 7.11 (d, *J* = 8.0 Hz, 2H), δ 6.99 (d, *J* = 9.6 Hz, 2H), δ 4.81 (d, *J* = 17.2 Hz, 2H), δ 4.67 (d, *J* = 17.2 Hz, 2H), δ 4.12 (br s, 2H), δ 3.88 (s, 6H), δ 3.63 (m, 2H), δ 3.55 (m, 2H), δ 2.45 (br s, 2H), δ 2.30-2.10 (m, 4H), δ 2.08-1.95 (br s, 8H), δ 1.93-1.82 (m, 2H). ESI-MS in CH<sub>3</sub>CN: [M-2CH<sub>3</sub>CN]<sup>2+</sup> m/z 219.5, [M-CH<sub>3</sub>CN]<sup>2+</sup> m/z 239.6, [M-2CH<sub>3</sub>CN+SbF<sub>6</sub>]<sup>+</sup> m/z 673.1, [ligand+H]<sup>+</sup> m/z 383.4; [SbF<sub>6</sub>]<sup>-</sup> m/z 235.3.

**[Fe(CH<sub>3</sub>CN)<sub>2</sub>(S,S-PDP-OMe)](BF<sub>4</sub>)<sub>2</sub> Fe5**



Under Ar, a solution of ligand **53** (300 mg, 0.78 mmol, 1 eq) in 10 mL CH<sub>3</sub>CN was transferred via cannula into a stirred solution of iron(II) tetrafluoroborate hexahydrate (97%, 273 mg, 0.78 mmol, 1 eq) in 10 mL CH<sub>3</sub>CN. The resulting pale yellow solution was stirred overnight at RT, then the solvent was evaporated and the yellow residue was washed with Et<sub>2</sub>O (2x), decanting off the solvent via syringe. Drying under high vacuum afforded a yellow-greenish solid in 47% yield. <sup>1</sup>H NMR (400 MHz, CD<sub>2</sub>Cl<sub>2</sub>): δ 8.1 (br, 2H), δ 7.4 (br, 2H), δ 6.7 (br, 2H), δ 5.2 (br, 2H), δ 4.9-4.6 (br, 4H), δ 4.03 (br, 8H), δ 3.0 (br, 2H), δ 3.2-2.5 (br, 10H), δ 2.39 (br, 2H), δ 1.3 (br, 2H). ESI-MS in CH<sub>3</sub>CN: [M-2CH<sub>3</sub>CN]<sup>2+</sup> m/z 219.3, [M-CH<sub>3</sub>CN]<sup>2+</sup> m/z 239.4, [M-2CH<sub>3</sub>CN+F]<sup>+</sup> m/z 457.3, [ligand+H]<sup>+</sup> m/z 383.3; [BF<sub>4</sub>]<sup>-</sup> m/z 87.1.

**[Fe(CH<sub>3</sub>CN)<sub>2</sub>(S,S-PDP-OMe)](BAr<sub>F</sub>)<sub>2</sub> Fe6**

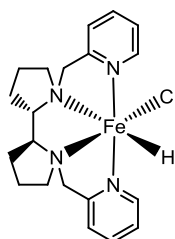


Method A. Under Ar, NaBAr<sub>F</sub> (230 mg, 0.26 mmol, 2 eq) was added to a stirred solution of **Fe5** (90 mg, 0.13 mmol, 1 eq) in 10 mL CH<sub>2</sub>Cl<sub>2</sub>. The reaction mixture became turbid and, after stirring for 1 hour, was filtered under Ar through celite. Evaporation of the filtrate gave **Fe6** as a whitish solid in 99% yield. Method B. Under Ar, AgBAr<sub>F</sub> (381 mg, 0.40 mmol, 2 eq) was added to a stirred thick brown solution of **Fe3** (100 mg, 0.20 mmol, 1 eq) in 8 mL CH<sub>3</sub>CN. Upon addition the reaction mixture became turbid and a white solid precipitated. The reaction mixture was stirred overnight with minimal light exposure and the precipitate was then filtered off under Ar. The filtrate was evaporated to dryness, the brown residue was taken up with 10 mL CH<sub>3</sub>CN and filtered through a 0.2 μm Acrodisc<sup>®</sup> LC PVDV syringe filter. The evaporation/filtration procedure was repeated to ensure no silver salts remains. Evaporation of solvents afforded **Fe16** as a dark brown solid in 78% yield. IR (Nujol):

## Chapter 3

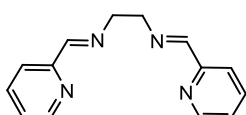
2306.45  $\text{cm}^{-1}$ , 2277.52  $\text{cm}^{-1}$  ( $\text{CH}_3\text{C}\equiv\text{N}$  stretching).

### $[\text{Fe}(\text{Cl})(\text{H})(\text{S,S-PDP})]^{34a}$ Fe7



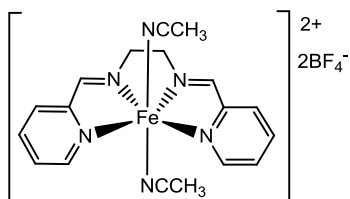
Attempted synthesis. Under Argon, a 1 M solution of  $\text{NaHBEt}_3$  in toluene (110  $\mu\text{L}$ , 0.11 mmol, 1 eq) was added dropwise to a stirred fine suspension of **Fe1** (50 mg, 0.11 mmol, 1 eq) in 3 mL THF. Upon addition the yellow reaction mixture darkened. Evaporation of solvents yielded to the isolation of a deep purple solid, which turned brown after short contact with air.

### (*E,E*)- $N^1,N^2$ -Bis(pyridin-2-ylmethylene)ethane-1,2-diamine (PED) **54**



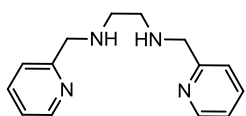
2-pyridinecarboxaldehyde (642 mg, 570  $\mu\text{L}$ , 5.93 mmol, 2 eq) was added to a stirred solution of ethylenediamine (180 mg, 200  $\mu\text{L}$ , 2.96 mmol, 1 eq) in 4 mL  $\text{Et}_2\text{O}$  and the resulting orange solution was stirred overnight at 70  $^\circ\text{C}$ . Solvents were removed and the residue was taken up with  $\text{Et}_2\text{O}$ /hexane 3:1, dissolving only the desired product. Solvents were thus decanted off and evaporated, obtaining **54** as an orange powder in 80% yield.  $^1\text{H}$  NMR (400 MHz,  $\text{CD}_2\text{Cl}_2$ ):  $\delta$  8.62 (ddd,  $J = 4.8, 1.7, 1.0$  Hz, 2H),  $\delta$  8.42 (s, 2H),  $\delta$  8.02 (dt,  $J = 7.9, 1.0$  Hz, 2H),  $\delta$  7.76 (td,  $J = 7.7, 1.7$  Hz, 2H),  $\delta$  7.34 (ddd,  $J = 7.5, 4.8, 1.2$  Hz, 2H),  $\delta$  4.05 (s, 4H).

### $[\text{Fe}(\text{CH}_3\text{CN})_2(\text{PED})](\text{BF}_4)_2$ Fe8



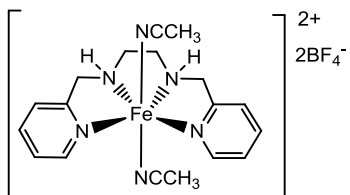
Under Ar, a yellow solution of ligand **54** (487 mg, 2.04 mmol, 1 eq) in 20 mL  $\text{CH}_3\text{CN}$  was added to a stirred solution of iron(II) tetrafluoroborate hexahydrate (97%, 711 mg, 2.04 mmol, 1 eq) in 10 mL  $\text{CH}_3\text{CN}$ . Upon addition the reaction mixture turned red and then darkened. After stirring overnight at RT, solvents were evaporated and the residue was washed with  $\text{Et}_2\text{O}$  (3x). The obtained dark red/purple solid was then dried under high vacuum. Yield: 91%. ESI-MS in  $\text{CH}_3\text{CN}$ :  $m/z$  167.6  $[\text{M}-\text{CH}_3\text{CN}]^+$ ;  $m/z$  87.2  $[\text{BF}_4]^-$ . IR (Nujol): 2282.34  $\text{cm}^{-1}$  ( $\text{CH}_3\text{C}\equiv\text{N}$  stretching).

### $N^1,N^2$ -Bis(pyridin-2-ylmethyl)ethane-1,2-diamine (PED-red) **55**



$\text{NaBH}_4$  (96%, 200 mg, 5.03 mmol, 3 eq) was added portion wise to a stirred solution of **54** (400 mg, 1.68 mmol, 1 eq) in 20 mL MeOH. The resulting mixture was stirred overnight at RT, then 15 mL 1M NaOH were added and MeOH was evaporated. The aqueous layer was extracted with  $\text{CH}_2\text{Cl}_2$  (4x) and the collected organic phases were washed with 1M NaOH, dried with  $\text{Na}_2\text{SO}_4$  and filtered. Evaporation of solvent afforded **55** as a yellow oil in 97% yield. The product was used without further purification.  $^1\text{H}$  NMR (400 MHz,  $\text{CD}_2\text{Cl}_2$ ):  $\delta$  8.55 (d,  $J = 4.8$  Hz, 2H),  $\delta$  7.67 (td,  $J = 7.7, 1.8$  Hz, 2H),  $\delta$  7.37 (d,  $J = 7.8$  Hz, 2H),  $\delta$  7.19 (dd,  $J = 7.5, 4.9$  Hz, 2H),  $\delta$  3.91 (s, 4H),  $\delta$  2.80 (s, 4H),  $\delta$  2.03 (s, 2H).

### $[\text{Fe}(\text{CH}_3\text{CN})_2(\text{PED-red})](\text{BF}_4)_2$ Fe9

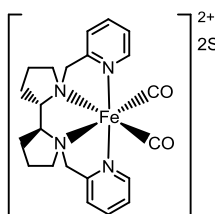


Under Ar, a solution of ligand **55** (240 mg, 1.0 mmol, 1 eq) in 10 mL  $\text{CH}_3\text{CN}$  was added via cannula into a stirred solution of iron(II) tetrafluoroborate hexahydrate in 10 mL  $\text{CH}_3\text{CN}$ . The solution turned red and then purple. After stirring for 1 hour, the solution was concentrated to 1 mL volume and 10 mL  $\text{Et}_2\text{O}$  were added. A



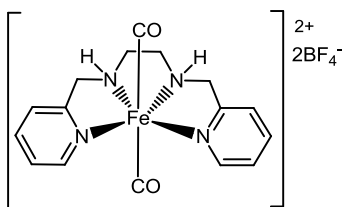
purple solid precipitated and the solvent was decanted off. The solid was washed once more with Et<sub>2</sub>O. Evaporation of solvents gave **Fe9** as a purple powder in 88% yield. ESI-MS in CH<sub>3</sub>CN: [M-2CH<sub>3</sub>CN]<sup>+</sup> *m/z* 149.4, [M-CH<sub>3</sub>CN]<sup>+</sup> *m/z* 169.5; [BF<sub>4</sub>]<sup>-</sup> *m/z* 87.1. IR (KBr): 3415.31cm<sup>-1</sup> (medium, broad N-H stretching), 2253.41 cm<sup>-1</sup> (medium, C≡N stretching). <sup>1</sup>H NMR (400 MHz, CD<sub>3</sub>CN): δ 26.0-23.5 (br, 2H), δ 20.0-17.5 (br, 2H), δ 14.0-13.0 (br, 4H), δ 12.5-12.0 (br, 2H), δ 9.3-8.7 (br, 4H), δ 6.2 (br, 2H), δ 3.4-1.9 (br, 8H).

### [Fe(CO)<sub>2</sub>(PDP)<sub>2</sub>](SbF<sub>6</sub>)<sub>2</sub> **Fe10**



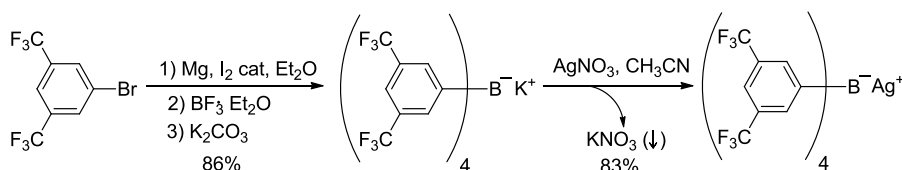
Complex **Fe2** (48 mg, 0.051 mmol) was dissolved in 4 mL acetone obtaining a purple solution. The latter was then purged three times with 1 bar CO and stirred under CO atmosphere for 2 hours. Evaporation of the resulting mixture afforded **Fe10** as a pale brown solid in 89% yield. ESI-MS in CH<sub>3</sub>CN: [M-CH<sub>3</sub>CN]<sup>2+</sup> *m/z* 209.5, [M-2CH<sub>3</sub>CN+SbF<sub>6</sub>]<sup>+</sup> *m/z* 613.0; [SbF<sub>6</sub>]<sup>-</sup> *m/z* 235.2. IR (KBr): disappearance of C≡N stretching bands.

### [Fe(CO)<sub>2</sub>(PED-red)<sub>2</sub>](BF<sub>4</sub>)<sub>2</sub> **Fe11**



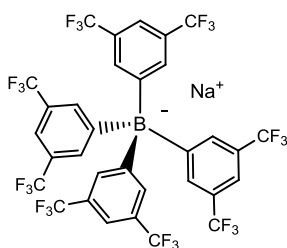
Complex **Fe9** [Fe(CH<sub>3</sub>CN)<sub>2</sub>(PED-red)](BF<sub>4</sub>)<sub>2</sub> (300 mg, 0.079 mmol) dissolved in 4 mL acetone was then purged three times with 1 bar CO and stirred under CO atmosphere for 2 hours. Evaporation of solvents gave **Fe11** as a dark green/black powder in 94% yield. ESI-MS in MeOH: [M-2CO-2H]<sup>2+</sup> *m/z* 296.2; [2BF<sub>4</sub>+Na]<sup>-</sup> *m/z* 197.3. IR (Nujol): 2091.42, 2043.21, 2010.43 cm<sup>-1</sup> (weak, C≡O stretching).

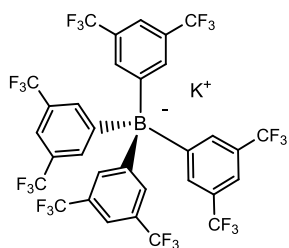
### Synthesis of AgBAR<sub>F</sub><sup>128</sup>



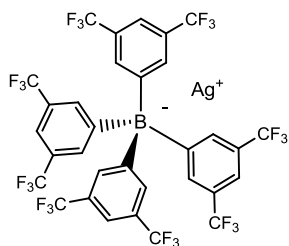
### Sodium tetrakis[3,5-bis(trifluoromethyl)phenyl]borate<sup>128</sup> NaBAR<sub>F</sub>

A brown suspension of activated Mg turnings (1.00 g, 41.2 mmol, 6.9 eq) and I<sub>2</sub> (catalytic, some crystals) in 10 mL Et<sub>2</sub>O was prepared. To this suspension a solution of 3,5-bis(trifluoromethyl)bromobenzene (10.0 g, 33.8 mmol, 5.6 eq) in 50 mL Et<sub>2</sub>O was added *dropwise*. The reaction mixture darkened and was heated to reflux for 45 minutes. After cooling down to RT, sodium tetrafluoroborate (0.67 g, 6.0 mmol, 1 eq) was added and the resulting mixture was stirred for 64 hours, at the end of which it was quenched by adding a saturated Na<sub>2</sub>CO<sub>3</sub> aqueous solution (50 mL) and stirring for 20 minutes. The mixture was then filtered through celite, phases were separated and the aqueous layer was extracted with Et<sub>2</sub>O (4x). The combined organic phases were dried with Na<sub>2</sub>SO<sub>4</sub>, filtered and evaporated to yield a brown gummy solid, which was crystallized from CH<sub>2</sub>Cl<sub>2</sub>/hexane 1:1. NaBAR<sub>F</sub> was obtained as an off-white powder in 94% yield. <sup>1</sup>H NMR (400 MHz, (CD<sub>3</sub>)<sub>2</sub>SO): δ 7.72 (s, 4H), δ 7.63 (s, 8H).



**Potassium tetrakis[3,5-bis(trifluoromethyl)phenyl]borate**<sup>128</sup>  $\text{KBAr}_F$ 

A solution of 3,5-bis(trifluoromethyl)bromobenzene (10.0 g, 33.8 mmol, 5.6 eq) in 50 mL  $\text{Et}_2\text{O}$  was added *dropwise* to a stirred suspension of Mg turnings (862 mg, 35.5 mmol, 5.9 eq) and catalytic iodine in 15 mL  $\text{Et}_2\text{O}$ . The reaction mixture initially discolored and started boiling, then became dark brown. It was heated to reflux for 50 minutes and then stirred at RT for 2 hours. A 20-mL  $\text{Et}_2\text{O}$  solution of  $\text{BF}_3 \cdot \text{Et}_2\text{O}$  (1.13 mL, 6.03 mmol, 1 eq) was dropped into the reaction flask over 20 minutes. After heating to reflux for 6 hours and stirring for further 18 hours, the reaction mixture was slowly poured into an Erlenmeyer flask containing a stirred solution of  $\text{K}_2\text{CO}_3$  (67 g, 485 mmol, 80 eq) in 276 mL  $\text{H}_2\text{O}$ ). The precipitated  $\text{MgCO}_3$  was filtered through celite washing with  $\text{Et}_2\text{O}$  (4x), and phases were separated. The aqueous layer was saturated with KBr and extracted with  $\text{Et}_2\text{O}$  (4x). The collected organic phases were evaporated to yield a pale orange solid. The solid was dissolved in 52 mL  $\text{CH}_2\text{Cl}_2/\text{THF}$  1:1 and layered with 52 mL hexane. After 3 days filtration on Buchner afforded  $\text{KBAr}_F$  as an off-white solid, which was then dried under high vacuum. Yield: 86%.

**Silver tetrakis[3,5-bis(trifluoromethyl)phenyl]borate**<sup>128</sup>  $\text{AgBAr}_F$ 

In an Erlenmeyer flask covered with an aluminum foil, a colorless solution of silver nitrate (380 mg, 2.22 mmol, 1 eq) in 14 mL  $\text{CH}_3\text{CN}$  was added to an orange solution of  $\text{KBAr}_F$  (2.00 g, 2.22 mmol, 1 eq) in 20 mL  $\text{CH}_3\text{CN}$ . Upon addition the solution became turbid. After stirring for 15 minutes, 25 mL of  $\text{Et}_2\text{O}$  were added and a white solid precipitated. The mixture was filtered through celite and the filtrate was concentrated to dryness. The residue was dissolved in THF and filtered again. Evaporation of solvent afforded a pale brown solid, which was crystallized as follows. The solid was dissolved in 50 mL THF and the solution was layered with 80 mL hexane, then kept at  $-30\text{ }^\circ\text{C}$  for 8 days with minimal light exposure. Filtration on Buchner gave  $\text{AgBAr}_F$  as a white solid in 83% yield (after drying under high vacuum).

**Hydrogenation's procedures**

**General procedure for the hydrogenation of methyl 2-acetamidoacrylate (S1).** A Parr multi-reactor was employed, allowing six reactions in parallel under hydrogen. The selected complex (4 mg, 0.05 eq) and methyl 2-acetamidoacrylate (15-20 mg, 1 eq) were weighted in 4-mL GC-vials with screw cap containing a magnetic stirring bar. The vessels were purged with nitrogen and solvent (2 mL) was added via syringe. A 25 gauge needle was inserted in the septum of the capped vials, which then were placed in the respective autoclaves and purged three times with 50 bar of hydrogen. The reactions were magnetically stirred under hydrogen pressure at the desired temperature for a given time and then analyzed for conversion and *ee* determination.

**General procedure for the hydrogenation of acetophenone (S2).** A Parr multi-reactor was employed, allowing six reactions in parallel under hydrogen pressure. The selected complex (5 mg, 0.05 eq) and the desired base (0.50 or 0.75 eq) were weighted in special glass vessels, which were then purged with nitrogen. Isopropanol (7 mL) and acetophenone (15-30  $\mu\text{L}$ , 1 eq) were added via syringe. The vessels were placed in the respective autoclaves and purged three times

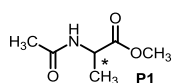


with 50 bar of hydrogen. The reactions were stirred under hydrogen pressure at the desired temperature for a given time and then analysed for conversion and *ee* determination.

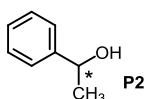
**General procedure for the transfer hydrogenation of acetophenone (S2).** A carousel multi-reactor was employed, allowing eight reactions in parallel under nitrogen atmosphere. Under N<sub>2</sub> flow, the selected complex (4 mg, 0.05 eq) and the desired base (0.50 or 0.75 eq) were introduced in special glass vessels, which were then closed with screw caps and purged with nitrogen. Distilled isopropanol (2 mL) and acetophenone (10-20 μL, 1 eq) were added via syringe and the reactions were stirred under nitrogen at the desired temperature for a given time, then analyzed for conversion and *ee* determination.

**Conditions for conversion and *ee* determination**

**Methyl 2-acetamidopropanoate P1.** Conversion and *ee* were determined by GC (capillary column: MEGADEX DACTBSβ, diacetyl-*tert*-butylsilyl-β-cyclodextrin, 0.25 μm; diameter = 0.25 mm; length = 25 m; carrier: hydrogen; flow: 1 mL/min; oven temperature: 140 °C for 6 min, then a 8 °C/min gradient is applied):  $t_{\text{substrate}}$  = 3.9 min;  $t_R$  = 5.2 min;  $t_S$  = 6.0 min.



**1-Phenylethanol P2.** Conversion and *ee* were determined by GC (capillary column: MEGADEX DACTBSβ, diacetyl-*tert*-butylsilyl-β-cyclodextrin, 0.25 μm; diameter = 0.25 mm; length = 25 m; carrier: hydrogen; hydrogen pressure: 1 bar; oven temperature: 75 °C for 5 min, 20 °C/min gradient until 95 °C, 95 °C for 15 min, then a 20 °C/min gradient is applied):  $t_{\text{substrate}}$  = 9.3 min;  $t_{\text{product-en1}}$  = 17.5 min;  $t_{\text{product-en2}}$  = 19.8 min.





## 4 Iron complexes with isonitrile ligands

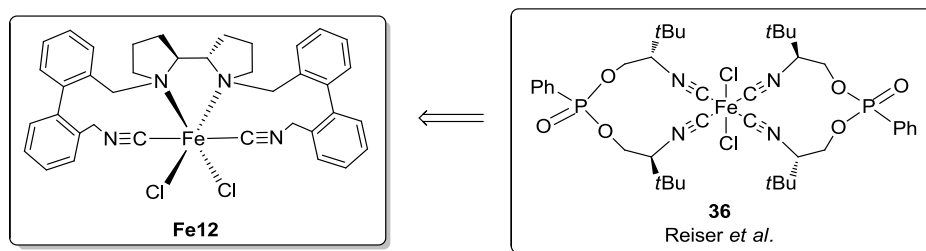
### 4.1 Isonitrile complexes

Isonitriles (also known as isocyanides) are organic molecules with peculiar reactivity, possessing a nucleophilic carbon which displays nucleophilic and electrophilic properties at the same time.<sup>131</sup> Isonitriles are also valuable ligands in coordination compounds. When an isocyanide coordinates to a metal, the lone electron pair on the formally divalent carbon atom (roughly corresponding to the HOMO) forms a  $\sigma$ -type bond to the metal. If the metal has filled d-orbitals which are capable of overlapping with empty anti-bonding orbital (LUMO) on the ligand, a second bond of  $\pi$ -type may form. Through the mechanism of back-donation, isonitriles efficiently stabilize metals in low oxidation states. They share this ability with some other ligands, such as CO and phosphines.

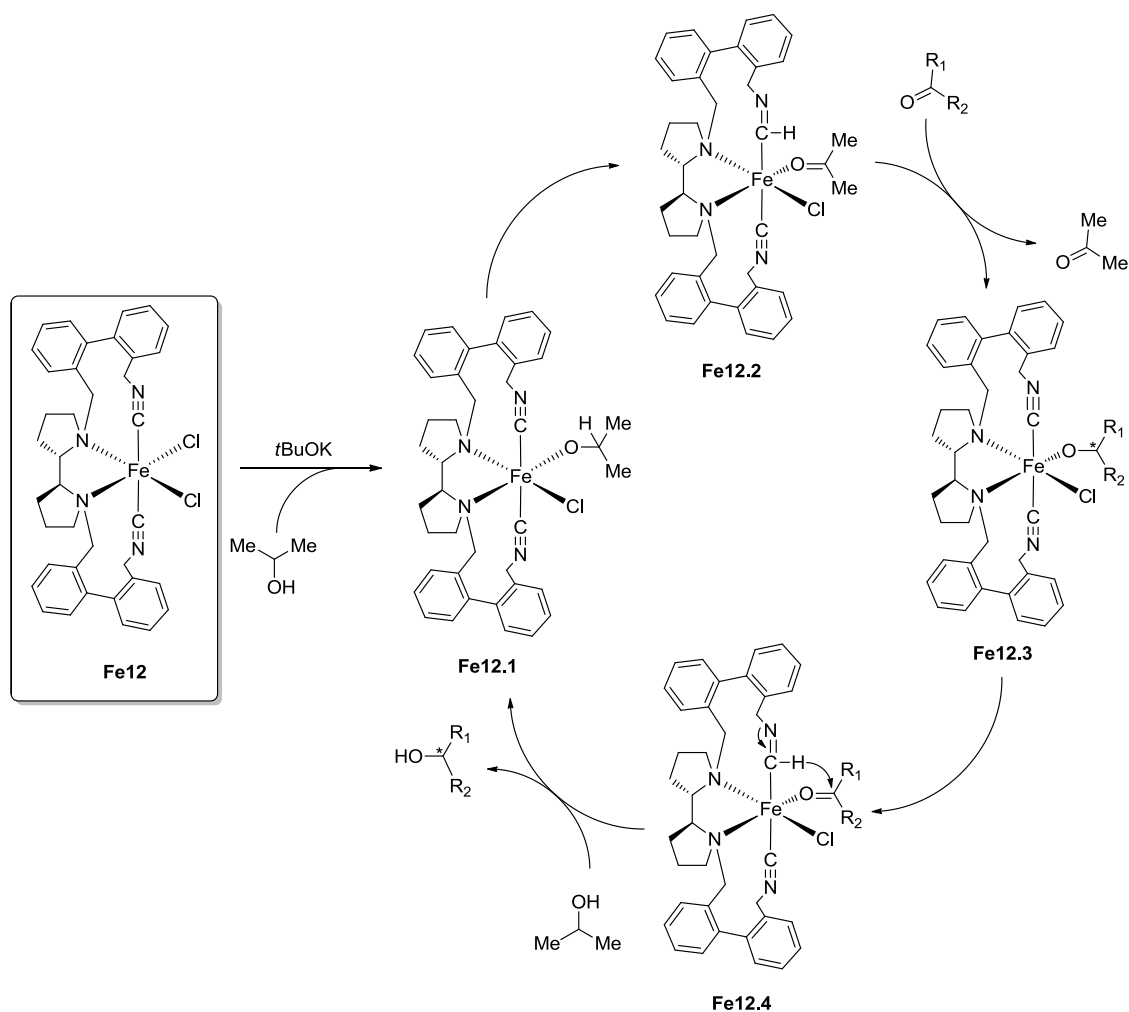
Low interest in this type of ligands may be attributed to their linear structure, which is rather prohibiting the arrangement of mononuclear chelates and can lead instead to multinuclear or polymeric metal complexes. The building of large-sized ligand backbones is required in order to encompass two isonitrile groups pointing toward the same metal centre.<sup>132</sup>

### 4.2 Novel complexes featuring bis(isonitrile) ligand

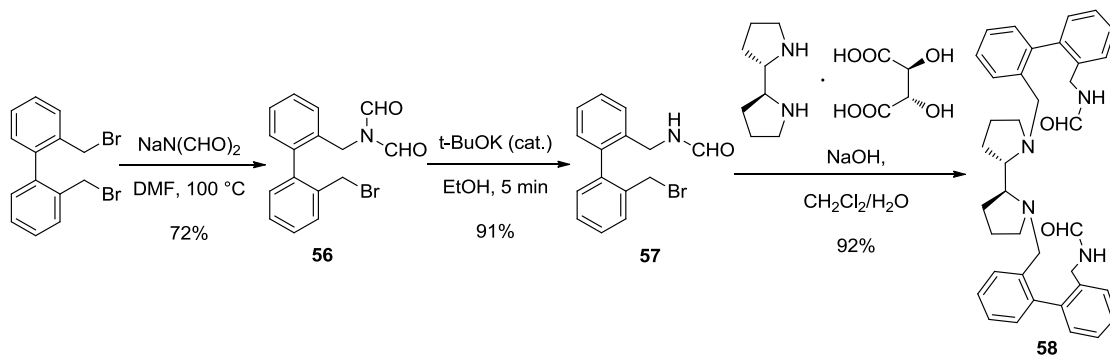
According to the considerations reported in the previous paragraph, the synthesis of novel complexes featuring isonitrile ligands was undertaken. Building on the chiral (*S,S*)-2,2'-bipyrrrolidine scaffold, already exploited for the design of *N,N,N,N*-ligands (see Paragraph 3.3),<sup>126</sup> the novel tetradentate complex **Fe12** was prepared (Figure 4.1). Iron(II) complex **Fe12** was inspired by Reiser's catalyst **36** (see Paragraph 2.4.6) and was expected to be active in the asymmetric transfer hydrogenation of aromatic ketones. Its ligand possesses two isonitrile groups, which can act as  $\pi$ -acceptors on one side and as non-innocent ligands on the other.

Figure 4.1 Novel bis(isonitrile) complex **Fe12**, inspired to the catalyst **36**.

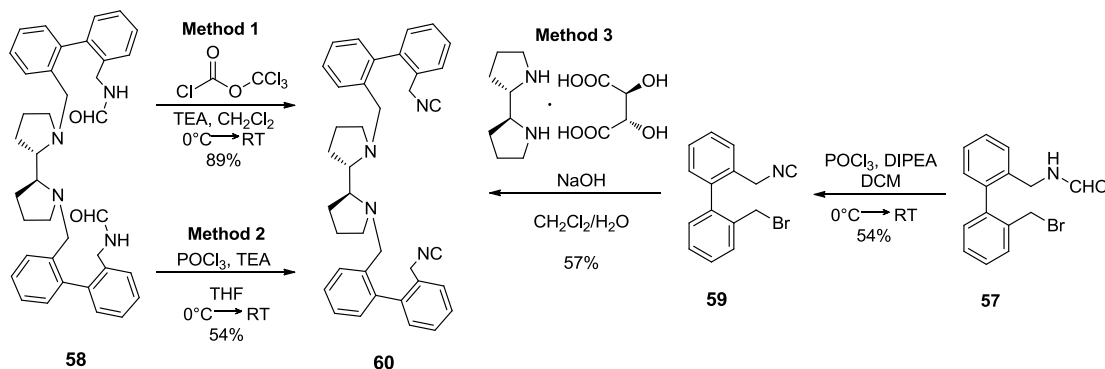
The proposed catalytic cycle for the asymmetric transfer-hydrogenation of ketones, could proceed according to the Meerwein-Ponndorf-Verley-type mechanism (see Scheme 4.1). We postulated activation of catalyst **Fe12** by *t*BuOK (or another base) and isopropanol coordination to form **Fe12.1**. After subsequent reduction of coordinated isonitrile to imine using a proton from isopropanol (**Fe12.2**), resultant acetone would be replaced by substrate to form **Fe12.3**. The final step would proceed by an inner-sphere mechanism where hydride transfer to the coordinated substrate is mediated by the imine part of the ligand (**Fe12.4**), rather than from iron, which role is limited just to coordinate the oxygen atom. Thus, as in the case of catalyst **36**, we postulated that desired catalyst would be a cooperative non-innocent one.

Scheme 4.1 Expected Meerwein-Ponndorf-Verley-like ATH mechanism for the new complex **Fe12**.

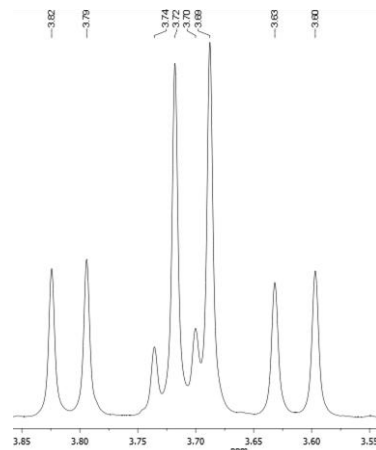
Synthesis of bis-formamide **58** starts relies on a different functionalization of the two benzyl bromide groups in commercially available 2,2'-bis(bromomethyl)-1,1'-biphenyl. First benzyl bromide was converted to mono-formamide **57** by reaction with  $\text{NaN}(\text{CHO})_2$  followed by treatment with *t*BuOK in ethanol (Scheme 4.2). Compound **57** was then reacted with 2,2'-bipyrrolidine to yield the bis-formamide **58**.

Scheme 4.2 Synthesis of **58**.

The bis-isonitrile **60** was obtained by dehydration of **58** using two different methods. Additionally also a third method was applied and contained dehydration of **57**, followed by nucleophilic substitution with the 2,2'-bispyrrolidine core. Irrespective of the synthetic approach employed (Scheme 4.3), ligand **60** was always isolated as a product showing two very close spots in TLC, which could not be separated by flash column chromatography or by RP-HPLC.

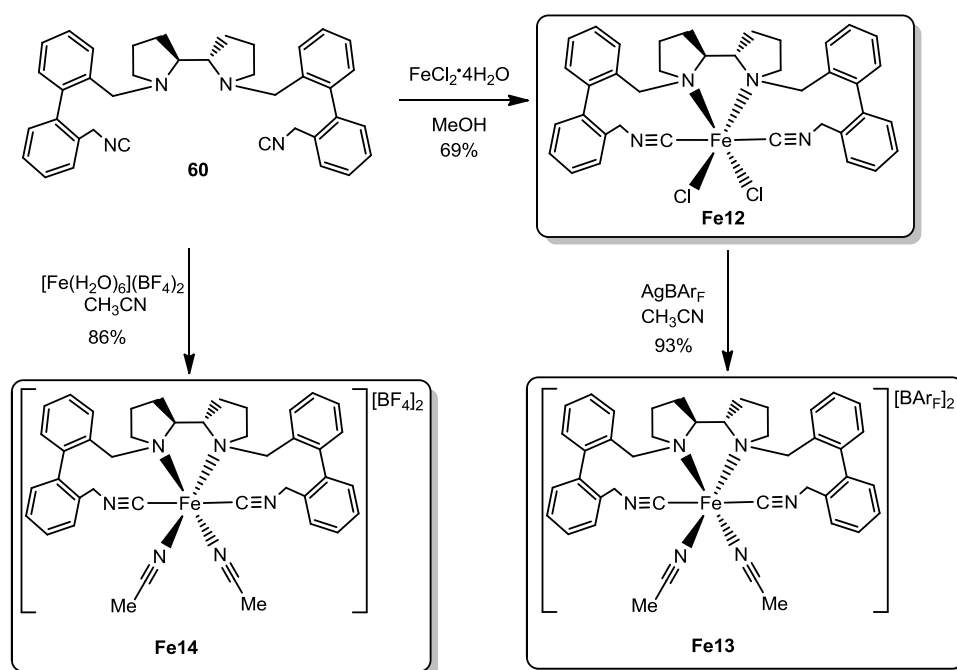
Scheme 4.3 Three different preparations of ligand **60**.

The NMR spectrum of **60** showed a peculiar signal splitting of benzylic  $\text{CH}_2$  group (Figure 4.2). The integral ratio between the split doublets was the same in all batches. Hindered rotation of the pyrrolidine-pyrrolidine bond or unusual configurational stability of the *N*-stereocenters might caused of the observed outcome.

Figure 4.2 Downfield part of  $\text{CH}_2$  AB spin system of **60** (4H).

ESI-MS spectra in CH<sub>3</sub>CN show two peaks at  $m/z$  551 (protonated ligand [M+H]<sup>+</sup>) and  $m/z$  1163 (Cu<sup>I</sup> complex [2M+Cu]<sup>+</sup>, whose formation occurs within the ESI source), thus indicated that ligand **60** is present as a single species.

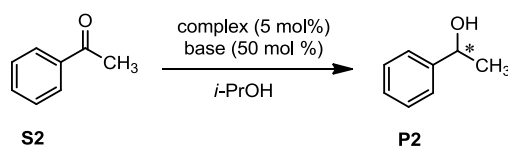
Ligand **60** was used to prepare complexes **Fe12-14** (Scheme 4.4). Use of iron(II) chloride tetrahydrate as iron source and methanol as solvent gave the neutral, highly insoluble complex **Fe12**. Treatment of the latter with AgBAR<sub>F</sub> in acetonitrile was found to be effective for obtaining the more soluble complex **Fe13**. Complexation reaction in acetonitrile between **60** and iron(II) tetrafluoroborate hexahydrate afforded the dicationic complex **Fe14**.



Scheme 4.4 Synthesis of bis(isonitrile) complexes **Fe12-Fe14**.

These new bis(isonitrile) complexes **Fe12-14** were then tested in the asymmetric transfer hydrogenation of acetophenone (Table 4.1).

Table 4.1 Catalytic screening of bis(isonitrile) complexes in the transfer hydrogenation of **S2**.



Entry	Complex	T (°C)	Time (h)	Base	Conv. (%)	ee (%)
1	<b>Fe12</b>	50	18	<i>t</i> -BuOK	51	13
2	<b>Fe12</b>	50	18	NaOH	52	5
3	<b>Fe12</b>	50	90	<i>t</i> -BuOK	87	11
4	<b>Fe13</b>	25	18	<i>t</i> -BuOK	11	14
5	<b>Fe13</b>	25	18	NaOH	48	16
6	<b>Fe13</b>	50	18	<i>t</i> -BuOK	12	5
7	<b>Fe13</b>	50	18	NaOH	73	12



8	<b>Fe14</b>	25	66	<i>t</i> -BuOK	34	0
9	<b>Fe14</b>	50	66	<i>t</i> -BuOK	36	9

All complexes turned out to be able to catalyze the transfer hydrogenation of acetophenone, although with a low level of stereocontrol (**Fe13**, *ee* up to 16%, entry 5).

The neutral complex **Fe12** promoted the reaction with up to 87% conversion (entry 13), but with a low enantiomeric excess (5-13% *ee*). Remarkably, a very long reaction time (90 hours) was necessary to achieve such level of conversion, while in the standard reaction time (18 hours) the maximum conversion was slightly above 50% (entry 1). This observation suggested that probably the catalyst **Fe12** did undergo degradation, but rather kept on promoting the reaction with a very slow rate. Regarding bases, NaOH afforded conversion comparable to *t*BuOK (entry 5), but with decreased *ee* - only 5%.

The most soluble complex **Fe13** gave the best result over 18 hours at 50 °C, achieving 73% conversion and 12% *ee* (entry 7). Remarkably, the catalytic activity of **Fe13** greatly depended upon the nature of the base used in the reaction. In each attempt, conversions with NaOH were higher than in the corresponding reactions with *t*-BuOK (entries 4 vs. 5, 6 vs. 7). A further base screening was conducted and it revealed that no reactions occurs in the presence of KOH, TEA, Na<sub>2</sub>CO<sub>3</sub> or K<sub>2</sub>CO<sub>3</sub>.

The dicationic complex **Fe14** was able to catalyze the reaction as well, but with lower conversions than the ones obtained with neutral complex **Fe12**. Complex **Fe14** afforded low enantiomeric excess and it required temperature elevated to 50 °C to obtain it (9% *ee*, entry 9).

The bis(isonitrile) complexes employed in this first catalytic screening showed ability to promote the transfer hydrogenation of acetophenone with moderate - yet not outstanding - activity. The positive results obtained prompted us to investigate more deeply the application of isonitrile Fe(II)-complexes for ketone reductions.

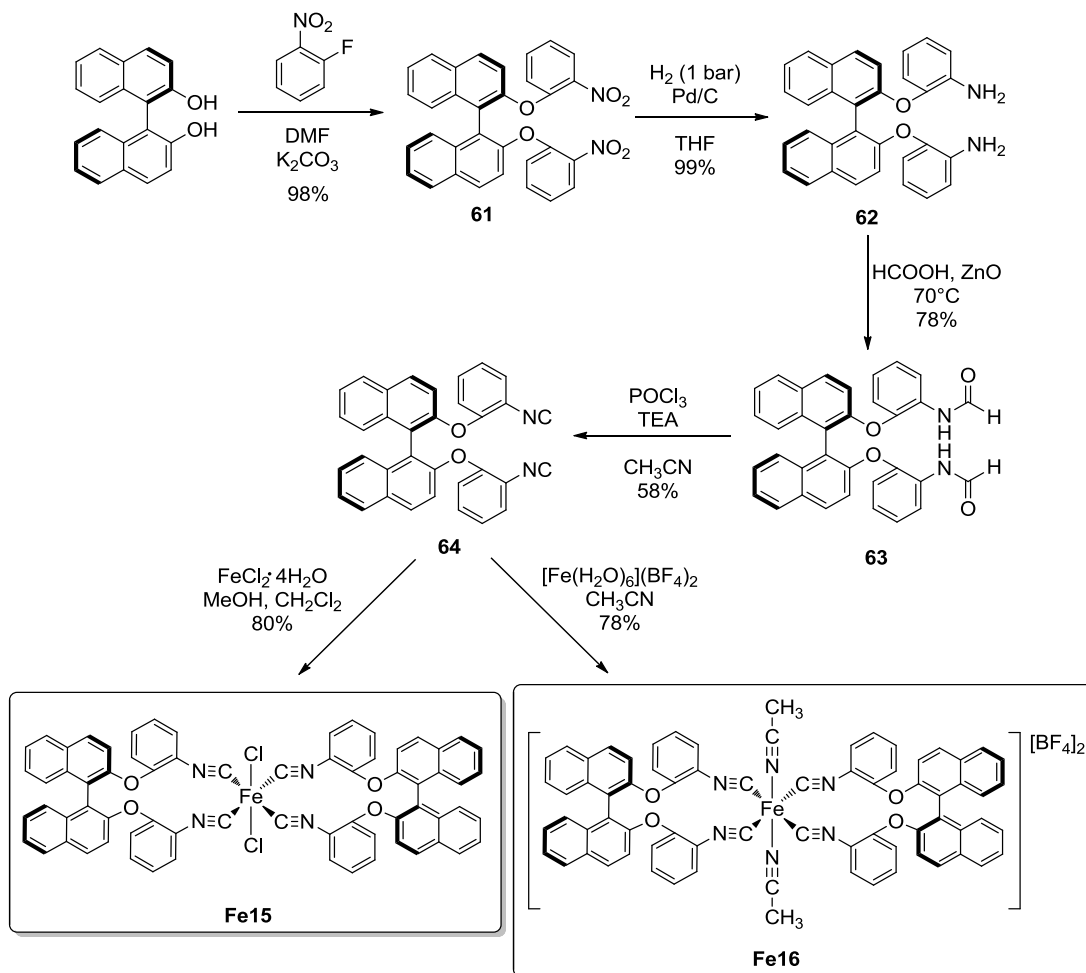
### 4.3 Tetra(isonitrile) complexes

We decided to synthesize new tetra(isonitrile) complexes **Fe15** and **Fe16**, which were more directly inspired to Reiser's catalyst **36** (Scheme 4.5). They were expected to display higher catalytic activity compared to the previously tested bis(isonitrile) complexes, because they possessed four isonitrile groups coordinated to the metal centre. The chiral scaffold was a binaphthyl moiety, connected to the linear isonitrile function by a rigid linker (benzene ring).

The synthetic route, started with a nucleophilic aromatic substitution between (*R*)-BINOL and *o*-fluoronitrobenzene, yielding **61**. The latter was reduced to diamine **62**, which was then subjected to bis-formylation in formic acid using zinc oxide as a promoter



to obtain bis-formamide **63**. Dehydration of **63** using phosphoryl chloride gave ligand **64** with 44% overall yield. Complexation of **64** with standard Fe(II) sources (iron chloride tetrahydrate and iron tetrafluoroborate hexahydrate) afforded complexes **Fe15** and **Fe16**.



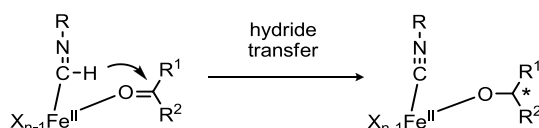
New complexes **Fe15** and **Fe16** were tested in the transfer hydrogenation of acetophenone Table 4.2.

Table 4.2 Catalytic screening of tetra(isonitrile) complexes in the transfer hydrogenation of **S2**.

Entry	Complex	T (°C)	Solvent	Base	Conv. (%)	ee (%)
1	<b>Fe15</b>	50	<i>i</i> -PrOH	<i>t</i> -BuOK	6	-
2	<b>Fe15</b>	50	<i>i</i> -PrOH	KOH	6	-
3	<b>Fe15</b>	50	H <sub>2</sub> O	HCOONa	0	-
4	<b>Fe15</b>	50	HCOOH:TEA 5:2	TEA	0	-
5	<b>Fe16</b>	50	<i>i</i> -PrOH	<i>t</i> -BuOK	2	-
6	<b>Fe16</b>	50	<i>i</i> -PrOH	NaOH	5	-

To our surprise, complexes **Fe15** and **Fe16** were not catalytically active in the transfer hydrogenation of ketones. Conversions at 50 °C over 18 hours were always very low, regardless of the base used. In particular, complex **Fe15** was tested employing different hydrogen donor reagents. Besides the standard isopropanol/potassium *tert*-butoxide and isopropanol/potassium hydroxide systems (entries 1 and 2), also the combinations water/sodium formate and formic acid/triethylamine were used, but without success (entries 3 and 4).

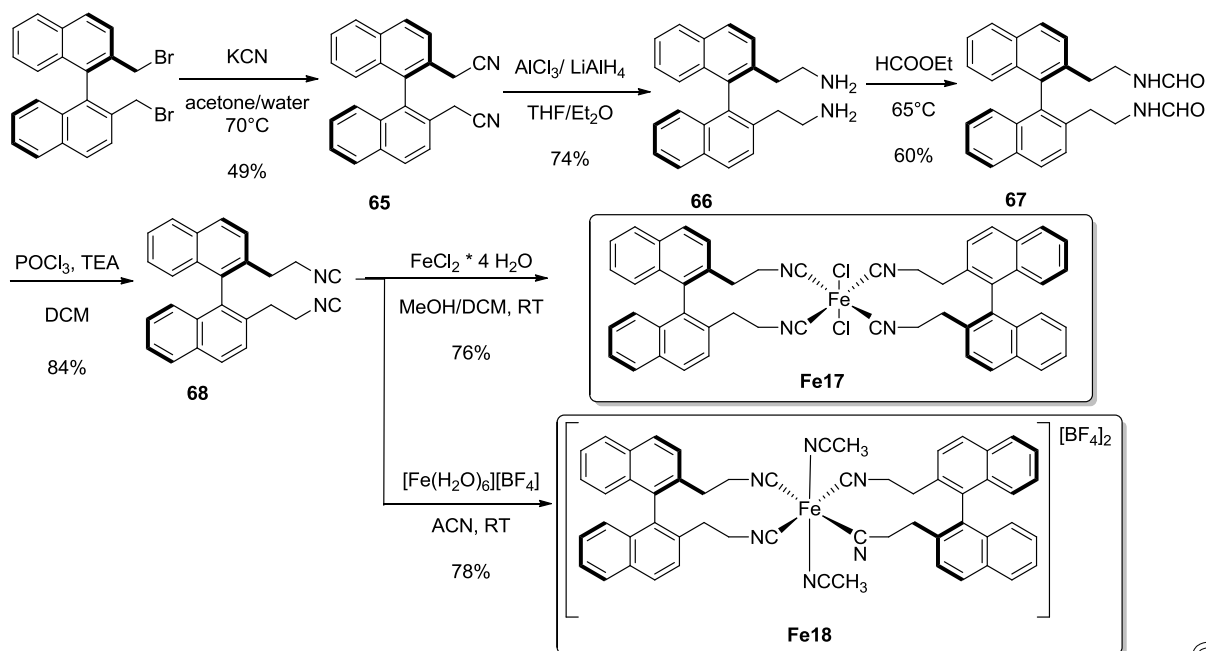
The observed lack of activity might be due to the fact that employed isonitriles are aromatic and not aliphatic as in complexes **36**, **Fe15** or **Fe16**. Under this hypothesis, the critical step of the catalytic cycle have to be the hydride transfer from the reduced isonitrile (imido) function to the coordinated substrate, as depicted in Scheme 4.6 (see Scheme 4.1 for the complete catalytic cycle). The hydride transfer may be disfavored when R is not aliphatic, as the isonitrile is less electron-rich.



Scheme 4.6 An aromatic isonitrile (R = Ar) can be less prone to transfer the hydride to the substrate, compared to an aliphatic one.

#### 4.4 Second generation of tetra(isonitrile) complexes

Considering possible reasons of failure of the previously synthesized tetra(isonitrile) complexes, our efforts continued to synthesize new aliphatic isonitrile iron(II) complexes, which were expected to be active catalysts for ketone transfer hydrogenation (Scheme 4.7).



Scheme 4.7. Synthesis of 2<sup>nd</sup> generation of isonitrile complexes **Fe17** and **Fe18**.

Synthesis of new complexes **Fe17** and **Fe18** started from commercially available (R)-2,2'-bis(bromomethyl)-1,1'-binaphthalene, which was converted into the bis-nitrile **65**. Various methods for reducing nitrile **65** to amine **66** were tested, but the one with LiAlH<sub>4</sub> / AlCl<sub>3</sub> proved to be the most efficient.<sup>133</sup> Bis-formylation of **66** and subsequent dehydration of **67** using phosphoryl chloride afforded ligand **68**. The workup of isonitrile **68** was problematic, as the use of a saturated aqueous solution of NaHCO<sub>3</sub> (generally used to quench isonitrile-forming reactions) caused product re-hydration to substrate **67**. We supposed that probably aq. NaHCO<sub>3</sub> did not quench the acidity generated from POCl<sub>3</sub> hydrolysis fast enough, which led to the acid-catalysed re-hydration to the isonitrile. As expected, use of a stronger base (10% aq. Na<sub>2</sub>CO<sub>3</sub>) prevented the re-hydration of **68**. Complexation with standard Fe(II) sources afforded complexes **Fe17** and **Fe18**, which were tested in transfer hydrogenation of acetophenone (Table 4.3).

Table 4.3 Catalytic screening of the second generation tetra(isonitrile) complexes in the transfer hydrogenation of **S2**.

Reaction scheme: Acetophenone (**S2**) reacts with a complex (5 mol%) and *t*BuOK (50 mol%) in *i*PrOH to form 1-phenylethanol (**P2**).

Entry	Complex	<i>T</i> (°C)	Time	Conv. (%)	<i>ee</i> (%)
1	<b>Fe17</b>	25	18	40	29
2	<b>Fe17</b>	25	48	42	26
3	<b>Fe17</b>	50	18	64	25
4	<b>Fe18</b>	25	18	12	15
5	<b>Fe18</b>	25	48	12	15
6	<b>Fe18</b>	50	18	13	8

The hypothesis of the necessity of aliphatic "arms" of isonitrile complexes to provide the efficient hydride transfer was confirmed. Catalyst **Fe17** was able to induce 29% *ee* with a 40% conversion (entry 1). Prolonged reaction time did not change this result, suggesting that catalyst **Fe17** got deactivated in the course of ATH (entry 2). Elevated temperature led to significantly higher conversion (64%), but along with an erosion of enantiomeric excess (25% *ee*, entry 3). Dicationic complex **Fe18** revealed much lower catalytic activity (entry 4) and much lower stability in time or at higher temperature (entries 5-6).

Upon comparison with the bis(isonitrile) complexes, obtained enantiomeric excess was nearly twice higher (29% *ee* for **Fe17** vs. 16% *ee* for **Fe13**), but it could be described only as very moderate when compared to the original catalyst **36** developed by Reiser and co-workers (up to 67% *ee*).<sup>91</sup>

#### 4.4.1 Possible improvements to the second generation isonitrile complexes

Positive results in ATH of acetophenone with the second generation tetra(isonitrile) complexes, encouraged us to think, how to increase the stereocontrol in the course of the reaction. Three possible structural modifications to tetra(isonitrile) complexes were evaluated as the most promising strategies (Figure 4.3):

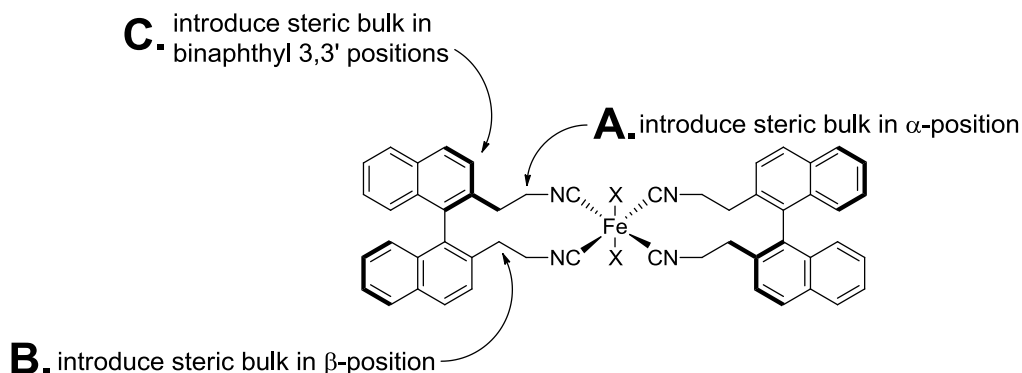
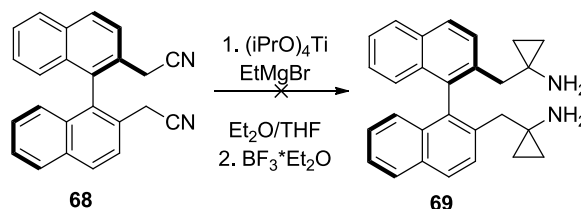


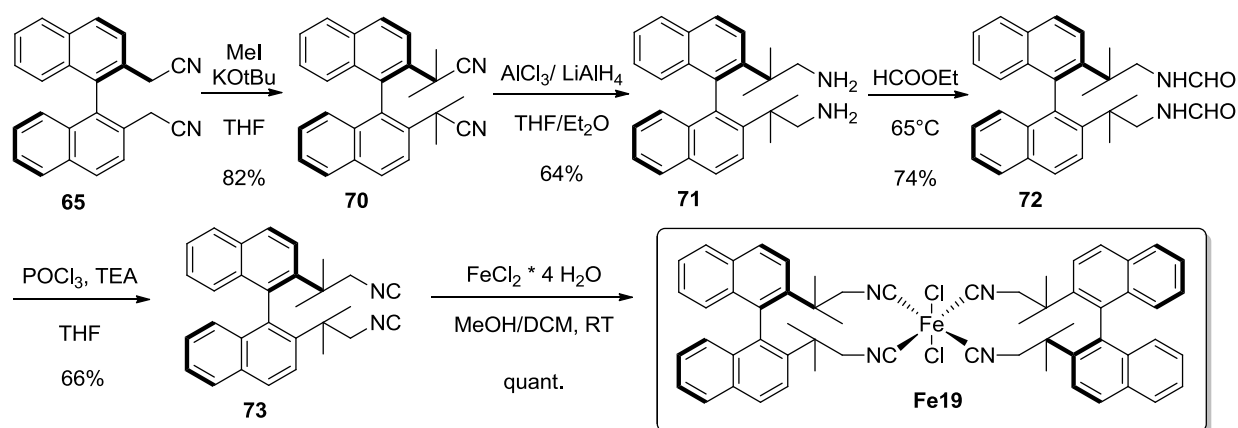
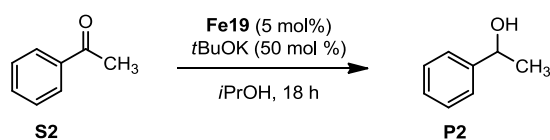
Figure 4.3 Possible structural improvements to the Fe-isonitrile catalysts.

Proceeding with the first proposal, we attempted to install substituents on the  $\alpha$  position of the alkyl chain. Unfortunately, this pathway was quickly abandoned. We were not able to synthesize a cyclopropane derivative according to a route published for phenylacetonitrile (Scheme 4.8).<sup>134</sup> Instead of the desired product **69**, only extensive degradation of the starting material **68** was observed.



Scheme 4.8 Unsuccessful attempt to introduce steric bulk in  $\beta$ -position of "isonitrile arm".

Our efforts to proceed with Strategy B and introduce steric bulk in  $\beta$ -positions of the isonitrile groups were successful. In addition to the previously reported synthesis of **Fe17** (Scheme 4.7), bis-nitrile **65** was methylated to **70** before being reduced to bis-amine **71** (Scheme 4.9). Following formylation and dehydration, new ligand **73** was obtained. Together with iron(II) chloride tetrahydrate, a new complex **Fe19** was successfully obtained and tested in ATH of acetophenone (Table 4.4).

Scheme 4.9. Introduction of steric bulk in  $\beta$ -positions of the isonitrile groups.Table 4.4 Catalytic screening of the improved second generation tetra(isonitrile) complex **Fe19** in the transfer hydrogenation of **S2**.

Entry	T (°C)	Conv. (%)	ee (%)
1	25	40	6
2	50	55	<2

To our great disappointment, installation of additional methyl groups on the alkyl chains led only to low or neglectable enantioselectivity along with lower conversions than in the case of previous Fe-isonitrile catalysts.

The last of proposed synthetic strategies, based on introducing steric bulk in binaphthyl 3,3'-positions (C from Figure 4.3) is still under investigation in our lab.

#### 4.5 Summary of the isonitrile complexes

In summary, being inspired by catalyst developed by Reiser and co-workers, we synthesized two new families of isonitrile complexes, eight of them in total. The first family of them, bis(isonitrile) iron catalysts **Fe12-14**, showed a moderate activity in terms of conversion and a low enantiomeric excess. The second family - tetra(isonitrile) complexes - proved to be better family of catalysts for the asymmetric transfer hydrogenation of ketones. Although initial attempts in the ATH with complexes **Fe15** and **Fe16** were unsuccessful, they were a confirmation of the postulated mechanism of this catalytic transformation, as required hydride transfer was disfavored when the isonitrile arm was aromatic and thus, less electron-rich. In second generation of tetra(isonitrile) complexes (**Fe17-Fe18**) this drawback was removed, but still obtained enantiomeric excess was rather low (up to 29% ee). In order to improve the transfer of the stereochemical information from the (*R*)-BINOL derived backbone, introductions of steric

bulk in different positions of the molecule were investigated, results obtained so far failed or led to lack of enantiocontrol in the ATH of ketones (**Fe19**). Synthesis of (*R*)-BINOL derived isonitriles with bulky 3,3'-substituents is currently underway in Gennari group.

## 4.6 Experimental section

### General remarks

All reactions were carried out in flame-dried glassware with magnetic stirring under nitrogen atmosphere, unless otherwise stated. Synthesis of complexes was performed under argon using standard Schlenk-techniques.

The solvents for reactions were distilled over the following drying agents and transferred under nitrogen: CH<sub>2</sub>Cl<sub>2</sub> (CaH<sub>2</sub>), MeOH (CaH<sub>2</sub>), CH<sub>3</sub>CN (CaH<sub>2</sub>), THF (Na), dioxane (Na), toluene (Na), hexane (Na), Et<sub>3</sub>N (CaH<sub>2</sub>). Acetophenone and *i*-PrOH were distilled on CaH<sub>2</sub> (a small amount of PPh<sub>3</sub> was added when distilling isopropanol) and stored over molecular sieves. Et<sub>2</sub>O and DMF were purchased in bottles with crown cap, over molecular sieves, and stored under nitrogen. The commercially available starting products [3,5-bis(trifluoromethyl)bromobenzene, (*S,S*)-2,2'-bipyrrrolidine D-tartrate trihydrate, 6-methoxy-2-pyridinecarboxaldehyde, 2-pyridine carboxaldehyde, 2,2'-bis(bromomethyl)-1,1'-biphenyl, 2-fluoronitrobenzene, (*R*)-binaphthol] were used as received.

The reactions were monitored by analytical thin-layer chromatography (TLC) using silica gel 60 F<sub>254</sub> pre-coated glass plates (0.25 mm thickness). Visualisation was accomplished by irradiation with a UV lamp and/or staining with a potassium permanganate alkaline solution, a ninydrine solution or a ceric ammonium molybdate solution. Flash column chromatography was performed using silica gel (60 Å, particle size 40-64 µm) as stationary phase, following the procedure by Still and co-workers.<sup>135</sup> Gas chromatography was performed by a GC instrument equipped with a flame ionization detector, using the chiral capillary column MEGADEX DACTBSβ, diacetyl-*t*-butylsilyl-β-cyclodextrin.

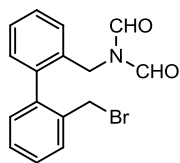
Proton NMR spectra were recorded on a spectrometer operating at 400.13 MHz. Proton chemical shifts are reported in ppm (δ) relative to tetramethylsilane (TMS) with the solvent resonance employed as the internal standard (CDCl<sub>3</sub>, δ = 7.26 ppm; CD<sub>2</sub>Cl<sub>2</sub>, δ = 5.32 ppm; (CD<sub>3</sub>)<sub>2</sub>SO, δ = 2.50 ppm; CD<sub>3</sub>OD, δ = 3.33 ppm; CD<sub>3</sub>CN, δ = 1.94 ppm). The following abbreviations are used to describe spin multiplicity: s = singlet, d = doublet, t = triplet, q = quartet, m = multiplet, br = broad signal. The coupling constant values are given in Hz. <sup>13</sup>C-NMR spectra were recorded on a 400 MHz spectrometer operating at 100.56 MHz, with complete proton decoupling. Carbon chemical shifts are reported in ppm (δ) relative to TMS with the respective solvent resonance as the internal standard (CDCl<sub>3</sub>, δ = 77.23 ppm; CD<sub>2</sub>Cl<sub>2</sub>, δ = 54.00 ppm; (CD<sub>3</sub>)<sub>2</sub>SO, δ = 39.51 ppm; CD<sub>3</sub>OD, δ = 49.05; CD<sub>3</sub>CN, δ = 118.26 ppm).

High resolution mass spectra (HRMS) were performed on a Fourier Transform Ion Cyclotron Resonance (FT-ICR) Mass Spectrometer APEX II & Xmass software (Bruker Daltonics) – 4.7 T Magnet (Magnex) equipped with ESI source, available at CIGA (Centro Interdipartimentale Grandi Apparecchiature) c/o Università degli Studi di Milano. Low resolution mass spectra (MS) were acquired either on a Thermo-Finnigan LCQ Advantage mass spectrometer (ESI ion source) or on a VG Autospec M246 spectrometer (FAB ion source).

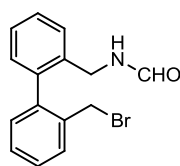
Elemental analyses were performed on a Perkin Elmer Series II CHNS/O Analyzer 2000.

Infrared spectra were recorded on a standard FT/IR spectrometer.

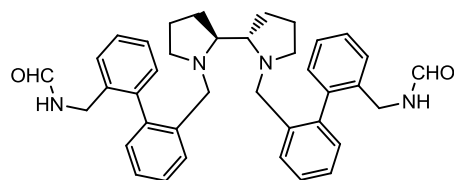


***N*-((2'-(Bromomethyl)biphenyl-2-yl)methyl)-*N*-formylformamide **56****

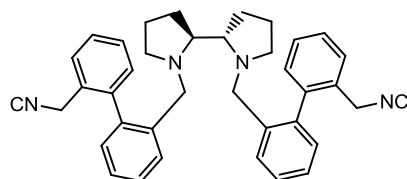
Sodium diformylamide (0.34 g, 3.5 mmol, 1.2 eq) was added to a stirred solution of 2,2'-bis(bromomethyl)-1,1'-biphenyl (1.00 g, 3.0 mmol, 1 eq) in 10 mL DMF. The reaction mixture was then stirred for 18 hours at 100 °C, then the solvent was evaporated. The residue was taken up with water and extracted with CH<sub>2</sub>Cl<sub>2</sub> (3x). The collected organic phases were dried with Na<sub>2</sub>SO<sub>4</sub>, filtered and evaporated. The crude was purified by FCC (hexane/AcOEt 8:2), giving **56** as a pale yellow oil in 72% yield. <sup>1</sup>H NMR (400 MHz, CDCl<sub>3</sub>): δ 8.90 (s, 2H), δ 7.60 (dd, *J* = 7.6, 1.4 Hz, 1H), δ 7.48-7.35 (m, 4 H), δ 7.34-7.30 (m, 1 H), δ 7.29-7.25 (m, 1H), δ 7.18 (br s, 1 H), δ 4.63 (d, *J* = 14.2 Hz, 1H), δ 4.56 (d, *J* = 14.2 Hz, 1H), δ 4.43 (d, *J* = 10.0 Hz, 1H), δ 4.24 (d, *J* = 10.0 Hz, 1H). ESI-MS in CH<sub>3</sub>CN: [M-CO+Na]<sup>+</sup> *m/z* 326.2, [M+Na]<sup>+</sup> *m/z* 354.2.

***N*-((2'-(Bromomethyl)biphenyl-2-yl)methyl)formamide **57****

Sodium *tert*-butoxide (20 mg, 0.18 mmol, 0.05 eq) was added to a stirred milky suspension of **56** (1.2 g, 3.6 mmol, 1 eq) in 20 mL EtOH. Upon addition the mixture became immediately clear. After 5 minutes, solid ammonium chloride was added and the reaction mixture was filtered through celite washing with CH<sub>2</sub>Cl<sub>2</sub>. Evaporation of the filtrate afforded **57** as a yellow oil which was purified with FCC (CH<sub>2</sub>Cl<sub>2</sub>/AcOEt 98:2). The product was obtained as a colourless oil in 91% yield. <sup>1</sup>H NMR (400 MHz, CDCl<sub>3</sub>): δ 8.12 (s, 1H), δ 7.56 (d, *J* = 10.7, 1H), δ 7.48-7.32 (m, 5H), δ 7.28-7.10 (m, 2H), δ 6.38 (br s, 1H), δ 4.32 (m, 2H), δ 4.27 (m, 2H). ESI-MS in CH<sub>3</sub>CN: [M+Na]<sup>+</sup> *m/z* 326.1.

***N,N'*-((2',2''-(2*S*,2'*S*)-2,2'-Bipyrrolidine-1,1'-diylbis(methylene)bis(biphenyl-2',2'-diyl))bismethylene)-diformamide **58****

NaOH (80 mg, 2.0 mmol, 6.7 eq) and **57** (204 mg, 0.66 mmol, 2.2 eq) were added in sequence to a stirred suspension of (*S,S*)-2,2'-bipyrrolidine D-tartrate trihydrate (104 mg, 0.30 mmol, 1 eq) in 24 mL H<sub>2</sub>O/CH<sub>2</sub>Cl<sub>2</sub> 1:1. The obtained mixture was stirred overnight at RT, then diluted with 1M NaOH and extracted with CH<sub>2</sub>Cl<sub>2</sub> (3x). The combined organic phases were dried with Na<sub>2</sub>SO<sub>4</sub> and concentrated in vacuo. The crude was purified by FCC (CH<sub>2</sub>Cl<sub>2</sub>/MeOH/aqueous NH<sub>3</sub> 33% 95:5:2). The collected fractions were combined, diluted with CH<sub>2</sub>Cl<sub>2</sub>, washed with water (2x) and dried with Na<sub>2</sub>SO<sub>4</sub>. Evaporation of solvents afforded **58** in 92% yield. <sup>1</sup>H NMR (400 MHz, CDCl<sub>3</sub>): δ 8.16 (s, 2H), δ 7.68 (s, 2H), δ 7.46-7.36 (m, 6H), δ 7.35-7.20 (m, 6H), δ 7.16 (m, 2H), δ 4.27 (m, 4H), δ 3.83 (d, *J* = 11.8 Hz, 2H), δ 2.72 (s, 2H), δ 2.56 (d, *J* = 11.8 Hz, 2H), δ 1.91 (br s, 2H), δ 1.56 (br s, 2H), δ 1.90-1.31 (m, 8H). ESI-MS in CH<sub>3</sub>CN: [M+H]<sup>+</sup> *m/z* 587.6; [M+Na]<sup>+</sup> *m/z* 609.5.

**(2*S*,2'*S*)-1,1'-Bis((2'-(isocyanomethyl)biphenyl-2-yl)methyl)-2,2'-bipyrrolidine (ISO) **60****

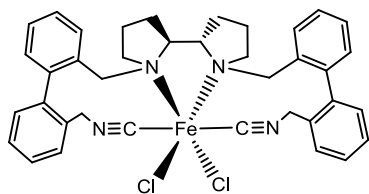
**Method 1.** To a mixture of **58** (1.34 g, 2.3 mmol, 1 eq) and triethylamine (0.86 mL, 9.6 mmol, 4.2 eq) in 13 mL CH<sub>2</sub>Cl<sub>2</sub> at 0 °C trichloromethyl chloroformate (diphosgene, 0.28 mL, 2.3 mmol, 1 eq) dissolved in 3 mL CH<sub>2</sub>Cl<sub>2</sub> was added with stirring over 1 h. After stirring for 25 minutes, the temperature was allowed to rise to 20 °C and the solution was washed with a saturated NaHCO<sub>3</sub>



## Chapter 4

aqueous solution. The organic phase was evaporated and the crude was purified by FCC (CH<sub>2</sub>Cl<sub>2</sub>/MeOH 99.5:0.5). Ligand **60** was obtained as a foamy solid in 89% yield. Method 2. A mixture of **58** (81 mg, 0.14 mmol, 1 eq) and TEA (0.13 mL, 1.38 mmol, 10 eq) in 1 mL THF was cooled to 0 °C. POCl<sub>3</sub> (28 μL, 0.30 mmol, 2.2 eq) was then added dropwise. After stirring overnight at RT, the yellow mixture was transferred into cold distilled water and extracted with CH<sub>2</sub>Cl<sub>2</sub> (3x). The collected organic phases were dried with Na<sub>2</sub>SO<sub>4</sub>, filtered and evaporated. Purification of the crude by FCC (CH<sub>2</sub>Cl<sub>2</sub>/MeOH 99.5:0.5) gave **60** as a yellow viscous oil in 54% yield. Method 3. NaOH (70 mg, 1.7 mmol, 6.3 eq) and **59** (170 mg, 0.60 mmol, 2.2 eq) were added in sequence to a stirred suspension of (*S,S*)-2,2'-bipyrrolidine D-tartrate trihydrate (94.0 mg, 0.27 mmol, 1 eq) in 20 mL H<sub>2</sub>O/CH<sub>2</sub>Cl<sub>2</sub> 1:1. The obtained mixture was stirred overnight at RT, then diluted with 1M NaOH and extracted with CH<sub>2</sub>Cl<sub>2</sub> (3x). The combined organic phases were dried with Na<sub>2</sub>SO<sub>4</sub> and concentrated in vacuo. The crude was purified by FCC (CH<sub>2</sub>Cl<sub>2</sub>/MeOH 99:1). Evaporation of solvents afforded **60** in 57% yield. <sup>1</sup>H NMR (400 MHz, CD<sub>2</sub>Cl<sub>2</sub>): δ 7.63 (d, *J* = 8.1 Hz, 2H), δ 7.57-7.31 (m, 10H), δ 7.19-7.05 (m, 4H), δ 4.50-4.24 (m, 4H), δ 3.75 (d, *J* = 12.4 Hz, 2H, rotamer I), δ 3.66 (d, *J* = 14.2 Hz, 2H, rotamer II), δ 3.64 (d, *J* = 12.1 Hz, 2H, rotamer III), δ 3.55 (d, *J* = 14.0 Hz, 2H, rotamer IV), δ 2.90-2.58 (m, 4H), δ 2.31 (m, 1H, rotamer I), δ 2.12 (m, 1H, rotamer II), δ 1.93-1.79 (m, 3H), δ 1.65-1.31 (m, 8H), δ 1.12 (m, 1H). <sup>13</sup>C NMR (100 MHz, CD<sub>2</sub>Cl<sub>2</sub>): δ 158.00, 139.95, 139.48, 137.62, 131.78, 129.51, 129.39, 128.05, 127.92, 127.74, 127.06, 126.48, 64.98, 57.23, 53.96, 43.82, 29.7, 25.04, 24.02. ESI-MS in CH<sub>3</sub>CN: [M+H]<sup>+</sup> *m/z* 551.6; [2M+Cu]<sup>+</sup> *m/z* 1163.5. HRMS: [M+H]<sup>+</sup> calculated *m/z* 551.31692, found 551.31741.

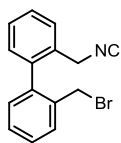
### [FeCl<sub>2</sub>(ISO)] Fe12



Under Ar, FeCl<sub>2</sub>·4H<sub>2</sub>O (56 mg, 0.27 mmol, 1 eq) was added to a stirred solution of ligand **60** (148 mg, 0.27 mmol, 1 eq) in 5 mL MeOH. Upon addition, the yellow solution became turbid brown. The reaction mixture was stirred overnight at RT, then Et<sub>2</sub>O was added to aid precipitation. The solvent was decanted off via syringe. The precipitate was washed again with Et<sub>2</sub>O (3x)

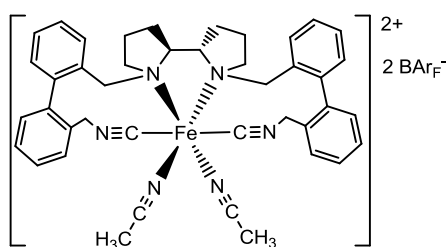
and CH<sub>2</sub>Cl<sub>2</sub> (1x). The beige solid was then dried under high vacuum. Yield: 69%. FAB-MS in MeOH: [M-Cl]<sup>+</sup> *m/z* 641.

### 2-(Bromomethyl)-2'-(isocyanomethyl)biphenyl **59**

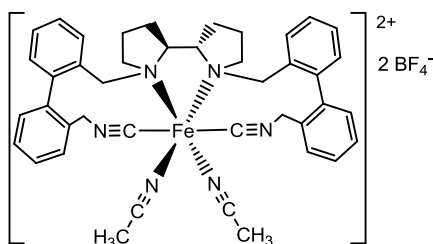


POCl<sub>3</sub> (37 μL, 0.40 mmol, 1.2 eq) was added dropwise to a stirred suspension of formamide **57** (102 mg, 0.34 mmol, 1 eq) and DIPEA (0.29 mL, 1.68 mmol, 5 eq) in 5 mL CH<sub>2</sub>Cl<sub>2</sub> kept at 0 °C. The reaction mixture was then stirred overnight at RT. On the next day a saturated NaHCO<sub>3</sub> aqueous solution and CH<sub>2</sub>Cl<sub>2</sub> were added, phases were

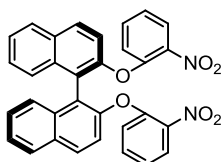
separated and the aqueous layer was extracted with CH<sub>2</sub>Cl<sub>2</sub> (3x). The collected organic phases were anhydriified with Na<sub>2</sub>SO<sub>4</sub>, filtered and evaporated. The crude was purified by FCC (hexane/AcOEt 9:1), obtaining **60** as a pale yellow foamy solid in 54% yield. <sup>1</sup>H NMR (400 MHz, CD<sub>2</sub>Cl<sub>2</sub>): δ 7.69 (dd, *J* = 7.6, 0.8 Hz, 1H), δ 7.62 (dd, *J* = 7.7, 1.6 Hz, 1H), δ 7.56 (td, *J* = 7.6, 1.6 Hz, 1H), δ 7.53-7.44 (m, 3H), δ 7.32 (dd, *J* = 7.6, 1.6 Hz, 1H), δ 7.24 (dd, *J* = 7.6, 1.6 Hz, 1H), δ 4.45 (d, *J* = 11.4 Hz, 1H), δ 4.42 (s, 2H), δ 4.34 (d, *J* = 11.4 Hz, 1H).

**[Fe(CH<sub>3</sub>CN)<sub>2</sub>(ISO)](BAR<sub>F</sub>)<sub>2</sub> Fe13**

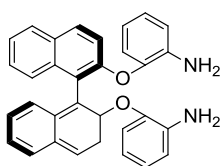
Under Ar, AgBAR<sub>F</sub> (245 mg, 0.25 mmol, 2 eq) was added to a stirred suspension of [FeCl<sub>2</sub>(ISO)] **Fe12** (85 mg, 0.13 mmol, 1 eq) in 4 mL CH<sub>3</sub>CN. Upon addition a whitish precipitate formed. After stirring for 4 hours with minimal light exposure, the reaction mixture was filtered under Ar through celite. Evaporation of the filtrate gave **Fe13** as a brown solid in 93% yield.

**[Fe(CH<sub>3</sub>CN)<sub>2</sub>(ISO)](BF<sub>4</sub>)<sub>2</sub> Fe14**

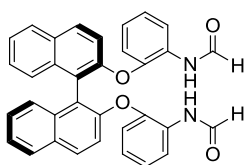
Under Ar, iron(II) tetrafluoroborate hexahydrate (97%, 356 mg, 1.02 mmol, 1 eq) was added to as stirred suspension of ligand **60** (561 mg, 1.02 mmol, 1 eq) in 10 mL CH<sub>3</sub>CN. After stirring overnight at RT, solvents were evaporated and the residue was washed with Et<sub>2</sub>O (3x). The obtained yellow solid was then dried under high vacuum. Yield: 86%. ESI-MS in CH<sub>3</sub>CN: [M-2CH<sub>3</sub>CN+F]<sup>+</sup> m/z 625.4.

**2,2'-Bis(2-nitrophenoxy)-1,1'-binaphthalene<sup>136</sup> 61**

2-fluoronitrobenzene (4.92 g, 34.9 mmol, 2 eq) was added to a stirred suspension of (*R*)-binaphthol (5.00 g, 17.4 mmol, 1 eq) and potassium carbonate (5.07 g, 36.7 mmol, 2.1 eq) in 60 mL DMF. The resulting yellow reaction mixture was heated overnight at 80 °C, then poured into cold water, with immediate precipitation of a yellow solid. The precipitate was filtered on Buchner washing with hot water (4x). After drying under high vacuum, **61** was obtained as a pale yellow solid in 98% yield. <sup>1</sup>H NMR (400 MHz, DMSO): δ 8.11 (d, *J* = 8.8 Hz, 2H), δ 8.02 (d, *J* = 8.0 Hz, 2H), δ 7.84 (dd, *J* = 8.0, 1.2 Hz, 2H), δ 7.48 (t, *J* = 7.6 Hz, 4H), δ 7.39-7.32 (m, 4H), δ 7.25-7.16 (m, 4H), δ 7.01 (d, *J* = 8.0 Hz, 2H).

**2,2'-([1,1'-Binaphthalene]-2,2'-diylbis(oxy))dianiline<sup>136</sup> 62**

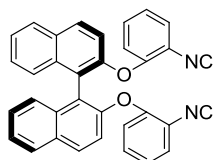
One drop of H<sub>2</sub>SO<sub>4</sub> was added to a stirred suspension of Pd/C (10%, 200 mg, 0.19 mmol, 0.01 eq) and **61** (9.09 g, 17.2 mmol, 1 eq) in 100 mL THF, then hydrogenated overnight under 1 bar H<sub>2</sub>. On the next day, the hydrogen burette was re-loaded and the reaction mixture was stirred for another night under 1 bar H<sub>2</sub>. The mixture was then filtered through celite washing with THF. Evaporation of the filtrate gave **62** as a whitish solid, which was used without purification in the following step. Yield: 99%. <sup>1</sup>H NMR (400 MHz, DMSO): δ 8.03 (d, *J* = 9.2 Hz, 2H), δ 7.99 (d, *J* = 8.0 Hz, 2H), δ 7.46 (td, *J* = 6.8, 1.2 Hz, 2H), δ 7.39 (td, *J* = 6.8, 1.2 Hz, 2H), δ 7.24 (d, *J* = 8.0 Hz, 2H), δ 7.10 (d, *J* = 9.2 Hz, 2H), δ 6.88 (td, *J* = 6.8, 1.2 Hz, 2H), δ 6.78-6.72 (m, 4H), δ 6.50 (td, *J* = 7.6, 1.2 Hz, 2H), δ 4.60 (s, 4H).

***N,N'*-([1,1'-Binaphthalene]-2,2'-diylbis(oxy))bis(2,1-phenylene)diformamide 63**

Dianiline **62** (1.00 g, 2.13 mmol, 1 eq) was added to a stirred suspension of ZnO (174 mg, 2.13 mmol, 1 eq) and formic acid (3.5 mL, excess). The reaction mixture was heated overnight at 70 °C, then was filtered through celite washing with CH<sub>2</sub>Cl<sub>2</sub> (3x). The filtrate was washed with water (x2)

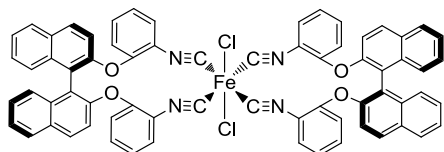
and saturated NaHCO<sub>3</sub> solution (1x). The organic layer was anhydriified with Na<sub>2</sub>SO<sub>4</sub>, filtered and evaporated to give a brown solid. Purification by FCC (CH<sub>2</sub>Cl<sub>2</sub>/AcOEt 93:7) afforded **63** as a pale pink solid in 78% yield. <sup>1</sup>H NMR (400 MHz, CDCl<sub>3</sub>): δ 8.55-8.38 (m, 1H), δ 8.23 (m, 1H), δ 8.00-7.88 (m, 4H), δ 7.82 (d, *J* = 1.2 Hz, 1H), δ 7.55-7.34 (m, 6H), δ 7.29-7.22 (m, 2H), δ 7.09-6.83 (m, 5H), δ 6.75-6.66 (m, 2H). <sup>13</sup>C NMR (100 MHz, CDCl<sub>3</sub>): δ 158.54, 151.47, 145.18, 133.81, 130.98, 130.54, 128.81, 128.35, 127.25, 125.39, 125.31, 124.25, 123.83, 122.00, 121.10, 118.76, 117.46. ESI-MS in CH<sub>3</sub>CN: [M+Na]<sup>+</sup> *m/z* 547.6, [2M+Na]<sup>+</sup> *m/z* 1071.2.

### 2,2'-Bis(2-isocyanophenoxy)-1,1'-binaphthalene (ISAR) **64**



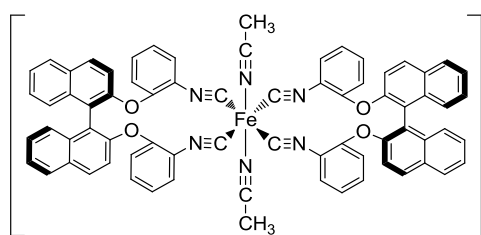
POCl<sub>3</sub> (287 μL, 3.07 mmol, 2.1 eq) was dropped into a stirred solution of **63** (767 mg, 1.46 mmol, 1 eq) and TEA (1.2 mL, 8.77 mmol, 6 eq) in 6 mL CH<sub>3</sub>CN. During the addition the reaction mixture darkened and became turbid. After stirring overnight at RT, the reaction mixture was poured into chilled NaHCO<sub>3</sub> aqueous solution and CH<sub>2</sub>Cl<sub>2</sub> was added. Phases were separated and the aqueous layer was extracted with CH<sub>2</sub>Cl<sub>2</sub> (3x). The combined organic phases were dried with Na<sub>2</sub>SO<sub>4</sub>, filtered and evaporated. Purification of the crude by FCC (hexane/AcOEt 95:5) afforded ligand **64** as an off-white foam in 58% yield. <sup>1</sup>H NMR (400 MHz, CD<sub>2</sub>Cl<sub>2</sub>): δ 7.99 (d, 11.9 Hz, 2H), δ 7.93 (d, 11.0 Hz, 2H), δ 7.46 (t, 10.3 Hz, 2H), δ 7.35 (m, 2H), δ 7.23 (t, 10.0 Hz, 2H), δ 7.15 (td, *J* = 10.1, 2.3 Hz, 2H), δ 6.91 (m, 2H).

### [FeCl<sub>2</sub>(ISAR)<sub>2</sub>] Fe15



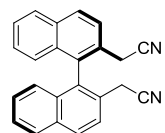
Under Ar, a solution of ligand **64** (181 mg, 0.38 mmol, 2 eq) in 5 mL CH<sub>2</sub>Cl<sub>2</sub> was added via cannula into a stirred solution of FeCl<sub>2</sub>·4H<sub>2</sub>O (38 mg, 0.19 mmol, 1 eq) in 7 mL MeOH. From the two yellow solution a reddish suspension formed. The reaction mixture was stirred overnight at RT, then solvents were removed under high vacuum and the residue was washed with hexane (2x), decanting the solvent off. **Fe15** was obtained as an orange solid in 80% yield. ESI-MS in CH<sub>3</sub>CN: [M-Cl]<sup>+</sup> *m/z* 1067.5.

### [Fe(CH<sub>3</sub>CN)<sub>2</sub>(ISAR)<sub>2</sub>](BF<sub>4</sub>)<sub>2</sub> Fe16



Under Ar, iron(II) tetrafluoroborate hexahydrate (107 mg, 0.31 mmol, 1 eq) was added to a stirred solution of ligand **64** (300 mg, 0.61 mmol, 2 eq) in 7 mL CH<sub>3</sub>CN. Upon addition the solution turned reddish/brown. The reaction mixture was stirred overnight at RT, then the solvent was concentrated to a volume of 1 mL. Addition of 15 mL Et<sub>2</sub>O caused precipitation of a dark yellow solid. Solvents were evaporated again and the residue was washed with Et<sub>2</sub>O, removing the solvent via syringe (3x). **Fe16** was obtained as a dark yellow powder in 78% yield. ESI-MS in CH<sub>3</sub>CN: [M-2CH<sub>3</sub>CN]<sup>2+</sup> *m/z* 516.7, [M-CH<sub>3</sub>CN]<sup>2+</sup> *m/z* 536.6; [2BF<sub>4</sub>+Na]<sup>-</sup> *m/z* 197.5.

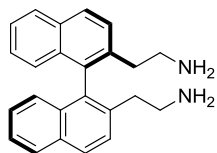
### (*R*)-2,2'-([1,1'-binaphthalene]-2,2'-diyl)diacetonitrile **65**



To a suspension of (*R*)-2,2'-bis(bromomethyl)-1,1'-binaphthalene (1.3 g, 2.95 mmol, 1 eq) in 6 mL DMF, solid KCN (0.44 g, 6.8 mmol, 2.3 eq) was added. After stirring overnight at 70 °C, DMF was evaporated and the reaction mixture was

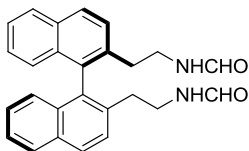
dissolved in  $\text{CH}_2\text{Cl}_2$  and water was added. Phases were separated and the aqueous layer was extracted with  $\text{CH}_2\text{Cl}_2$  (3x). The combined organic phases were dried with  $\text{Na}_2\text{SO}_4$ , filtered and evaporated. Purification of the crude by FCC (hexane/AcOEt 8:2) allowed to obtain **65** with 49% yield.  $^1\text{H}$  NMR (400 MHz,  $\text{CDCl}_3$ ):  $\delta$  8.1 (d,  $J$  = 8.8 Hz, 2H),  $\delta$  8.0 (d,  $J$  = 8.4 Hz, 2H),  $\delta$  7.8 (d,  $J$  = 8.4 Hz, 2H),  $\delta$  7.6 (dt,  $J$  = 7.2, 1.2 Hz, 2H),  $\delta$  7.4 (dt,  $J$  = 7.2, 1.2 Hz, 2H),  $\delta$  7.1 (d,  $J$  = 8.8 Hz, 2H),  $\delta$  3.4 (d,  $J$  = 9.5 Hz, 2H),  $\delta$  3.3 (d,  $J$  = 9.5 Hz, 2H).

**(R)-2,2'-([1,1'-binaphthalene]-2,2'-diyl)diethanamine 66**



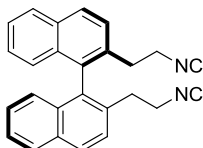
To a solution of  $\text{AlCl}_3$  (0.81 g, 6.1 mmol, 4.2 eq) and  $\text{LiAlH}_4$  (0.23 g, 6.1 mmol, 4.2 eq) in 15 mL of THF, a solution of **65** (0.48 g, 1.44 mmol, 1 eq) was added dropwise. Mixture was stirring overnight under low  $\text{N}_2$  flow. Reaction was diluted with 5 mL of water and 8 mL of 3 M  $\text{H}_2\text{SO}_4$  was added dropwise under  $\text{N}_2$  flow. Reaction mixture was diluted with  $\text{CH}_2\text{Cl}_2$ . Phases were separated and the aqueous layer was extracted with  $\text{CH}_2\text{Cl}_2$  (3x). The combined organic phases were dried with  $\text{Na}_2\text{SO}_4$ , filtered and evaporated. Crude **66** was used without purification in the following step.  $^1\text{H}$  NMR (400 MHz,  $\text{CDCl}_3$ ):  $\delta$  7.9 (m, 2H),  $\delta$  7.7 (m, 2H),  $\delta$  7.6 (m, 2H),  $\delta$  7.5 (m, 2H),  $\delta$  7.4 (m, 2H),  $\delta$  7.1 (m, 2H),  $\delta$  2.8 (m, 2H),  $\delta$  2.6 (m, 2H),  $\delta$  1.6 (br, 2H)

**(R)-N,N'-([1,1'-binaphthalene]-2,2'-diyl)bis(ethane-2,1-diyl)diformamide 67**



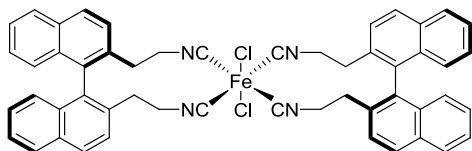
Crude **66** was dissolved in 5 mL of ethyl formate and refluxed for 48 h. Purification of the crude by FCC (DCM/MeOH 97:3) allowed to obtain **67** in 60% yield.  $^1\text{H}$  NMR (400 MHz,  $\text{CDCl}_3$ ):  $\delta$  8.0 (d,  $J$  = 8.8 Hz, 2H),  $\delta$  7.9 (d,  $J$  = 8.4 Hz, 2H),  $\delta$  7.7 (d,  $J$  = 8.4 Hz, 2H),  $\delta$  7.5 (dt,  $J$  = 7.2, 1.2 Hz, 2H),  $\delta$  7.3 (dt,  $J$  = 7.2, 1.2 Hz, 2H),  $\delta$  7.0 (d,  $J$  = 8.8 Hz, 2H),  $\delta$  3.5 (m, 2H),  $\delta$  3.3 (m, 2H),  $\delta$  2.6 (m, 2H). ESI-MS in  $\text{CH}_3\text{CN}$ :  $[\text{M}-\text{Na}]^+$   $m/z$  419.6.

**(R)-2,2'-bis(2-isocyanoethyl)-1,1'-binaphthalene (ISAL)68**

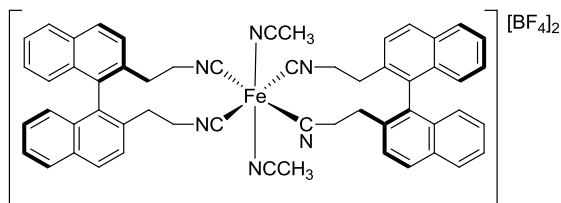


$\text{POCl}_3$  (90  $\mu\text{L}$ , 0.9 mmol, 2.2 eq) was dropped into a stirred solution of **67** (165 mg, 4.2 mmol, 1 eq) and TEA (0.3 mL, 3.35 mmol, 8 eq) in 6 mL DCM. During the addition the reaction mixture darkened and became turbid. After stirring 3 h at RT, the reaction mixture was poured into chilled  $\text{NaCO}_3$  aqueous solution and  $\text{CH}_2\text{Cl}_2$  was added. Phases were separated and the aqueous layer was extracted with  $\text{CH}_2\text{Cl}_2$  (3x). The combined organic phases were dried with  $\text{Na}_2\text{SO}_4$ , filtered and evaporated. Purification of the crude by FCC (DCM) afforded ligand **64** as an off-white foam in 84% yield.  $^1\text{H}$  NMR (400 MHz,  $\text{CDCl}_3$ ):  $\delta$  8.1 (d,  $J$  = 8.8 Hz, 2H),  $\delta$  8.0 (d,  $J$  = 8.4 Hz, 2H),  $\delta$  7.6 (d,  $J$  = 8.4 Hz, 2H),  $\delta$  7.5 (m, Hz, 2H),  $\delta$  7.3 (m, 2H),  $\delta$  7.0 (d,  $J$  = 8.4 Hz, 2H),  $\delta$  3.3 (m, 4H),  $\delta$  2.8 (m, 4H).

**$[\text{FeCl}_2(\text{ISAL})_2]$  Fe17**

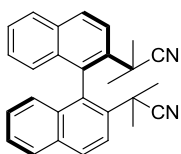


Under Ar, a solution of ligand **68** (111 mg, 0.39 mmol, 2 eq) in 5 mL  $\text{CH}_2\text{Cl}_2$  was added via cannula into a stirred solution of  $\text{FeCl}_2 \cdot 4\text{H}_2\text{O}$  (39 mg, 0.20 mmol, 1 eq) in 7 mL MeOH. From the two yellow solution a reddish suspension formed. The reaction mixture was stirred overnight at RT, then solvents were removed under high vacuum and the residue was washed with hexane (2x), decanting the solvent off. **Fe17** was obtained as an orange solid in 76% yield. ESI-MS in  $\text{CH}_3\text{CN}$ :  $[\text{M}-\text{Cl}+\text{ACN}]^+$   $m/z$  851.9.

**[Fe(CH<sub>3</sub>CN)<sub>2</sub>(ISAL)<sub>2</sub>](BF<sub>4</sub>)<sub>2</sub> Fe18**

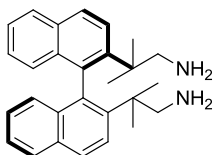
Under Ar, iron(II) tetrafluoroborate hexahydrate (70 mg, 0.20 mmol, 1 eq) was added to a stirred solution of ligand **68** (145 mg, 0.4 mmol, 2 eq) in 5 mL CH<sub>3</sub>CN. Upon addition the solution turned brown. The

reaction mixture was stirred overnight at RT, then the solvent was concentrated to a volume of 1 mL. Addition of 15 mL Et<sub>2</sub>O caused precipitation of a dark yellow solid. Solvents were evaporated again and the residue was washed with Et<sub>2</sub>O, removing the solvent via syringe (3x). **Fe18** was obtained as a dark yellow powder in 78% yield. ESI-MS in CH<sub>3</sub>CN: [M-2CH<sub>3</sub>CN]<sup>2+</sup> m/z 516.7, [M-CH<sub>3</sub>CN]<sup>2+</sup> m/z 858.3; [2BF<sub>4</sub>+Na]<sup>-</sup> m/z 1055.5.

**(R)-2,2'-([1,1'-binaphthalene]-2,2'-diyl)bis(2-methylpropanenitrile) 70**

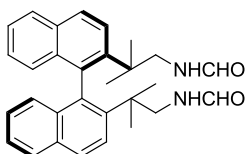
Under N<sub>2</sub>, in a Shlenk flask, to a solution of tBuOK (0.93 g, 8.25 mmol, 5.5 eq) in THF (3 mL) at -30°C, a solution of nitrile **65** (0.50 g, 1.5 mmol, 1 eq) and methyl iodide (0.84 mL, 13.5 mmol, 9 eq) in THF (4 mL) is added slowly over 20 minutes. The reaction was allowed to reach R.T. and was stirred for 1 hour. The

reaction was quenched with water (8 mL) and diluted with EtOAc (15 mL). Phases were separated and the aqueous layer was washed with EtOAc (2 x 10 mL). The combined organic layers were washed with water (20 mL), brine (20 mL) and dried over Na<sub>2</sub>SO<sub>4</sub>, filtered and evaporated affording **70** in 82% yield (0.48 g, 1.23 mmol). <sup>1</sup>H NMR (400 MHz, CDCl<sub>3</sub>) δ 8.09 (d, *J* = 8.9 Hz, 2H), 7.91 (d, *J* = 8.2 Hz, 2H), 7.62 (d, *J* = 8.9 Hz, 2H), 7.46 (t, *J* = 7.5 Hz, 2H), 7.23 (d, *J* = 7.8 Hz, 2H), 6.98 (d, *J* = 8.6 Hz, 2H), 1.89 (s, 6H), 1.56 (s, 6H). ESI-MS in MeOH: [M+Na]<sup>+</sup> m/z 411.4 (calcd. for C<sub>28</sub>H<sub>24</sub>N<sub>2</sub> 388.5).

**(R)-2,2'-([1,1'-binaphthalene]-2,2'-diyl)bis(2-methylpropan-1-amine) 71**

To a solution of AlCl<sub>3</sub> (260 mg, 1.96 mmol, 3 eq) and LiAlH<sub>4</sub> (75 mg, 1.96 mmol, 3 eq) in 5 mL of Et<sub>2</sub>O, a solution of **70** (250 mg, 0.65 mmol, 1 eq) in THF (5 mL) was added dropwise. Mixture was stirring overnight under low N<sub>2</sub>

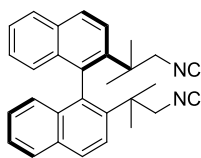
flow. Reaction was diluted with 5 mL of water and 8 mL of 3 M H<sub>2</sub>SO<sub>4</sub> was added dropwise under N<sub>2</sub> flow. Reaction mixture was diluted with CH<sub>2</sub>Cl<sub>2</sub>. Phases were separated and the aqueous layer was extracted with CH<sub>2</sub>Cl<sub>2</sub> (3x). The combined organic phases were dried with Na<sub>2</sub>SO<sub>4</sub>, filtered and evaporated. Crude **71** was used without purification in the following step. <sup>1</sup>H NMR (400 MHz, CDCl<sub>3</sub>): δ 8.0 (m, 2H), δ 7.8 (m, 2H), δ 7.7 (m, 2H), δ 7.5 (m, 2H), δ 7.4 (m, 2H), δ 7.1 (m, 2H), δ 2.8 (m, 2H), δ 2.6 (m, 2H), δ 1.16 (s, 6H), δ 0.70 (s, 6H).

**(R)-N,N'-([1,1'-binaphthalene]-2,2'-diyl)bis(2-methylpropane-2,1-diyl)diformamide 72**

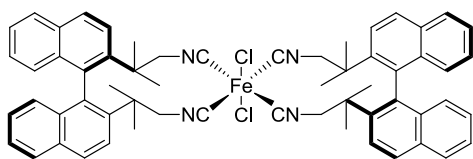
Crude **71** was dissolved in 5 mL of ethyl formate and refluxed for 48 h.

Purification of the crude by FCC (DCM/MeOH 97:3) allowed to obtain **67** in 64% yield. <sup>1</sup>H NMR (400 MHz, DMSO) δ 8.00 (d, *J* = 9.0 Hz, 2H), 7.90 (d, *J* = 7.7 Hz, 2H), 7.83 (d, *J* = 9.0 Hz, 2H), 7.77 (s, *J* = 17.6 Hz, 2H), 7.40 (t, *J* = 7.3

Hz, 2H), 7.18 (t, *J* = 7.3 Hz, 2H), 6.90 (d, *J* = 8.6 Hz, 2H), 3.24 (dd, *J* = 13.2, 5.9 Hz, 2H), 3.17 (d, *J* = 4.8 Hz, 2H), 1.03 (s, *J* = 6.5 Hz, 6H), 0.70 (s, 6H).

**(R)-2,2'-bis(1-isocyano-2-methylpropan-2-yl)-1,1'-binaphthalene 73**

$\text{POCl}_3$  (50  $\mu\text{L}$ , 0.59 mmol, 2.2 eq) was dropped into a stirred solution of **72** (120 mg, 0.265 mmol, 1 eq) and TEA (0.3 mL, 2.12 mmol, 8 eq) in 3 mL THF. During the addition the reaction mixture darkened and became turbid. After stirring overnight at RT, the reaction mixture was poured into chilled  $\text{NaCO}_3$  aqueous solution and  $\text{CH}_2\text{Cl}_2$  was added. Phases were separated and the aqueous layer was extracted with  $\text{CH}_2\text{Cl}_2$  (3x). The combined organic phases were dried with  $\text{Na}_2\text{SO}_4$ , filtered and evaporated. Purification of the crude by FCC (DCM/MeOH 95:5) afforded ligand **73** as an off-white foam in 66% yield.  $^1\text{H}$  NMR (400 MHz,  $\text{CD}_2\text{Cl}_2$ )  $\delta$  8.05 (d,  $J = 9.0$  Hz, 2H), 7.93 (d,  $J = 8.1$  Hz, 2H), 7.76 (d,  $J = 9.0$  Hz, 2H), 7.48 (s, 2H), 7.24 (s, 2H), 6.95 (d,  $J = 8.6$  Hz, 2H), 3.44 (s, 4H), 1.34 (s, 6H), 1.02 (s, 6H).

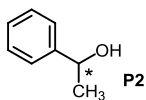
**Fe19**

Under Ar, a solution of ligand **72** (65 mg, 0.144 mmol, 2 eq) in 2.5 mL  $\text{CH}_2\text{Cl}_2$  was added via cannula into a stirred solution of  $\text{FeCl}_2 \cdot 4\text{H}_2\text{O}$  (14 mg, 0.072 mmol, 1 eq) in 2.5 mL MeOH. From the two yellow solution a orange suspension formed. The reaction mixture was stirred overnight at RT, then solvents were removed under high vacuum and the residue was washed with hexane (2x), decanting the solvent off. **Fe19** was obtained as an orange solid in quantitative yield. ESI-MS in  $\text{CH}_3\text{CN}$ :  $[\text{M}-\text{Cl}+\text{ACN}]^+$   $m/z$  964.1 (calcd. for  $\text{C}_{60}\text{H}_{56}\text{Cl}_2\text{FeN}_4$  958.3).

**General procedure for the transfer hydrogenation of acetophenone (S2).** A carousel multi-reactor was employed, allowing eight reactions in parallel under nitrogen atmosphere. Under  $\text{N}_2$  flow, the selected complex (4 mg, 0.05 eq) and the desired base (0.50 or 0.75 eq) were introduced in special glass vessels, which were then closed with screw caps and purged with nitrogen. Distilled isopropanol (2 mL) and acetophenone (10-20  $\mu\text{L}$ , 1 eq) were added via syringe and the reactions were stirred under nitrogen at the desired temperature for a given time, then analyzed for conversion and *ee* determination.

**Conditions for conversion and *ee* determination**

**1-Phenylethanol P2.** Conversion and *ee* were determined by GC (capillary column: MEGADEX DACTBS $\beta$ , diacetyl-*tert*-butylsilyl- $\beta$ -cyclodextrin, 0.25  $\mu\text{m}$ ; diameter = 0.25 mm; length = 25 m; carrier: hydrogen; hydrogen pressure: 1 bar; oven temperature: 75  $^\circ\text{C}$  for 5 min, 20  $^\circ\text{C}/\text{min}$  gradient until 95  $^\circ\text{C}$ , 95  $^\circ\text{C}$  for 15 min, then a 20  $^\circ\text{C}/\text{min}$  gradient is applied):  $t_{\text{substrate}}$  = 9.3 min;  $t_{\text{product-en1}}$  = 17.5 min;  $t_{\text{product-en2}}$  = 19.8 min.



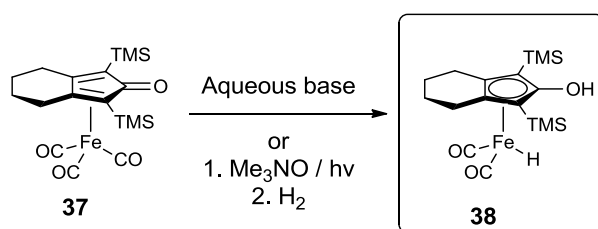




## 5 Chiral (cyclopentadienone)iron complexes

### 5.1 (*R*)-BINOL derived complexes<sup>137</sup>

Cyclopentadienone(iron) complexes are very robust pre-catalysts which can be used in a range of hydrogenations and transfer hydrogenations, as it was described in the Paragraph 2.4.7. When compared to other iron complexes described in Chapter 2, they present the advantage of not being sensitive to air or moisture, besides being easy to synthesize and purify using simple silica gel chromatography. The most well known cyclopentadienone(iron) is complex **37**, which can be activated *in situ* and transformed into active (cyclopentadienyl)iron hydride **38** – best known as “Knölker-Casey catalyst”. The transformation **37** → **38** can be accomplished by the Hieber base reaction<sup>101</sup> or by oxidative/photolytic cleavage of CO ligand with subsequent H<sub>2</sub> splitting (Scheme 5.1).<sup>99,100</sup>



Scheme 5.1 Activation of cyclopentadienone(iron) pre-catalyst **37** to form the Knölker-Casey catalyst **38**.

Despite their inherent advantages of cyclopentadienone(iron) complexes, the development of chiral complexes to be used as enantioselective pre-catalysts still remains a major challenge (see Paragraph 2.4.7.2). Replacement of one of the CO ligands with a chiral phosphoramidite by Berkessel and co-workers led to formation of two diastereoisomers, which in effect led to only 31% *ee* in the AH of ketones (Figure 5.1a).<sup>104</sup> Insertion of a stereocenter in the ring fused with cyclopentadienone made by Wills and co-workers, led to only 25% *ee*, most likely as an effect of the excessive distance between the stereocentre and the reaction centre (Figure 5.1b).<sup>105</sup> The best result so far was obtained by Beller and co-workers, who used a chiral phosphoric acid additive as a sort of "chiral template" between catalyst **38** and the substrate: ketimines could be hydrogenated with excellent conversions and enantiomeric excesses (up to 98% *ee*), but this methodology was not be applied for ketones (Figure 5.1c).<sup>106-109</sup>

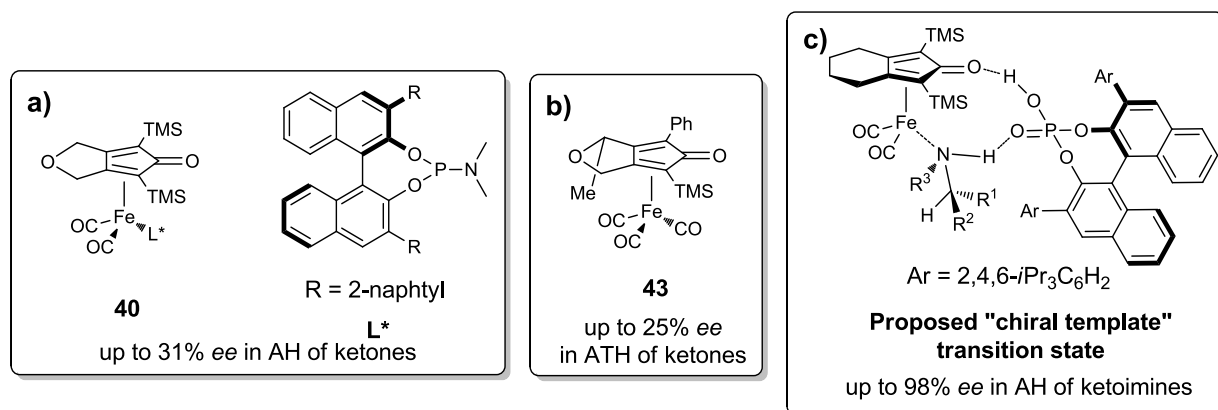


Figure 5.1 Reported attempts for enantioselective transformations using cyclopentadienone(iron) complexes.

Seeking room for improvement of chiral transformations with cyclopentadienone(iron) complexes, we decided to investigate this field, particularly focusing on the asymmetric hydrogenation of ketones. In principle, our approach was related to that used by Wills and co-workers,<sup>105</sup> as we wanted to introduce the stereocentre directly to the cyclopentadienone ligand. We thus decided to develop new chiral complex basing on (*R*)-BINOL [(*R*)-1,1'-bi-2-naphthol] backbone (Figure 5.2), analogously to what done by Cramer *et al.*<sup>138</sup> for their chiral rhodium(I) Cp complex **74**. The selected (*R*)-BINOL backbone possesses numerous advantages, as it is a stable, rigid, readily available and relatively cheap chiral starting material (it costs ~1 €/g).<sup>139</sup>

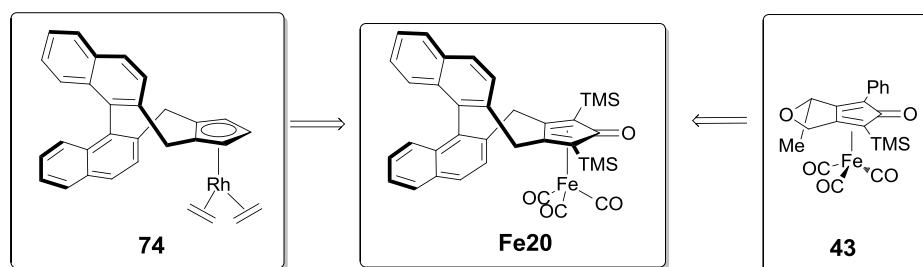
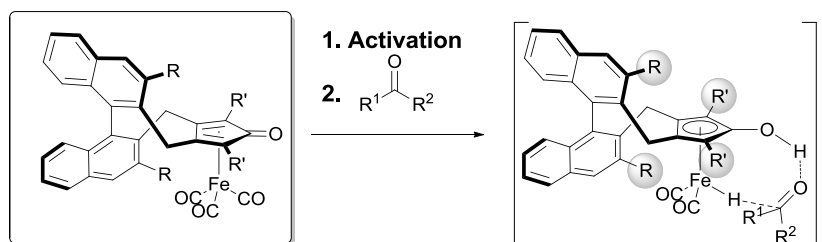


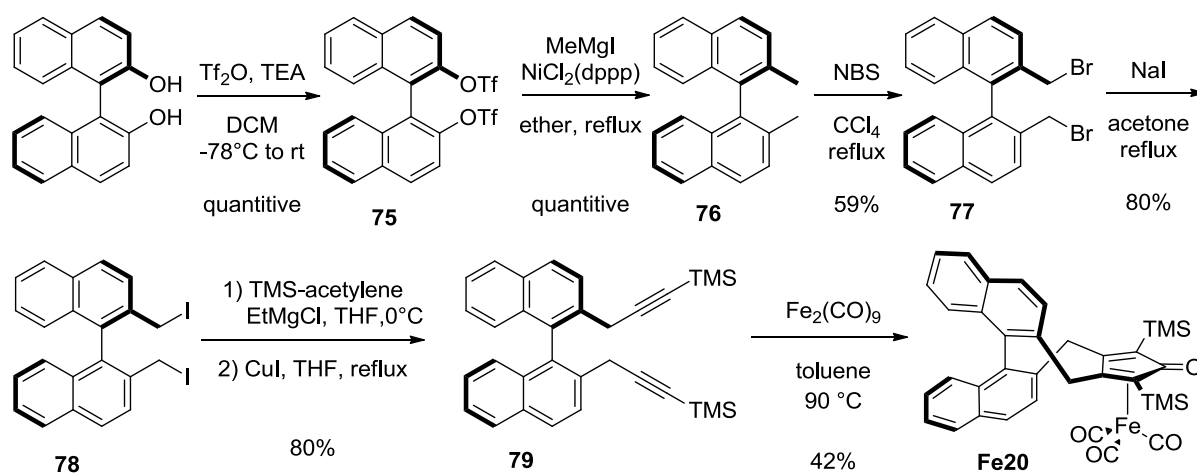
Figure 5.2 Idea for synthesizing a new chiral iron pre-catalyst **Fe20**.

As we foresaw that the binaphthyl stereoaxis would be relatively far from the reaction centre, we speculated that certain structural modifications could improve the transfer of the stereochemical information or just act as a directing groups for substrates (Scheme 5.2). This is observations were in line with previously used BINOL-derived complexes.<sup>138,140</sup>

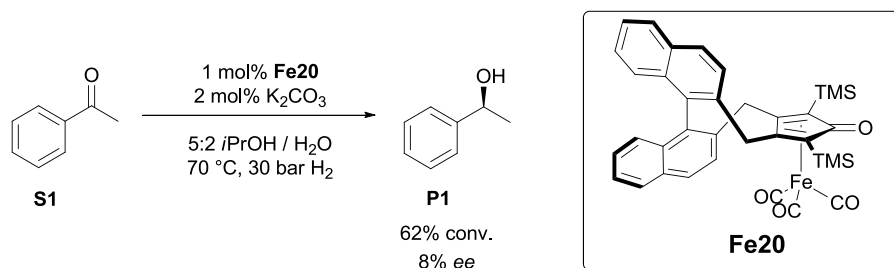


Scheme 5.2 General structure of new chiral iron pre-catalysts and expected importance of binaphthyl 3,3'-substituents and cyclopentadienone 2,5-substituents in AH.

We first decided to synthesize the 3,3'-unsubstituted pre-catalyst **Fe20**, featuring TMS groups in the 2,5-positions of cyclopentadienone ring (Scheme 5.3). The early steps of our synthesis (up to **77**) involved quite simple chemical transformations, already described by Maruoka and co-workers.<sup>141</sup> The sequence started from (*R*)-BINOL which was triflated to **75**. Following bis-methyl derivative **76** was obtained by Kumada cross-coupling with a Grignard reagent without a loss of enantiopurity.<sup>142</sup> Radical bromination of compound **76** using NBS yielded the bis-bromide **77**. Following a procedure reported for related benzyl bromide substrates,<sup>143</sup> the bis-bromide **77** was treated with (TMS-ethynyl)magnesium bromide in the presence of CuI, but no conversion was observed. However, the synthesis of the bis-alkyne **79** could be achieved under similar conditions using the bis-iodide **78**, readily obtained from **77** by halogen exchange, as a substrate. Cyclization of **79** in the presence of Fe<sub>2</sub>(CO)<sub>9</sub> under the conditions reported by Renaud and co-workers<sup>99a</sup> afforded a new pre-catalyst **Fe20**. Complex **Fe20** met our expectations and proved to be stable in air and upon purification using silica column chromatography.

Scheme 5.3 Synthesis of new chiral iron complex **Fe20**.

The new chiral cyclopentadienone(iron) pre-catalyst **Fe20** was tested in the asymmetric hydrogenation of acetophenone under conditions similar to the one reported by Beller and co-workers for the achiral pre-catalyst **37** (Scheme 5.4).<sup>101</sup>

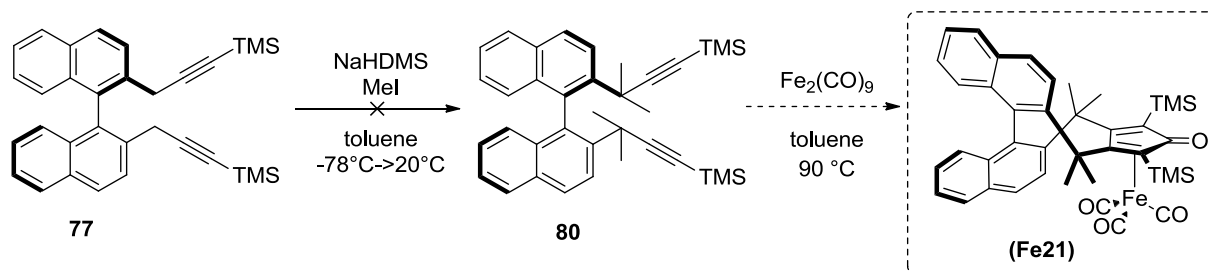
Scheme 5.4 AH of acetophenone **S1** using chiral complex **Fe20**.

The first catalytic attempt led to 62% conversion and low enantiomeric excess - just 8% *ee*. Moderate conversion was not discouraging, as we expected to that the newly synthesized pre-catalyst **Fe20** may require optimization of the hydrogenation's



conditions. As for the low enantiomeric excess, the result confirmed our suspects that the pre-catalyst without 3,3'-substituents could have problems of inefficient transfer of stereochemical information from the stereocentre to the reaction centre (Scheme 5.2).

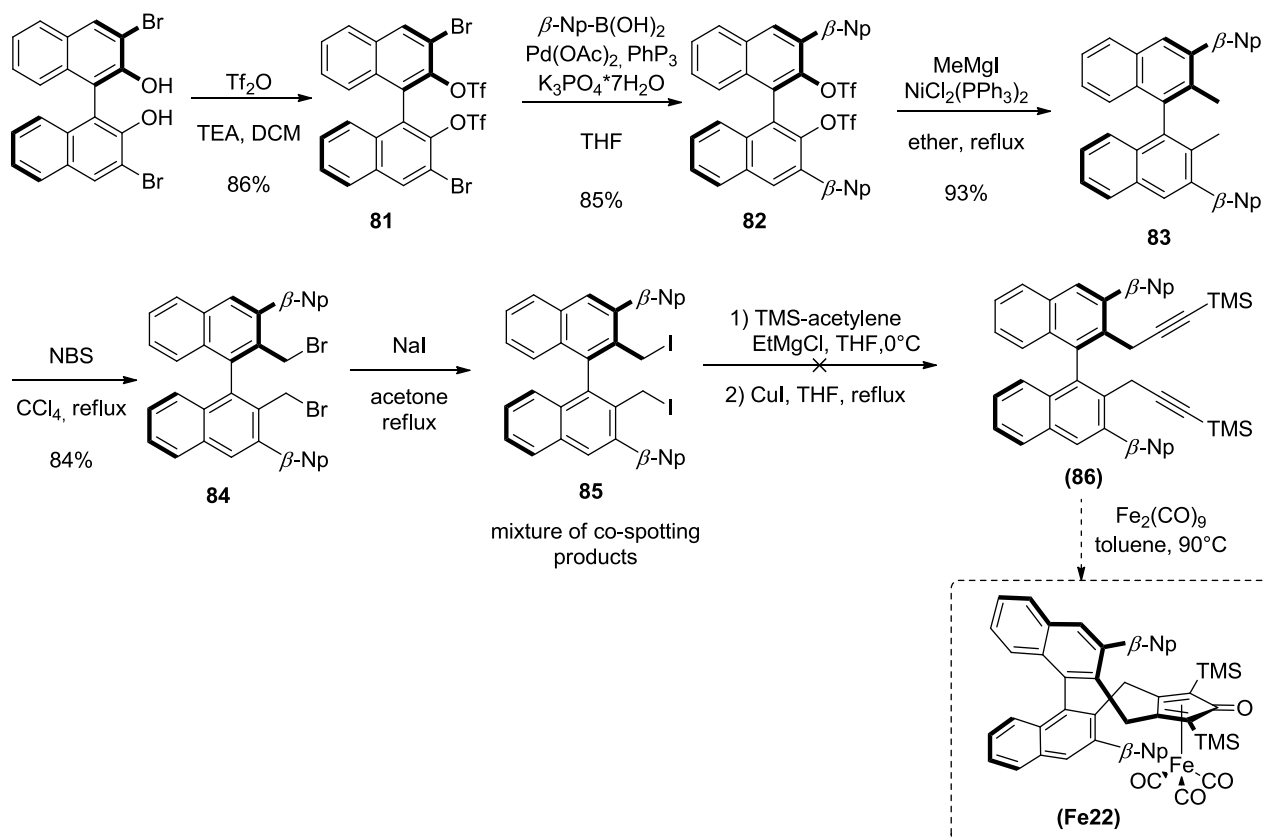
With the expectation that an enhanced steric bulk next to the cyclopentadienone ring could enhance the transmission of stereochemical information, we tried to prepare the pre-catalyst **Fe21**, featuring four methyl groups next to the cyclopentadienone ring. Thus, we tried to methylate compound **77**, but unfortunately this reaction was unsuccessful and only led to decomposition of the starting material (Scheme 5.5).



Scheme 5.5 Attempt to increase the steric bulk by introducing methyl groups.

This additional attempt led us back to conclusion that it would be the best to install bulky substituents in the 3,3'-positions of the binaphthyl moiety. Molecular modeling suggested that the best substituent would be the flat and rigid  $\beta$ -naphthyl. We selected commercially available (*R*)-3,3'-dibromo-[1,1'-binaphthalene]-2,2'-diol as the starting point of the new synthetic pathway (Scheme 5.6). This chiral substrate was triflated to yield **81** and then compound **82** was obtained, using Suzuki-Miyaura cross coupling with  $\beta$ -naphthyl boronic acid. The latter reaction proceeded very slowly, most likely because of the bulkiness of  $\beta$ -naphthyl substituents. Subsequent Kumada coupling with MeMgI afforded **83**, which was brominated under radical conditions to yield the bis-bromide **84**. As it was expected that that the bis-bromide **84** would not be reactive with (TMS-ethynyl)magnesium bromide, conversion into the corresponding diiodide was attempted by Filkenstein reaction with NaI. To our disappointment, this reaction did not proceed as easily as in the case of the bis-bromide **77** (devoid of 3,3'-substituents). Three compounds (co-spotting in TLC) were present in the reaction crude, and it was not possible to separate them. Moreover, crude compound **85** turned out to be very unstable (it immediately decomposed after contact with  $\text{CDCl}_3$  and shortly after contact with DCM). Nevertheless, crude compound **85** was used in following reaction with (TMS-ethynyl)magnesium bromide without any purification.  $^1\text{H}$  NMR of the obtained crude was inconclusive, but it was decided to use the putative compound **86** as such in the reaction with  $\text{Fe}_2(\text{CO})_9$ . Unfortunately, the bis- $\beta$ -naphthyl complex **Fe22** did not form.

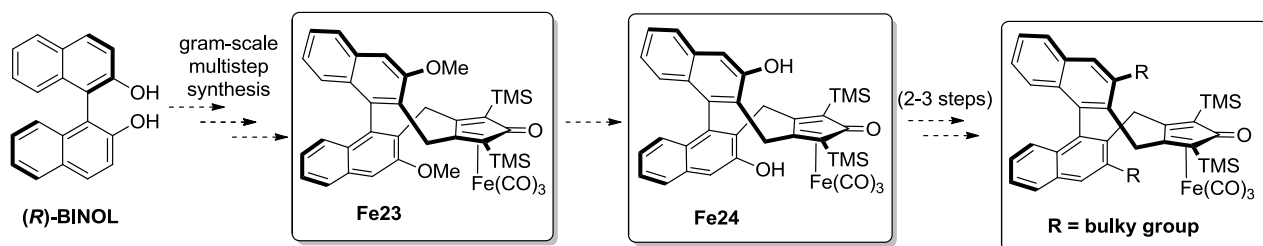
## Chiral (cyclopentadienone)iron complexes



Scheme 5.6 Attempts to synthesize  $\beta$ -naphthyl complex **Fe22**.

## 5.2 Towards a new family of chiral cyclopentadienone(iron) complexes<sup>144</sup>

The lesson learned from the first, unsuccessful attempt to obtain **Fe22** was that the bulky 3,3'-substituents had to be introduced at a late stage of the synthetic pathway, as their presence hampered the functionalization of the 2,2'-positions of the binaphthyl system. Moreover, we started to analyze the possibility to prepare differently 3,3'-substituted complexes from a common precursor synthesized on gram scale. Ideally, this versatile "scaffold complex" could be easily modified in one or two synthetic steps, allowing to obtain a library of different new 3,3'-substituted complexes (Scheme 5.7), and to evaluate the importance of their 3,3'-substituents.

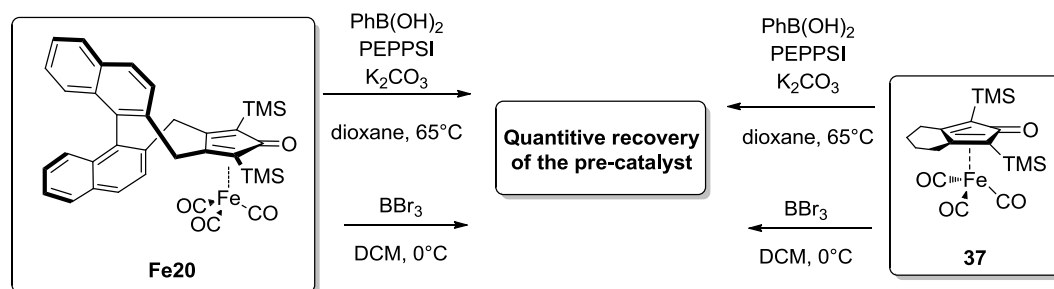


Scheme 5.7 New approach to synthesize new family of chiral iron complexes.

Before starting such plan, it was necessary to verify if the chiral cyclopentadienone(iron) complexes are stable to conditions we wanted to apply for their subsequent modifications. In a series of preliminary tests we evaluated if the



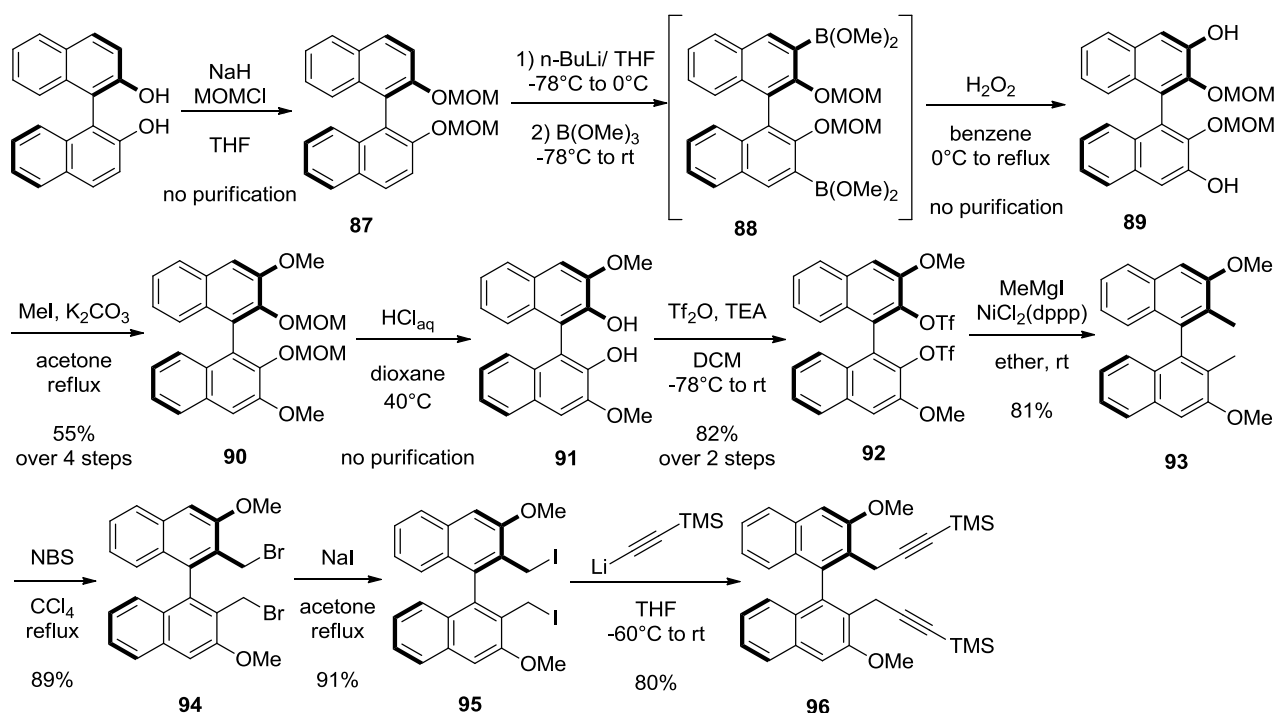
demethylating agent  $\text{BBr}_3$  (and its side product -  $\text{HBr}$ ) would interfere with our complex or whether in the typical experimental conditions of the Suzuki-Miyaura coupling can cause *in situ* Hieber reaction, which would form the sensitive iron hydride complex and eventually lead to decomposition of the complex. We prepared a series of test reactions, using two pre-catalysts available in our lab - **Fe20** and **37** (Scheme 5.8). In every case, a quantitative recovery of iron complexes was accomplished. This proved that our concept and gave a "green light" for the new synthetic strategy.



Scheme 5.8 Verification of stability of cyclopentadienone(iron) complexes.

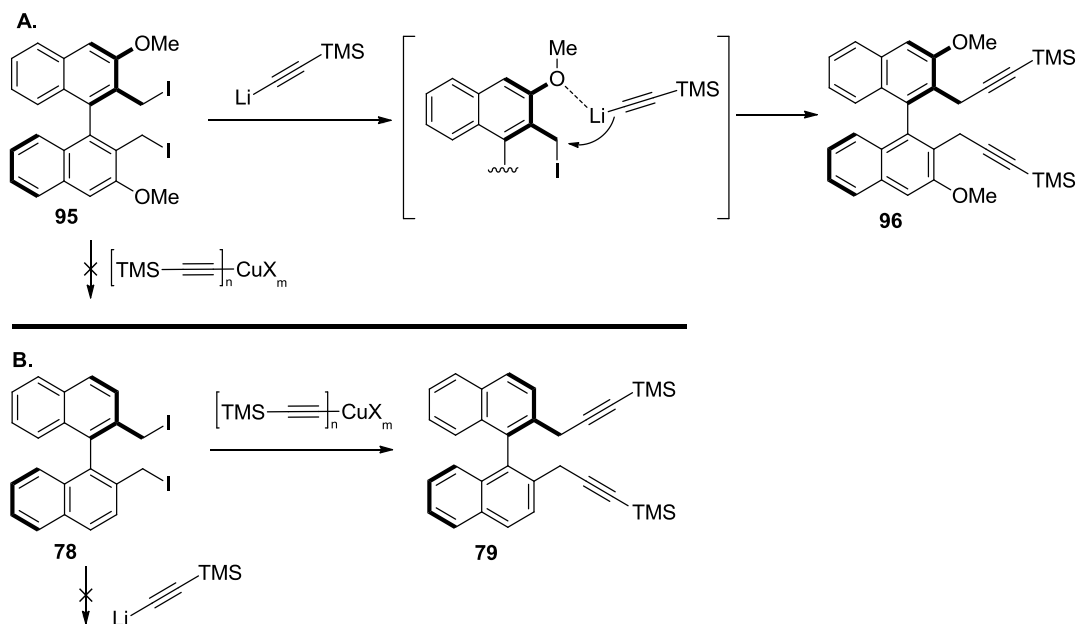
We individuated a synthetic plan to access the 3,3'-dimethoxy-substituted complex **Fe23**. Based on the observations made by Maruoka and co-workers<sup>145</sup> for related BINOL-derivatives, we expected that the relatively small methoxy group should give less steric problems than the bulky  $\beta$ -naphthyl group used in the previous synthetic attempt (Scheme 5.6). The first synthetic steps (up to **93**) were carried out as described by Maruoka and co-workers (Scheme 5.9).<sup>145</sup> The synthetic pathway started from (*R*)-BINOL, which was protected using methyl chloromethyl ether (MOMCl). Protected **87** was subjected to *ortho*-lithiation, followed by formation of the bis-borate **88** and subsequent oxidation to **89**. The hydroxy groups of **89** were methylated using MeI in the presence of  $\text{K}_2\text{CO}_3$  to yield **90**. The MOM protection was removed by acidic hydrolysis and afforded 3,3'-dimethoxy-2,2'-BINOL derivative **91**. The latter compound was converted into the bis-triflate **92**, which was methylated by Kumada coupling in the presence of MeMgI and  $[\text{Ni}(\text{dppp})\text{Cl}_2]$  to yield the known compound **93**. The radical bromination to yield the bis-bromide **94** was carried out under the conditions described by Cramer and co-workers.<sup>138</sup> Compound **94** was converted into the bis-iodide **95**. Unexpectedly, the reaction of **95** with (TMS-ethynyl)magnesium bromide in the presence of CuI, which was effective for the of 3,3'-unsubstituted analog **78**, did not work with compound **95**. We then screened without success a number of different possible conditions to synthesize compound **96**: i) additional to CuI use of  $\text{Pd}(\text{PPh}_3)_4$ ; ii) reaction of **95** with the Gilman's cuprate  $(\text{TMS-ethynyl})_2\text{CuLi}$ ; iii) Kumada cross coupling using **92** and (TMS-ethynyl)magnesium bromide. To our delight, substitution of **95** with (TMS-ethynyl)lithium allowed to obtain the diyne **96** with a high yield.

## Chiral (cyclopentadienone)iron complexes



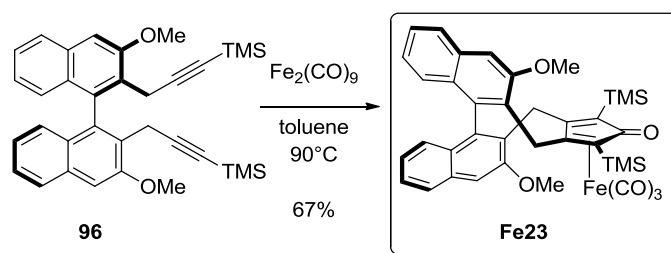
Scheme 5.9 Synthesis of direct precursor of complex **Fe23** - the diyne **96**.

We assumed that the alkylation of **95** in the presence of (TMS-ethynyl)lithium was assisted by the methoxy groups in the adjacent 3,3'-position of the binaphthyl moiety (see Scheme 5.10 A). The latter hypothesis was confirmed by the fact that the 3,3'-unsubstituted bis-iodide **78** did not react with (TMS-ethynyl)lithium (Scheme 5.10 B).



Scheme 5.10 Directing effect of the 3,3'-dimethoxy groups on the nucleophilic substitution in **95**.

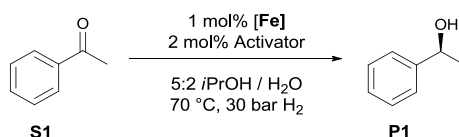
Cyclization of diyne **96** in the presence of  $\text{Fe}_2(\text{CO})_9$  yielded a new chiral complex **Fe23** with 67% yield (Scheme 5.11).

Scheme 5.11 Synthesis of complex **Fe23**

To simplify our work and proceed with multi-gram step synthesis (starting from up to 20 g of (*R*)-BINOL) of complex **Fe23**, a number of purifications were skipped in order to optimize our synthetic protocol. In this eleven-step synthetic pathway, no purification was used until compound **90** which was purified using column chromatography with 55% yield calculated from starting (*R*)-BINOL. Only three more chromatographic purification were used - for **92**, **93** and the final complex **Fe23**. The bis-bromide **94** could be efficiently crystallized with comparable yield to initially used column chromatography (84% vs. 89%) and the latter bis-iodide **95** was purified by simple filtration. Purification of the diyne **96** was also skipped, resulting later in exactly the same yield (54% for two steps) of final complex **Fe23**. Calculating from starting material (*R*)-BINOL, overall yield of this chiral (cyclopentadienone)iron complex **Fe23** was 15.8%. Theoretically speaking, this accounts for 0.38 g of **Fe23** from every 1 g of (*R*)-BINOL used in the synthetic pathway.

### 5.3 Conditions screening

The new cyclopentadienone(iron) complex **Fe23** was tested in the AH of acetophenone. It allowed to obtain similar conversion to the **Fe20**, but the enantiomeric excess (48% *ee*) was nearly 6 times higher (Table 5.1, entry 1 and 2), thus demonstrating the importance of 3,3'-substituents. We decided to optimize the experimental conditions for this reaction. Firstly, we performed a screening of different activators in order to improve the catalytic results.

Table 5.1 Screening of the activators for new cyclopentadienone(iron) complexes.<sup>[a]</sup>

Entry	Complex	Activator	Conv. (%) <sup>[b]</sup>	<i>ee</i> (%) <sup>[b,c]</sup>
1	<b>Fe20</b>	K <sub>2</sub> CO <sub>3</sub>	62	8
2	<b>Fe23</b>	K <sub>2</sub> CO <sub>3</sub>	54	49
3	<b>Fe23</b>	Li <sub>2</sub> CO <sub>3</sub>	9	52
4	<b>Fe23</b>	Na <sub>2</sub> CO <sub>3</sub>	25	53
5	<b>Fe23</b>	Cs <sub>2</sub> CO <sub>3</sub>	29	51
6	<b>Fe23</b>	LiOH	49	51



## Chiral (cyclopentadienone)iron complexes

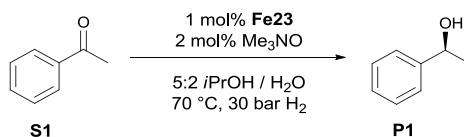
7	<b>Fe23</b>	NaOH	35	50
8	<b>Fe23</b>	KOH	30	52
9	<b>Fe23</b>	K <sub>3</sub> PO <sub>4</sub>	23	53
10	<b>Fe23</b>	Me <sub>3</sub> NO	84	50

<sup>[a]</sup> Reaction conditions: **S1**/[**Fe**]/activator = 100:1:2,  $P_{H_2}$  = 30 bar, solvent = 5:2 *i*PrOH/H<sub>2</sub>O,  $c_0$  (**S1**) = 1.43 M,  $T$  = 70 °C, time = 18 h. <sup>[b]</sup> Determined by GC equipped with a chiral capillary column (MEGADEX DACTBSβ, diacetyl-*t*-butylsilyl-β-cyclodextrin). <sup>[c]</sup> Absolute configuration: *S* in all cases (assigned by comparison of the optical rotation sign with literature data).<sup>168</sup>

This screening revealed that the enantiomeric excess is almost independent on applied activator (entries 2-10). In terms of conversion, the most efficient inorganic activator appeared to be initially selected K<sub>2</sub>CO<sub>3</sub> (entry 2), but the best result was obtained with trimethylamine *N*-oxide (TMNO, entry 11), whose use was firstly reported by Renaud and co-workers.<sup>99</sup> TMNO oxidatively removes one of CO ligand from **Fe23**, forming a vacant site which is filled with subsequent H<sub>2</sub> splitting, compared to the Hieber base activation with inorganic bases.

After finding the optimal activation pathway for the pre-catalyst **Fe23**, optimization studies continued to assess effects of applied hydrogen pressure, temperature and solvent (Table 5.2).

Table 5.2 Optimization of reaction parameters of the AH of acetophenone **S1** promoted by pre-catalyst **Fe23**.<sup>[a]</sup>

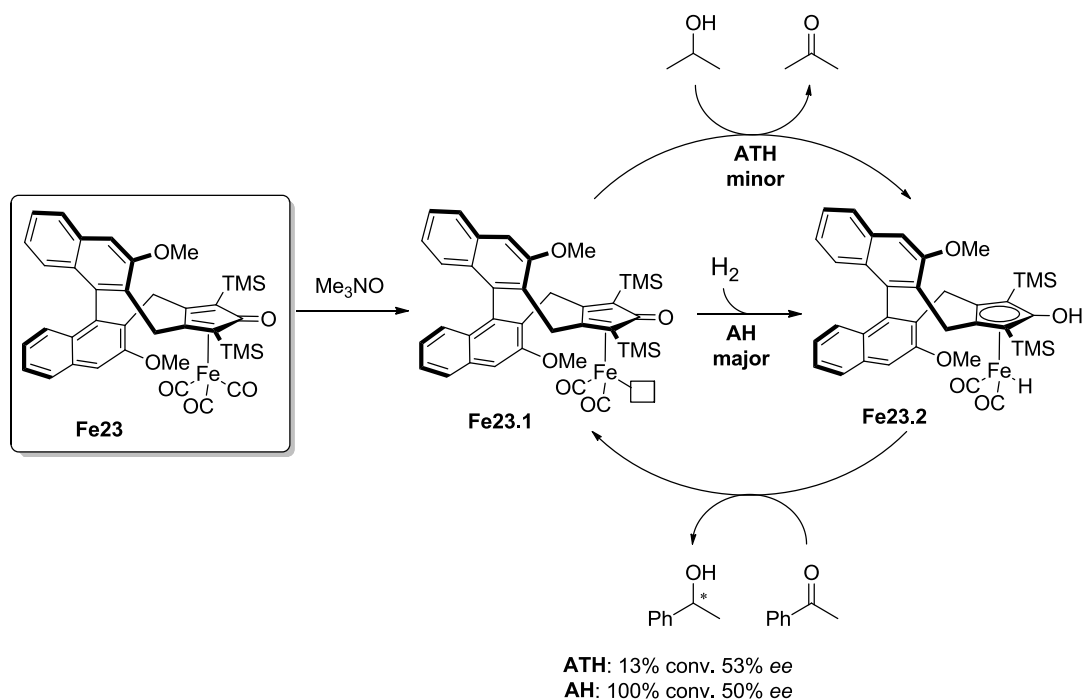


Entry	Solvent	$P$ (bar)	$T$ (°C)	Conv. (%) <sup>[b]</sup>	<i>ee</i> (%) <sup>[b,c]</sup>
1	5:2 <i>i</i> PrOH/H <sub>2</sub> O	30	70	84	50
2	5:2 <i>i</i> PrOH/H <sub>2</sub> O	50	70	85	51
3	5:2 <i>i</i> PrOH/H <sub>2</sub> O	30	80	59	50
4	5:2 <i>i</i> PrOH/H <sub>2</sub> O	30	50	33	55
5 <sup>[d]</sup>	5:2 <i>i</i> PrOH/H <sub>2</sub> O	30	70	100 <sup>[e]</sup>	50
6 <sup>[f]</sup>	5:2 <i>i</i> PrOH/H <sub>2</sub> O	30	70	58	51
7 <sup>[g]</sup>	5:2 <i>i</i> PrOH/H <sub>2</sub> O	--	70	13	53
8	<i>i</i> PrOH	30	70	15	54
9	5:2 EtOH/H <sub>2</sub> O	30	70	21	49
10	5:2 CF <sub>3</sub> CH <sub>2</sub> OH/H <sub>2</sub> O	30	70	74	42
11	5:2 DME/H <sub>2</sub> O	30	70	56	52
12	5:2 dioxane/H <sub>2</sub> O	30	70	56	52
13	5:2 CH <sub>3</sub> CN/H <sub>2</sub> O	30	70	3	53
14	5:2 DMF/H <sub>2</sub> O	30	70	26	54
15	5:2 DCE/H <sub>2</sub> O	30	70	34	54
16	5:2 toluene/H <sub>2</sub> O	30	70	8	53

<sup>[a]</sup> Reaction conditions: **S1**/**Fe23**/Me<sub>3</sub>NO = 100:1:2,  $P_{H_2}$  = 30 bar,  $c_0$  (**S1**) = 1.43 M <sup>[b,c]</sup> See the footnotes of Table 5.1. <sup>[d]</sup> 2 mol% **CK2** (4 mol% Me<sub>3</sub>NO) employed. <sup>[e]</sup> Yield of the isolated product **P1** = 94%. <sup>[f]</sup>  $c_0$  (**S1**) = 0.72 M. <sup>[g]</sup> no hydrogen was applied to perform only ATH



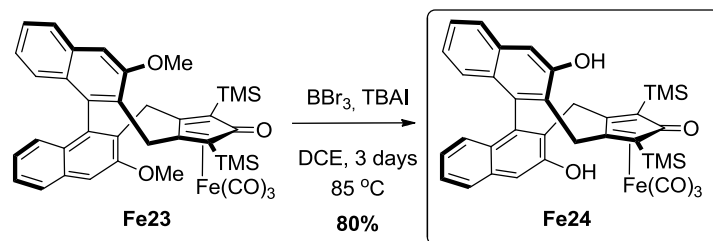
Increased pressure (entry 2) or temperature (entry 3) did not lead to full conversion. To achieve that, 2 mol% of the **Fe23** had to be used (entry 5). A slightly increased enantiomeric excess was observed at lower temperature (entry 4), but at the cost of the conversion. Additional solvent mixtures were tested (entries 9-16), but none of them led to better results than the 5:2 isopropanol/water mixture. Interestingly, the presence of water appeared to be crucial for the conversion (entry 8), possibly due to the poor solubility of TMNO in isopropanol. Also the substrate concentration appeared to be important, because when the reaction was diluted twice (entry 6 vs. 1), a remarkable erosion of conversion was observed. Pre-catalyst **Fe23** was also tested in the absence of H<sub>2</sub> (entry 7). Under these conditions, a low conversion was obtained, which proves that the main catalytic activity is coming from the hydrogenation pathway, although a background ATH with isopropanol is also occurring (Scheme 5.12). Nevertheless, obtained enantiomeric excess was nearly exactly the same as in the case of the AH and thus it had no negative effect on overall results.

Scheme 5.12 Comparison of ATH and AH with **Fe23**.

#### 5.4 Synthesis of a library of new chiral pre-catalysts

The promising enantiomeric excess obtained with **Fe23**, encouraged us to pursue the planned synthetic strategy to prepare complexes bearing different 3,3'-substituents from the common precursor **Fe23**. We thus tried to demethylate complex **Fe23**, which turned out to be very stable to  $\text{BBr}_3$ . Under typical conditions for the demethylation of aryl methyl ethers (0 °C, DCM), no conversion could be achieved, but the unreacted substrate gave no sign of decomposition (as expected after initial experiments with

similar complexes presented on Scheme 5.8). However, using tetra-*n*-butylammonium iodide (TBAI) as an additive<sup>146</sup> and with the reaction temperature raised to 85 °C (in DCE), the bis-phenol **Fe24** was obtained in good yield of 80% (Scheme 5.13). Again, this harsh conditions proved the great stability of cyclopentadienone(iron) complexes.



Scheme 5.13 Demethylation of **Fe23**.

To our delight, we were able to grow a crystal of **Fe24** suitable for a single-crystal X-ray diffraction analysis (Figure 5.3).

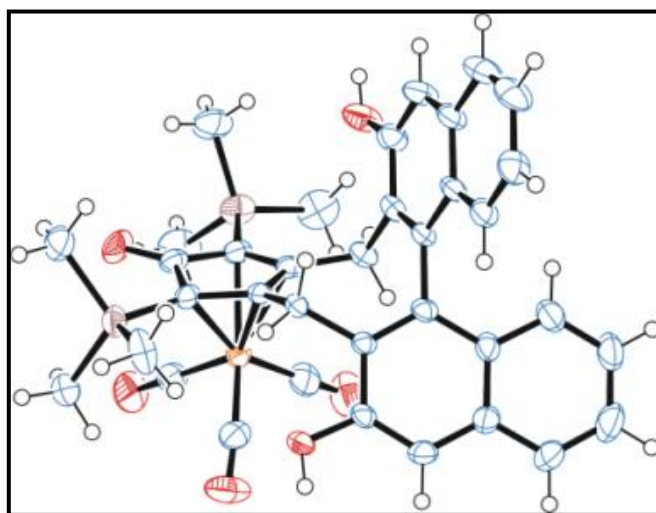
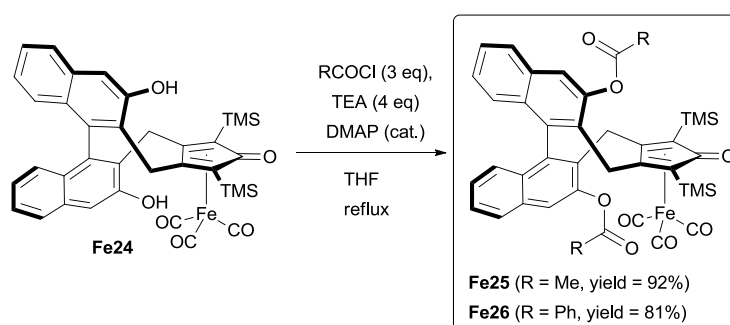


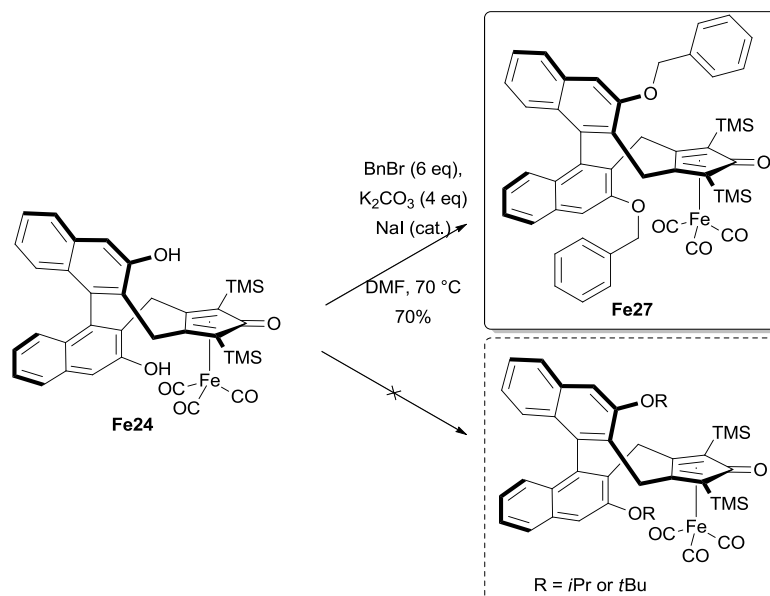
Figure 5.3 ORTEP diagram (CCDC 1037376) of the molecular structure of **Fe24** (thermal ellipsoids set at the 50% probability level).

With the "scaffold complex" **Fe24** in our hands, we set to pursue our strategy of using simple transformation for preparing complexes with more bulky 3,3'-substituents. Starting with one of the most trivial chemical transformations, under classical conditions for esterification, two new pre-catalysts were obtained in good yields: the bis-acetate **Fe25** and bis-benzoate **Fe26** (Scheme 5.14).



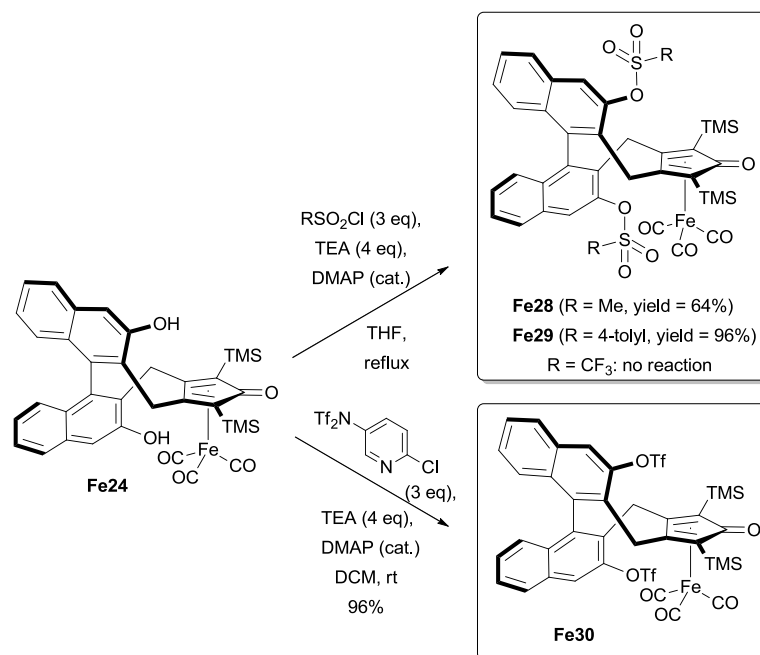
Scheme 5.14 Synthesis of esters **Fe25** and **Fe26**.

Our next goal was to prepare bis-ether derivatives of **Fe24**. Unfortunately, the etherification did not proceed as good as in the previously described esterification. We managed to obtain only the bis(benzyl ether) complex **Fe27** with a good and useful yield (Scheme 5.15). Attempt to use similar conditions for synthesizing the bis(isopropyl ether), failed, as efforts in the case of synthesizing the bis(*tert*-butyl ether) with isobutene or  $(t\text{BuO})_2\text{CHNMe}_2$ .

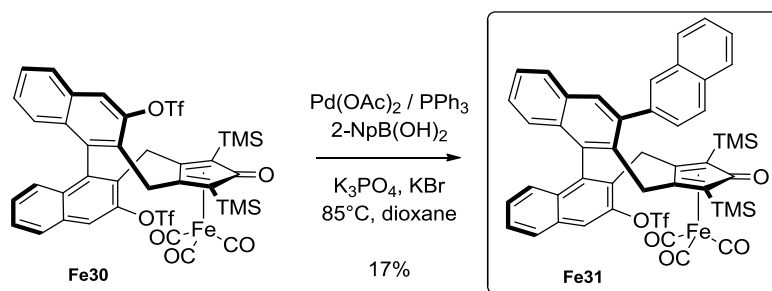


Scheme 5.15 Synthesis of 3,3'-bis(benzyl ether) (*R*)-**1c**, and attempted preparation of other 3,3'-bis(ether) derivatives.

Sulfonylation of **Fe24** with methanesulfonyl chloride (MsCl) or *p*-toluenesulfonyl chloride (TsCl) occurred in high yield in the presence of triethylamine (TEA) and catalytic amount of 4-dimethylaminopyridine (DMAP), yielding complexes **Fe28** and **Fe29** (Scheme 5.16). Surprisingly, the reaction with trifluoromethanesulfonyl chloride (TfCl) or trifluoromethanesulfonyl anhydride ( $\text{Tf}_2\text{O}$ ) under analogous conditions did not afford the bis-triflate derivative **Fe30**. To obtain this complex, we used a less common method using the Comins' reagent [*N*-(5-chloro-2-pyridyl)bis(trifluoromethanesulfonylimide)].<sup>147</sup> Its application led to complex **Fe30** in a nearly quantitative way.

Scheme 5.16 Synthesis of sulfonyl esters **Fe28-30**.

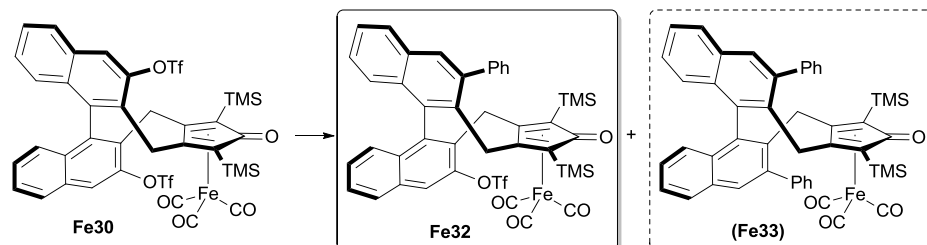
As the main goal of our synthetic strategy remained the installation of aryl substituents in the 3,3'-positions of the binaphthyl moiety, we wanted to use the obtained bis-triflate **Fe30** in the Suzuki-Miyaura cross-coupling. Under typical conditions for this cross-coupling,<sup>148</sup> using  $\beta$ -naphthyl boronic acid, only a mono-substituted complex **Fe31** was obtained with just 17% yield (Scheme 5.17). As the triflate group located nearby the  $\text{Fe}(\text{CO})_3$  group is sterically less accessible, we assigned to the obtained monosubstitution product **Fe31** the structure shown in Scheme 5.17, where the bulky aryl group is located far from the Fe centre.

Scheme 5.17 Suzuki-Miyaura coupling with **Fe30**.

We addressed this low conversion to the steric bulkiness of the  $\beta$ -naphthyl group and we decided to carry out further attempts using phenylboronic acid. Application of the same conditions led also to only a mono-substituted complex **Fe32** (Table 5.3, entry 1), but this time in a nearly quantitative way. Slightly modified conditions ( $\text{Pd}(\text{OAc})_2/\text{PPh}_3$  instead of  $[\text{Pd}(\text{PPh}_3)_4]$ ) gave almost the same result, with no sign of the desired complex (entry 2). Different conditions were tested, but without success as well (Table 5.3, entry 3-4).<sup>149,150</sup> In general, when using relatively strong bases and/or in the presence of water, decomposition of the iron complex was observed. This was most likely caused by the



Hieber-base reaction, in which light-sensitive (hydroxycyclopentadienyl)iron complex was produced. In total, 24 different palladium and nickel catalyzed cross coupling conditions were tested, varying ligands, base, solvent and temperature. In any of them we were able to obtain the desired bis-coupled complex **Fe33**.

Table 5.3 Arylation of bis-triflate **Fe30** by Suzuki-Miyaura cross-coupling.

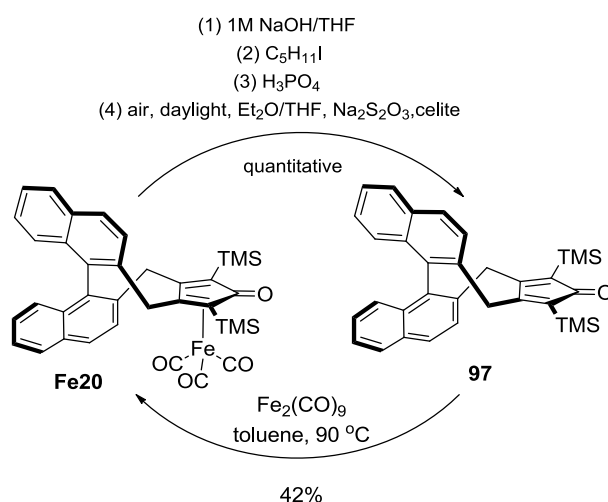
Entry	Catalyst	Equiv. PhB(OH) <sub>2</sub>	Base [equiv.]	Additive [equiv.]	T (°C)	Solvent	NMR ratio (%) <sup>[a]</sup>		
							Fe30	Fe32	Fe33
1 <sup>148</sup>	Pd(PPh <sub>3</sub> ) <sub>4</sub> [10%]	2.5	K <sub>3</sub> PO <sub>4</sub> [3]	KBr [2.2]	85	dioxane	5	95 (74)	0
2	Pd(OAc) <sub>2</sub> [20%] PPh <sub>3</sub> [40%]	2.5	K <sub>3</sub> PO <sub>4</sub> [3]	KBr [2.2]	85	dioxane	2	98 (80)	0
3 <sup>149</sup>	Pd(OAc) <sub>2</sub> [15%] PCy <sub>3</sub> [18%]	2.5	KF [3.3]	KBr [2.2]	60	THF	97	3	0
4 <sup>150</sup>	Pd(PPh <sub>3</sub> ) <sub>4</sub> [10%]	5	Ba(OH) <sub>2</sub> ·8 H <sub>2</sub> O [3]		85	DME/H <sub>2</sub> O	<i>decomposition</i>		
5 <sup>149</sup>	Pd(OAc) <sub>2</sub> [15%] PCy <sub>3</sub> [18%]	2.5	KF [3.3]		60	THF	97	3	
6 <sup>151</sup>	Pd(OAc) <sub>2</sub> [25%] SPhos [50%]	3	K <sub>3</sub> PO <sub>4</sub> [4]		85	toluene		100	
7	Pd(OAc) <sub>2</sub> [20%] PPh <sub>3</sub> [40%]	2.5	K <sub>3</sub> PO <sub>4</sub> [3]	KBr [2.2]	85	dioxane		95 (80)	
8 <sup>152</sup>	Pd(PPh <sub>3</sub> ) <sub>4</sub> [5%+5%]	2.5	K <sub>3</sub> PO <sub>4</sub> [3]	KBr [2.2]	85	dioxane		93 (74)	
9	Pd(PPh <sub>3</sub> ) <sub>4</sub> [10%]	2.5	K <sub>3</sub> PO <sub>4</sub> [3]	KBr [2.2] H <sub>2</sub> O [6]	85	dioxane		100	
10	Pd(PPh <sub>3</sub> ) <sub>4</sub> [5%]	2.5	K <sub>3</sub> PO <sub>4</sub> [3]	KBr [5.6]	110	dioxane		100	
11	Pd(PPh <sub>3</sub> ) <sub>4</sub> [5%]	2.5	K <sub>3</sub> PO <sub>4</sub> [5]		100	DMF	<i>decomposition</i>		
12	Pd(PPh <sub>3</sub> ) <sub>4</sub> [5%]	2.5	K <sub>3</sub> PO <sub>4</sub> [3]	TBAB [2.2]	85	dioxane	100		
13	Pd(PPh <sub>3</sub> ) <sub>4</sub> [10%]	5	K <sub>3</sub> PO <sub>4</sub> [6]	KBr [2.2]	85	dioxane/H <sub>2</sub> O	<i>decomposition</i>		
14	Pd(PPh <sub>3</sub> ) <sub>4</sub> [10%]	5	K <sub>3</sub> PO <sub>4</sub> [6]	KBr [2.2]	85	dioxane		100	
15	Pd(PPh <sub>3</sub> ) <sub>4</sub> [5%]	2.5	Ba(OH) <sub>2</sub> ·8 H <sub>2</sub> O [3]	KBr [2.2]	85	dioxane		100	
16 <sup>150</sup>	Pd(PPh <sub>3</sub> ) <sub>4</sub> [10%]	5	Ba(OH) <sub>2</sub> ·8 H <sub>2</sub> O [6]		85	DME/H <sub>2</sub> O	<i>decomposition</i>		
17	Pd(PPh <sub>3</sub> ) <sub>4</sub> [10%]	2.5	Ba(OH) <sub>2</sub> [3]	KBr [2.2]	85	dioxane	65	35	
18	Pd(PPh <sub>3</sub> ) <sub>4</sub> [5%]	2.5	<i>t</i> BuOK [3]	KBr [2.2]	85	dioxane	<i>decomposition</i>		
18 <sup>153</sup>	PEPPSI- <i>i</i> Pr [4%]	2.5	K <sub>2</sub> CO <sub>3</sub> [6]		60	dioxane	100		
19	PEPPSI- <i>i</i> Pr [5%]	2.5	K <sub>3</sub> PO <sub>4</sub> [3]		85	dioxane	100		
20	PEPPSI- <i>i</i> Pr [5%]	2.5	<i>t</i> BuOK [2.6]		60	IPA	<i>decomposition</i>		
21 <sup>154</sup>	Pd(cinnamyl) ( <i>i</i> Pr*)Cl [5%]	3	K <sub>2</sub> CO <sub>3</sub> [4]		40	EtOH	<i>decomposition</i>		

22 <sup>155</sup>	NiCl <sub>2</sub> (dppp) [5%]	4	K <sub>3</sub> PO <sub>4</sub> [8]		100	dioxane	<i>decomposition</i>	
23	PdCl <sub>2</sub> (dppp) [10%]	2.5	K <sub>3</sub> PO <sub>4</sub> [3]	KBr [2.2]	85	dioxane	50	50
24	PdCl <sub>2</sub> (dppp) [10%]	2.5	Ba(OH) <sub>2</sub> ·8 H <sub>2</sub> O [3]	KBr [2.2]	85	dioxane	50	50

<sup>[a]</sup> Conversion determined by NMR; isolated yields are indicated in brackets.

Despite the possibility of a non-selective mono cross-coupling on both sides of **Fe30**, NMR studies confirmed that it was occurring only on one side of the molecule. As we did not managed to grow a suitable crystal of **Fe32**, a 100% assessment of which of the two diastereotopic OTf groups of **Fe30** was substituted, was not possible. We postulated that the cross-coupling occurs only on the triflate group located on the cyclopentadienone side opposite to Fe(CO)<sub>3</sub>, as it is sterically less hindered and thus allows an easier access for the cross-coupling.

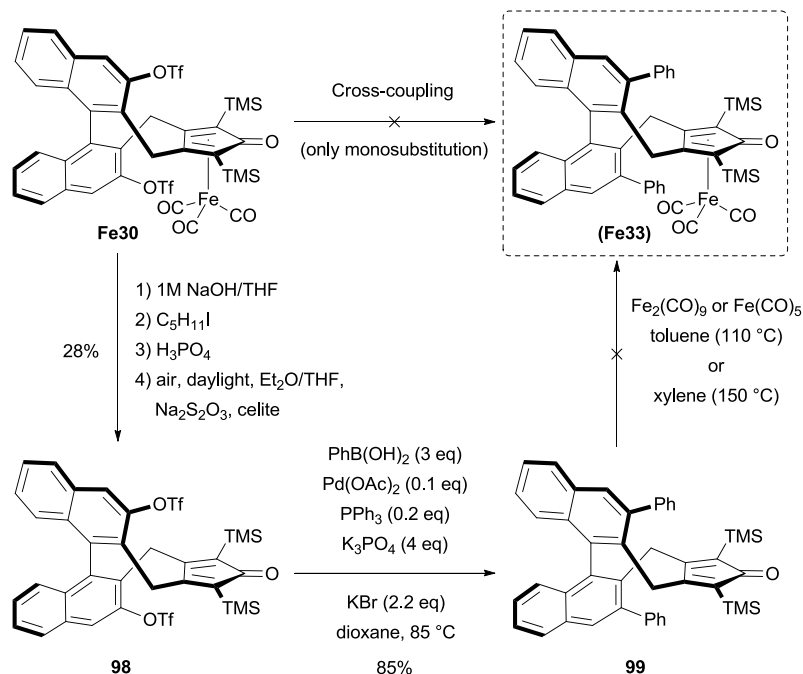
We attempted a different approach to obtain the bis-phenyl derivative **Fe33**. As we assumed that the Fe(CO)<sub>3</sub> was interfering with Suzuki-Miyaura cross-coupling, we decided to remove that obstacle by decomplexation, in order to perform the cross-coupling just on a 3,3'-substituted cyclopentadienone ligand. We believed that subsequent recomplexation of the 3,3'-bisphenyl ligand with Fe<sub>2</sub>(CO)<sub>9</sub> could occur easier than the cross-coupling with the metal complex. To asses this proposal, using the methodology developed by Knölker,<sup>95</sup> we decomplexated Fe(CO)<sub>3</sub> from **Fe20** in a quantitative manner obtaining free ligand **97**, and successfully recomplexate **97** into **Fe20** (Scheme 5.18).



Scheme 5.18 Reversible de-complexation of **Fe20**

We performed the decomplexation directly on the bis-triflate **Fe30**, as it would give us direct access to the Suzuki-Miyaura coupling with obtained ligand **98** (Scheme 5.19). The reaction worked, although ligand **98** was obtained with only 28% yield. As expected, the cross coupling of compound **98** with phenylboronic acid easily afforded ligand **99**, bearing with two phenyl groups in 3,3'-positions. This results provides indirect proof of the fact that, in the mono-substitution products **Fe31** and **Fe32**, the unreacted

triflate group is the one located close to the  $\text{Fe}(\text{CO})_3$  residue. Unfortunately, recomplexation of ligand **99** failed, although different iron sources were tried, together with higher temperatures and prolonged reaction times. No sign of desired iron complex **Fe33** was observed.

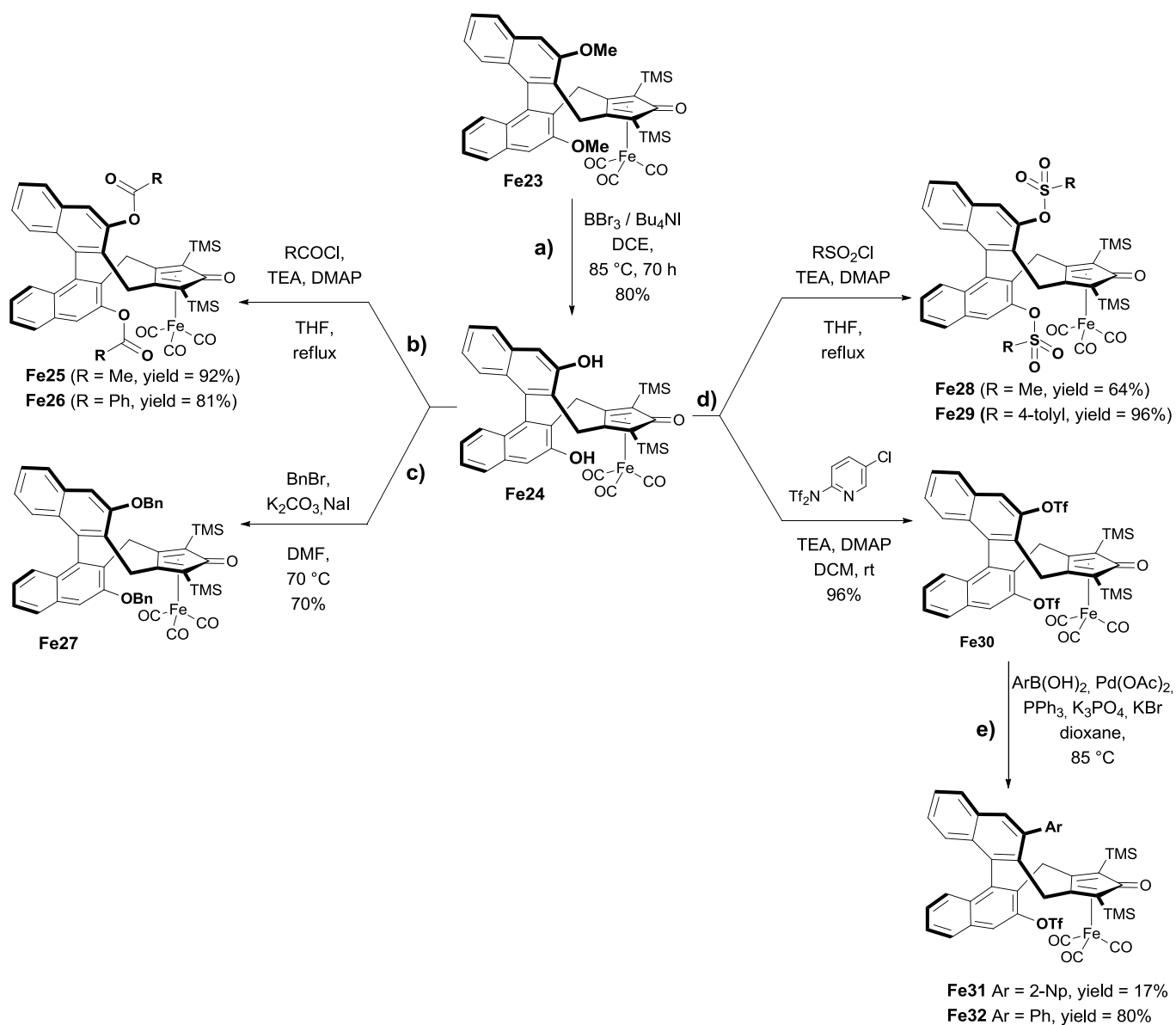


Scheme 5.19 Attempted synthesis of complex **Fe33** from **Fe30** by a de-complexation/cross-coupling/re-complexation sequence.

In summary, our synthetic efforts led us to a new family of chiral iron complexes, starting from one "parent scaffold" complex **Fe23**. Our unprecedented synthetic pathway based on the high chemical and thermal stability of cyclopentadienone(iron) complexes and their direct modifications, using relatively simple transformations (Scheme 5.20). The strategy involved (a) deprotection of **Fe23** followed by: (b) esterification, (c) etherification, (d) sulfonylation or (e) cross-coupling with the triflate derivative. In this way, although synthesis of **Fe23** required twelve steps from (*R*)-BINOL (with overall yield of 16%), we were able to synthesize nine of new pre-catalysts with just few synthetic steps. In this way we omitted time-consuming parallel synthesis of each new complex and possible synthetic complications during multi-step synthesis.



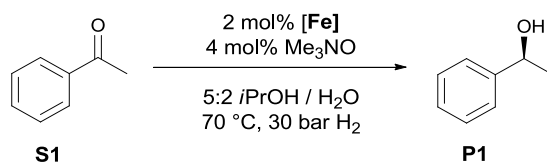
## Chiral (cyclopentadienone)iron complexes



Scheme 5.20 Synthetic routs from "parent scaffold" complex **Fe23** to 9 different pre-catalysts.

## 5.5 Catalytic test with new chiral cyclopentadienone(iron) complexes

Using the optimized conditions found for **Fe23**, all of the obtained chiral 3,3-substituted cyclopentadienone(iron) pre-catalysts were tested in the AH of acetophenone.

Table 5.4 Screening of pre-catalysts **Fe23-32** in the AH of acetophenone **S1**.<sup>[a]</sup>

Entry	Pre-catalyst	Conv. (%)	ee (%)	Entry	Pre-catalyst	Conv. (%)	ee (%)
1		100	50	6		14	39
2		63	46	7		20	37
3		3	46	8		7	35
4		16	38	9		12	47
5		38	39	10		22	52

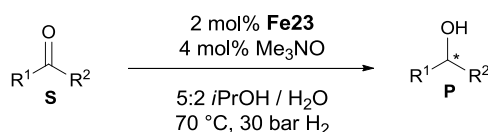
<sup>[a]</sup> Reaction conditions: substrate/[Fe]/Me<sub>3</sub>NO = 100:2:4, P<sub>H<sub>2</sub></sub> = 30 bar, solvent = 5:2 *i*PrOH/H<sub>2</sub>O, c<sub>0</sub> (substrate) = 1.43 M, T = 70 °C, reaction time = 18 h. <sup>[b,c]</sup> See the footnotes of Table 5.1

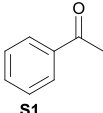
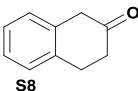
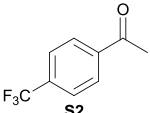
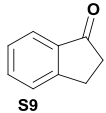
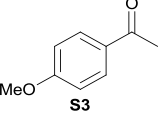
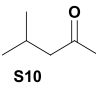
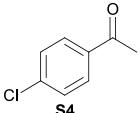
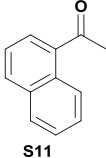
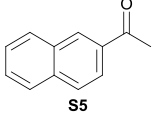
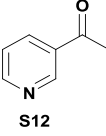
All of the newly synthesized pre-catalysts showed significantly lower catalytic activities and lower stereoselectivity compared to parent pre-catalyst **Fe23**. A full conversion of the substrate **S1** was not observed at any case. In terms of catalytic activity, the best result was obtained with the dihydroxy-substituted pre-catalyst **Fe24**, directly derived from **Fe23**. In terms of stereoselectivity, only **Fe31** and **Fe32** pre-catalysts granted the same level as **Fe23**, whereas the other complexes showed significantly lower *ee*'s (entries 3-8). While the slightly decreased enantiomeric excess reached of **Fe24** (compared to **Fe23**) can be explained by the lesser steric bulk of the 3,3'-substituents, the low stereoselectivity of the other complexes is not simple to explain, as they bear bigger 3,3'-substituents. In the case of esters **Fe25-26**, low conversion could be obtained because of the possible carbonyl oxygen coordination to the iron centre and its deactivation.<sup>156</sup> Moreover, it is likely that the bulky substituent of ethers and esters tends to stay clear from the zone of approach of the substrate because of free rotation of the C-O bond.

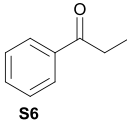
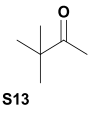
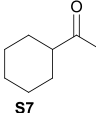
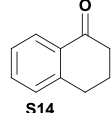
## 5.6 Substrate screening with the best complex

As the best catalyst for the AH of acetophenone remained the 3,3'-bis-methoxy pre-catalyst **Fe23**, a substrate screening was performed using that complex (Table 5.5).

Table 5.5 Substrate screening for pre-catalyst **Fe23**.<sup>[a]</sup>



Entry	Substrate	Conv. (%) <sup>[b]</sup>	<i>ee</i> (%), <sup>[c]</sup> abs. conf. <sup>[d]</sup>	Entry	Substrate	Conv. (%) <sup>[b]</sup>	<i>ee</i> (%), <sup>[c]</sup> abs. conf. <sup>[d]</sup>
1		100	50, S	8		100	13, R
2		100	46, S	9		78	59, R
3		64	50, S	10		76	0
4		100	51, S	11		43	68, R
5		99	51, S	12		35	50, S

6		97	57, S	13		22	77, S
7		89	61, S	14 <sup>[e]</sup>		25	77, S

<sup>a)</sup> Reaction conditions: substrate/**Fe23**/ $\text{Me}_3\text{NO}$  = 100:2:4,  $P_{\text{H}_2}$  = 30 bar, solvent = 5:2 *i*PrOH/ $\text{H}_2\text{O}$ ,  $c_0$  (substrate) = 1.43 M,  $T$  = 70 °C, reaction time = 18 h. <sup>[b]</sup> Determined by GC equipped with a chiral capillary column (see the Experimental section). <sup>[c]</sup> Determined by GC or HPLC equipped with a chiral capillary column (see the Experimental section). <sup>[d]</sup> Assigned by comparison of the sign of optical rotation with literature data (see the Experimental section). <sup>[e]</sup>  $\text{S14}/\text{Fe23}/\text{Me}_3\text{NO}$  = 100:5:10.

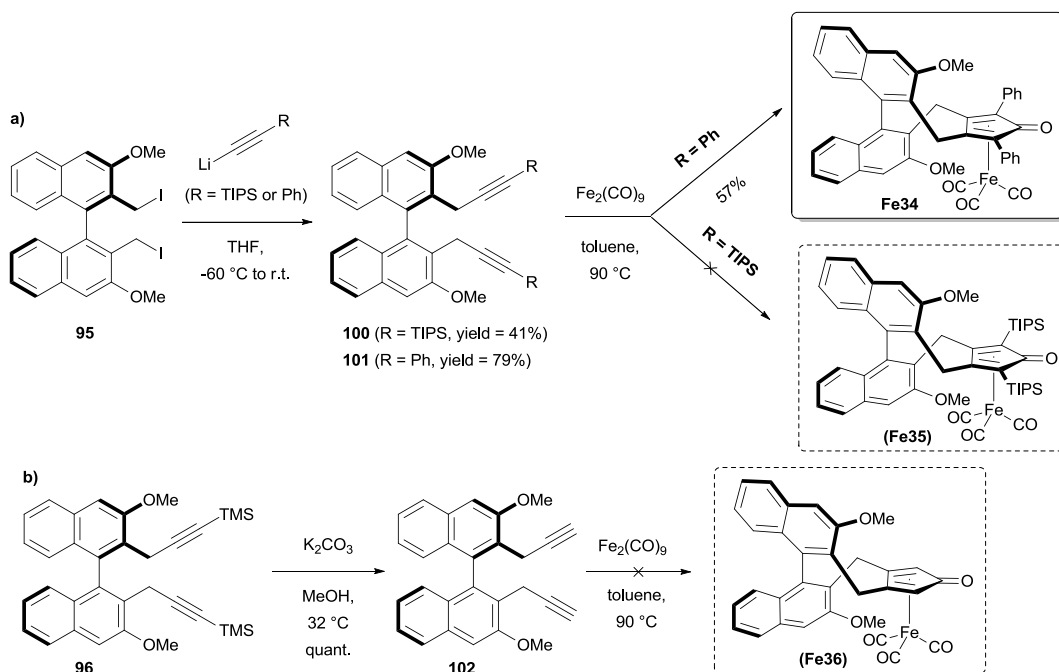
Pre-catalyst **Fe23** showed quite a broad application scope. It worked with range of acetophenone derivatives (entries 1-6, 9, 11, 14), as well with heteroaromatic (entries 12), cyclic non aromatic (entries 7, 8) and aliphatic ketones (entries 10, 13). A general trend can be observed, as bulkier the substituents next to the carbonyl group, the higher *ee* was observed (up to 77% for **S13** and **S14**), but along with a decreased conversion as well. With a low steric hindrance, low (13% *ee* for **S8**) or no enantioselectivity (0% *ee* for **S10**) was observed, along with good to full conversion (entries 8-10).

## 5.7 Variation of the 2,5-substituents of the cyclopentadienone ring

Although in the substrate scope with 3,3'-substituted pre-catalyst **Fe23**, we obtained up to 77% *ee*, they came along with quite low conversions of 22-25%. The most commonly used substrate in ketone hydrogenation, acetophenone **S1**, was fully hydrogenated with 50% *ee*. According to our initial speculation, also 2,5-substituents of the cyclopentadienone ring could influence the transmission of stereochemical information and thus affect the catalytic performance of the iron complex. Therefore, we decided to modify the best working pre-catalyst **Fe23**, by replacing its TMS groups in the 2,5-positions with other groups. In particular, we selected the TIPS group, because of its increased steric bulk compared to TMS, and the flat phenyl group, which could possibly allow to install bulky 3,3'-substituents by cross-coupling reaction. The last investigated option was just the removal of any substituents from the 2,5-positions.

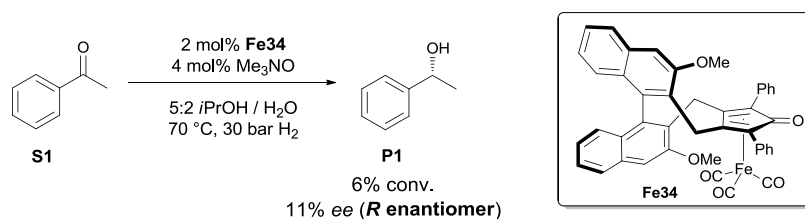
Previously synthesized advanced intermediates were used for the synthesis of the new derivatives. We functionalized the bis-iodide **95** with different ethynyl-lithium compounds in analogous way to described before (Scheme 5.21a). Upon treatment of **95** with [(TIPS)ethynyl]lithium and [(phenyl)ethynyl]lithium, new diyne compounds **100** and **101** were obtained. However, the following cyclization of the TIPS derivative **100** in the presence of  $\text{Fe}_2(\text{CO})_9$  gave no conversion, most likely due to the excessive steric bulk of the TIPS groups. The 2,5-bis-phenyl-substituted derivative **101** did cyclize with  $\text{Fe}_2(\text{CO})_9$  and afforded the new chiral iron complex **Fe34**. In order to obtain 2,5-unsubstituted

complex, we removed the TMS groups from diyne **96**, in the presence of sodium carbonate in methanol (Scheme 5.21b). In these mild conditions we obtained quantitative conversion to diyne **102**, which unfortunately was not stable enough under the cyclization conditions, so that only decomposition was observed.



Scheme 5.21 Synthesis of **Fe23** analogs modified at the 2,5-positions of the cyclopentadienone ring.

The new complex **Fe34** was tested in the AH of acetophenone, applying our optimized conditions for **Fe23** (Scheme 5.22).

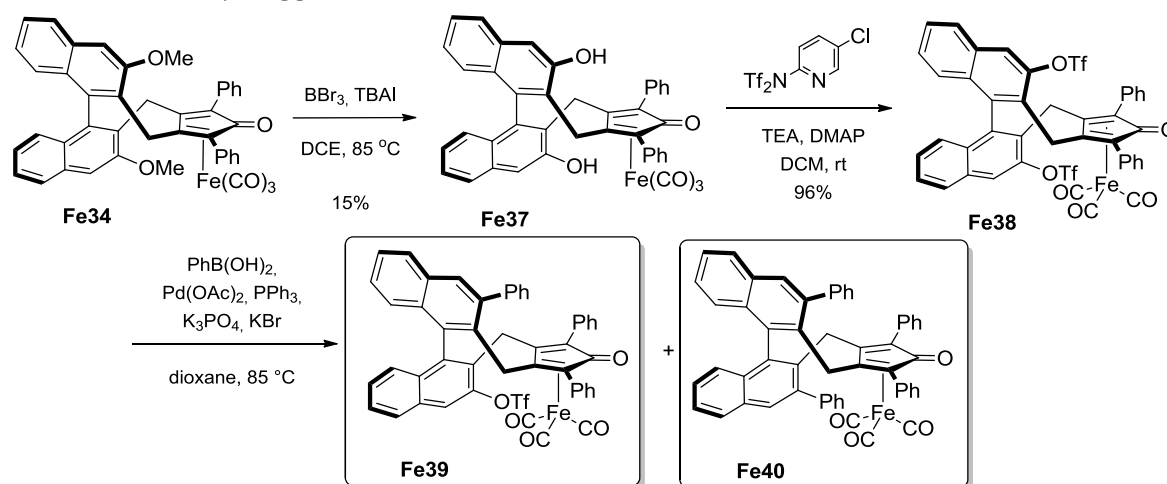


Scheme 5.22 Test of pre-catalyst **Fe34** in the AH of acetophenone **S1**.

To our disappointment, newly prepared pre-catalyst **Fe34** presented very low catalytic activity. Only 6% of the substrate **S1** was converted to (*R*)-phenylethanol, with only 11% *ee*. A possible rationalization of that result, might be that the phenyl groups on the cyclopentadienone ring are not bulky enough to prevent dimerization of the activated hydride of **Fe34**, which could lead to a decomposition as reported by Guan and co-workers for a related iron complex.<sup>157</sup> Additionally, computational studies on a related achiral cyclopentadienone(iron) complex with 2,5-phenyl groups, confirmed that phenyl groups lead to an increase of the activation energy of the hydrogenation process.<sup>158</sup>

Despite this negative result, we still attempted to install 3,3'-phenyl substituents and to verify if bulky 2,5-TMS groups are really interfering with the Suzuki-Miyaura cross-coupling or not. Complex **Fe34** was subjected to deprotection at room temperature in the

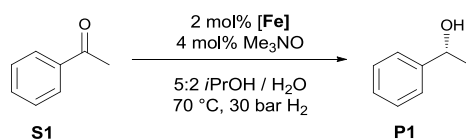
presence of  $\text{BBr}_3$  (Scheme 5.23). The reaction did not proceed to the dihydroxy derivative **Fe37** and, as in the synthesis of **Fe24**, use of very harsh conditions for a long period of time was required. After 3 days of reflux, only a small amount of the desired product was obtained (15% yield), thus suggesting that, in the case of **Fe23**, the TMS groups exert also some stabilizing effect on the cyclopentadienone ring. **Fe37** was converted in the corresponding triflate **Fe38** using the Comin's reagent. Subjecting **Fe38** into the Suzuki-Miyaura cross-coupling with phenylboronic acid under the best conditions found for **Fe30** (Table 5.3), afforded a mixture of mono and bis-substituted products **Fe39** and **Fe40**. This result proved that, together with the  $\text{Fe}(\text{CO})_3$  group, also the bulky TMS groups interfered with the Suzuki-Miyaura coupling during our attempts to synthesize **Fe33**. The flat phenyl group allowed the cross-coupling to occur on the both sides of the molecule, although reaction was very sluggish.



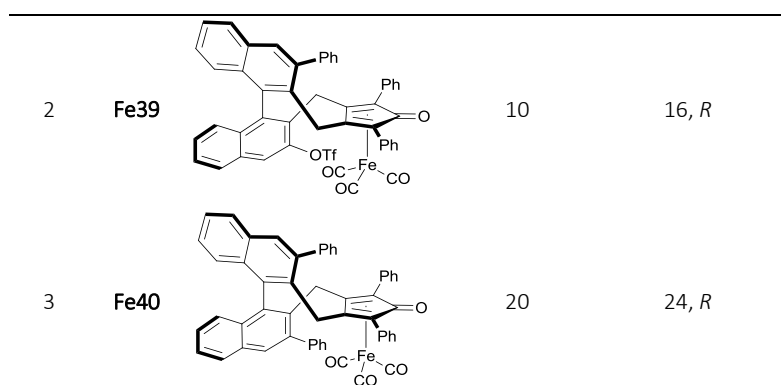
Scheme 5.23 Synthesis of 3,3-bisphenyl (cyclopentadienone)iron complex **Fe40**.

The catalytic activity of complexes **Fe34**, **Fe39** and **Fe40** in the AH of acetophenone **S1** was studied (Table 5.6).

Table 5.6 Screening of pre-catalysts in the AH of acetophenone **S1**.<sup>[a]</sup>



Entry	Pre-catalyst	Conv. (%) <sup>[b]</sup>	ee (%), <sup>[c]</sup> abs. conf. <sup>[d]</sup>
1	<b>Fe34</b> 	6	11, R



<sup>[a]</sup> Reaction conditions: substrate/[Fe]/Me<sub>3</sub>NO = 100:2:4, *P*<sub>H<sub>2</sub></sub> = 30 bar, solvent = 5:2 *i*PrOH/H<sub>2</sub>O, *c*<sub>0</sub> (substrate) = 1.43 M, *T* = 70 °C, reaction time = 18 h. <sup>[b,c]</sup> See the footnotes of Table 5.1

In comparison to the bis-methoxy pre-catalyst **Fe34**, both new catalyst revealed increased catalytic activity. The best result was obtained with catalyst **Fe40**, which led to 20% conversion of acetophenone with 24% *ee*. With **Fe39**, lower conversion (10%) and *ee* (16%) were obtained. Interestingly, complexes with 2,5-phenyl substituents (**Fe34**, **Fe39**, **Fe40**) produced (*R*)-phenylethanol, whereas use of 2,5-TMS pre-catalysts (**Fe20**, **Fe23-32**) led to the (*S*)-enantiomer. This inversion in the stereochemical preference demonstrates that the cyclopentadienone 2,5-substituents play an important role in the transmission of the stereochemical information to the substrate, not less than the binaphthyl 3,3'-substituents. As we were not able to grow crystals of any of the 2,5-phenyl catalysts, it is not certain how phenyls are positioned and how this effect the reverse enantioselectivity of these catalysts.

## 5.8 Cyclopentadienone(iron) complexes bearing chiral 2,5-substituents

We decided to investigate also a new approach to the development of chiral (cyclopentadienone)iron pre-catalysts, which consists in the introduction of chiral substituents at the 2,5-positions of the cyclopentadienone ring, rather than employing a chiral cyclopentadienone backbone as was done in the examples described above. In particular, we envisaged the possibility of using chiral silyl groups easily prepared from (*R*)-BINOL (Figure 5.4).

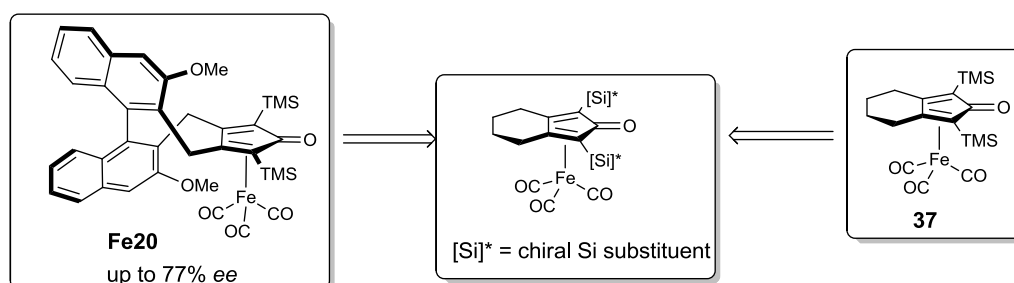
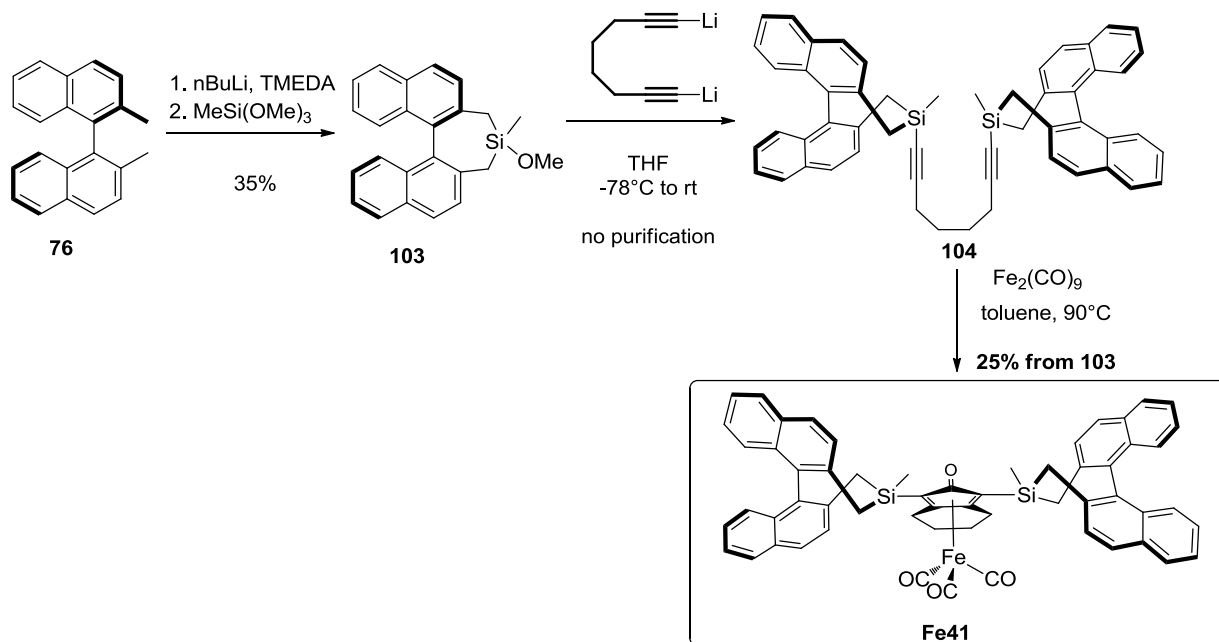


Figure 5.4 New ideas for the development of chiral (cyclopentadienone)iron complexes.

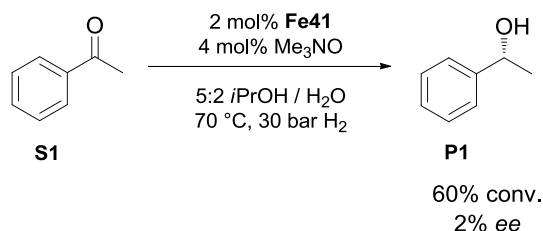
The new chiral iron complex **Fe41** was prepared as shown in the Scheme 5.24. Previously synthesized (*R*)-2,2'-dimethyl-1,1'-binaphthalene **76**, was dilithiated using

*n*BuLi/TMEDA complex and subsequently treated with trimethoxy(methyl)silane to afford the methoxysilacyle **103**. Diyne **104** was obtained from **103** and dilithiated octa-1,7-diyne, and subsequently cyclized in the presence of  $\text{Fe}_2(\text{CO})_9$  to afford the new complex **Fe41**.



Scheme 5.24 Synthesis of new complex **Fe41**.

The new complex **Fe41**, was tested in the AH of acetophenone, applying our optimized conditions for **Fe24** (Scheme 5.25).



Scheme 5.25 Hydrogenation of acetophenone **S1** using pre-catalyst **Fe41**.

Pre-catalyst **Fe41** proved to be active in the AH of **S1** and the phenylethanol **P1** was obtained with a good conversion (under conditions optimized for a different catalysts). Remarkably there was almost no transfer of stereochemical information from the chiral fragments of the complex as the product **P1** was nearly a racemate (just 2% *ee*). This outcome is probably due to the free rotation of the C-Si bond connecting the cyclopentadienone ring to the chiral silacycles. This result discouraged us from any further investigations of chiral 2,5-substituents on the cyclopentadienone ring.



## 5.9 Complexes derived from chiral diamines

The new diamine-derived (cyclopentadienone)iron complex **45** and its use as a pre-catalyst for reductive amination and  $\text{NaHCO}_3$  hydrogenation was reported by Renaud and co-workers (see Paragraph 2.5.1).<sup>111</sup> Thanks to the 3,4-ethylenediamino-substitution, complex **45** possesses a more electron-rich cyclopentadienone framework compared to **37**, which was enhancing the overall Lewis base character of the carbonyl group in the cyclopentadienone ligand. Using DFT calculations, Renaud and co-workers proved that their new complex, after de-complexation of a CO ligand, had a lower energy barrier to split  $\text{H}_2$  and to form the active hydride species. Considering that a number of chiral 1,2-diamine are commercially available or synthetically accessible, we decided to synthesize new chiral analogues of **45** bearing a chiral diamino moiety, hoping to achieve new effective chiral iron pre-catalysts (Figure 5.5).

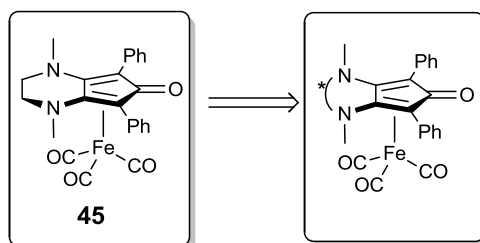
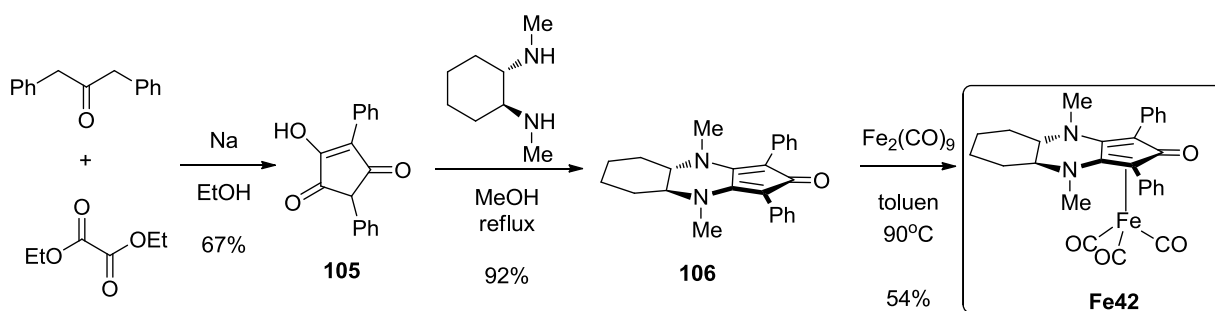


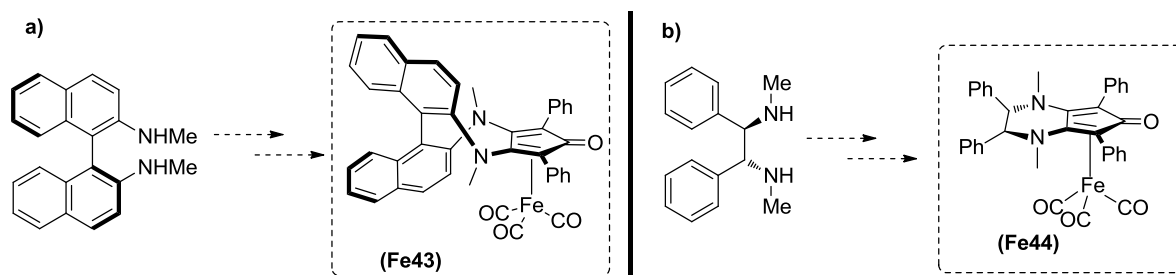
Figure 5.5 Idea for new chiral iron pre-catalysts.

Using Claisen condensation of commercially available 1,3-diphenylpropan-2-one with diethyl oxalate we obtained **105**, which reacted with (*S,S*)-*N,N'*-dimethyl-1,2-cyclohexanediamine to afford ligand **106** (Scheme 5.26). Subsequent cyclisation with  $\text{Fe}_2(\text{CO})_9$  allowed to obtain a new chiral complex **Fe42**.

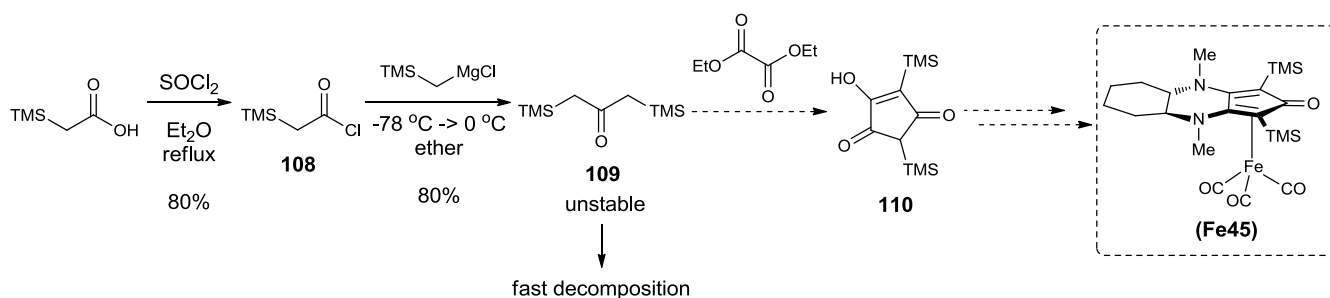


Scheme 5.26 Synthesis of a new chiral pre-catalyst **Fe42**.

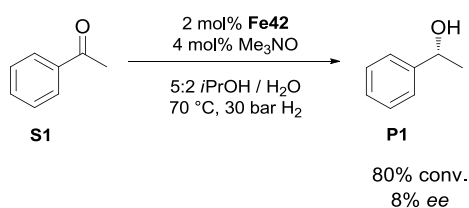
We tried to apply this methodology with two other commercially available amines but, unfortunately, no sign of reaction was observed between them and **105**, and thus the corresponding complexes **Fe43** and **Fe44** could not be prepared (Scheme 5.27).

Scheme 5.27 Unaccomplished plans for synthesizing new chiral complexes a) **Fe43** and b) **Fe44**.

We also tried to synthesize a new chiral complex similar to **Fe42** but with TMS groups at the 2,5-positions (Scheme 5.28). (TMS)acetyl chloride **108** was obtained from corresponding carboxylic acid using thionyl chloride. Using prepared *in situ* prepared (TMS)magnesium chloride, TMS-acetone **109** was obtained with a good yield. Unfortunately it appeared to be very sensitive and it underwent decomposition shortly after being prepared. For this reason, the synthesis of a **Fe42** analogue bearing TMS groups could not be carried out.

Scheme 5.28 Attempt to synthesize new complex **Fe45**.

Complex **Fe42** was tested in the AH of acetophenone, applying our optimized conditions for **Fe23** (Scheme 5.29).

Scheme 5.29 Hydrogenation of acetophenone **S1** using pre-catalyst **Fe42**.

Pre-catalyst **Fe42** was found to be catalytically active, giving 80% conversion of acetophenone, but with only low enantiomeric excess (8% *ee*). A plausible reason for such low enantiocontrol is that the catalyst's stereocenters are too remote from the zone from where the reaction occurs, thus preventing an efficient transfer of the stereochemical information. To tackle this issue, the synthesis of new pre-catalysts bearing bulkier substituents in the 2,5-positions of the cyclopentadienone ring is currently underway.

## 5.10 Summary of chiral (cyclopentadienone)iron complexes

In our studies we developed a series of new chiral cyclopentadienone(iron) complexes (Figure 5.6). We were confident that with their advantages (like easy synthesis or working with them without a glove-box), they can bring a positive contribution to the field of iron catalysis. In our research towards new, effective chiral iron complexes, we focused our attention to investigate various structural modifications of the cyclopentadienone ring.

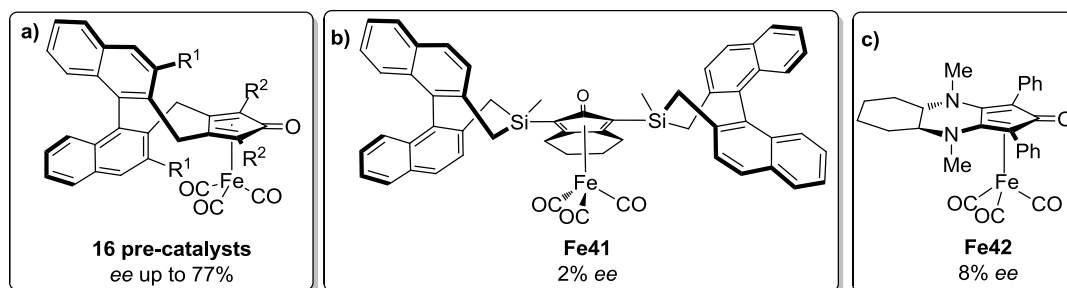


Figure 5.6 Summary of obtained new chiral (cyclopentadienone)iron pre-catalysts for ketone hydrogenation.

The most extensive research was directed towards new pre-catalysts derived from (*R*)-BINOL (Figure 5.6a). In total 16 novel iron complexes for ketone hydrogenation were obtained and the best one, **Fe23**, allowed to get up to 77% *ee* in ketone AH. In our research, we found out that 3,3'-substituents play a crucial role in the transfer of stereogenic information to the reaction centre, although the range of suitable 3,3'-substituents was found to be rather limited. They should not possess heteroatoms which might coordinate to the iron centre and deactivate the catalyst. Moreover, we were not able to install really bulky substituents like phenyl or 2-naphthyl when 2,5-positions of the cyclopentadienone rings were substituted with TMS groups. Replacing them with phenyl groups allowed to install phenyl substituents at the 3,3'-positions, but the catalytic studies revealed that overall results of the asymmetric hydrogenation, are also dependent on the cyclopentadienone 2,5-substituents. Thus, replacement of TMS groups with phenyl groups led to decrease of catalytic activity of (cyclopentadienone)iron pre-catalysts even in the presence of bulky 3,3'-substituents.

Following an alternative approach aimed at bringing the stereogenic units closer to the reaction centre, we introduced chiral substituents at 2,5-positions of the cyclopentadienone ring (Figure 5.6b). However, almost no *ee* was observed with **Fe41**, most probably due to the conformational flexibility of the new complex.

With a different synthetic route, we tried to obtain a new family of chiral diamine-derived (cyclopentadienone)iron complexes, but we managed to synthesize just the iron pre-catalyst **Fe42** (Figure 5.6c). In the hydrogenation of acetophenone, the obtained *ee* was low - just 8%, most probably due to the long distance between the catalyst's stereocentres and the reaction site, typical problem met with chiral (cyclopentadienone)iron complexes.

## 5.11 Experimental section

### General Remarks

All reactions were carried out in flame-dried glassware with magnetic stirring under nitrogen or argon atmosphere, unless otherwise stated.

The solvents for reactions were distilled over the following drying agents and transferred under nitrogen: CH<sub>2</sub>Cl<sub>2</sub> (CaH<sub>2</sub>), MeOH (CaH<sub>2</sub>), THF (Na), dioxane (Na), Et<sub>3</sub>N (CaH<sub>2</sub>). Dry Et<sub>2</sub>O, acetone and CHCl<sub>3</sub> (over molecular sieves in bottles with crown cap) were purchased from Sigma Aldrich and stored under nitrogen.

The reactions were monitored by analytical thin-layer chromatography (TLC) using silica gel 60 F254 pre-coated glass plates (0.25 mm thickness). Visualization was accomplished by irradiation with a UV lamp and/or staining with a potassium permanganate alkaline solution. Flash column chromatography was performed using silica gel (60 Å, particle size 40-64 μm) as stationary phase, following the procedure by Still and co-workers.<sup>159</sup>

Proton NMR spectra were recorded on a spectrometer operating at 400.13 MHz. Proton chemical shifts are reported in ppm (δ) with the solvent reference relative to tetramethylsilane (TMS) employed as the internal standard (CDCl<sub>3</sub> δ = 7.26 ppm; CD<sub>2</sub>Cl<sub>2</sub>, δ = 5.32 ppm; [D]<sub>6</sub>acetone, δ = 2.05 ppm; [D]<sub>6</sub>DMSO, δ = 2.50 ppm; CD<sub>3</sub>OD, δ = 3.33 ppm). The following abbreviations are used to describe spin multiplicity: s = singlet, d = doublet, t = triplet, q = quartet, m = multiplet, br = broad signal, dd = doublet-doublet, td = triplet-doublet. <sup>13</sup>C-NMR spectra were recorded on a 400 MHz spectrometer operating at 100.56 MHz, with complete proton decoupling. Carbon chemical shifts are reported in ppm (δ) relative to TMS with the respective solvent resonance as the internal standard (CDCl<sub>3</sub>, δ = 77.16 ppm; CD<sub>2</sub>Cl<sub>2</sub>, δ = 54.00 ppm; [D]<sub>6</sub>acetone, δ = 29.84 ppm, 206.26 ppm; [D]<sub>6</sub>DMSO, δ = 39.51 ppm; CD<sub>3</sub>OD, δ = 49.05 ppm). The coupling constant values are given in Hz.

Infrared spectra were recorded on a standard FT/IR spectrometer. Optical rotation values were measured on an automatic polarimeter with a 1 dm cell at the sodium D line (λ = 589 nm). Gas chromatography was performed on a GC instrument equipped with a flame ionization detector, using a chiral capillary column.

High resolution mass spectra (HRMS) were performed on a Fourier Transform Ion Cyclotron Resonance (FT-ICR) Mass Spectrometer APEX II & Xmass software (Bruker Daltonics) – 4.7 T Magnet (Magnex) equipped with ESI source, available at CIGA (Centro Interdipartimentale Grandi Apparecchiature) c/o Università degli Studi di Milano.

Low resolution mass spectra (MS) were acquired either on a Thermo-Finnigan LCQ Advantage mass spectrometer (ESI ion source) or on a VG Autospec M246 spectrometer (FAB ion source).

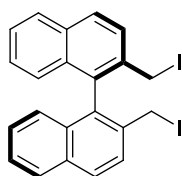
Elemental analyses were performed on a Perkin Elmer Series II CHNS/O Analyzer 2000. X-ray intensity data were collected with a Bruker Apex II CCD area detector by using graphite monochromated Mo-Kα radiation.

### Materials

Commercially available reagents were used as received. While both (*R*)-(+)-1,1'-bi(2-naphthol) (BINOL) and (*R*)-3,3'-dibromo-[1,1'-binaphthalene]-2,2'-diol are commercially available, (*R*)-2,2'-bis(bromomethyl)-1,1'-binaphthyl **77** and (*R*)-2'',3'-bis(bromomethyl)-2,2':4',1'':3'',2'''-

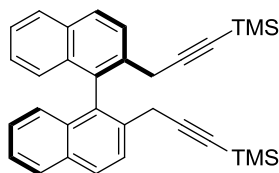
quaternaphthalene **84** were synthesized from BINOL according to the procedure described by Ooi *et al.*<sup>160</sup> (*R*)-2,2'-bis(bromomethyl)-3,3'-dimethoxy-1,1'-binaphthyl **94** was synthesized according to the procedure described by Crammer and co-workers.<sup>138</sup> 4-Hydroxy-2,5-diphenylcyclopent-4-ene-1,3-dione **105** was synthesized following the procedure by Claisen *et al.*<sup>161</sup> 1,3-Bis(trimethylsilyl)propan-2-one **109** was synthesized according to the paper of Hosomi *et al.*<sup>162</sup> Ethynyltrimethylsilane, ethylmagnesium bromide (1 M in THF), *n*-BuLi (1.6 M in hexanes), BBr<sub>3</sub> (1 M in DCM), Bu<sub>4</sub>NI, NaI, CuI, Fe<sub>2</sub>(CO)<sub>9</sub>, DMAP, acetyl chloride, benzoyl chloride, benzyl bromide, methanesulfonyl chloride, *p*-toluenesulfonyl chloride, N-(5-chloro-2-pyridyl)bis(trifluoromethanesulfonimide), Pd(OAc)<sub>2</sub>, K<sub>3</sub>PO<sub>4</sub>, PPh<sub>3</sub>, KBr, phenylboronic acid, PCy<sub>3</sub>, SPhos, Pd(cinnamyl)(IPr)Cl, PdCl<sub>2</sub>(dppp), NiCl<sub>2</sub>(dppp), Ba(OH)<sub>2</sub>·H<sub>2</sub>O, Ba(OH)<sub>2</sub> anhydrous, Bu<sub>4</sub>NBr, KF, K<sub>2</sub>CO<sub>3</sub>, *t*BuOK, 1-iodopentane, ethynyltriisopropylsilane, ethynylbenzene and the ketones used in the substrate screening were purchased from commercial suppliers (TCI Chemicals, ACROS, Sigma Aldrich) and used as received.

#### (*R*)-2,2'-Bis(iodomethyl)-1,1'-binaphthyl **78**



Under nitrogen in a Schlenk tube fitted with a Teflon screw cap, NaI (13.6 g, 91 mmol, 10 eq) was added to a stirred suspension of compound **77**<sup>138</sup> (4.01 g, 9.1 mmol) in acetone (50 mL). The Schlenk was sealed and the mixture was heated to 58 °C and stirred overnight. To prevent possible photodegradation of **78**, the reaction vessel was covered tightly with aluminum foil and the reaction workup was done in the presence of the smallest possible amount of light. After cooling down to 40 °C, acetone was removed *in vacuo*, and the obtained solid was dried under high vacuum for 30 min. Water (100 mL) was added, and the obtained suspension was stirred for 30 min. The mixture was filtered on a ceramic frit, and the crude product **78** was washed with water (100 mL), sat. aq. Na<sub>2</sub>S<sub>2</sub>O<sub>3</sub> (100 mL), water (100 mL), and ice-cold 2:1 MeOH/hexane mixture (100 mL). Product **78** – a pale yellow powder – was dried on the frit and then under high vacuum. Yield: 3.89 g (80%); m.p. = 130-132 °C (dec.); [α]<sub>D</sub><sup>24</sup> = + 112.81 (*c* = 0.345 in DCM); <sup>1</sup>H NMR (400 MHz, [D<sub>6</sub>]acetone): δ = 7.34 (d, <sup>3</sup>*J*(H,H) = 8.6 Hz, 2H), 7.25 (d, <sup>3</sup>*J*(H,H) = 8.2 Hz, 2H), 7.06 (d, <sup>3</sup>*J*(H,H) = 8.6 Hz, 2H), 6.77 (td, <sup>3</sup>*J*(H,H) = 8.2 Hz, <sup>4</sup>*J*(H,H) = 1.1 Hz, 2H), 6.55 (td, <sup>3</sup>*J*(H,H) = 8.2 Hz, <sup>4</sup>*J*(H,H) = 1.2 Hz, 2H), 6.25 (d, <sup>3</sup>*J*(H,H) = 8.6 Hz, 2H), 3.62 (d, <sup>2</sup>*J*(H,H) = 9.5 Hz, 2H, AB system), 3.51 (d, <sup>2</sup>*J*(H,H) = 9.5 Hz, 2H, AB system); <sup>13</sup>C NMR (100 MHz, [D<sub>6</sub>]acetone): δ = 136.2, 134.1, 133.0, 130.3, 129.2, 129.1, 127.8, 127.5, 127.3, 5.7; IR (film): ν = 2292.2, 1461.9, 1377.3, 1156.6 cm<sup>-1</sup>; elemental analysis (%): C 49.26, H 3.03 (calcd. for C<sub>22</sub>H<sub>16</sub>I<sub>2</sub>: C 49.47, H 3.02).

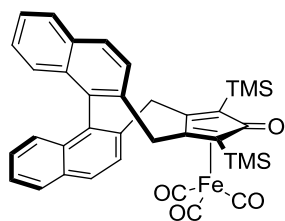
#### (*R*)-2,2'-Bis(3-(trimethylsilyl)prop-2-ynyl)-1,1'-binaphthyl **79**.



A solution of ethynyltrimethylsilane (0.565 mL, 4.0 mmol, 4 eq) in THF (5 mL) was added dropwise to a 1 M solution of ethylmagnesium bromide in THF (4.0 mL, 4.0 mmol, 4 eq) kept at 0 °C. The reaction mixture was heated to reflux and stirred for 1 h. After cooling to room temperature, CuI (0.095 g, 0.500 mmol, 0.5 eq) and compound **78** (0.534 g, 1.0 mmol, 1 eq) were added. The mixture was heated to reflux and stirred overnight. After cooling down to R.T., the reaction was quenched with sat. aq. NH<sub>4</sub>Cl (5 mL), and the obtained aqueous phase was extracted with AcOEt (3 × 25 mL). The organic layer was washed with H<sub>2</sub>O (20 mL) and brine (20 mL), dried over Na<sub>2</sub>SO<sub>4</sub> and concentrated *in vacuo*. Purification by column chromatography (95:5 hexane/DCM) gave the product **79** as a light yellow oil. Yield: 0.38 g

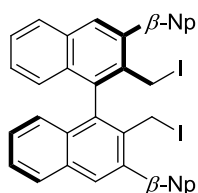
(80%); m.p. = 56 °C;  $[\alpha]_D^{24} = +134.55$  ( $c = 0.348$  in DCM);  $^1\text{H NMR}$  (400 MHz,  $\text{CD}_2\text{Cl}_2$ ):  $\delta = 8.03$  (d,  $^3J(\text{H,H}) = 8.5$  Hz, 2H), 7.95 (d,  $^3J(\text{H,H}) = 8.2$  Hz, 2H), 7.89 (d,  $^3J(\text{H,H}) = 8.5$  Hz, 2H), 7.45 (td,  $^3J(\text{H,H}) = 8.2$  Hz,  $^4J(\text{H,H}) = 1.1$  Hz, 2H), 7.24 (td,  $^3J(\text{H,H}) = 8.2$  Hz,  $^4J(\text{H,H}) = 1.3$  Hz, 2H), 6.99 (d,  $^3J(\text{H,H}) = 8.5$  Hz, 2H), 3.35 (d,  $^2J(\text{H,H}) = 19$  Hz, 2H, AB system), 3.22 (d,  $^2J(\text{H,H}) = 19$  Hz, 2H, AB system), 0.12 (s, 18H);  $^{13}\text{C NMR}$  (100 MHz,  $\text{CD}_2\text{Cl}_2$ ):  $\delta = 134.2, 133.7, 133.4, 133.0, 129.1, 128.7, 127.2, 127.2, 126.3, 126.0, 104.5, 87.6, 25.1, 0.3$ ; IR (film):  $\nu = 3059.0, 2959.8, 2174.8, 1484.9, 1265.1, 1249.8$   $\text{cm}^{-1}$ ; HRMS (ESI+):  $m/z$  497.20980  $[\text{M} + \text{Na}]^+$  (calcd. for  $\text{C}_{32}\text{H}_{34}\text{Si}_2\text{Na}$ : 497.20913).

#### Complex Fe20.

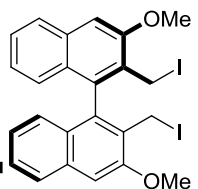


Under argon, diyne **79** (0.510 g, 1.07 mmol, 1 eq) and  $\text{Fe}_2(\text{CO})_9$  (0.781 g, 2.14 mmol, 2 eq) were dissolved in dry toluene (9 mL) and heated to 90 °C for 4 h. After cooling down to room temperature, the reaction mixture was filtered through a pad of Celite (rinsing with DCM). The filtrate was concentrated *in vacuo*, and the residue was purified by flash column chromatography (8:2 hexane/DCM) to obtain (**R**)-Fe20 as a pale yellow solid. Yield: 0.320 g (46%); m.p. = 209 °C (dec.);  $[\alpha]_D^{19} = -32.24$  ( $c = 0.9$  in DCM);  $^1\text{H NMR}$  (400 MHz,  $\text{CD}_2\text{Cl}_2$ ):  $\delta = 8.04$  (d,  $^3J(\text{H,H}) = 8.5$  Hz, 2H), 7.99 (d,  $^3J(\text{H,H}) = 8.8$  Hz, 1H), 7.97 (d,  $^3J(\text{H,H}) = 8.8$  Hz, 1H), 7.68 (d,  $^3J(\text{H,H}) = 8.5$  Hz, 1H), 7.55 (d,  $^3J(\text{H,H}) = 8.5$  Hz, 1H), 7.52-7.45 (m, 2H), 7.30 (td,  $^3J(\text{H,H}) = 8.5$  Hz,  $^4J(\text{H,H}) = 1.1$  Hz, 1H), 7.25 (td,  $^3J(\text{H,H}) = 8.5$  Hz,  $^4J(\text{H,H}) = 1.1$  Hz, 1H), 7.20 (d,  $^3J(\text{H,H}) = 8.5$  Hz, 1H), 7.09 (d,  $^3J(\text{H,H}) = 8.5$  Hz, 1H), 3.76 (d,  $^2J(\text{H,H}) = 15.7$  Hz, 1H), 3.67 (d,  $^2J(\text{H,H}) = 14.1$  Hz, 1H), 3.45 (d,  $^2J(\text{H,H}) = 15.7$  Hz, 1H), 3.38 (d,  $^2J(\text{H,H}) = 14.1$  Hz, 1H), 0.41 (s, 9H), 0.26 (s, 9H);  $^{13}\text{C NMR}$  (100 MHz,  $\text{CD}_2\text{Cl}_2$ ):  $\delta = 209.8, 181.4, 137.0, 135.6, 135.0, 134.6, 133.4, 132.5, 130.0, 129.7, 128.9, 128.7, 127.5, 127.3, 127.1, 127.0, 126.9, 126.5, 113.1, 111.5, 76.0, 74.0, 34.8, 32.8, 0.9, 0.5$ ; IR (film):  $\nu = 3054.69, 2953.93, 2060.1, 2005.1, 1985.4, 1626.2, 1507.6, 1429.5, 1264.1, 1248.7$   $\text{cm}^{-1}$ ; HRMS (ESI+):  $m/z$  643.14164  $[\text{M} + \text{H}]^+$  (calcd. for  $\text{C}_{36}\text{H}_{35}\text{O}_4\text{Si}_2\text{Fe}$ : 643.14294).

#### (R)-2'',3'-bis(iodomethyl)-2,2':4',1'':3'',2'''-quaternaphthalene **85**



Under nitrogen in a Schlenk tube fitted with a Teflon screw cap, NaI (1.33 g, 8.9 mmol, 8 eq) was added to a stirred suspension of (**R**)-2,2'-bis(bromomethyl)-3,3'-dimethoxy-1,1'-binaphthyl **84** (0.77 g, 1.1 mmol, 1 eq) in acetone (6 mL). The Schlenk was sealed and the mixture was heated to 58 °C and stirred overnight. To prevent possible photodegradation of **84**, the reaction vessel was covered tightly with aluminum foil and the reaction workup was done in the presence of the smallest possible amount of light. After cooling down to 40 °C, acetone was removed *in vacuo*, and the obtained solid was dried under high vacuum for 30 min. Water (100 mL) was added, and the obtained suspension was stirred for 30 min. The mixture was filtered on a ceramic frit, and the crude product **84** was washed with water (15 mL), sat. aq.  $\text{Na}_2\text{S}_2\text{O}_3$  (15 mL), water (15 mL), and ice-cold 2:1 MeOH/hexane mixture (15 mL). Product **84** – a pale yellow powder – was dried on the frit and then under high vacuum. Yield: 0.83 g (95%);  $^1\text{H NMR}$  (400 MHz,  $\text{CD}_2\text{Cl}_2$ ):  $\delta = 8.24$  (s, 2H), 7.97-8.07 (10 H, m), 7.89 (d, 2H,  $^3J(\text{H,H}) = 8.0$  Hz), 7.58-7.65 (6H, m), 7.31-7.43 (4H, m), 4.52 (d,  $^2J(\text{H,H}) = 12$  Hz, 2H, AB system), 4.41 (d,  $^2J(\text{H,H}) = 8.0$  Hz, 2H, AB system).

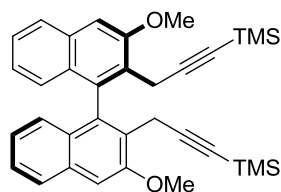


#### (R)-2,2'-Bis(iodomethyl)-3,3'-dimethoxy-1,1'-binaphthyl **95**.

Under nitrogen in a Schlenk tube fitted with a Teflon screw cap, NaI (16.5 g, 110 mmol, 10 eq) was added to a stirred suspension of (**R**)-2,2'-bis(bromomethyl)-3,3'-dimethoxy-1,1'-binaphthyl **94**<sup>138</sup> (5.50 g, 11.0 mmol) in

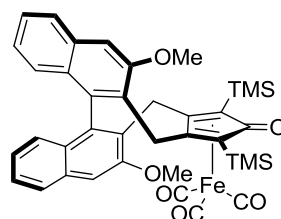
acetone (55 mL). The Schlenk was sealed and the mixture was heated to 58 °C and stirred overnight. To prevent possible photodegradation of **95**, the reaction vessel was covered tightly with aluminum foil and the reaction workup was done in the presence of the smallest possible amount of light. After cooling down to 40 °C, acetone was removed *in vacuo*, and the obtained solid was dried under high vacuum for 30 min. Water (100 mL) was added, and the obtained suspension was stirred for 30 min. The mixture was filtered on a ceramic frit, and the crude product **95** was washed with water (100 mL), sat. aq. Na<sub>2</sub>S<sub>2</sub>O<sub>3</sub> (120 mL), water (150 mL), and ice-cold 2:1 MeOH/hexane mixture (100 mL). Product **95** – a pale yellow powder – was dried on the frit and then under high vacuum. Yield: 5.94 g (91%); m.p. = 169-173 °C (dec.); [ $\alpha$ ]<sub>D</sub><sup>24</sup> = +133.48 (*c* = 0.52 in acetone); <sup>1</sup>H NMR (400 MHz, [D<sub>6</sub>]acetone):  $\delta$  = 7.93 (d, <sup>3</sup>*J*(H,H) = 8.2 Hz, 2H), 7.57 (s, 2H), 7.47 (td, <sup>3</sup>*J*(H,H) = 8.1 Hz, <sup>4</sup>*J*(H,H) = 1.1 Hz, 2H), 7.13 (td, <sup>3</sup>*J*(H,H) = 8.1 Hz, <sup>4</sup>*J*(H,H) = 1.2 Hz, 2H), 6.9 (d, <sup>3</sup>*J*(H,H) = 8.1 Hz, 2H), 4.28 (d, <sup>2</sup>*J*(H,H) = 8.9 Hz, 2H, AB system), 4.20 (d, <sup>2</sup>*J*(H,H) = 8.9 Hz, 2H, AB system), 4.15 (s, 6H); <sup>13</sup>C NMR (100 MHz, [D<sub>6</sub>]acetone):  $\delta$  = 156.5, 136.1, 135.7, 128.1, 128.1, 128.0, 127.9, 127.6, 125.1, 107.6, 56.3, 0.1; IR (film):  $\nu$  = 3060.5, 2959.7, 2935.6, 1618.0, 1597.7, 1570.7, 1445.9, 1422.7, 1327.3, 1158.0 cm<sup>-1</sup>; HRMS (ESI+): *m/z* 616.94566 [M + Na]<sup>+</sup> (calcd. for C<sub>24</sub>H<sub>20</sub>O<sub>2</sub>Na: 616.94449).

**(R)-(3,3'-(3,3'-dimethoxy-1,1'-binaphthyl-2,2'-diyl)bis(prop-1-yne-3,1-diyl))bis(trimethylsilane) 96**



*n*-BuLi (1.6 M hexane solution, 11.6 mL, 18.5 mmol, 3 eq) was added dropwise to a solution of ethynyltrimethylsilane (1.82 g, 2.62 mL, 18.5 mmol, 3 eq) in THF (12 mL) kept at -60 °C. The obtained mixture was allowed to warm to 0 °C and stirred for 30 min at this temperature, then it was cooled down again to -60 °C. A solution of bis-iodide **95** (3.63 g, 6.11 mmol, 1 eq) in THF (45 mL) was added and then the mixture was allowed to warm to R.T. and stirred overnight. The reaction was quenched with sat. aq. NH<sub>4</sub>Cl (50 mL) and extracted with Et<sub>2</sub>O (3 × 20 mL). The combined organic extracts were dried over Na<sub>2</sub>SO<sub>4</sub> and concentrated *in vacuo*. Diyne **96** can be either purified by flash column chromatography (8:2 hexane/DCM) or used in the following step without further purification. Yield after chromatography: 2.61 g (80%); m.p. = 75-83 °C; [ $\alpha$ ]<sub>D</sub><sup>24</sup> = +55.56 (*c* = 0.555 in CHCl<sub>3</sub>); <sup>1</sup>H NMR (400 MHz, CDCl<sub>3</sub>):  $\delta$  = 7.81 (d, <sup>3</sup>*J*(H,H) = 8.2 Hz, 2H), 7.40 (t, <sup>3</sup>*J*(H,H) = 8.2 Hz, 2H), 7.32 (s, 2H), 7.09-7.02 (m, 4H), 4.08 (s, 6H), 3.40 (d, <sup>2</sup>*J*(H,H) = 16.6 Hz, 2H, AB system), 3.29 (d, <sup>2</sup>*J*(H,H) = 16.6 Hz, 2H, AB system), 0.00 (s, 18H); <sup>13</sup>C NMR (100 MHz, CDCl<sub>3</sub>):  $\delta$  = 155.9, 136.1, 134.0, 128.3, 126.9, 126.6, 126.6, 126.3, 124.0, 106.0, 104.5, 83.6, 55.8, 19.6, 0.16; IR (film):  $\nu$  = 3062.9, 2958.3, 2898.0, 2173.9, 1620.4, 1597.7, 1446.8, 1327.3, 1248.7, 1109.8 cm<sup>-1</sup>; HRMS (ESI+): *m/z* 557.23139 [M + Na]<sup>+</sup> (calcd. for C<sub>34</sub>H<sub>38</sub>O<sub>2</sub>Si<sub>2</sub>Na: 557.23025).

**Complex Fe23**

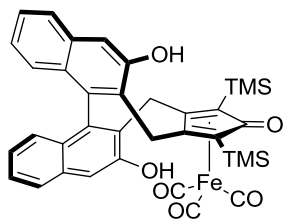


Under argon, diyne **96** (3.27 g, 6.11 mmol, 1 eq) and Fe<sub>2</sub>(CO)<sub>9</sub> (4.55g, 12.5 mmol, 2 eq) were dissolved in dry toluene (45 mL) and heated to 90 °C for 4.5 h. After cooling down to room temperature, the reaction mixture was filtered through a pad of Celite (rinsing with DCM). The filtrate was concentrated *in vacuo*, and the residue was purified by flash column chromatography (93:7 hexane/AcOEt) to obtain (*R*)-Fe**23** as a

pale yellow solid. Yield: 2.88 g (67% yield); m.p. = 233-237 °C (dec.); [ $\alpha$ ]<sub>D</sub><sup>23</sup> = -129.38 (*c* = 0.41 in DCM); <sup>1</sup>H NMR (400 MHz, CDCl<sub>3</sub>):  $\delta$  = 7.84 (m, 2H), 7.42 (t, <sup>3</sup>*J*(H,H) = 7.2 Hz, 2H), 7.33 (s, 1H), 7.30

(s, 1H), 7.11-7.03 (m, 2H), 6.92 (d,  $^3J(\text{H,H}) = 8.4$  Hz, 2H), 4.37 (d,  $^2J(\text{H,H}) = 15.5$  Hz, 1H), 4.15 (d,  $^2J(\text{H,H}) = 13.7$  Hz, 1H), 4.04 (s, 3H), 3.94 (s, 3H), 3.26 (d,  $^2J(\text{H,H}) = 13.7$  Hz, 1H), 3.12 (d,  $^2J(\text{H,H}) = 15.5$  Hz, 1H), 0.43 (s, 9H), 0.32 (s, 9H);  $^{13}\text{C}$  NMR (100 MHz,  $\text{CDCl}_3$ ):  $\delta = 208.7, 181.1, 155.1, 154.8, 138.6, 137.2, 133.9, 133.8, 127.4, 127.2, 127.1, 127.0, 126.9, 126.8, 126.6, 126.5, 126.4, 124.3, 124.1, 115.4, 107.8, 106.3, 105.7, 75.2, 74.9, 55.6, 54.8, 26.3, 26.2, 0.7, 0.2$ ; IR (film):  $\nu = 3059.5, 2960.2, 2169.0, 2059.6, 2004.2, 1987.3, 1620.4, 1598.7, 1454.1, 1246.3, 1111.3$   $\text{cm}^{-1}$ ; HRMS (ESI+):  $m/z$  703.16264  $[\text{M} + \text{H}]^+$  (calcd. for  $\text{C}_{38}\text{H}_{39}\text{O}_6\text{Si}_2\text{Fe}$ : 703.16410).

### Complex Fe24



Under nitrogen in a Schlenk tube fitted with a Teflon screw cap,  $\text{BBr}_3$  (1 M DCM solution, 14.0 mL, 14.0 mmol, 10 eq) was added dropwise to a stirred solution of (*R*)-**Fe23** (0.99 g, 1.41 mmol, 1 eq) and  $\text{Bu}_4\text{NI}$  (1.30 g, 3.52 mmol, 2.5 eq) in DCE (40 mL) kept at 0 °C. The Schlenk was sealed and the mixture was heated to 84 °C and stirred for 3 days. After this time, the reaction was cooled down to 0 °C and ice-cold  $\text{H}_2\text{O}$  (50 mL)

was added. The mixture was extracted with DCM (3 × 20 mL), washed with brine (30 mL) and then dried over  $\text{Na}_2\text{SO}_4$ . Filtration of the DCM solution through a short pad of silica allowed to remove the ammonium salts (which eluted before the product), then complex (*R*)-**Fe24** – a pale yellow solid – was purified by flash column chromatography (83:17 to 77:23 hexane/AcOEt). Yield: 0.762 g (80%); m.p. = 187-195 °C (dec.);  $[\alpha]_{\text{D}}^{23} = -115.07$  ( $c = 0.515$  in DCM);  $^1\text{H}$  NMR (400 MHz,  $\text{CDCl}_3$ ):  $\delta = 7.71$  (d,  $^3J(\text{H,H}) = 8.2$  Hz, 2H), 7.39-7.35 (m, 3H), 7.31 (s, 1H), 7.06 (t,  $^3J(\text{H,H}) = 7.5$  Hz, 2H), 6.98 (dd,  $^3J(\text{H,H}) = 8.3$  Hz,  $^4J(\text{H,H}) = 2.3$  Hz, 2H), 6.32 (br s, 2H), 4.34 (d,  $^2J(\text{H,H}) = 15.6$  Hz, 1H), 4.14 (d,  $^2J(\text{H,H}) = 13.8$  Hz, 1H), 3.24 (d,  $^2J(\text{H,H}) = 13.8$  Hz, 1H), 3.11 (d,  $^2J(\text{H,H}) = 15.5$  Hz, 1H), 0.41 (s, 9H), 0.31 (s, 9H);  $^{13}\text{C}$  NMR (100 MHz,  $\text{CDCl}_3$ ):  $\delta = 208.4, 180.3, 152.3, 152.2, 138.9, 137.7, 134.0, 133.9, 127.3, 127.3, 127.1, 126.4, 126.1, 125.5, 123.8, 123.6, 114.7, 110.4, 109.5, 76.3, 75.4, 29.8, 26.4, 0.9, 0.5$ ; IR (film):  $\nu = 3236.0, 2953.4, 2852.7, 2065.9, 2010.4, 1996.9, 1575.1, 1342.2, 1248.2$   $\text{cm}^{-1}$ ; HRMS (ESI+):  $m/z$  675.13152  $[\text{M} + \text{H}]^+$  (calcd. for  $\text{C}_{36}\text{H}_{35}\text{O}_6\text{Si}_2\text{Fe}$ : 675.13277).

### X-Ray Crystal Structure Analysis Of Complex Fe24

Crystals suitable for X-ray diffraction analysis have been obtained by slow diffusion of hexane into a DCM solution of complex (*R*)-**Fe24**. Crystal data and details of data collection and refinement are given in Table 5.7. Intensity data were collected with a Bruker Apex II CCD area detector by using graphite monochromated Mo- $K\alpha$  radiation. Data reduction was performed with SAINT, and absorption corrections based on multiscan were obtained with SADABS.<sup>163</sup> The structure was solved by direct methods using SHELXS-97 and refined by SHELXL-2013.<sup>164</sup> The program ORTEP-III was used for graphics.<sup>165</sup> Anisotropic thermal parameters were used for all non-hydrogen atoms. The isotropic thermal parameters of H atoms were fixed at 1.2 (1.5 for methyl groups) times those of the atom to which they were attached. All H atoms were placed in calculated positions and refined using a riding model with freely rotating methyl groups.

Table 5.7 Details of the Crystal Data and Structure Refinement for Compound (*R*)-**Fe24**

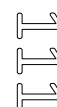
Crystal Data	
Empirical formula	$\text{C}_{40}\text{H}_{44}\text{FeO}_8\text{Si}_2$
Moiety formula	$\text{C}_{36}\text{H}_{34}\text{FeO}_6\text{Si}_2 \cdot \text{C}_4\text{H}_{10}\text{O} \cdot \text{H}_2\text{O}$
Formula weight	764.78



Crystal system	Orthorhombic
Space group	$P2_12_12_1$
$a/\text{\AA}$	11.1452(5)
$b/\text{\AA}$	16.4340(7)
$c/\text{\AA}$	22.8671(10)
$V/\text{\AA}^3$	4188.3(3) $\text{\AA}^3$
$Z$	4
Temperature/K	130(2)
Density (calculated) $D_x/\text{Mg m}^{-3}$	1.213
Absorption coefficient $\mu/\text{mm}^{-1}$	0.464
Color, habit	orange, prism
Dimensions /mm	0.30×0.30×0.20
<i>Data Collection</i>	
radiation, $\lambda/\text{\AA}$	Mo $K\alpha$ , 0.71073
$2\theta_{\text{max}}/^\circ$	49.34
$h$ range	-13→13
$k$ range	-19→19
$l$ range	-26→26
Measured reflections	55474
Independent reflections	7102
Reflections with $I > 2\sigma(I)$	6162
$R_{\text{int}}$	0.0577
<i>Refinement on <math>F^2</math></i>	
Data, restraints, parameters	7102, 1, 488
$S$	1.049
Final $R$ , $wR$ [ $F^2 > 2\sigma(F^2)$ ]	0.0377, 0.0920
Final $R$ , $wR$ (all data)	0.0478, 0.0985
Flack parameter	0.000(7)
$(\Delta/\sigma)_{\text{max}}$	0.001
$\Delta\rho_{\text{max}}, \Delta\rho_{\text{min}}/e\text{\AA}^{-3}$	0.359, -0.270

An ORTEP view of the complex is presented in Figure 5.7 and selected geometrical parameters are collected in Table 5.8. The structure includes one water molecule, disordered over three positions labeled Ow1, Ow2 and Ow3 with occupancies 0.4, 0.4 and 0.2, respectively (only Ow1 is shown in Figure 5.7 for clarity) and one Et<sub>2</sub>O molecule. The latter, which is strongly hydrogen-bonded to one hydroxyl group (O1–H1) of the complex through its oxygen atom O7 (O1⋯O7, 2.752 Å; O1–H1⋯O7, 164.4°), was probably bonded to the complex during solubilization attempts made before the crystallization.

The crystal structure of (*R*)-**Fe24** shows typical geometrical parameters observed in related structures. In particular, the cyclopentadienone ring strongly deviates from planarity, with atom C24 significantly bent away from the iron atom (see Table 5.8). The dihedral angle between the l.s. plane through the coordinated butadiene and the plane defined by C23, C24 and C25, 13.9(2)°, is typical for cyclopentadienone-iron complexes.<sup>95</sup> The dihedral angle between the l.s.



planes through the carbon atoms of the naphthyl moieties,  $67.9(1)^\circ$ , is quite similar to that found in other binaphthyl derivatives where the *ortho* positions are connected through a (diylidimethylene)cyclopentadienyl group.<sup>166</sup> In Table 5.8 are also reported the relevant distances concerning atom O2, which remarkably affects the level of enantioselectivity in ketone hydrogenation, as discussed in the article.

CCDC 1037376 contains the supplementary crystallographic data for this structure. These data can be obtained free of charge from The Cambridge Crystallographic Data Centre via [www.ccdc.cam.ac.uk/data\\_request/cif](http://www.ccdc.cam.ac.uk/data_request/cif).

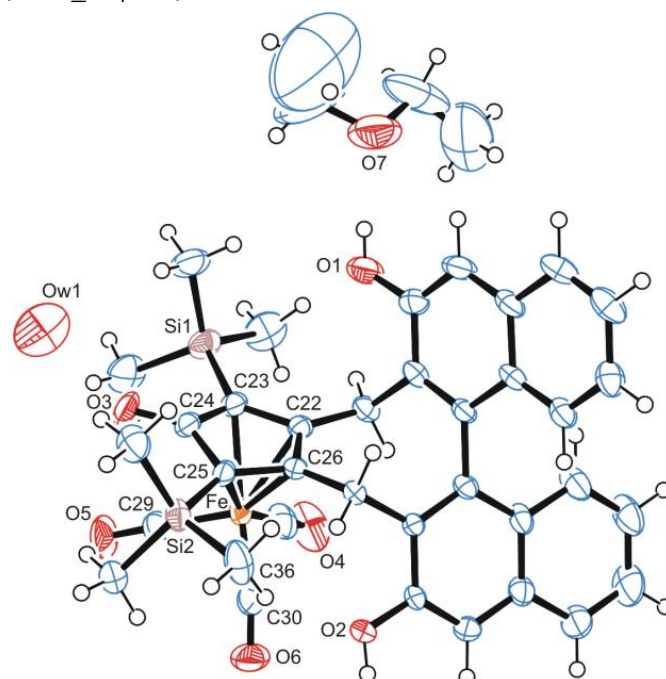
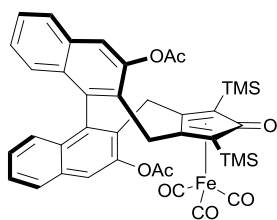


Figure 5.7 ORTEP view of the asymmetric unit of **Fe24**·Et<sub>2</sub>O·H<sub>2</sub>O. Thermal ellipsoids are drawn at the 50% probability level.

Table 5.8 Selected interatomic distances (Å) for **Fe24**.

Fe–C22	2.095(4)	O2...C29	5.356(3)
Fe–C26	2.115(4)	O2...O5	6.296(3)
Fe–C23	2.139(4)	O2...Fe	4.016(2)
Fe–C25	2.145(4)	O2...O3	6.429(2)
Fe–C24	2.310(4)	O2...Si2	4.408(2)
		O2...C36	3.641(4)

### Complex Fe25



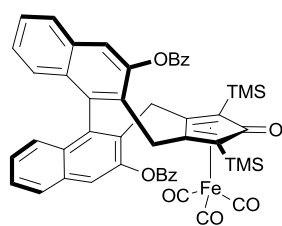
Acetyl chloride (32  $\mu$ L, 0.44 mmol, 3 eq) was slowly added to a stirred solution of **Fe24** (100 mg, 0.15 mmol, 1 eq), Et<sub>3</sub>N (83  $\mu$ L, 0.59 mmol, 4 eq) and DMAP (1.6 mg, 0.015 mmol, 0.1 eq) in THF (2 mL), then the mixture was refluxed for 3 h. After this time, the mixture was diluted DCM and washed with 0.5 M HCl (2  $\times$  5 mL), sat. aq. NaHCO<sub>3</sub> (5 mL) and brine (5 mL). The organic phase was then dried over Na<sub>2</sub>SO<sub>4</sub>. Complex

112

**Fe25** – a pale yellow solid – was purified by flash column chromatography (90:10 to 85:15 hexane/AcOEt). Yield: 103.3 g (92%); m.p. = 162–166  $^\circ$ C;  $[\alpha]_D^{22} = +19.37$  ( $c = 0.51$  in DCM); <sup>1</sup>H

NMR (400 MHz, CDCl<sub>3</sub>)  $\delta$  7.90 (d,  $^3J(\text{H,H}) = 8.2$  Hz, 1H), 7.87 (d,  $^3J(\text{H,H}) = 8.2$  Hz, 1H), 7.80 (s, 1H), 7.73 (s, 1H), 7.52-7.43 (m, 2H), 7.25-7.17 (m, 2H), 6.99 (d,  $^3J(\text{H,H}) = 8.4$  Hz, 1H), 6.85 (d,  $^3J(\text{H,H}) = 8.4$  Hz, 1H), 4.00 (d,  $^2J(\text{H,H}) = 16.0$  Hz, 1H), 3.89 (d,  $^2J(\text{H,H}) = 14.3$  Hz, 1H), 3.36 (d,  $^2J(\text{H,H}) = 14.3$  Hz, 1H), 3.34 (d,  $^2J(\text{H,H}) = 16.0$  Hz, 1H), 2.45 (s, 3H), 2.39 (s, 3H), 0.45 (s, 9H), 0.32 (s, 9H); <sup>13</sup>C NMR (100 MHz, CDCl<sub>3</sub>)  $\delta$  208.2, 181.0, 170.1, 169.8, 146.1, 138.8, 137.5, 133.0, 132.9, 130.2, 130.1, 128.7, 127.9, 127.8, 127.5, 127.0, 126.8, 126.7, 126.6, 121.6, 121.1, 112.0, 110.2, 74.9, 74.6, 27.5, 26.6, 22.3, 21.9, 0.9, 0.5; IR (film):  $\nu = 3062.4, 2953.9, 2923.6, 2903.3, 2852.7, 2062.5, 2007.5, 1989.7, 1768.4, 1624.25, 1189.4, 1155.6, 1087.7, 849.0$  cm<sup>-1</sup>; HRMS (ESI+):  $m/z$  759.15207 [M + H]<sup>+</sup> (calcd. for C<sub>50</sub>H<sub>43</sub>O<sub>8</sub>Si<sub>2</sub>Fe: 759.15395).

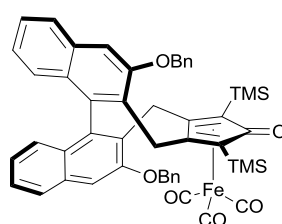
### Complex Fe26



Benzoyl chloride (26  $\mu\text{L}$ , 0.22 mmol, 3 eq) was slowly added to a stirred solution of **Fe24** (50 mg, 0.07 mmol, 1 eq), Et<sub>3</sub>N (41  $\mu\text{L}$ , 0.3 mmol, 4 eq) and DMAP (0.8 mg, 0.007 mmol, 0.1 eq) in THF (1 mL), then the mixture was refluxed for 4 h. After this time, the mixture was diluted with DCM and washed with 0.5 M HCl (2  $\times$  5 mL), sat. aq. NaHCO<sub>3</sub> (5 mL) and brine (5 mL). The organic phase was then dried over Na<sub>2</sub>SO<sub>4</sub>. After

concentration, the pure complex (*R*)-1e - a pale yellow solid - was purified by flash column chromatography (95:5 to 9:1 hexane/AcOEt). Yield: 53 mg (81%); m.p. = 176 °C (dec.);  $[\alpha]_{436}^{27} = -108.6$  ( $c = 0.25$  in DCM); <sup>1</sup>H NMR (400 MHz, CDCl<sub>3</sub>)  $\delta$  8.26 (m, 1H), 8.24 (m, 1H), 8.21 (m, 1H), 8.19 (m, 1H), 7.92 (d,  $^3J(\text{H,H}) = 4.7$  Hz, 1H), 7.90 (d,  $^3J(\text{H,H}) = 4.6$  Hz, 1H), 7.83 (s, 1H), 7.82 (s, 1H), 7.72-7.64 (m, 2H), 7.59-7.46 (m, 6H), 7.31-7.26 (m, 2H), 7.01 (dd,  $^3J(\text{H,H}) = 8.4$ ,  $^4J(\text{H,H}) = 0.6$  Hz, 1H), 6.97 (dd,  $^3J(\text{H,H}) = 8.5$ ,  $^4J(\text{H,H}) = 0.6$  Hz, 1H), 4.01 (d,  $^2J(\text{H,H}) = 14.5$  Hz, 1H), 3.98 (d,  $^2J(\text{H,H}) = 16.1$  Hz, 1H), 3.58 (d,  $^2J(\text{H,H}) = 14.6$  Hz, 1H), 3.49 (d,  $^2J(\text{H,H}) = 16.1$  Hz, 1H), 0.10 (s, 9H), 0.03 (s, 9H); <sup>13</sup>C NMR (100 MHz, CDCl<sub>3</sub>)  $\delta$  208.1, 181.0, 167.0, 166.6, 147.3, 147.1, 139.0, 137.8, 134.2, 134.1, 133.3, 131.1, 130.7, 129.7, 129.7, 129.5, 129.2, 128.7, 127.8, 127.1, 126.9, 126.7, 121.1, 120.7, 113.2, 109.1, 75.7, 74.8, 27.7, 27.2, 0.7, 0.3; IR (film):  $\nu = 3062.9, 2953.9, 2897.5, 2062.0, 2007.5, 1990.2, 1740.4, 1624.7, 1266.0, 1246.3, 1090.1, 1022.1, 847.1, 711.1$  cm<sup>-1</sup>; HRMS (ESI+):  $m/z$  883.187411 [M + H]<sup>+</sup> (calcd. for C<sub>50</sub>H<sub>43</sub>O<sub>8</sub>Si<sub>2</sub>Fe: 883.18537).

### Complex Fe27

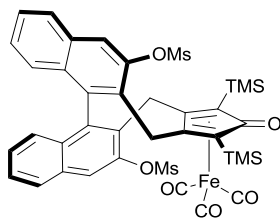


Benzyl bromide (53  $\mu\text{L}$ , 0.45 mmol, 6 eq) was slowly added to a stirred solution of **Fe24** (50 mg, 0.07 mmol, 1 eq) and K<sub>2</sub>CO<sub>3</sub> (41 mg, 0.30 mmol, 4 eq) in DMF (0.37 mL) and stirred at 70 °C overnight. After this time, the reaction was cooled down to R.T. and diluted with Et<sub>2</sub>O (8 mL). The mixture was washed with H<sub>2</sub>O (3  $\times$  5 mL) and the organic phase dried over Na<sub>2</sub>SO<sub>4</sub>. Complex **Fe27** - a pale yellow solid - was

purified by flash column chromatography (9:1 DCM/hexane). Yield: 42 mg (70%); m.p. = 155 °C (dec.);  $[\alpha]_{\text{D}}^{32} = -20.6$  ( $c = 0.92$  in DCM); <sup>1</sup>H NMR (400 MHz, CDCl<sub>3</sub>)  $\delta$  7.80 (d,  $^3J(\text{H,H}) = 8.1$  Hz, 1H), 7.71 (d,  $^3J(\text{H,H}) = 8.1$  Hz, 1H), 7.46-7.23 (m, 14H), 7.11-7.03 (m, 2H), 6.91-6.84 (m, 2H), 5.51 (d,  $^2J(\text{H,H}) = 13.5$  Hz, 1H), 5.46 (d,  $^2J(\text{H,H}) = 13.5$  Hz, 1H), 5.26 (d,  $^2J(\text{H,H}) = 11.3$  Hz, 1H), 5.17 (d,  $^2J(\text{H,H}) = 11.3$  Hz, 1H), 4.38 (d,  $^2J(\text{H,H}) = 15.6$  Hz, 1H), 4.29 (d,  $^2J(\text{H,H}) = 13.8$  Hz, 1H), 3.35 (d,  $^2J(\text{H,H}) = 13.8$  Hz, 1H), 3.15 (d,  $^2J(\text{H,H}) = 15.6$  Hz, 1H), 0.32 (s, 9H), 0.08 (s, 9H); <sup>13</sup>C NMR (100 MHz, CDCl<sub>3</sub>)  $\delta$  208.6, 181.1, 154.1, 153.6, 139.0, 137.6, 136.7, 136.1, 133.8, 133.6, 129.1, 128.9, 128.7, 128.5, 128.1, 127.4, 127.4, 127.2, 127.1, 127.1, 127.0, 126.9, 126.9, 126.6, 126.4, 124.3, 124.3,

114.8, 108.7, 108.6, 107.3, 75.8, 75.1, 70.5, 70.1, 26.4, 26.2, 0.8, 0.2; IR (film):  $\nu = 3063.4, 3034.4, 2953.0, 2899.0, 2060.1, 2004.2, 1987.3, 1757.3, 1620.9, 1596.8, 1246.3, 1105.5, 850.5, 738.1 \text{ cm}^{-1}$ ; HRMS (ESI+):  $m/z$  855.22583  $[\text{M} + \text{H}]^+$  (calcd. for  $\text{C}_{50}\text{H}_{47}\text{O}_6\text{Si}_2\text{Fe}$ : 855.22685).

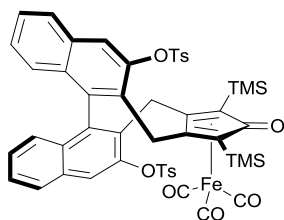
### Complex Fe28



Methanesulfonyl chloride (17  $\mu\text{L}$ , 0.22 mmol, 3 eq) was slowly added to a stirred solution of **Fe24** (50 mg, 0.07 mmol, 1 eq),  $\text{Et}_3\text{N}$  (41  $\mu\text{L}$ , 0.30 mmol, 4 eq) and DMAP (0.8 mg, 0.007 mmol, 0.1 eq) in THF (1 mL), then the mixture was refluxed for 5 h. After this time, the reaction was cooled down to R.T., diluted with AcOEt (5 mL) and washed with 0.5 M HCl (2  $\times$  5 mL), sat. aq.  $\text{NaHCO}_3$  (5 mL) and brine (5 mL). The organic

phase was dried over  $\text{Na}_2\text{SO}_4$ . After concentration, the pure complex **Fe28** was obtained as a pale yellow solid. Yield: 40 mg (65%); m.p. = 172  $^\circ\text{C}$  (dec.);  $[\alpha]_{\text{D}}^{27} = -6.8$  ( $c = 1.4$  in DCM);  $^1\text{H}$  NMR (400 MHz,  $\text{CDCl}_3$ )  $\delta$  8.12 (s, 1H), 8.09 (s, 1H), 7.99 (d,  $^3J(\text{H,H}) = 8.3$  Hz, 1H), 7.96 (d,  $^3J(\text{H,H}) = 8.3$  Hz, 1H), 7.56 (dd,  $^3J(\text{H,H}) = 8.3$  Hz,  $^3J(\text{H,H}) = 7.0$  Hz, 1H), 7.53 (dd,  $^3J(\text{H,H}) = 8.3$  Hz,  $^3J(\text{H,H}) = 6.9$  Hz, 1H), 7.33 (dd,  $^3J(\text{H,H}) = 8.4$  Hz,  $^3J(\text{H,H}) = 7.0$  Hz, 1H), 7.28 (dd,  $^3J(\text{H,H}) = 8.5$  Hz,  $^3J(\text{H,H}) = 6.9$  Hz, 1H), 6.99 (d,  $^3J(\text{H,H}) = 8.4$  Hz, 1H), 6.85 (d,  $^3J(\text{H,H}) = 8.5$  Hz, 1H), 4.25 (d,  $^2J(\text{H,H}) = 16.2$  Hz, 1H), 4.15 (d,  $^2J(\text{H,H}) = 14.4$  Hz, 1H), 3.35 (d,  $^2J(\text{H,H}) = 14.4$  Hz, 1H), 3.33 (d,  $^2J(\text{H,H}) = 16.2$  Hz, 1H), 3.31 (s, 3H), 3.29 (s, 3H), 0.45 (s, 9H), 0.33 (m, 9H);  $^{13}\text{C}$  NMR (100 MHz,  $\text{CDCl}_3$ )  $\delta$  208.2, 181.4, 144.4, 143.5, 139.3, 138.0, 132.8, 132.7, 130.5, 130.5, 128.8, 128.5, 128.4, 128.2, 128.0, 127.8, 127.8, 127.7, 126.6, 126.3, 121.9, 121.4, 111.1, 110.1, 75.5, 75.1, 38.8, 38.6, 27.7, 26.7, 0.7, 0.5; IR (film):  $\nu = 3054.2, 2986.7, 2066.4, 2010.4, 1994.5, 1617.5, 1265.6, 739.1, 705.3 \text{ cm}^{-1}$ ; HRMS (ESI+):  $m/z$  853.06820  $[\text{M} + \text{Na}]^+$  (calcd. for  $\text{C}_{38}\text{H}_{38}\text{O}_{10}\text{S}_2\text{Si}_2\text{FeNa}$ : 853.06985).

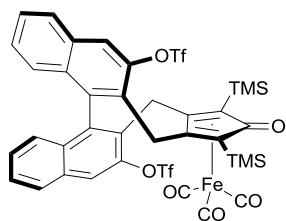
### Complex Fe29



*p*-Toluenesulfonyl chloride (43 mg, 0.22 mmol, 3 eq) was slowly added to a stirred solution of **Fe24** (50 mg, 0.07 mmol, 1 eq),  $\text{Et}_3\text{N}$  (41  $\mu\text{L}$ , 0.30 mmol, 4 eq) and DMAP (0.8 mg, 0.007 mmol, 0.1 eq) in THF (1 mL), then the mixture was refluxed overnight. The reaction was cooled down to R.T., diluted with AcOEt (5 mL) and washed with 0.5 M HCl (2  $\times$  5 mL), sat. aq.  $\text{NaHCO}_3$  (5 mL) and brine (5 mL). The organic phase was

dried over  $\text{Na}_2\text{SO}_4$  and then concentrated. Complex **Fe29** – a pale yellow solid – was purified by flash column chromatography (8:2 hexane/AcOEt). Yield: 63 mg (96%); m.p. = 166-168  $^\circ\text{C}$  (dec.);  $[\alpha]_{\text{D}}^{23} = +168.6$  ( $c = 1.2$  in DCM);  $^1\text{H}$  NMR (400 MHz,  $\text{CDCl}_3$ )  $\delta$  7.92 (s, 1H), 7.85 (d,  $^3J(\text{H,H}) = 8.3$  Hz, 1H), 7.82 (d,  $^3J(\text{H,H}) = 8.3$  Hz, 1H), 7.79 (s, 1H), 7.70 (d,  $^3J(\text{H,H}) = 8.0$  Hz, 2H), 7.65 (d,  $^3J(\text{H,H}) = 8.0$  Hz, 2H), 7.51 (t,  $^3J(\text{H,H}) = 7.5$  Hz, 2H), 7.29-7.19 (m, 6H), 6.65 (d,  $^3J(\text{H,H}) = 8.4$  Hz, 1H), 6.54 (d,  $^3J(\text{H,H}) = 8.5$  Hz, 1H), 3.93 (d,  $^2J(\text{H,H}) = 16.1$  Hz, 1H), 3.92 (d,  $^2J(\text{H,H}) = 14.3$  Hz, 1H), 3.01 (d,  $^2J(\text{H,H}) = 14.3$  Hz, 1H), 2.86 (d,  $^2J(\text{H,H}) = 16.1$  Hz, 1H), 2.40 (s, 3H), 2.37 (s, 3H), 0.43 (s, 9H), 0.27 (s, 9H);  $^{13}\text{C}$  NMR (100 MHz,  $\text{CDCl}_3$ )  $\delta$  208.0, 181.3, 145.9, 145.9, 145.0, 145.0, 138.8, 137.3, 132.7, 132.5, 132.4, 130.2, 130.1, 130.0, 129.9, 129.3, 128.9, 128.8, 128.5, 128.4, 128.3, 127.4, 127.3, 127.3, 126.2, 126.1, 121.2, 121.2, 111.5, 108.6, 75.3, 74.9, 27.3, 26.4, 21.9, 21.9, 0.6, 0.6. IR (film):  $\nu = 3054.2, 2986.7, 2916.8, 2066.4, 2010.9, 1422.2, 1265.6, 895.8, 740.5, 705.3 \text{ cm}^{-1}$ ; HRMS (ESI+):  $m/z$  983.14923  $[\text{M} + \text{H}]^+$  (calcd. for  $\text{C}_{50}\text{H}_{47}\text{O}_{10}\text{S}_2\text{Si}_2\text{Fe}$ : 983.15069).

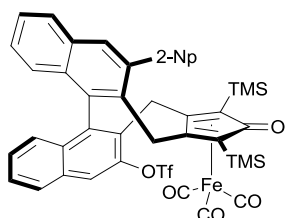
## Complex Fe30



*N*-(5-Chloro-2-pyridyl)bis(trifluoromethanesulfonimide) (1.2 g, 3.0 mmol, 3 eq) was added to a stirred solution of **Fe24** (670 mg, 1.0 mmol, 1 eq), Et<sub>3</sub>N (550 μL, 4.0 mmol, 4 eq) and DMAP (12 mg, 0.1 mmol, 0.1 eq) in DCM (30 mL) and stirred at R.T. overnight. The reaction was diluted with DCM (30 mL) and washed with 0.5 M HCl (2 × 50 mL), 0.5 M NaOH (2 × 50 mL) and brine (50 mL). The organic phase was then dried

over Na<sub>2</sub>SO<sub>4</sub>. Complex **Fe30** – a pale yellow solid – was purified by flash column chromatography (10:1 hexane/AcOEt). Yield: 882 mg (94%); m.p. = 142-143 °C (dec.); [α]<sub>D</sub><sup>24</sup> = + 43.9 (*c* = 1.9 in DCM); <sup>1</sup>H NMR (400 MHz, CDCl<sub>3</sub>) δ 8.14 (s, 1H), 8.12 (s, 1H), 8.03 (d, <sup>3</sup>*J*(H,H) = 8.5 Hz, 1H), 8.01 (d, <sup>3</sup>*J*(H,H) = 8.3 Hz, 1H), 7.62 (t, <sup>3</sup>*J*(H,H) = 7.5 Hz, 1H), 7.61 (t, <sup>3</sup>*J*(H,H) = 7.5 Hz, 1H), 7.40 (t, <sup>3</sup>*J*(H,H) = 8.2 Hz, 1H), 7.38 (t, <sup>3</sup>*J*(H,H) = 8.1 Hz, 1H), 6.90 (d, <sup>3</sup>*J*(H,H) = 8.5 Hz, 1H), 6.84 (d, <sup>3</sup>*J*(H,H) = 8.5 Hz, 1H), 4.18 (d, <sup>2</sup>*J*(H,H) = 16.2 Hz, 1H), 4.13 (d, <sup>2</sup>*J*(H,H) = 14.6 Hz, 1H), 3.40 (d, <sup>2</sup>*J*(H,H) = 14.7 Hz, 1H), 3.35 (d, <sup>2</sup>*J*(H,H) = 16.2 Hz, 1H), 0.41 (s, 9H), 0.31 (s, 9H); <sup>13</sup>C NMR (100 MHz, CDCl<sub>3</sub>) δ 207.9, 181.3, 145.2, 144.9, 139.4, 137.9, 132.7, 132.6, 130.8, 130.7, 128.9, 128.8, 128.8, 128.7, 128.4, 128.3, 127.8, 127.1, 126.2, 126.0, 120.9, 120.8, 119.0 (q, <sup>1</sup>*J*(C,F) = 324.5 Hz), 118.9 (q, <sup>1</sup>*J*(C,F) = 324.5 Hz), 110.7, 108.7, 75.5, 75.5, 27.6, 26.8, 0.5, 0.4; <sup>19</sup>F NMR (282 MHz, CDCl<sub>3</sub>) δ -71.7, -72.7; IR (film): ν = 3066.7, 2954.9, 2925.5, 2903.3, 2852.7, 2065.4, 2011.9, 1993.6, 1629.1, 1427.6, 1245.8, 1212.5, 1138.3, 915.5, 883.2, 844.7, 822.0 cm<sup>-1</sup>; HRMS (ESI+): *m/z* 961.01272 [M + Na]<sup>+</sup> (calcd. for C<sub>38</sub>H<sub>32</sub>O<sub>10</sub>F<sub>6</sub>Si<sub>2</sub>FeNa: 961.01332).

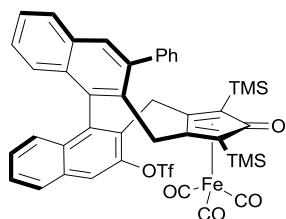
## Complex Fe31



**Fe30** (100 mg, 0.1 mmol, 1 eq), Pd(OAc)<sub>2</sub> (4.5 mg, 0.02 mmol, 0.2 eq), PPh<sub>3</sub> (10.5 mg, 0.04 mmol, 0.4 eq), K<sub>3</sub>PO<sub>4</sub> (63 mg, 0.3 mmol, 3 eq), KBr (26 mg, 0.22 mmol, 2.2 eq) and phenylboronic acid (30.5 mg, 0.25 mmol, 2.5 eq) were dissolved in dioxane (2.5 mL). The reaction was heated to 85 °C and stirred overnight. The mixture was diluted with DCM (5 mL) and washed with 1 M NaOH (5 mL), H<sub>2</sub>O (5 mL) and brine (5

mL), then dried over Na<sub>2</sub>SO<sub>4</sub>. Complex **Fe31** – a yellow solid – was purified by flash column chromatography (DCM/hexane 7:3). Yield: 15 mg (17%); <sup>1</sup>H NMR (400 MHz, CDCl<sub>3</sub>) δ 8.12 (s, 1H), 7.89-8.02 (m 6H), 7.81 (m, 2H), 7.62 (t, <sup>3</sup>*J*(H,H) = 8.0 Hz, 1H), 7.54 (m, 3H), 7.41 (m 2H), 7.29 (t, <sup>3</sup>*J*(H,H) = 8.0 Hz, 1H), 7.09 (m, 1H), 6.74 (d, <sup>3</sup>*J*(H,H) = 8.0 Hz, 1H), 4.24 (d, <sup>2</sup>*J*(H,H) = 14.8 Hz, 1H), 4.13 (d, <sup>2</sup>*J*(H,H) = 15.8 Hz, 1H), 3.64 (d, <sup>2</sup>*J*(H,H) = 14.8 Hz, 1H), 3.52 (d, <sup>2</sup>*J*(H,H) = 15.8 Hz, 1H), 0.34 (s, 9H), -0.40 (s, 9H); ESI-MS in CH<sub>3</sub>CN: [M+H]<sup>2+</sup> *m/z* 917.2

## Complex Fe32

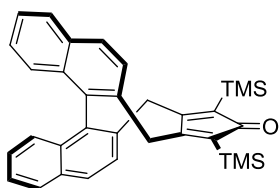


**Fe30** (100 mg, 0.1 mmol, 1 eq), Pd(OAc)<sub>2</sub> (4.5 mg, 0.02 mmol, 0.2 eq), PPh<sub>3</sub> (10.5 mg, 0.04 mmol, 0.4 eq), K<sub>3</sub>PO<sub>4</sub> (63 mg, 0.3 mmol, 3 eq), KBr (26 mg, 0.22 mmol, 2.2 eq) and phenylboronic acid (30.5 mg, 0.25 mmol, 2.5 eq) were dissolved in dioxane (2.5 mL). The reaction was heated to 85 °C and stirred overnight. The mixture was diluted with DCM (5 mL) and washed with 1 M NaOH (5 mL), H<sub>2</sub>O (5 mL) and brine (5

mL), then dried over Na<sub>2</sub>SO<sub>4</sub>. Complex **Fe32** – a yellow solid – was purified by flash column chromatography (6:4 to 8:2 DCM/hexane). Yield: 69 mg (80%); m.p. = 157-158 °C (dec.); [α]<sub>D</sub><sup>21</sup> = +

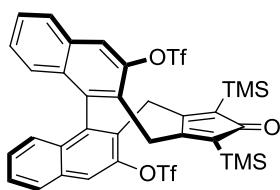
88.3 ( $c = 0.6$  in DCM);  $^1\text{H}$  NMR (400 MHz,  $\text{CDCl}_3$ )  $\delta$  8.10 (s, 1H), 8.01 (d,  $^3J(\text{H,H}) = 8.2$  Hz, 1H), 7.93 (d,  $^3J(\text{H,H}) = 8.2$  Hz, 1H), 7.90 (s, 1H), 7.63–7.31 (m, 8H), 7.26 (dd,  $^3J(\text{H,H}) = 8.5$  Hz,  $^3J(\text{H,H}) = 7.3$  Hz, 1H), 7.02 (d,  $^3J(\text{H,H}) = 8.5$  Hz, 1H), 6.70 (d,  $^3J(\text{H,H}) = 8.5$  Hz, 1H), 4.27 (d,  $^2J(\text{H,H}) = 14.8$  Hz, 1H), 4.11 (d,  $^2J(\text{H,H}) = 15.8$  Hz, 1H), 3.58 (d,  $^2J(\text{H,H}) = 14.8$  Hz, 1H), 3.50 (d,  $^2J(\text{H,H}) = 15.8$  Hz, 1H), 0.33 (s, 9H), -0.15 (s, 9H);  $^{13}\text{C}$  NMR (100 MHz,  $\text{CDCl}_3$ )  $\delta$  208.1, 180.8, 144.9, 141.6, 141.3, 139.4, 136.1, 132.7, 132.5, 132.5, 132.1, 131.1, 130.9, 128.6, 128.3, 128.1, 127.9, 127.6, 127.4, 127.0, 126.4, 125.7, 120.0, 118.9 (q,  $^1J(\text{C,F}) = 321.3$  Hz), 111.8, 111.2, 75.9, 75.5, 29.5, 27.5, 0.5, 0.4;  $^{19}\text{F}$  NMR (282 MHz,  $\text{CDCl}_3$ )  $\delta$  -72.1; IR (film):  $\nu = 3054.7, 2987.2, 2065.4, 2009.5, 1639.7, 1421.8, 1265.6, 744.4, 705.3$   $\text{cm}^{-1}$ ; HRMS (ESI+):  $m/z$  889.10212  $[\text{M} + \text{Na}]^+$  (calcd. for  $\text{C}_{43}\text{H}_{37}\text{O}_7\text{F}_3\text{S}_1\text{Si}_2\text{FeNa}$ : 889.10049).

### 1,3-bis(trimethylsilyl)-4,17-dihydro-2H-cyclopenta[6,7]cycloocta[2,1-a:3,4-a']dinaphthalen-2-one **97**



A solution of complex **Fe20** (104 mg, 0.16 mmol, 1 eq), in THF (2.7 mL) and aqueous 1 M NaOH (1.3 mL) was stirred for 2.5 h under an argon atmosphere. Then 1-iodopentane was added (50  $\mu\text{L}$ , 0.38 mmol, 2.4 eq) and the yellow solution turned brown. After stirring the mixture for an additional 15 min under argon,  $\text{H}_3\text{PO}_4$  (85%, 50  $\mu\text{L}$ ) was added, the reaction stirred for 5 min and the organic layer separated. The aqueous layer was extracted with  $\text{Et}_2\text{O}$  ( $2 \times 7$  mL). The combined organic layers were dried over  $\text{Na}_2\text{SO}_4$  and filtered through a short path of silica gel. After addition of  $\text{Na}_2\text{S}_2\text{O}_3 \cdot 5 \text{H}_2\text{O}$  (105 mg) and Celite (65 mg) the filtrate was stirred slowly in the air for 16 h in the presence of daylight. Filtration through a short path of Celite, evaporation of the solvent, and flash chromatography (9:1 hexane/DCM) of the residue on silica gel provided the free ligand **97**. Yield: 79 mg (99%)  $^1\text{H}$  NMR (400 MHz,  $\text{CDCl}_3$ )  $\delta$  7.95 (d,  $J = 8.4$  Hz, 4H), 7.53 (d,  $J = 8.4$  Hz, 2H), 7.51 – 7.46 (m, 2H), 7.30 (d,  $J = 3.6$  Hz, 4H), 4.02 (d,  $J = 14.8$  Hz, 2H), 3.22 (d,  $J = 14.8$  Hz, 2H), 0.27 (s, 18H).

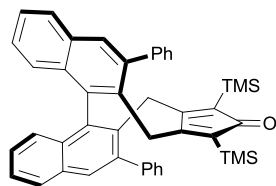
### (*R*)-2-Oxo-1,3-bis(trimethylsilyl)-4,17-dihydro-2-cyclopenta[6,7]cycloocta[2,1-a:3,4-a']-dinaphthalene-5,16-diyl bis(trifluoromethanesulfonate) **98**



A solution of complex **Fe30** (150 mg, 0.16 mmol, 1 eq), in THF (2.7 mL) and aqueous 1 M NaOH (1.3 mL) was stirred for 2.5 h under an argon atmosphere. Then 1-iodopentane was added (50  $\mu\text{L}$ , 0.38 mmol, 2.4 eq) and the yellow solution turned brown. After stirring the mixture for an additional 15 min under argon,  $\text{H}_3\text{PO}_4$  (85%, 50  $\mu\text{L}$ ) was added, the reaction stirred for 5 min and the organic layer separated. The aqueous layer was extracted with  $\text{Et}_2\text{O}$  ( $2 \times 7$  mL). The combined organic layers were dried over  $\text{Na}_2\text{SO}_4$  and filtered through a short path of silica gel. After addition of  $\text{Na}_2\text{S}_2\text{O}_3 \cdot 5 \text{H}_2\text{O}$  (105 mg) and Celite (65 mg) the filtrate was stirred slowly in the air for 16 h in the presence of daylight. Filtration through a short path of Celite, evaporation of the solvent, and flash chromatography (9:1 hexane/DCM) of the residue on silica gel provided the free ligand **98**. Yield: 35 mg (28%); m.p. = 204–207  $^\circ\text{C}$ ;  $[\alpha]_{\text{D}}^{21} = +112.4$  ( $c = 0.6$  in DCM);  $^1\text{H}$  NMR (400 MHz,  $\text{CDCl}_3$ )  $\delta$  8.07 (s, 2H), 8.01 (d,  $^3J(\text{H,H}) = 8.3$  Hz, 2H), 7.62 (dd,  $^3J(\text{H,H}) = 8.3, 6.4$  Hz, 1H), 7.41 (dd,  $^3J(\text{H,H}) = 8.4, 6.4$  Hz, 1H), 7.20 (d,  $^3J(\text{H,H}) = 8.5$  Hz, 2H), 4.36 (d,  $^2J(\text{H,H}) = 15.6$  Hz, 2H), 3.06 (d,  $^2J(\text{H,H}) = 15.6$  Hz, 2H), 0.22 (s, 18H);  $^{13}\text{C}$  NMR (100 MHz,  $\text{CDCl}_3$ )  $\delta$  209.6, 164.7, 147.5, 138.9, 132.8, 132.1, 130.6, 129.1, 128.8, 128.3, 128.0, 126.7, 119.0, 118.9 (q,  $^1J(\text{C,F}) = 321.5$  Hz), 30.1, 0.2;  $^{19}\text{F}$  NMR (282 MHz,  $\text{CDCl}_3$ )  $\delta$  -72.75; IR (film):  $\nu = 2953.5, 2906.2, 1685.0, 1426.1, 1241.0, 1214.0, 1138.8, 847.1$   $\text{cm}^{-1}$ ; HRMS (ESI+):  $m/z$  821.08966  $[\text{M} + \text{Na}]^+$  (calcd.

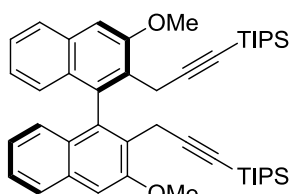
for C<sub>35</sub>H<sub>32</sub>O<sub>7</sub>F<sub>6</sub>S<sub>2</sub>Si<sub>2</sub>Na: 821.09244).

**(R)-5,16-Diphenyl-1,3-bis(trimethylsilyl)-4,17-dihydro-2H-cyclopenta[6,7]cycloocta[2,1-a:3,4-a']dinaphthalen-2-one 99**



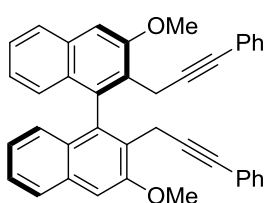
**99** (35 mg, 0.044 mmol, 1 eq), Pd(OAc)<sub>2</sub> (2 mg, 0.009 mmol, 0.2 eq), PPh<sub>3</sub> (4.6 mg, 0.018 mmol, 0.4 eq), K<sub>3</sub>PO<sub>4</sub> (37 mg, 0.18 mmol, 3 eq), KBr (12 mg, 0.10 mmol, 2.2 eq) and phenylboronic acid (16 mg, 0.13 mmol, 3 eq) were dissolved in dioxane (1 mL). The reaction was stirred at 85 °C overnight. The mixture was diluted with DCM (5 mL) and washed with 1 M NaOH (5 mL), H<sub>2</sub>O (5 mL) and brine (5 mL), then dried over Na<sub>2</sub>SO<sub>4</sub>. Ligand **99** – a yellow solid – was purified by flash column chromatography (29:1 hexane/DCM). Yield: 25 mg (86%); m.p. = 264-266 °C; [α]<sub>D</sub><sup>20</sup> = +150.5 (*c* = 0.5 in DCM); <sup>1</sup>H NMR (400 MHz, CDCl<sub>3</sub>) δ 7.92 (d, <sup>3</sup>*J*(H,H) = 8.2 Hz, 2H), 7.79 (s, 2H), 7.51 (ddd, <sup>3</sup>*J*(H,H) = 8.1, 6.7 Hz, <sup>4</sup>*J*(H,H) = 1.2 Hz, 2H), 7.45-7.38 (m, 6H), 7.38-7.29 (m, 6H), 7.24 (d, <sup>3</sup>*J*(H,H) = 8.4 Hz, 2H), 4.00 (d, <sup>2</sup>*J*(H,H) = 15.4 Hz, 2H), 3.30 (d, <sup>2</sup>*J*(H,H) = 15.4 Hz, 2H), -0.20 (s, 18H); <sup>13</sup>C NMR (100 MHz, CDCl<sub>3</sub>) δ 210.8, 169.5, 142.1, 141.7, 137.7, 134.1, 132.3, 131.5, 129.9, 129.6, 128.6, 128.1, 127.5, 126.9, 126.5, 126.4, 33.8, 0.0.; IR (film): ν = 3058.6, 2958.8, 2896.1, 1679.7, 1542.3, 1245.3, 850.5, 748.2, 701.0 cm<sup>-1</sup>; HRMS (ESI+): *m/z* 655.28304 [M + H]<sup>+</sup> (calcd. for C<sub>45</sub>H<sub>43</sub>O<sub>1</sub>Si<sub>2</sub>: 655.28470).

**(R)-((3,3'-Dimethoxy-[1,1'-binaphthalene]-2,2'-diyl)bis(prop-1-yne-3,1-diyl))bis-(triisopropylsilane)100**



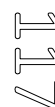
*n*-BuLi (1.6 M hexane solution, 560 μL, 0.9 mmol, 3 eq) was added dropwise to a solution of ethynyltriisopropylsilane (200 μL, 0.9 mmol, 3 eq) in THF (1 mL) kept at -60 °C. The obtained mixture was allowed to warm to 0 °C and stirred for 30 min at this temperature, and then it was cooled down again to -60 °C. A solution of bis-iodide **95** (178 mg, 0.3 mmol, 1 eq) in THF (3 mL) was added and then the mixture was allowed to warm to R.T. and stirred overnight. The reaction was quenched with sat. aq. NH<sub>4</sub>Cl (5 mL) and extracted with Et<sub>2</sub>O (3 × 5 mL). The combined organic extracts were dried over Na<sub>2</sub>SO<sub>4</sub> and concentrated in *vacuo*. Diyne **100** was purified by flash column chromatography (8:2 hexane/DCM). Yield: 86 mg (41%); m.p. = 61-62 °C; [α]<sub>D</sub><sup>20</sup> = +22.4 (*c* = 0.6 in DCM); <sup>1</sup>H NMR (400 MHz, CDCl<sub>3</sub>) δ 7.80 (d, <sup>3</sup>*J*(H,H) = 8.1 Hz, 2H), 7.40 (ddd, <sup>3</sup>*J*(H,H) = 8.1, 6.6 Hz, <sup>4</sup>*J*(H,H) = 1.4 Hz, 2H), 7.29 (s, 2H), 7.10-6.99 (m, 4H), 4.05 (s, 6H), 3.34 (s, 4H), 0.98-0.92 (m, 36H); <sup>13</sup>C NMR (100 MHz, CDCl<sub>3</sub>) δ 156.2, 135.8, 133.9, 128.5, 127.1, 127.0, 126.6, 126.2, 124.2, 106.4, 105.6, 79.3, 55.5, 20.1, 18.7, 11.4; IR (film): ν = 2962.1, 2941.9, 2862.8, 2171.5, 1260.3, 1092.5, 1020.2, 799.4 cm<sup>-1</sup>; HRMS (ESI+): *m/z* 725.41937 [M + Na]<sup>+</sup> (calcd. for C<sub>46</sub>H<sub>62</sub>O<sub>2</sub>Si<sub>2</sub>Na: 725.41806).

**(R)-3,3'-Dimethoxy-2,2'-bis(3-phenylprop-2-yn-1-yl)-1,1'-binaphthalene 101**



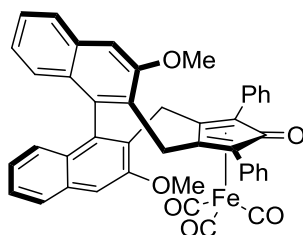
*n*-BuLi (1.6 M hexane solution, 790 μL, 1.26 mmol, 3 eq) was added dropwise to a solution of ethynylbenzene (140 μL, 1.26 mmol, 3 eq) in THF (1.5 mL) kept at -60 °C. The obtained mixture was allowed to warm to 0 °C and stirred for 30 min at this temperature, and then it was cooled down again to -60 °C. A solution of bis-iodide **95** (250 mg, 0.42 mmol, 1 eq) in THF (4 mL) was added and then the mixture was allowed to warm

to R.T. and stirred overnight. The reaction was quenched with sat. aq. NH<sub>4</sub>Cl (5 mL) and extracted with Et<sub>2</sub>O (3 × 5 mL). The combined organic extracts were dried over Na<sub>2</sub>SO<sub>4</sub> and concentrated in



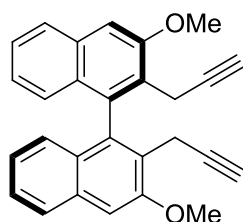
*vacuo*. Diyne **101** was purified by flash column chromatography (8:2 hexane/DCM). Yield: 180 mg (79%); m.p. = 94-95 °C;  $[\alpha]_D^{16} = -20.9$  ( $c = 0.7$  in DCM);  $^1\text{H NMR}$  (400 MHz,  $\text{CDCl}_3$ )  $\delta$  7.82 (d,  $^3J(\text{H,H}) = 8.2$  Hz, 2H), 7.39 (ddd,  $^3J(\text{H,H}) = 8.1$ , 6.5 Hz,  $^4J(\text{H,H}) = 1.4$  Hz, 2H), 7.35 (s, 2H), 7.21-7.12 (m, 10H), 7.12-7.02 (m, 4H), 4.10 (s, 6H), 3.64 (d,  $^2J(\text{H,H}) = 16.5$  Hz, 2H), 3.51 (d,  $^2J(\text{H,H}) = 16.5$  Hz, 2H);  $^{13}\text{C NMR}$  (100 MHz,  $\text{CDCl}_3$ )  $\delta$  156.0, 136.3, 134.0, 131.7, 128.5, 128.0, 127.4, 126.9, 126.7, 126.7, 126.4, 124.2, 124.0, 106.0, 88.2, 80.0, 55.9, 19.0.; IR (film):  $\nu = 3060.5, 2934.2, 2365.3, 1619.0, 1596.8, 1422.2, 1107.9, 1020.2, 755.0, 691.4$   $\text{cm}^{-1}$ ; HRMS (ESI+):  $m/z$  565.21535  $[\text{M} + \text{Na}]^+$  (calcd. for  $\text{C}_{40}\text{H}_{30}\text{O}_2\text{Na}$ : 565.21380).

#### Complex Fe34



Diyne **101** (271 mg, 0.50 mmol, 1 eq) and  $\text{Fe}_2(\text{CO})_9$  (455 mg, 1.25 mmol, 2.5 eq) were dissolved in toluene (6 mL) and stirred to 90 °C overnight. After cooling down to room temperature, the reaction mixture was filtered through a pad of Celite (rinsing with DCM). The filtrate was concentrated in *vacuo*, and the residue was purified by flash column chromatography (8:2 hexane/DCM) to obtain **Fe34** as a pale yellow solid. Yield: 201 mg (57% yield); m.p. = 156-158 °C;  $[\alpha]_D^{17} = -92.1$  ( $c = 0.4$  in DCM);  $^1\text{H NMR}$  (400 MHz,  $\text{CDCl}_3$ )  $\delta$  7.85 (d,  $^3J(\text{H,H}) = 8.2$  Hz, 1H), 7.80 (d,  $^3J(\text{H,H}) = 8.2$  Hz, 1H), 7.46-7.30 (m, 5H), 7.30 (s, 1H), 7.26 (s, 1H), 7.21-7.01 (m, 9H), 6.91 (m, 1H), 6.81 (m, 1H), 3.97 (d,  $^2J(\text{H,H}) = 15.2$  Hz, 1H), 3.96 (s, 3H), 3.86 (d,  $^2J(\text{H,H}) = 14.3$  Hz, 1H), 3.80 (s, 3H), 3.08 (d,  $^2J(\text{H,H}) = 15.1$  Hz, 1H), 2.99 (d,  $^2J(\text{H,H}) = 14.3$  Hz, 1H);  $^{13}\text{C NMR}$  (100 MHz,  $\text{CDCl}_3$ )  $\delta$  213.8, 212.2, 205.9, 204.7, 183.1, 167.3, 155.6, 155.1, 148.7, 148.6, 138.6, 138.4, 134.0, 133.8, 132.7, 129.8, 128.6, 128.2, 128.0, 127.5, 127.2, 127.0, 127.0, 127.0, 126.9, 126.6, 126.5, 126.4, 126.4, 126.3, 124.1, 123.9, 105.9, 105.6, 55.1, 54.8, 30.2, 29.3; IR (film):  $\nu = 3055.7, 2919.7, 2858.0, 2061.5, 1985.4, 2024.9, 1599.6, 1451.2, 1111.8, 1025.9$   $\text{cm}^{-1}$ ; HRMS (ESI+):  $m/z$  733.13041  $[\text{M} + \text{Na}]^+$  (calcd. for  $\text{C}_{40}\text{H}_{30}\text{O}_2\text{Na}$ : 733.12972).

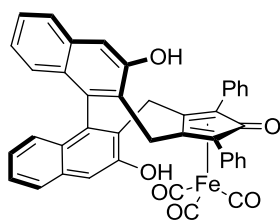
#### (R)-3,3'-Dimethoxy-2,2'-di(prop-2-yn-1-yl)-1,1'-binaphthalene **102**



A solution of **96** (244 mg, 0.34 mmol, 1 eq) in MeOH (5 mL) and DCM (2.5 mL) was treated with  $\text{K}_2\text{CO}_3$  (276 mg, 2 mmol, 5.9 eq) and stirred at 30 °C overnight. After this time,  $\text{H}_2\text{O}$  (10 mL) were added and the mixture was extracted with DCM. The combined organic extracts were dried over  $\text{Na}_2\text{SO}_4$  and concentrated in *vacuo*. Diyne **102** was recrystallized from a mixture hexane/DCM (9:1) Yield: 120 mg (90%); m.p. = 150-152 °C;  $[\alpha]_D^{16} = +112.0$  ( $c = 0.5$  in DCM);  $^1\text{H NMR}$  (400 MHz,  $\text{CDCl}_3$ )  $\delta$  7.81 (d,  $^3J(\text{H,H}) = 8.2$  Hz, 2H), 7.40 (ddd,  $^3J(\text{H,H}) = 8.2$  Hz,  $^3J(\text{H,H}) = 6.7$  Hz,  $^4J(\text{H,H}) = 1.4$  Hz, 2H), 7.32 (s, 2H), 7.07 (ddd,  $^3J(\text{H,H}) = 8.4$  Hz,  $^3J(\text{H,H}) = 6.7$  Hz,  $^4J(\text{H,H}) = 1.2$  Hz, 2H), 7.01 (d,  $^3J(\text{H,H}) = 8.4$  Hz, 2H), 4.09 (s, 6H), 3.36 (dd,  $^2J(\text{H,H}) = 16.5$  Hz,  $^4J(\text{H,H}) = 2.7$  Hz, 2H), 3.24 (dd,  $^2J(\text{H,H}) = 16.5$  Hz,  $^4J(\text{H,H}) = 2.7$  Hz, 2H), 1.71 (t,  $^4J(\text{H,H}) = 2.7$  Hz, 2H).;  $^{13}\text{C NMR}$  (100 MHz,  $\text{CDCl}_3$ )  $\delta$  155.8, 136.2, 134.0, 128.3, 126.9, 126.7, 126.5, 126.3, 124.0, 106.0, 82.2, 67.8, 55.9, 18.3; IR (film):  $\nu = 3290.9, 3058.6, 2934.2, 2118.4, 1619.0, 1597.7, 1447.3, 1422.2, 1326.8, 1217.8, 1108.9, 1020.2$   $\text{cm}^{-1}$ ; HRMS (ESI+):  $m/z$  413.15186  $[\text{M} + \text{Na}]^+$  (calcd. for  $\text{C}_{40}\text{H}_{30}\text{O}_2\text{Na}$ : 413.15120).



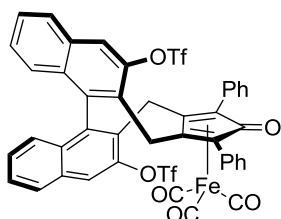
## Complex Fe37



Under argon in a Schlenk tube fitted with a Teflon screw cap,  $\text{BBr}_3$  (1 M DCM solution, 10.0 mL, 10.0 mmol, 10 eq) was added dropwise to a stirred solution of (*R*)-**Fe34** (0.71 g, 1.0 mmol, 1 eq) and  $\text{Bu}_4\text{NI}$  (0.92 g, 2.5 mmol, 2.5 eq) in DCE (25 mL) kept at 0 °C. The Schlenk was sealed and the mixture was heated to 84 °C and stirred for 3 days. After this time, the reaction was cooled down to 0 °C and ice-cold  $\text{H}_2\text{O}$  (30 mL)

was added. The mixture was extracted with DCM (3 × 15 mL), washed with brine (25 mL) and then dried over  $\text{Na}_2\text{SO}_4$ . Filtration of the DCM solution through a short pad of silica allowed to remove the ammonium salts (which eluted before the product), then complex (*R*)-**Fe37** – a pale yellow solid – was purified by flash column chromatography (7:3 heptane/AcOEt). Yield: 0.105 g (15%);  $^1\text{H}$  NMR (300 MHz,  $\text{CDCl}_3$ ):  $\delta$  = 7.72 (d,  $^3J(\text{H,H})$  = 9 Hz, 1H), 7.80 (d,  $^3J(\text{H,H})$  = 9 Hz, 1H), 7.38-7.21 (m, 5H), 7.16-6.97 (m, 11 H), 6.89 (m, 1H), 6.79 (m, 1H), 5.11 (bs, 1H), 5.02 (bs, 1H), 3.92 (d,  $^2J(\text{H,H})$  = 15 Hz, 1H), 3.65 (d,  $^2J(\text{H,H})$  = 15 Hz, 1H), 3.12 (d,  $^2J(\text{H,H})$  = 15 Hz, 1H), 3.02 (d,  $^2J(\text{H,H})$  = 15 Hz, 1H).

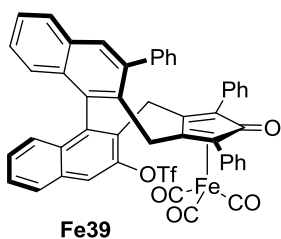
## Complex Fe38



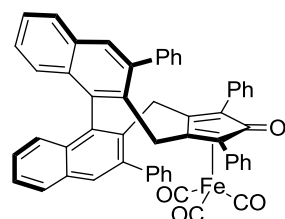
*N*-(5-Chloro-2-pyridyl)bis(trifluoromethanesulfonimide) (0.12 g, 0.3 mmol, 3 eq) was added to a stirred solution of **Fe37** (68 mg, 0.1 mmol, 1 eq),  $\text{Et}_3\text{N}$  (55  $\mu\text{L}$ , 0.4 mmol, 4 eq) and DMAP (1.2 mg, 0.01 mmol, 0.1 eq) in DCM (3 mL) and stirred at R.T. overnight. The reaction was diluted with DCM (5 mL) and washed with 0.5 M HCl (2 × 10 mL), 0.5 M NaOH (2 × 10 mL) and brine (20 mL). The organic phase was then dried over

$\text{Na}_2\text{SO}_4$ . Complex **Fe38** – a pale yellow solid – was purified by flash column chromatography (10:2 heptane/AcOEt). Yield: 91 mg (96%).  $^1\text{H}$  NMR (300 MHz,  $\text{CDCl}_3$ )  $\delta$  8.25 (s, 1H), 8.07 (t,  $J$  = 4.0 Hz, 2H), 8.03 (d,  $J$  = 8.3 Hz, 1H), 7.61 (dd,  $J$  = 15.8, 7.8 Hz, 2H), 7.48 – 7.25 (m, 5H), 7.25 – 7.09 (m, 5H), 7.04 (d,  $J$  = 8.3 Hz, 1H), 6.99 (d,  $J$  = 8.3 Hz, 1H), 6.93 – 6.81 (m, 1H), 6.75 – 6.66 (m, 1H), 3.98 (d,  $J$  = 11.8 Hz, 1H), 3.93 (d,  $J$  = 12.1 Hz, 1H), 3.31 (d,  $J$  = 15.6 Hz, 1H), 3.12 (d,  $J$  = 15.3 Hz, 1H).  $^{19}\text{F}$  NMR (282 MHz,  $\text{CDCl}_3$ )  $\delta$  -73.3, -74.1.

## Complexes Fe39 and Fe40



Fe39



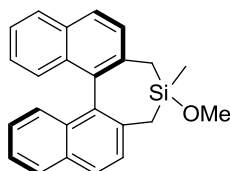
Fe40

**Fe38** (90 mg, 0.1 mmol, 1 eq),  $\text{Pd}(\text{OAc})_2$  (4.5 mg, 0.02 mmol, 0.2 eq),  $\text{PPh}_3$  (10.5 mg, 0.04 mmol, 0.4 eq),  $\text{K}_3\text{PO}_4$  (63 mg, 0.3 mmol, 3 eq), KBr (26 mg, 0.22 mmol, 2.2 eq) and phenylboronic acid (30.5 mg, 0.25 mmol, 2.5 eq) were dissolved in dioxane (3 mL). The reaction was heated to 85 °C and stirred overnight. The mixture was diluted with DCM (5 mL) and washed with 1 M NaOH (5 mL),  $\text{H}_2\text{O}$  (5 mL) and brine

(10 mL), then dried over  $\text{Na}_2\text{SO}_4$ . Mixture of complexes **Fe39** and **Fe40** – a yellow solid – was purified by flash column chromatography (7:3 heptane/AcOEt). Yield **Fe39**: 25 mg (30%).  $^1\text{H}$  NMR (600 MHz,  $\text{CD}_2\text{Cl}_2$ )  $\delta$  8.07 (s, 1H), 8.05 (d,  $J$  = 8.3 Hz, 1H), 7.95 (d,  $J$  = 8.2 Hz, 1H), 7.83 (s, 1H), 7.63 (t,  $J$  = 7.2 Hz, 1H), 7.60 – 7.57 (m, 1H), 7.56 – 7.50 (m, 3H), 7.44 – 7.41 (m, 2H), 7.40 – 7.37 (m, 2H), 7.36 (t,  $J$  = 6.9 Hz, 2H), 7.28 – 7.26 (m, 1H), 7.24 – 7.20 (m, 4H), 7.02 – 6.94 (m, 3H), 6.88 (d,  $J$  = 8.8 Hz, 1H), 6.86 – 6.83 (m, 1H), 3.96 (d,  $J$  = 15.9 Hz, 1H), 3.87 (d,  $J$  = 15.4 Hz, 1H), 3.40 (d,  $J$  = 12.5 Hz, 1H), 3.17 (d,  $J$  = 15.9 Hz, 1H). ESI-MS:

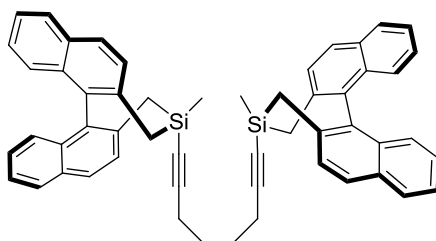
$m/z$  897.0  $[M + Na]^+$  (calcd. for  $C_{49}H_{29}F_3FeO_7S$ : 874.1). Yield **Fe40**: 28 mg (35%).  $^1H$  NMR (600 MHz,  $CD_2Cl_2$ )  $\delta$  7.98 (s, 1H), 7.97 (s, 1H), 7.89 (d,  $J = 8.1$  Hz, 1H), 7.71 (s, 1H), 7.53 – 7.48 (m, 1H), 7.48 – 7.44 (m, 1H), 7.40 – 7.32 (m, 4H), 7.32 – 7.28 (m, 3H), 7.27 – 7.18 (m, 6H), 7.09 (dt,  $J = 19.9$ , 7.1 Hz, 3H), 7.00 (dd,  $J = 15.3$ , 7.9 Hz, 2H), 6.96 (d,  $J = 8.1$  Hz, 2H), 6.94 – 6.89 (m, 2H), 6.84 (t,  $J = 7.3$  Hz, 1H), 6.80 (d,  $J = 7.4$  Hz, 1H), 4.16 (d,  $J = 15.7$  Hz, 1H), 4.03 (d,  $J = 15.0$  Hz, 1H), 3.41 (d,  $J = 15.0$  Hz, 1H), 3.31 (d,  $J = 15.7$  Hz, 1H). ESI-MS:  $m/z$  825.2  $[M + Na]^+$  (calcd. for  $C_{54}H_{34}FeO_4$ : 802.2).

#### 4-methoxy-4-methyl-4,5-dihydro-3H-dinaphtho[2,1-c:1',2'-e]silepine **103**



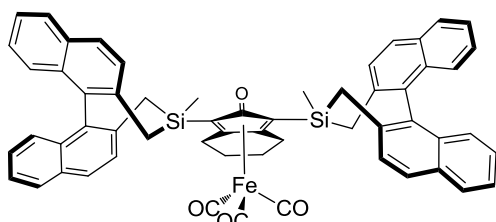
Adapting the procedure described by Mattson and co-workers,<sup>167</sup> under argon a Schlenk flask was charged with *n*-BuLi (2.7 M heptane solution, 8.3 mL, 22.5 mmol, 3 eq) and cooled to 0 °C. **76** (2.12 g, 7.5 mmol) was dissolved in dry  $Et_2O$  (25 mL) and added dropwise to the Schlenk tube. The solution was stirred at 0 °C for 10 minutes, then dry *N,N,N,N*-tetramethylethylenediamine (TMEDA, 3.5 mL, 22.5 mmol, 3 eq) was added dropwise at 0 °C. Solution changed color to yellow and it was stirred for 24 h at R.T. The resulting dark red mixture was cooled to 0 °C and trimethoxy(methyl)silane (4.2 mL, 29.2 mmol, 3.9 eq) in dry  $Et_2O$  (25 mL) was added dropwise. The mixture was stirred overnight at R.T. The solution was concentrated and purified using column chromatography (95:5 heptane/AcOEt). Yield 53% (1.4 g).  $^1H$  NMR (300 MHz,  $CDCl_3$ )  $\delta$  7.89 (d,  $J = 8.4$  Hz, 2H), 7.84 (d,  $J = 8.4$  Hz, 2H), 7.49 (d,  $J = 8.4$  Hz, 1H), 7.42 (d,  $J = 8.4$  Hz, 1H), 7.37 (t,  $J = 9.0$  Hz, 2H), 7.18 (t,  $J = 9.0$  Hz, 2H), 7.12-7.08 (m, 2H), 3.40 (s, 3H), 2.24-2.07 (m, 3H), 1.89 (d,  $J = 15$  Hz, 1H), 0.13 (s, 3H).

#### 1,8-bis((4*S*,11*B**R*)-4-methyl-4,5-dihydro-3H-dinaphtho[2,1-c:1',2'-e]silepin-4-yl)octa-1,7-diyne **104**



Under argon, in a Schlenk flask, a stirred solution of with 1,7-octadiyne (0.09 mL, 0.66 mmol, 0.45 eq) in THF (2.5 mL) was cooled to -78 °C. *n*-BuLi (2.7 M heptane solution, 0.5 mL, 1.35 mmol, 0.93 eq) was added dropwise and the reaction was stirred for 10 min. at -78 °C and then 30 min. at 0 °C. A THF solution (2.5 mL) of **103** (0.52 g, 1.46 mmol, 1 eq) was added dropwise at 0 °C. After addition, mixture was stirred for 2 h at R.T. and quenched with 1 M HCl (5 mL) at 0 °C. Organic materials were extracted with  $Et_2O$  (2x 10 mL) and washed with water (2x 15 mL) and brine (1x 20 mL). After drying over anhydrous  $Na_2SO_4$  the solvent was removed *in vacuo*, and the residue was purified by flash column chromatography (7:3 heptane/DCM) to obtain **104** as a white foamy solid. Yield 80 mg (36% when calculated from diyne).  $^1H$  NMR (300 MHz,  $CDCl_3$ )  $\delta$  7.89 (d,  $J = 8.4$  Hz, 4H), 7.84 (d,  $J = 8.4$  Hz, 4H), 7.48 (d,  $J = 8.4$  Hz, 2H), 7.39-7.32 (m, 6H), 7.19-7.08 (m, 8H), 2.12-2.04 (m, 6H), 1.87 (d,  $J = 15$  Hz, 2H), 1.59-1.54 (m, 4H), 0.91-0.86 (m, 4H), 0.17 (s, 6H). ESI-MS  $m/z$  773.6  $[M + Na]^+$  (calcd. for  $C_{54}H_{46}Si_2$ : 750.3).

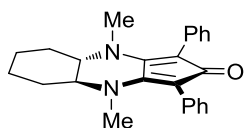
#### Complex **Fe41**



Under argon, diyne **104** (153 mg, 0.2 mmol, 1 eq) and  $Fe_2(CO)_9$  (185 mg, 0.5 mmol, 2.5 eq) were dissolved in dry toluene (3 mL) and heated to 90 °C for 6 h. After cooling down to room temperature, the reaction mixture was filtered through a pad of Celite (rinsing with DCM). The filtrate was concentrated *in vacuo*, and the residue was purified by flash column chromatography (9:1 heptane/AcOEt) to obtain **Fe41**

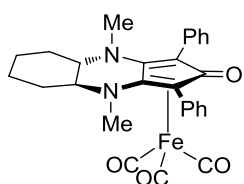
as a pale yellow solid. Yield: 130 mg (70%).  $^1\text{H}$  NMR (300 MHz,  $\text{CDCl}_3$ )  $\delta$  7.89-7.84 (m, 8H), 7.52-7.33 (m, 8H), 7.23-7.03 (m, 8H), 2.35-2.19 (m, 4H), 2.07-1.93 (m, 4H), 1.40-1.33 (m, 4H), 1.30-1.25 (m, 4H), 0.43 (s, 3H), 0.28 (s, 3H). ESI-MS  $m/z$  941.3  $[\text{M} + \text{Na}]^+$  (calcd. for  $\text{C}_{58}\text{H}_{46}\text{FeO}_4\text{Si}_2$ : 918.2).

**(4S,8S)-4,9-dimethyl-1,3-diphenyl-4,4,5,6,7,8,8,9-octahydro-2H-cyclopenta[b]quinoxalin-2-one 106**



Adapting the procedure described by Renoud and co-workers,<sup>111</sup> in a Schlenk tube, the diphenylcyclopentanetrione **105** (500 mg, 1.90 mmol, 1 eq) and (*R,R*)-*N,N*-dimethylcyclohexane-1,2-diamine (280 mg, 1.90 mmol, 1 eq) were mixed in methanol (10 mL). The reaction mixture was heated under reflux for 3 h. After removing solvent *in vacuo*, the pure **106** was obtained as a dark purple powder. Yield 660 mg (92%).  $^1\text{H}$  NMR (300 MHz,  $\text{CDCl}_3$ )  $\delta$  7.30-7.25 (m, 8H), 7.16-7.12 (m, 2H), 3.13 (m, 2H), 2.78 (s, 6H), 1.90-1.83 (m, 4H), 1.40-1.35 (m, 4H).

**Complex Fe42**



Under argon, the cyclopentadienone derivative **106** (0.66 g, 1.75 mmol, 1 eq) and  $\text{Fe}_2(\text{CO})_9$  (1.25 g, 3.5 mmol, 2 eq) were dissolved in dry toluene (12 mL) and heated to 90 °C for 4 h. After cooling down to room temperature, the reaction mixture was filtered through a pad of Celite (rinsing with DCM). The filtrate was concentrated *in vacuo*, and the residue was purified by flash column chromatography (9:1 heptane/EtOAc) to obtain **Fe42**. Yield: 0.50 g (54%).  $^1\text{H}$  NMR (300 MHz,  $\text{CDCl}_3$ )  $\delta$  7.28-7.23 (m, 8H), 7.12-7.08 (m, 2H), 3.25 (m, 2H), 2.37 (s, 6H), 1.99-1.89 (m, 4H), 1.45-1.40 (m, 4H). ESI-MS  $m/z$  533.1  $[\text{M} + \text{Na}]^+$  (calcd. for  $\text{C}_{28}\text{H}_{26}\text{FeN}_2\text{O}_4$ : 510.1).

**General Procedure for the Asymmetric Hydrogenation**

Hydrogenations were run in a 450 mL Parr autoclave equipped with a removable aluminum block that can accommodate up to fifteen magnetically stirred 7 mL glass vials. The catalyst [0.01 mmol (2 mol-%)] was weighed in glass vials, which were accommodated in the aluminum block after adding magnetic stir bars in each of them. The block was placed in a Schlenk tube, where it was subjected to three vacuum/nitrogen cycles. *i*PrOH (0.25 mL) was added to each vial, and stirring was started.  $\text{Me}_3\text{NO}$  [0.02 mmol (4 mol-%)] was added to each vial as an  $\text{H}_2\text{O}$  solution (0.1 mL). After stirring at room temperature under nitrogen for 10 min, the substrate (0.5 mmol) was added to the mixtures. Each vial was capped with a Teflon septum pierced by a needle, the block was transferred into the autoclave, and stirring was started. After purging four times with hydrogen at the selected pressure, heating was started. The reactions were stirred under hydrogen pressure overnight and then analyzed for conversion and *ee* determination.

**Conditions for conversion and *ee* determination**

Products' absolute configurations were assigned by comparison of the sign of optical rotation with literature data (see the references cited for each compound).

**(S)-1-Phenylethanol P1 (GC):** capillary column: MEGADEX DACTBS $\beta$ , diacetyl-*tert*-butylsilyl- $\beta$ -cyclodextrin, 0.25  $\mu\text{m}$ ; diameter = 0.25 mm; length = 25 m; carrier: hydrogen; inlet pressure: 1 bar; oven temperature: 95 °C for 20 min:  $t_{\text{substrate}}$  = 6.0 min;  $t_{\text{R}}$  = 13.2 min;  $t_{\text{S}}$  = 15.1 min.<sup>168</sup>

**(S)-1-(4-(Trifluoromethyl)phenyl)ethanol P2 (GC):** capillary column: MEGADEX DACTBS $\beta$ , diacetyl-*tert*-butylsilyl- $\beta$ -cyclodextrin, 0.25  $\mu\text{m}$ ; diameter = 0.25 mm; length = 25 m; carrier: hydrogen; inlet pressure: 1 bar; oven temperature: 110 °C for 20 min:  $t_{\text{substrate}}$  = 6.4 min;  $t_{\text{R}}$  = 14.3 min;  $t_{\text{S}}$  = 15.4 min.<sup>169</sup>

**(S)-1-(4-Methoxyphenyl)ethanol P3 (GC):** capillary column: MEGADEX DACTBS $\beta$ , diacetyl-*tert*-

butylsilyl- $\beta$ -cyclodextrin, 0.25  $\mu\text{m}$ ; diameter = 0.25 mm; length = 25 m; carrier: hydrogen; inlet pressure: 1 bar; oven temperature: 110  $^{\circ}\text{C}$  for 10 min; 30  $^{\circ}\text{C}/\text{min}$  gradient; 120  $^{\circ}\text{C}$  for 10 min; 30  $^{\circ}\text{C}/\text{min}$  gradient; 130  $^{\circ}\text{C}$ :  $t_{\text{substrate}} = 20.1$  min;  $t_R = 21.1$  min;  $t_S = 22.6$  min.<sup>170</sup>

**(S)-1-(4-Chlorophenyl)ethanol P4 (GC):** capillary column: MEGADEX DACTBS $\beta$ , diacetyl-*tert*-butylsilyl- $\beta$ -cyclodextrin, 0.25  $\mu\text{m}$ ; diameter = 0.25 mm; length = 25 m; carrier: hydrogen; inlet pressure: 1 bar; oven temperature: 110  $^{\circ}\text{C}$  for 10 min; 30  $^{\circ}\text{C}/\text{min}$  gradient; 120  $^{\circ}\text{C}$  for 10 min; 30  $^{\circ}\text{C}/\text{min}$  gradient; 130  $^{\circ}\text{C}$ :  $t_{\text{substrate}} = 12.8$  min;  $t_R = 23.4$  min;  $t_S = 24.3$  min.<sup>170</sup>

**(S)-1-(Naphthalen-2-yl)ethanol P5 (GC):** capillary column: MEGADEX DACTBS $\beta$ , diacetyl-*tert*-butylsilyl- $\beta$ -cyclodextrin, 0.25  $\mu\text{m}$ ; diameter = 0.25 mm; length = 25 m; carrier: hydrogen; inlet pressure: 1 bar; oven temperature: 150  $^{\circ}\text{C}$  for 20 min:  $t_{\text{substrate}} = 10.6$  min;  $t_R = 16.9$  min;  $t_S = 17.9$  min.<sup>170</sup>

**(S)-1-Phenylpropan-1-ol P6 (GC):** capillary column: MEGADEX DACTBS $\beta$ , diacetyl-*tert*-butylsilyl- $\beta$ -cyclodextrin, 0.25  $\mu\text{m}$ ; diameter = 0.25 mm; length = 25 m; carrier: hydrogen; inlet pressure: 1 bar; oven temperature: 95  $^{\circ}\text{C}$  for 20 min:  $t_{\text{substrate}} = 9.4$  min;  $t_R = 16.6$  min;  $t_S = 18.5$  min.<sup>171</sup>

**(S)-1-Cyclohexylethanol P7 (GC):** capillary column: MEGADEX DACTBS $\beta$ , diacetyl-*tert*-butylsilyl- $\beta$ -cyclodextrin, 0.25  $\mu\text{m}$ ; diameter = 0.25 mm; length = 25 m; carrier: hydrogen; inlet pressure: 1 bar; oven temperature: 120  $^{\circ}\text{C}$  for 20 min:  $t_{\text{substrate}} = 4.9$  min;  $t_S = 6.2$  min;  $t_R = 7.6$  min.<sup>172</sup>

**(R)-1,2,3,4-Tetrahydronaphthalen-2-ol P8 (GC):** the product was derivatized as acetate before injection. Capillary column: MEGADEX DACTBS $\beta$ , diacetyl-*tert*-butylsilyl- $\beta$ -cyclodextrin, 0.25  $\mu\text{m}$ ; diameter = 0.25 mm; length = 25 m; carrier: hydrogen; inlet pressure: 1 bar; oven temperature: 110  $^{\circ}\text{C}$  for 40 min:  $t_R = 29.3$  min;  $t_S = 30.3$  min;  $t_{\text{substrate}} = 35.1$  min.<sup>173</sup>

**(R)-2,3-Dihydro-1H-inden-1-ol P9 (GC):** capillary column: MEGADEX DACTBS $\beta$ , diacetyl-*tert*-butylsilyl- $\beta$ -cyclodextrin, 0.25  $\mu\text{m}$ ; diameter = 0.25 mm; length = 25 m; carrier: hydrogen; inlet pressure: 1 bar; oven temperature: 110  $^{\circ}\text{C}$  for 20 min:  $t_{\text{substrate}} = 12.9$  min;  $t_S = 11.8$  min;  $t_R = 14.2$  min.<sup>174</sup>

**rac-4-Methylpentan-2-ol P10 (GC):** capillary column: MEGADEX DACTBS $\beta$ , diacetyl-*tert*-butylsilyl- $\beta$ -cyclodextrin, 0.25  $\mu\text{m}$ ; diameter = 0.25 mm; length = 25 m; carrier: hydrogen; inlet pressure: 1 bar; oven temperature: 120  $^{\circ}\text{C}$  for 20 min:  $t_{\text{substrate}} = 10.6$  min;  $t_{\text{en},1} = 11.6$  min;  $t_{\text{en},2} = 13.5$  min.

**(S)-1-(Naphthalen-1-yl)ethanol P11 (GC and HPLC):** GC conditions for conversion determination: capillary column: MEGADEX DACTBS $\beta$ , diacetyl-*tert*-butylsilyl- $\beta$ -cyclodextrin, 0.25  $\mu\text{m}$ ; diameter = 0.25 mm; length = 25 m; carrier: hydrogen; inlet pressure: 1 bar; oven temperature: 150  $^{\circ}\text{C}$  for 15 min):  $t_{\text{substrate}} = 8.0$  min;  $t_{R+S} = 10.4$  min. HPLC conditions of ee determination: column: Daicel Chiralcel OD-H; eluent: 9:1 *n*-hexane/*i*-PrOH; flow: 1 mL/min;  $\lambda = 210$  nm;  $t_{\text{substrate}} = 7.1$  min;  $t_S = 9.3$  min;  $t_R = 13.3$  min.<sup>170</sup>

**(S)-1-(Pyridin-3-yl)ethanol P12 (GC and HPLC):** GC conditions for conversion determination: capillary column: MEGADEX DACTBS $\beta$ , diacetyl-*tert*-butylsilyl- $\beta$ -cyclodextrin, 0.25  $\mu\text{m}$ ; diameter = 0.25 mm; length = 25 m; carrier: hydrogen; inlet pressure: 1 bar; oven temperature: 130  $^{\circ}\text{C}$  for 15 min:  $t_{\text{substrate}} = 3.4$  min;  $t_{R+S} = 12.0$  min. HPLC conditions of ee determination: column: Daicel Chiralcel OB-H; eluent: 9:1 *n*-hexane/*i*-PrOH; flow: 0.8 mL/min;  $\lambda = 210$  nm;  $t_S = 10.6$  min;  $t_R = 17.4$  min;  $t_{\text{substrate}} = 20.1$  min.<sup>170</sup>

**(S)-3,3-Dimethylbutan-2-ol P13 (GC):** capillary column: CP-Chirasil-Dex CB, 0.25  $\mu\text{m}$ ; diameter = 0.25 mm; length = 25 m; carrier: hydrogen; inlet pressure: 1.89 bar; oven temperature: 60  $^{\circ}\text{C}$  for

11 min:  $t_{\text{substrate}} = 3.3$  min;  $t_S = 10.1$  min;  $t_R = 10.6$  min.<sup>175</sup>

**(S)-1,2,3,4-Tetrahydronaphthalen-1-ol P14 (GC):** capillary column: MEGADEX DACTBS $\beta$ , diacetyl-*tert*-butylsilyl- $\beta$ -cyclodextrin, 0.25  $\mu\text{m}$ ; diameter = 0.25 mm; length = 25 m; carrier: hydrogen; inlet pressure: 1 bar; oven temperature: 120 °C for 20 min:  $t_{\text{substrate}} = 9.5$  min;  $t_R = 11.0$  min;  $t_S = 12.2$  min.<sup>176</sup>



## 6 New application of cyclopentadienone(iron) complexes

### 6.1 Ester hydrogenation with (cyclopentadienone)iron complex

Until 2014, application of iron catalysts for ester hydrogenation was unreported. As described in Paragraph 2.5.2, this situation changed thanks to contribution made by three research groups. Firstly, Milstein and co-workers proved that the *P,N,P*-complex **47** (Figure 6.1a) could be applied in the hydrogenation of strongly activated trifluoroacetic esters.<sup>119</sup> Although the reduction of trifluoroacetates is not particularly appealing from the synthetic point of view, this was the first report of an iron-catalytic methodology for the ester reduction. Shortly after the Milstein's seminal report, important contributions were made, nearly simultaneously, by the research groups of Beller<sup>120</sup> and Guan/Fairweather.<sup>121</sup> Using catalyst **49** (Figure 6.1b) both groups were able to hydrogenate various esters, including fatty esters under base-free, neat conditions. Catalysts **47** and **49** clearly opened a new chapter in the ester hydrogenation, proving that it can be accomplished using complexes with a cheap and abundant metal such as iron. Yet, in order for these catalysts to become really suitable for industrial use, their catalytic activity still has to be improved and the pincer *P,N,P*-ligands ideally should be replaced with less expensive and easy-to-handle ones.

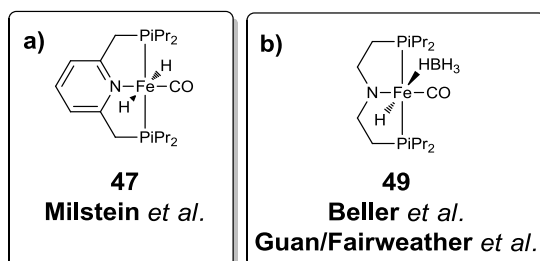
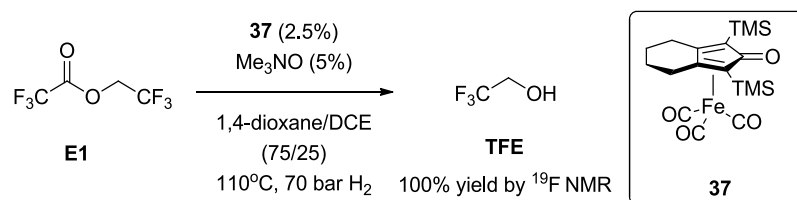


Figure 6.1 Catalysts used for hydrogenation of a) activated and b) "normal" esters.

As described in Chapter 5, during my research, I deeply investigated asymmetric hydrogenations using various (cyclopentadienone)iron complexes. As I had become quite familiar with their synthesis and setting up catalytic reactions with them, I started to

wonder if we can find a new field to apply them. As discussed in Paragraph 2.4.7, (cyclopentadienone)iron complexes are especially effective in ketone and imine hydrogenation, but they were also found active in the hydrogenation of sodium bicarbonate. They were also used in reductive amination or hydrogen borrowing reactions. What was for sure unaccomplished with them was the ester hydrogenation, and we decided approach this challenging field with them. (Cyclopentadienone)iron complexes for sure would be much welcome in ester hydrogenation as, compared to *P,N,P*-pincer ligands, they are easier to synthesize and to handle.

It was decided to carry out the initial experiments with the activated ester 2,2,2-trifluoroethyl 2,2,2-trifluoroacetate **E1** (Scheme 6.1). We chose to work with the most well studied iron complex **37** and to activate it using Me<sub>3</sub>NO to form the Knölker-Casey catalyst **38** *in situ*. Knowing the high thermal stability of (cyclopentadienone)iron complexes, we decided to start our catalytic experiments using rather harsh conditions: 110 °C and 70 bar H<sub>2</sub>. We did that as we rather wanted to see some conversion and possibly lower the temperature and hydrogen pressure in course of the optimization of the reaction's conditions, than not to observe any conversion because of the mild conditions applied. 1,4-Dioxane was selected as a higher-boiling surrogate of tetrahydrofuran (b.p. = 101 °C vs. 66 °C), which is commonly used in ester hydrogenation. A co-solvent was also employed to dissolve Me<sub>3</sub>NO, which is poorly soluble in 1,4-dioxane, thus ensuring the possibility to work with stock solutions while preparing the reaction.



Scheme 6.1 Hydrogenation of 2,2,2-trifluoroethyl 2,2,2-trifluoroacetate with complex **37**.

Delightfully, the first attempt, carried out using 1,2-dichloroethane (DCE) as co-solvent, led to full conversion. As the 2,2,2-trifluoroethyl 2,2,2-trifluoroacetate or 2,2,2-trifluoroethanol (TFE) have too low boiling point to be detected by GC, we measured the ester conversion using <sup>19</sup>F NMR analysis of the reaction crude. This method allowed us to measure the conversion and the yield of TFE, but also to detect possible fluorine byproducts such as the 2,2,2-trifluoroacetic acid (TFA) potentially formed by ester hydrolysis (Figure 6.2).



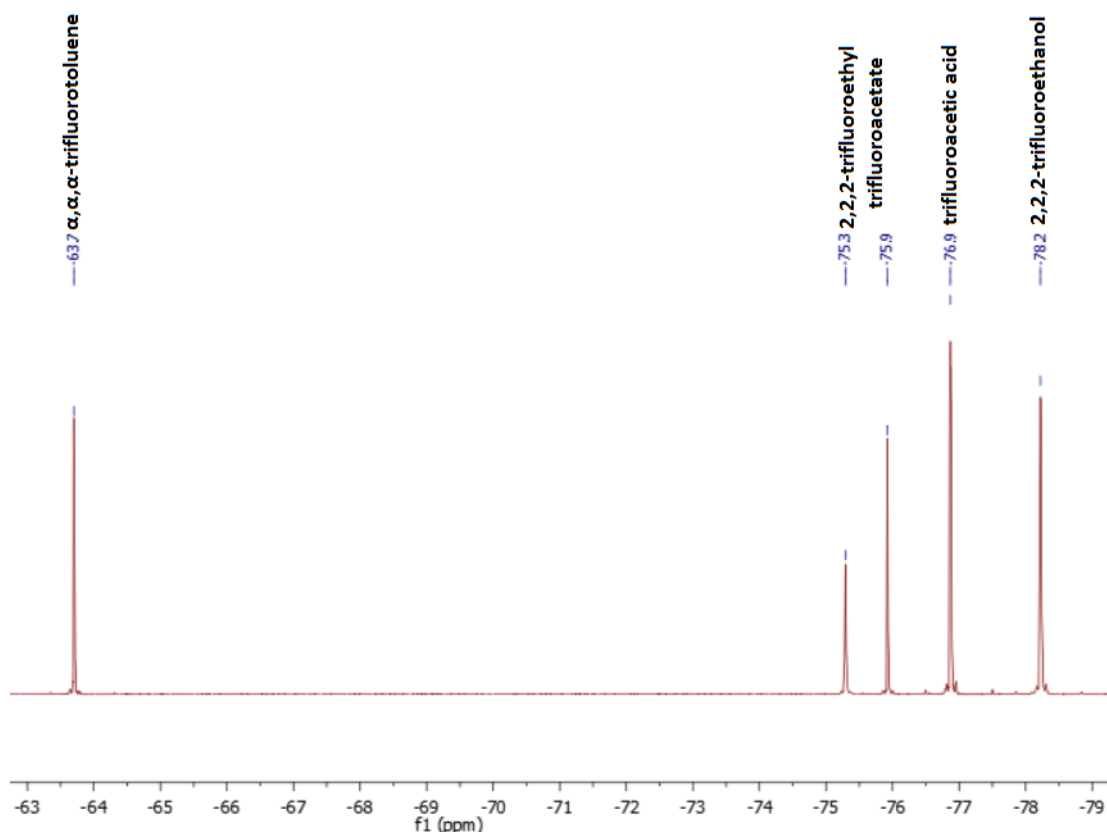
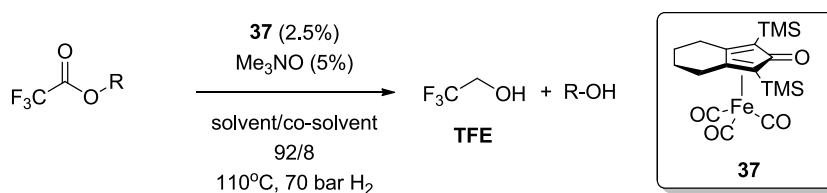


Figure 6.2 An exemplary  $^{19}\text{F}$  NMR spectra (decoupled) of  $\alpha,\alpha,\alpha$ -trifluorotoluene (used as  $^{19}\text{F}$  NMR shift reference), 2,2,2-trifluoroethyl trifluoroacetate (substrate), trifluoroacetic acid (possible by-product) and 2,2,2-trifluoroethanol (product).

## 6.2 Conditions screening

We decided to test this new methodology for ester hydrogenation using (cyclopentadienone)iron pre-catalyst **37** with more challenging substrates - cyclohexylmethyl 2,2,2-trifluoroacetate **E2** and hexyl 2,2,2-trifluoroacetate **E3** (Table 6.1).

Table 6.1 Solvent screening with esters **E2** and **E3**.



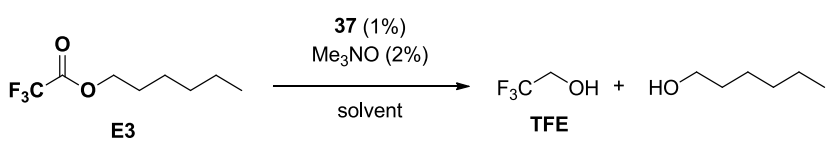
Entry	Solvent	Yield (%) <sup>[a]</sup>	
		Substrate E2	Substrate E3
1	1,4-Dioxane/DCE 75:25	77	82
2	1,4-Dioxane/DCE 85:15	94	88
3	1,4-dioxane	100	100
4	DCE	89	90
5	CPME	100	100
6	Toluene	100	100

[a] Yield of TFE by  $^{19}\text{F}$  NMR.

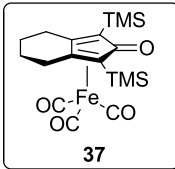
Upon applying for esters **E2** and **E3** the same conditions as for substrate **E1**, we were positively surprised upon obtaining high yields for both esters (entry 1). The bulky cyclohexylmethyl group clearly was not an obstacle during the hydrogenation. When we tried to lower the amount of co-solvent (DCE), we were able to obtain higher yields (entry 2). As we observed that the amount of DCE clearly affected the results, we tried to run catalytic tests without using any co-solvent, despite the bad solubility of Me<sub>3</sub>NO in most common solvents. Remarkably, using pure 1,4-dioxane led to 100% yield (entry 3), whereas the use of pure DCE afforded slightly lower yields, 89% for **E1** and 90% for **E3** (entry 4). Following the lead of pure solvents we tested also cyclopentyl methyl ether (CPME) and toluene, obtaining in every case 100% yield in each case.

As we did not see any difference between two substrates **E2** and **E3**, we run the further optimization study using only **E3**, together with three best solvents - 1,4-dioxane, CPME and toluene (Table 6.2). We wanted to evaluate the effects of lowering catalyst loading, temperature and pressure.

Table 6.2 Optimization of the ester hydrogenation using complex **37**.



**E3**  $\xrightarrow[\text{solvent}]{\text{37 (1\%)}, \text{Me}_3\text{NO (2\%)}}$  **TFE** + HO-CH<sub>2</sub>-CH<sub>2</sub>-CH<sub>2</sub>-CH<sub>2</sub>-CH<sub>2</sub>-CH<sub>2</sub>-CH<sub>2</sub>-CH<sub>2</sub>-OH



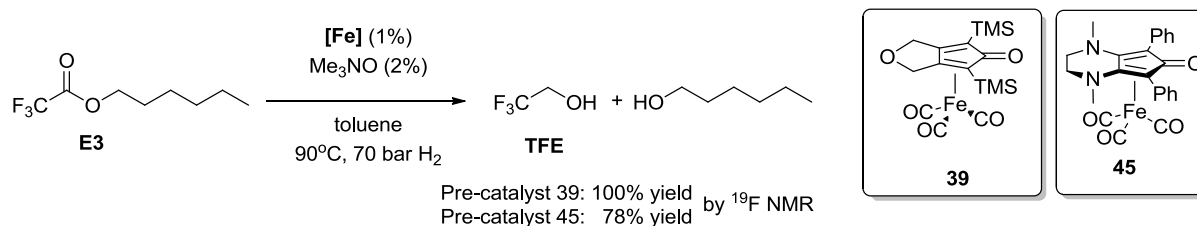
**37**

Entry	Temp (°C)	Pressure (bar)	Yield (%) <sup>[a]</sup>		
			1,4-dioxane	CPME	toluene
1	110	70	100	100	100
2	90	70	98	100	100
3	90	35	91	99	98
4	70	70	83	96	99

[a] Yield of TFE by <sup>19</sup>F NMR.

We started our optimization by lowering the catalyst loading from 2.5% to 1% which did not affect results at all (entry 1 from Table 6.2 vs. entries 3, 5-6 from Table 6.1). Decrease of the temperature by 20 °C, lowered the yield only in the case of 1,4-dioxane, but only by 2% (entry 2). Moreover, lowering the pressure (35 bar vs. 70 bar) led to lower yields, but the most significant change was observed again with 1,4-dioxane (entry 3). Keeping the original pressure (70 bar), but lowering the temperature to 70 °C, led to lower yields, most distinguishable in the case of 1,4-dioxane (entry 4). Overall, reactions performed in toluene were the least affected by changes of pressure or temperature. However, we did not undertake further reaction optimization, but rather used the best conditions (i.e. with 100% yield) for a substrate screening in which we wanted to include also more challenging "non-activated" esters. Before carrying out the solvent screening, we decided to test two other (cyclopentadienone)iron pre-catalysts (Scheme 6.2).

## New application of cyclopentadienone(iron) complexes



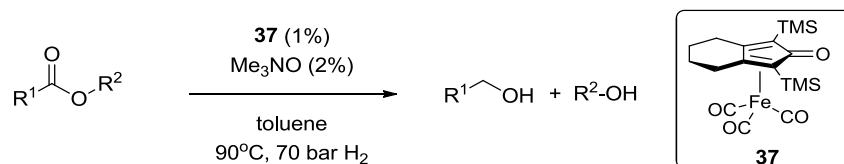
Scheme 6.2 Additional screening of two other (cyclopentadienone)iron complexes in ester hydrogenation.

With complex **39**, the reaction worked as good as with the pre-catalyst **37**, but complex **45** lowered the yield to 78%. We decided to keep the pre-catalyst **37** for the substrate screening, as it is the most commonly used (cyclopentadienone)iron pre-catalyst.

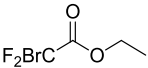
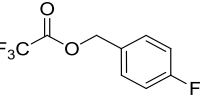
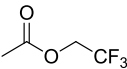
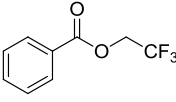
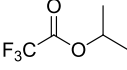
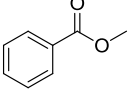
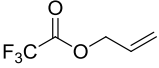
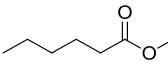
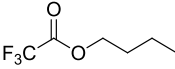
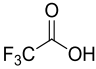
### 6.3 Substrate screening

In the substrate screening (Table 6.3), besides testing other 2,2,2-trifluoroacetic esters, we wanted to verify whether  $\text{CF}_3$  group on the acyl group is indispensable to observe conversion (substrates **E5-6**). Also esters derived from 2,2,2-trifluoroethanol were synthesized (**E7** and **E17**), to test if their  $\text{CF}_3$  group can affect the hydrogenation. Besides that we included other, more classical "non-activated" esters (**E18-19**) and 2,2,2-trifluoroacetic acid (**E20**).

Table 6.3 Substrate screening for ester hydrogenation, using pre-catalyst **37**.



Entry	Substrate	Yield (%)	Milstein's yield (%) <sup>[a]</sup>	Entry	Substrate	Yield (%)	Milstein's yield (%) <sup>[a]</sup>
1	<b>E1</b> 	100	>99	11	<b>E11</b> 	100	>99
2	<b>E2</b> 	100	52, 95 <sup>[b]</sup>	12	<b>E12</b> 	0	
3	<b>E3</b> 	100		13	<b>E13</b> 	0	
4	<b>E4</b> 	100		14	<b>E14</b> 	100	78
5	<b>E5</b> 	0	0	15	<b>E15</b> 	100	>99

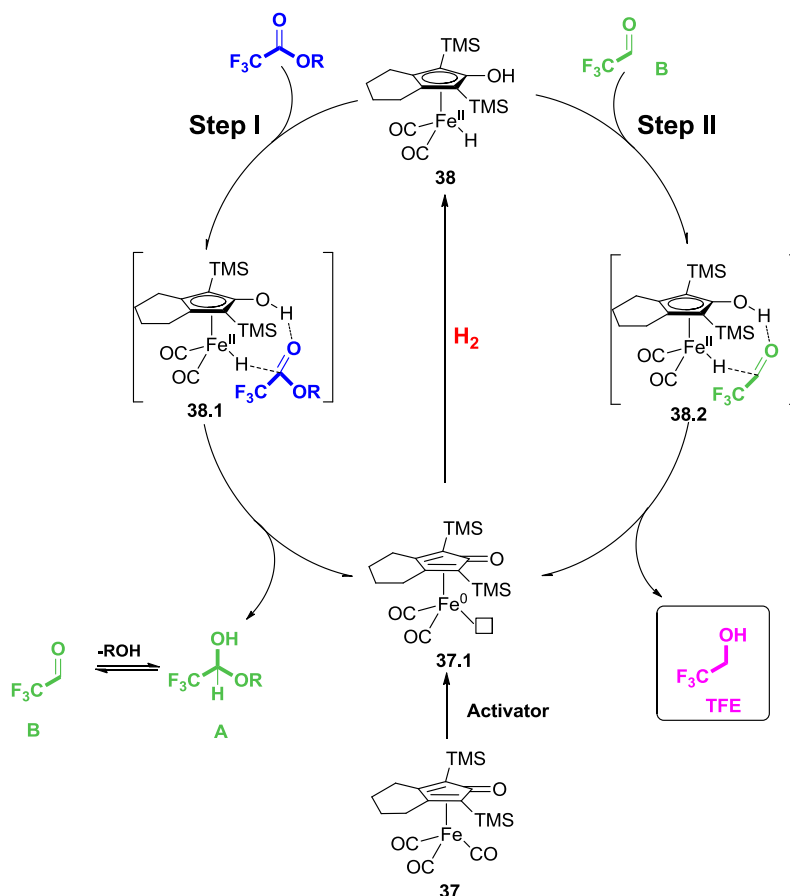
6	<b>E6</b>		0	0	16	<b>E16</b>		100	97
7	<b>E7</b>		0	0	17	<b>E17</b>		0	
8	<b>E8</b>		100	25, 77 <sup>[c]</sup>	18	<b>E18</b>		0	
9	<b>E9</b>		100	95	19	<b>E19</b>		0	
10	<b>E10</b>		100	77	20	<b>E20</b>		0	

[a] Yields reported by Milstein and co-workers with iron catalyst **47** (conditions: 1 mol% catalyst, 5 mol% NaOMe, 16h, 40 °C); [b] higher yield required 48 h reaction time [c] higher yield required 3 mol% catalyst, 15 mol% NaOMe, 60h)

Remarkably, the hydrogenation did either not work at all or lead to 100% yield. None of the "non-activated" esters was hydrogenated (entries 7, 17-19), as well as "less-activated" substrates **E5** and **E6** featuring a CHF<sub>2</sub> group instead of CF<sub>3</sub> (entries 5-6). Also 2,2,2-trifluoroacetic acid **E20** did not react (entry 20). On the contrary, the activated esters all gave full conversion with the exception of esters **E12** and **E13**, featuring electron-poor phenol groups (entries 12-13). We tried to hydrogenate them using pre-catalyst **39** and **45**, but also without obtaining any conversion. Upon comparison with iron catalyst **47** used by Milstein and co-workers for hydrogenation of majority of tested here esters, it can be clearly seen that (cyclopentadienone)iron catalyst **37** is having a broader scope of substrates, being able to hydrogenate esters with the bulky alkoxy groups (entry 2 and 8) without prolonged reaction times or increased catalyst loading.

#### 6.4 Tentative mechanism of ester hydrogenation

Based on the outcome of the ester hydrogenation experiments and on the commonly accepted mechanism of the hydrogenation of carbonyl compound promoted by the Knölker-Casey catalyst, a tentative mechanism can be proposed for the ester hydrogenation with the pre-catalyst **37** (Scheme 6.3). After removal of a CO ligand by Me<sub>3</sub>NO and subsequent hydrogen splitting, the catalyst **38** is able to promote the reduction of ester C=O group according to a concerted outer-sphere mechanism, in which its OH group is activating the ester by a hydrogen-bonding. As the ester C=O group is poorly reactive, a strong electron withdrawing group such as CF<sub>3</sub> is indispensable to make it more electrophilic and thus activate it towards the nucleophilic attack of the hydride in the pericyclic transition state **38.1**. Formed 2,2,2-trifluorohemiacetal **A** is then converted into the corresponding 2,2,2-trifluoroaldehyde **B**, which then is hydrogenated by the regenerated iron hydride **38** to form TFE.



Scheme 6.3 Plausible mechanism of activated ester hydrogenation with pre-catalyst **37**.

This proposed mechanism explains why the hydrogenation is not working with other than 2,2,2-trifluoroacetic esters, as in "non-activated" esters, the carbonyl carbon is a weaker electrophile. Nor hemiacetal or aldehyde intermediates are observed by  $^{19}\text{F}$  NMR, suggesting that the hemiacetal dissociation and subsequent hydrogenation of 2,2,2-trifluoroaldehyde take place with a fast rate.

## 6.5 Summary

In summary, a new reactivity of (cyclopentadienone/hydroxycyclopentadienyl)iron complexes has been discovered. Ester hydrogenation promoted by these complexes has been investigated and shown to work with trifluoroacetic esters. It has been shown that (cyclopentadienone)iron complexes, upon activation with  $\text{Me}_3\text{NO}$ , can catalyze hydrogenation of variety of trifluoroacetic esters, almost independently on alcohol part of the ester (with the exception of phenyl esters bearing electron-poor substituents, which did not reacted). Unfortunately, up to date we have been unable to perform the hydrogenation of more "typical" esters **E18** and **E19**, and for this reason the outcome of this research has mostly academic impact, without possible industrial applications. Nevertheless, the catalytic performances obtained on trifluoroacetate esters are superior to those previously reported by Milstein (with catalyst **47**) and co-workers on this narrow class of substrates.



## 6.6 Experimental section

### General Remarks

Dry toluene and tetrahydrofuran were obtained from MBraun SPS system. Dry diethyl ether, dichloroethane, CPME and 1,4-dioxane (over molecular sieves in bottles with crown cap) were purchased from Sigma Aldrich and stored under nitrogen.

The reactions were monitored by analytical thin-layer chromatography (TLC) using silica gel 60 F254 pre-coated glass plates (0.25 mm thickness). Visualization was accomplished by irradiation with a UV lamp and/or staining with a potassium permanganate alkaline solution. Flash column chromatography was performed using Grace Reveleris® X2 Flash Chromatography System (silica gel cartridges with particle size 40 µm).

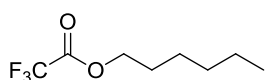
Proton NMR spectra were recorded on a spectrometer operating at 300 MHz. Proton chemical shifts are reported in ppm ( $\delta$ ) with the solvent reference relative to tetramethylsilane (TMS) employed as the internal standard ( $\text{CDCl}_3 = 7.26$  ppm). The following abbreviations are used to describe spin multiplicity: s = singlet, d = doublet, t = triplet, q = quartet, m = multiplet, dd = doublet-doublet.  $^{13}\text{C}$  NMR spectra were recorded on a 300 MHz spectrometer operating at 75 MHz, with complete proton decoupling. Carbon chemical shifts are reported in ppm ( $\delta$ ) relative to TMS with the respective solvent resonance as the internal standard ( $\text{CDCl}_3$ ,  $\delta = 77.2$  ppm). The coupling constant values are given in Hz.

Gas chromatography was performed on a Hewlett Packard 6890 instrument, equipped with a flame ionization detector, using capillary columns. Mass analysis was performed using a Hewlett Packard 6890 instrument coupled with a mass spectrometer.

### Materials

The following substrates were obtained from commercial sources (Sigma and VWR): 2,2,2-trifluoroethyl trifluoroacetate **E1**, ethyl 2,2,2-trifluoroacetate **E4**, ethyl difluoroacetate **E5**, ethyl bromodifluoroacetate **E6**, 2,2,2-trifluoroethyl acetate **E7**, *i*-propyl trifluoroacetate **E8**, allyl trifluoroacetate **E9**, butyl 2,2,2-trifluoroacetate **E10**, phenyl 2,2,2-trifluoroacetate **E11**, 4-nitrophenyl 2,2,2-trifluoroacetate **E12**, perfluorophenyl 2,2,2-trifluoroacetate **E13**, methyl benzoate **E18**, methyl hexanoate **E19**, 2,2,2-trifluoroacetic acid **E20**. Esters: cyclohexylmethyl 2,2,2-trifluoroacetate **E2**, phenethyl 2,2,2-trifluoroacetate **E14**, benzyl 2,2,2-trifluoroacetate **E15**, 4-fluorobenzyl 2,2,2-trifluoroacetate **E16** were prepared as reported by Milstein and co-workers.<sup>119</sup> 2,2,2-Trifluoroethyl benzoate **E17** was prepared using the procedure reported by Studer and co-workers.<sup>177</sup> Complexes **37** and **45** were prepared following procedures reported by Renaud and co-workers.<sup>111</sup> Complex **39** was prepared as described by Wills and co-workers.<sup>105</sup>

### Hexyl 2,2,2-trifluoroacetate **E3**



Under argon, 1-hexanol (0.06 mol, 7.5 mL, 1 eq) was diluted with dry  $\text{Et}_2\text{O}$  (60 mL) and cooled down to 0 °C. 2,2,2-Trifluoroacetic anhydride (0.072 mol, 10 mL, 1.2 eq) was slowly added and the reaction mixture was stirred for 0.5 h at 0 °C. Then the ice bath was removed and the reaction was stirred for 2 h. GC-MS and  $^{19}\text{F}$  NMR analysis confirmed full conversion of 1-hexanol to hexyl 2,2,2-trifluoroacetate

**E3**. The reaction mixture was diluted with ether (50 mL). The organic layer was washed with  $\text{NaHCO}_3$  saturated solution (2x 100 mL) and with brine (1x 100 mL). The organic phases were combined and filtered using phase-separation paper. Ester **E3** was purified by distillation (boiling

point 145 °C). Yield 84%.  $^1\text{H}$  NMR (300 MHz)  $\delta$  4.34 (t,  $^3J(\text{H,H}) = 6.7$  Hz, 2H), 1.76-1.69 (m, 2H), 1.39-1.30 (m, 6H), 0.90 (t,  $^3J(\text{H,H}) = 6.7$  Hz, 3H).  $^{19}\text{F}$  NMR (282 MHz,  $\text{CDCl}_3$ )  $\delta$  -75.72.  $^{13}\text{C}$  NMR (75 MHz)  $\delta$  157.8 (q,  $^2J(\text{C,F}) = 42.0$  Hz), 114.8 (q,  $^1J(\text{C,F}) = 285.6$  Hz), 68.5, 31.4, 28.2, 25.3, 22.6, 14.0. GCI-MS  $m/z$  198 [M] (calcd. for  $\text{C}_8\text{H}_{13}\text{F}_3\text{O}_2$ : 198.1).

#### **General Procedure for the Hydrogenation**

In a nitrogen filled mBraun glovebox, a solution of catalyst (0.01 mmol, 1 mol% in 0.25 mL solvent) was dispensed to a glass vial with solid  $\text{Me}_3\text{NO}$  (0.02 mmol, 2 mol%). Vial was capped and solution was stirred for 1h at 30 °C. After that vial was opened and ester substrate (1 mmol) was added. Vial was capped again and put inside the Premex 96er Reactor. The system was purged three times with 10 bar of nitrogen and three times with 10 bar of hydrogen. Catalytic reactions were stirred overnight under selected pressure and temperature. After this time, the reaction crudes were directly analyzed by  $^{19}\text{F}$  NMR with  $\alpha,\alpha,\alpha$ -trifluorotoluene (1 mmol in 0.5 mL solvent) as  $^{19}\text{F}$  NMR internal shift reference.





## 7 Conclusions and perspectives

In my thesis *Reductions catalyzed by first-row transition metals*, I decided to particularly focus on the most abundant transition metal – iron. In the last 15 years, this cheap and non-toxic metal is becoming the object of increasing interest in the scientific community, and a remarkable progress has been made in the development of iron-catalyzed reactions. The new iron catalysts started to reach activities reported so far only for noble metal complexes. Nevertheless, there is still much room for improvement, as many of these iron catalysts are highly air- and/or moisture-sensitive, and their synthesis can be very difficult. In order for the homogeneous iron catalysts to become industrially relevant, more easy-to-prepare and stable catalysts have to be developed. My thesis contributes particularly to the field of asymmetric catalysis, seen often as a domain of noble metals.

In Chapter 3 iron complexes with *N,N,N,N*-ligands are described (Figure 7.1). Eleven iron complexes were synthesized and tested in catalytic reductions. The negative results obtained with *N,N,N,N*-ligand complexes in the hydrogenation of C=C and C=O double bonds indicate that *N*-based tetradentate ligands, despite being an effective option for stabilizing the Fe(II) metal centre, are not particularly good candidates for promoting Fe-catalyzed reductions. In addition to the *N*-based tetradentate ligand, they require strong  $\pi$ -acceptors like CO, to stabilize the low-valent iron species produced in the course of the reaction.

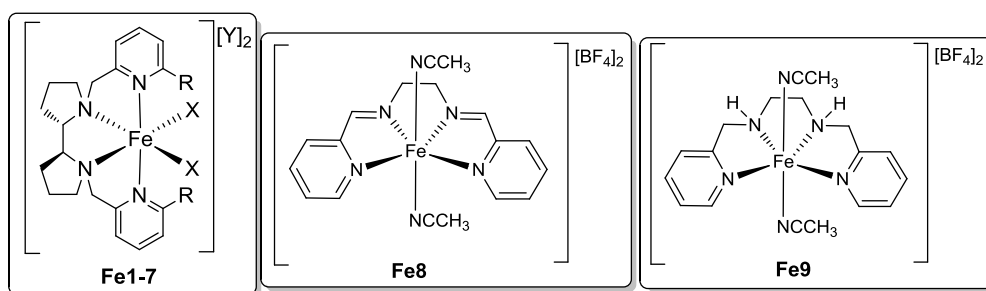


Figure 7.1 Examples of synthesized iron complexes with *N,N,N,N*-ligands.

In Chapter 4 new iron complexes with isonitrile ligands are described. Overall, three families of iron complexes were synthesized and tested in asymmetric transfer hydrogenation of ketones. The best catalyst, **Fe17** (Figure 7.2), was able to induce up to 29% *ee* in transfer hydrogenation of acetophenone. In order to improve the transfer of the stereochemical information from the (*R*)-BINOL derived backbone, the introduction of steric bulk in different positions of the molecule was investigated, but no improvement could be obtained. Research towards more effective catalysts is still underway in Gennari group.

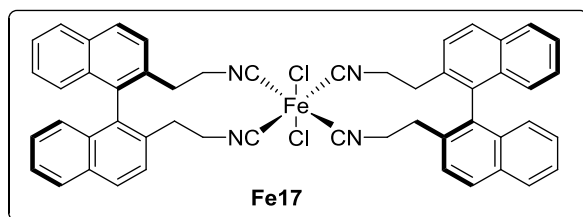


Figure 7.2 The most effective tetra(isonitrile) complex for ketone transfer-hydrogenation.

In Chapter 5, chiral cyclopentadienone(iron) complexes are presented, which represent the core of my PhD work. Compared to other iron complexes used for homogenous asymmetric hydrogenation, (cyclopentadienone)iron complexes have the advantage of being easy to synthesize and stable to air, water and light. By reaction with bases or  $\text{Me}_3\text{NO}$ , these complexes can be activated *in situ* and converted in catalysts for reduction reactions such as the hydrogenation of ketones and imines. A series of eighteen new chiral (cyclopentadienone)iron pre-catalysts were developed. Most of these complexes are derived from (*R*)-BINOL and differ one from the other in the substitution at the 3,3'-positions of the dinaphthalene backbone, as well as at the 2,5-positions of the cyclopentadienone ring. Among these (*R*)-BINOL-derived iron complexes, the best one, **Fe23** (Figure 7.3), allowed to obtain up to 77% *ee* in the asymmetric hydrogenation of ketones. Remarkably, this result was nearly three times higher than previously reported in the literature for chiral (cyclopentadienone)iron derivatives.

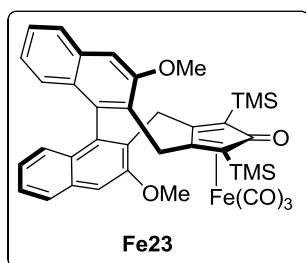
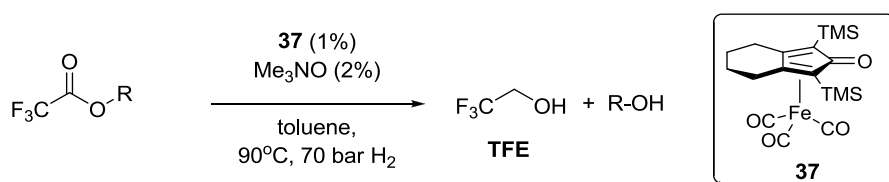


Figure 7.3 The most effective chiral cyclopentadienone(iron) complexes for ketone hydrogenation.

Other approaches to the development of chiral cyclopentadienone(iron) complexes were also investigated, such as replacement of the (*R*)-BINOL-derived backbone with chiral diamine-derived one, and introduction of stereocentres at the 2,5-

positions of the cyclopentadienone ring. However, these approaches did not lead to any improvement, in terms of stereocontrol, with respect to the (*R*)-BINOL-derived complexes.

Building on the expertise achieved with cyclopentadienone(iron) complexes, it was decided to use the most well-known complex **37** to investigate the reduction of substrates different from ketones and imines. In Chapter 6, ester hydrogenation with iron complex **37** is described (Scheme 7.1). Hydrogenation of a variety of 2,2,2-trifluoroacetate esters could be achieved with a 100% yield, although classical esters remained inactive under these reaction conditions.



Scheme 7.1 Ester hydrogenation with cyclopentadienone(iron) complex **37**.

To conclude, in my work of thesis nearly 40 iron complexes have been developed and tested in catalytic hydrogenation reactions, giving in some cases very promising results, and providing new knowledge and directions for future developments in this field.

## 8 List of publications

1. *Chiral (Cyclopentadienone)iron Complexes for the Catalytic Asymmetric Hydrogenation of Ketones*, P. Gajewski, M. Renom-Carrasco, S. Vailati Facchini, L. Pignataro, L. Lefort, J. G. de Vries, R. Ferraccioli, A. Forni, U. Piarulli and C. Gennari, *Eur. J. Org. Chem.* **2015**, 1887-1893.

In this thesis, research from this paper is presented under copyright license with John Wiley and Sons – license number 3773900427152 from 21<sup>st</sup> December 2015.

This communication was highlighted as *Iron-Catalyzed Asymmetric Hydrogenation of Ketones*, *SynFacts* **2015**, *11*, 626.

2. *Synthesis of (R)-BINOL-Derived (Cyclopentadienone)iron Complexes and Their Application in the Catalytic Asymmetric Hydrogenation of Ketones*, P. Gajewski, M. Renom-Carrasco, S. Vailati Facchini, L. Pignataro, L. Lefort, J. G. de Vries, R. Ferraccioli, U. Piarulli and C. Gennari, *Eur. J. Org. Chem.* **2015**, 5526–5536.

In this thesis, research from this paper is presented under copyright license with John Wiley and Sons – license number 3773900159497 from 21<sup>st</sup> December 2015.

3. *Assisted Tandem Catalysis: Metathesis Followed by Asymmetric Hydrogenation from a Single Ruthenium Source*, M. Renom-Carrasco, P. Gajewski, L. Pignataro, J. G. de Vries, U. Piarulli, C. Gennari and L. Lefort. *Adv. Synth. Catal.* **2015**, *10*, 2223-2228.

4. *Asymmetric Transfer Hydrogenation of Ketones with modified Grubbs Metathesis Catalysts: On the Way to a Tandem Process*, M. Renom-Carrasco, P. Gajewski, L. Pignataro, J. G. de Vries, U. Piarulli, C. Gennari and L. Lefort. *Adv. Synth. Catal.* **2016**, DOI: 10.1002/adsc.201500933, *in press*.

## 9 Acknowledgments

I sincerely acknowledge my supervisors, Prof. Cesare Gennari and Prof. Johannes de Vries, for giving me the opportunity to work on a challenging and multidisciplinary project, for their steady support, and for their huge contribution to my scientific education.

I thank Dr. Laurent Lefort for giving me insights into working in the industry, and Prof. Umberto Piarulli for the copious advice about my project.

I do not thank Dr. Luca Pignataro. I simply do not know how. Words cannot express my gratitude for his excellent support, advice on every topic, innumerable visits to the university bar, and countless ridiculously bad *small* jokes.

Words of appreciation go to Allegra, with whom I started my iron adventure. Cheers to Alberto, my party-hard companion! *Dottore, dottore, dottore...*! I hope that you were right and I will return to Italy someday! Salute to Simone, a quiet and self-possessed member of the group. Congratulations to my first student Marco, who somehow survived my supervision and decided to return to Gennari Group! Many thanks also to Sofia for her input to my project.

Last from the University of Milan, but definitely not least – Marc. We started together and we will finish together, but we never really worked together. A unique collaboration which will always stay in my memory. And what an outcome! Seven papers (fingers crossed!), two weeks in Poland and one week in Spain! It was great to have you as my tandem co-worker!

From my stay at DSM I would like to thank Joanne, as she was always there to chat about chemistry, and not only that (and I hope I did not bore you to death with my trivial problems!). I cannot forget about Mr. Mike! It was a pleasure to work with you. You work very hard, but you never forget about other people – this truly makes you a great person! Besides that, I would like to thank Felix for all the tips and tricks, from chemistry to cycling and climbing. Thanks to the whole department of Innovative Synthesis for a warm welcome and see you all on the next ODS!

I dedicate this work to my parents, Joanna (pomijając to ziewanie przed Skypem, to chyba jednak całkiem dobrze mnie wychowałaś skoro kończę doktorat!) and Tadeusz (chemia nie jest programowaniem, ale też jest fajna), my sister Eliza (I still believe that art is a little bit more joyful for the soul than chemistry, so keep it up!), and to my beloved wife – Agnieszka. Without Agnieszka, this thesis would not have been written, and even this PhD would not have been started. If this doctorate was our honeymoon, what will happen next? For sure, the future is bright!

PS: To everyone who arrived on this page after reading my thesis – many thanks! But if you have not read it and skipped straight to acknowledgments, think about your actions, your life, and the Universe – and then return to page 1! May the iron be with you!

# 10 Bibliography

- <sup>1</sup> J. J. Berzelius, *Årsberättelsen om framsteg i fysik och kemi* [Annual report on progress in physics and chemistry], 1808.
- <sup>2</sup> P. T. Anastas, J. Warner, *Green chemistry: theory and practice*, Oxford University Press, Oxford, **1988**.
- <sup>3</sup> (a) A. Corma, S. Iborra and A. Velty, *Chem. Rev.*, **2007**, *107*, 2411; (b) J. G. de Vries, C. J. Elsevier, *Handbook of Homogeneous Hydrogenation*, Wiley-VCH, Weinheim, **2007**.
- <sup>4</sup> E. Bauer, *Iron Catalysis II, Top Organomet Chem* **2015**, *50*.
- <sup>5</sup> G. Patrick, *Instant Notes in Medicinal Chemistry*, BIOS Scientific Publishers, **2001**.
- <sup>6</sup> <http://www.fda.gov/Drugs/GuidanceComplianceRegulatoryInformation/Guidances/ucm122883.htm>
- <sup>7</sup> V. Farina, J. T. Reeves, C. H. Senanayake, J. J. Song, *Chem. Soc. Rev.* **2006**, *106*, 2734-2793.
- <sup>8</sup> M. Calvin, *J. Am. Chem. Soc.* **1939**, *61*, 2230-2234.
- <sup>9</sup> J. A. Osborn, F. H. Jardine, J. F. Young, G. Wilkinson, *J. Chem. Soc. A* **1966**, *12*, 1711-1732.
- <sup>10</sup> (a) W. S. Knowles, M. J. Sabacky, *Chem. Commun.* **1968**, *22*, 1445-1446; (b) W. S. Knowles, M. J. Sabacky, B. D. Vineyard, *J. Chem. Soc., Chem. Commun.* **1972**, 10-11.
- <sup>11</sup> L. Horner, H. Siegel, H. Büthe, *Angew. Chem., Int. Ed. Engl.* **1968**, *7*, 941.
- <sup>12</sup> Berry, A. J.: *Modern Chemistry*, Cambridge, University Press, **1946**.
- <sup>13</sup> H. B. Kagan, T. P. Dang, *J. Am. Chem. Soc.* **1972**, *94*, 6429-6433.
- <sup>14</sup> B. D. Vineyard, W. S. Knowles, M. J. Sabacky, G. L. Bachman, D. J. Weinkauff, *J. Am. Chem. Soc.* **1977**, *99*, 5946-5952.
- <sup>15</sup> (a) R. Noyori, H. Takaya, *Acc. Chem. Res.* **1990**, *23*, 345-350; (b) R. Noyori, M. Kitamura, T. Ohkuma, *Proc. Natl. Ac. Sci. U. S. A.* **2004**, *101*, 5356-5362.
- <sup>16</sup> R. Noyori, *Angew. Chem. Int. Ed.* **2002**, *41*, 2008-2022.
- <sup>17</sup> W. S. Knowles, *Angew. Chem. Int. Ed.* **2002**, *41*, 1998-2007.
- <sup>18</sup> K. B. Sharpless *Angew. Chem. Int. Ed.* **2002**, *41*, 2024-2032.
- <sup>19</sup> (a) Hydrogenation of olefins: R. Noyori, T. Ohkuma, M. Kitamura, *J. Am. Chem. Soc.* **1987**, *109*, 5856-5858; (b) Hydrogenation of functionalised ketones: M. Kitamura, T. Ohkuma, S. Inoue, N. Sayo, H. Kumobayashi, S. Akutagawa, T. Ohta, H. Takaya, R. Noyori, *J. Am. Chem. Soc.* **1988**, *110*, 629-631; (c) Hydrogenation of unfunctionalised ketones: T. Ohkuma, H. Ooka, S. Hashiguchi, T. Ikariya, R. Noyori, *J. Am. Chem. Soc.* **2005**, *117*, 2675-2676.
- <sup>20</sup> (a) A. Gillon, K. Heslop, D. J. Hyett, A. Martorell, A. G. Orpen, P. G. Pringle, C. Claver, E. Fernandez, *Chem. Commun.* **2000**, 961-962; (b) M. T. Reetz, G. Mehler, *Angew. Chem. Int. Ed.* **2000**, *39*, 3889-3890; (c) F. Guillen, J.-C. Fiaud, *Tetrahedron Lett.* **1999**, *40*, 2939-2942; (d) M. van den Berg, A. J. Minnaard, E. P. Schudde, J. van Esch, A. H. M. de Vries, J. G. de Vries, B. L. Feringa, *J. Am. Chem. Soc.* **2000**, *122*, 11539-11540; (e) A. Börner, *Phosphorus Ligands in Asymmetric Catalysis: Synthesis and Applications*, Wiley-VCH, **2008**.
- <sup>21</sup> M. T. Reetz, T. Sell, A. Meiswinkel, G. Mehler, *Angew. Chem. Int. Ed.* **2003**, *42*, 790-793.
- <sup>22</sup> D. Peña, A. J. Minnaard, J. A. F. Boogers, A. H. M. de Vries, J. G. de Vries, B. L. Feringa, *Org. Biomol. Chem.* **2003**, *1*, 1087-1089.
- <sup>23</sup> Schneider, H.-J.; Yatsimirsky, A. K., *Principles and Methods in Supramolecular Chemistry*, Wiley-VCH, New York, **2000**
- <sup>24</sup> B. Plietker *Iron Catalysis in Organic Chemistry*, Wiley-VCH Verlag, Weinheim, **2008**.
- <sup>25</sup> For reviews on asymmetric homogeneous hydrogenation, see: (a) D. J. Ager, A. H. M. de Vries, J. G. de Vries, *Chem. Soc. Rev.* **2012**, *41*, 3340-3380; (b) H. U. Blaser, C. Malan, B. Pugin, F. Spindler, H. Steiner, M. Studer, *Adv. Synth. Catal.* **2003**, *345*, 103-151; (c) J. G. de Vries, C. J. Elsevier, *Handbook of*

---

*Homogeneous Hydrogenation*, Wiley-VCH, **2006**; (d) G. Shang, W. Li, X. Zhang, *Transition metal-catalyzed homogeneous asymmetric hydrogenation*, in *Catalytic Asymmetric Synthesis*, 3rd ed., Wiley-VCH, **2010**, 343-436.

<sup>26</sup> S. Gladiali, E. Alberico, *Chem. Soc. Rev.* **2006**, *35*, 226-236.

<sup>27</sup> H.U. Blaser, H.-J. Federsel *Asymmetric Catalysis on Industrial Scale*, 2<sup>nd</sup> ed. *Challenges, Approaches, Solutions*, Wiley-VCH, Weinheim, **2010**

<sup>28</sup> Prices obtained on <http://www.infomine.com/investment/metal-prices/> as for 1.12.2015.

<sup>29</sup> R. M. Bullock, *Catalysis without Precious Metals*, Wiley-VCH, **2010**.

<sup>30</sup> (a) M. Darwish, M. Wills, *Catal. Sci. Technol.* **2012**, *2*, 243-255; (b) specifically on Fe-catalysed reduction methodologies: R. H. Morris, *Chem. Soc. Rev.* **2009**, *38*, 2282-2291; (c) K. Gopalaiah, *Chem. Rev.* **2013**, *113*, 3248-3296; (d) I. Bauer, H. J. Knolker *Chem. Rev.* **2015**, *115*, 3170-3387; (e) D. S. Mérela, M. Loan Tran Doa, S. Gaillarda, P. Dupaud, J. L. Renauda, *Coord. Chem. Rev.* **2015**, *288*, 50-68; (f) A. Pinaka, G.C. Vougioukalakis *Coord. Chem. Rev.* **2015**, *288*, 69-97; (g) L. C. Misal Castro, H. Li, J. B. Sortais, C. Darcel, *Green Chem.* **2015**, *17*, 2283-2303.

<sup>31</sup> (a) B. Plietker, A. Dieskau *Eur. J. Org. Chem.* **2009**, 775 (b) O. G. Manchegno *Angew. Chem., Int. Ed.* **2011**, *50*, 2216. (c) I. Bauer, H.-J. Knolker *Chem. Rev.* **2015**, *115*, 3170-3387.

<sup>32</sup> S. J. Lippard, J. M. Berg *Principles of Bioinorganic Chemistry*, University Science Books, Mill Valley, **1994**.

<sup>33</sup> F. Naud, F. Spindler, C. J. Rueggeberg, A. T. Schmidt, H. U. Blaser, *Org. Process Res. Dev.*, **2007**, *11*, 519.

<sup>34</sup> C. Bolm *Nat. Chem.* **2009**, *1*, 420.

<sup>35</sup> P. J. Chirik, *J. Am. Chem. Soc.* **2009**, *131*, 3788-3789.

<sup>36</sup> H. U. Blaser, C. Malan, B. Pugin, F. Spindler, H. Steiner and M. Studer, *Adv. Synth. Catal.*, **2003**, *345*, 103; J. I. van der Vlugt, J. N. H. Reek, *Angew. Chem., Int. Ed.*, **2009**, *48*, 8832.

<sup>37</sup> B. de Bruin *Eur. J. Inorg. Chem.* **2012**, 340-342.

<sup>38</sup> K. Jørgensen, *Coord. Chem. Rev.* **1966**, *1*, 164-178.

<sup>39</sup> H. Grützmacher, *Angew. Chem. Int. Ed.* **2008**, *47*, 1814; J. I. van der Vlugt, J. N. H. Reek, *Angew. Chem. Int. Ed.* **2009**, *48*, 8832.

<sup>40</sup> J. R. Partington *A History of Chemistry*, MacMillan & Co, New York, **1964**.

<sup>41</sup> L. Mond, F. Quinke, *J. Chem. Soc.* **1891**, 59,604.

<sup>42</sup> For early studies using iron salts activated by aluminum compounds see: Y. Takegami, T. Ueno, T. Fujii *Bull. Chem. Soc. Jpn* **1969**, *42*, 1663.

<sup>43</sup> E. N. Frankel, E. A. Emken, H. M. Peters, V. K. Davison, R. O. and Butterfield *J. Org. Chem.* **1964**, *29*, 3292.

<sup>44</sup> R. Noyori, I. Umeda, T. Ishigami *J. Org. Chem.*, **1972**, *37*, 1542.

<sup>45</sup> M. A. Schroeder, M. S. Wrighton, *J. Am. Chem. Soc.*, **1976**, *98*, 551.

<sup>46</sup> (a) B. H. Weiller, M. E. Miller, E. R. Grant *J. Am. Chem. Soc.*, **1987**, *109*, 352; (b)

B. H. Weiller, E. R. Grant *J. Am. Chem. Soc.*, **1987**, *109*, 1051; (c) M. E. Miller, E. R. Grant *J. Am. Chem. Soc.*, **1987**, *109*, 7951.

<sup>47</sup> K. Kano, M. Takeuchi, S. Hashimoto, Z. I. Yoshida, *J. Chem. Soc., Chem. Commun.*, **1991**, 1728.

<sup>48</sup> (a) S. Sakaki, T. Sagura, T. Arai, T. Kojima, T. Ogata and K. Ohkubo, *J. Mol. Catal.*, **1992**, *75*, L33; (b) S. Sakaki, T. I. Kojima and T. Arai, *J. Chem. Soc., Dalton Trans.*, **1994**, 7.

<sup>49</sup> (a) H. Inoue, M. Sato, *J. Chem. Soc., Chem. Commun.* **1983**, 983-984; (b) H. Inoue, M. Suzuki, *J.*

---

*Chem. Soc., Chem. Commun.* **1980**, 817–818.

<sup>50</sup> C. Bianchini, A. Meli, M. Peruzzini, P. Frediani, C. Bohanna, M. A. Esteruelas and L. A. Oro, *Organometallics*, **1992**, *11*, 138.

<sup>51</sup> E. J. Daida, J. C. Peters, *Inorg. Chem.* **2004**, *43*, 7474–7485.

<sup>52</sup> H. Fong, M. Moret, Y. Lee, J. C. Peters, *Organometallics*, **2013**, *32*, 3053.

<sup>53</sup> G. Wienhofer, F. Westerhaus, R. V. Jagadeesh, K. Junge, H. Junge, M. Beller *Chem. Commun.* **2012**, *48*, 4827.

<sup>54</sup> D. Srimani, Y. Diskin-Posner, Y. Ben-David, D. Milstein, *Angew. Chem., Int. Ed.* **2013**, *52*, 14131.

<sup>55</sup> D. J. Frank, L. Guet, A. Kaslin, E. Murphy, S. P. Thomas, *RSC Adv.* **2013**, *3*, 25698.

<sup>56</sup> M. Kamitani, Y. Nishiguchi, R. Tada, M. Itazaki, H. Nakazawa, *Organometallics* **2014**, *33*, 1532.

<sup>57</sup> S. C. Bart, E. Lobkovsky, P. J. Chirik, *J. Am. Chem. Soc.* **2004**, *126*, 13794–13807.

<sup>58</sup> (a) G. J. P. Britovsek, V. C. Gibson, B. S. Kimberley, P. J. Maddox, S. J. McTavish, G. A. Solan, A. J. P. White, D. J. Williams *Chem. Commun.* **1998**, *59*, 849–850; (b) B. L. Small, M. Brookhart, A. M. A. Bennett *J. Am. Chem. Soc.* **1998**, *120*, 4049–4050.

<sup>59</sup> V. C. Gibson, C. Redshaw, G. A. Solan *Chem. Rev.* **2007**, *107*, 1745–1776.

<sup>60</sup> S. C. Bart, K. Chlopek, E. Bill, M. W. Bouwkamp, E. Lobkovsky, F. Neese, K. Wieghardt and P. J. Chirik, *J. Am. Chem. Soc.*, **2006**, *128*, 13901.

<sup>61</sup> Studies on the non-innocent nature of the bis(imino)pyridine ligand: (a) S. Stieber, E. Chantal, C. Milsman, J. M. Hoyt, Z. R. Turner, K. D. Finkelstein, K. Wieghardt, S. DeBeer, J. P. Chirik, *Inorg. Chem.* **2012**, *51*, 3770–3785; (b) A. M. Tondreau, S. Stieber, E. Chantal, C. Milsman, E. Lobkovsky, T. Weyhermuller, S. Semproni, J. P. Chirik, *Inorg. Chem.* **2013**, *52*, 635–646.

<sup>62</sup> R. J. Trovitch, E. Lobkovsky, P. J. Chirik, *Inorg. Chem.* **2006**, *45*, 7252–7260.

<sup>63</sup> S. C. Bart, E. J. Hawrelak, E. Lobkovsky, *Organometallics* **2005**, *24*, 5518–5527.

<sup>64</sup> P. Phua, L. Lefort, J. A. F. Boogers, M. Tristany and J. G. de Vries, *Chem. Commun.*, **2009**, 3747.

<sup>65</sup> R. Bedford, M. Betham, D. Bruce, S. Davis, R. Frost and M. Hird, *Chem. Commun.*, **2006**, 1398.

<sup>66</sup> M. Stein, J. Wieland, P. Steurer, F. Teolle, R. Moulhaupt, B. Breit, *Adv. Synth. Catal.* **2011**, *353*, 523.

<sup>67</sup> T. N. Gieshoff, A. Welther, M. T. Kessler, M. H. G. Pechtl, A. von Wangelin, *J. Chem. Commun.* **2014**, *50*, 2261.

<sup>68</sup> V. Kelsen, B. Wendt, S. Werkmeister, K. Junge, M. Beller, B. Chaudret, *Chem. Commun.* **2013**, *49*, 3416.

<sup>69</sup> (a) L. Markó, M. A. Radhi *J. Organomet. Chem.* **1981**, *218*, 369; (b) L. Markó, J. Pala, *Transition Met. Chem.* **1983**, *8*, 207.

<sup>70</sup> J.-S. Chen, L.-L. Chen, Y. Xing, G. Chen, W.-Y. Shen, Z.-R. Dong, Y.-Y. Li, J.-X. Gao *Acta Chim. Sin.* **2004**, *62*, 1745.

<sup>71</sup> C. Sui-Seng, F. Freutel, A. Lough, R. H. Morris, *Angew. Chem., Int. Ed.* **2008**, *47*, 940.

<sup>72</sup> J. F. Sonnenberg, R. H. Morris, *ACS Catal.* **2013**, *3*, 1092–1102.

<sup>73</sup> (a) A. A. Mikhailine, E. Kim, C. Dingels, A. J. Lough, R. H. Morris, *Inorg. Chem.*, **2008**, *47*, 6587–6589; (b) A. A. Mikhailine, A. J. Lough, R. H. Morris, *J. Am. Chem. Soc.* **2009**, *131*, 1394–1395; (c) P. O. Lagaditis, A. A. Mikhailine, A. J. Lough, R. H. Morris, *Inorg. Chem.* **2010**, *49*, 1094–1102.

<sup>74</sup> P. E. Sues, A. J. Lough, R. H. Morris, *Organometallics* **2011**, *30*, 4418–4431.

<sup>75</sup> A. A. Mikhailine, M. I. Maishan, A. J. Lough, R. H. Morris, *J. Am. Chem. Soc.* **2012**, *134*, 12266–12280.

<sup>76</sup> (a) W. W. Zuo, A. J. Lough, Y. F. Li, R. H. Morris, *Science* **2013**, *342*, 1080–1083; (b) W. Zuo, S. Tauer, D. E. Prokopchuk, R. H. Morris, *Organometallics* **2014**, *33*, 5791–5801; (c)



- 
- S. A. M. Smith, R. H. Morris, *Synthesis* **2015**, DOI: 10.1055/s-0034-1380147.
- <sup>77</sup> (a) C. A. Sandoval, T. Ohkuma, K. Muniz, R. Noyori, *J. Am. Chem. Soc.* **2003**, *125*, 13490-13503; (b) R. Noyori, M. Kitamura, T. Ohkuma, *Proc. Natl. Ac. Sci.* **2004**, *101*, 5356-5362.
- <sup>78</sup> (a) W. Zuo, Y. Li, A. J. Lough, R. H. Morris *Science* **2013**, *342*, 1080; (b) W. Zuo, S. Tauer, D. E. Prokopchuk, R. H. Morris *Organometallics* **2014**, *33*, 5791; (c) S. A. M. Smith, R. H. Morris *Synthesis* **2015**, *47*, 1775-1779.
- <sup>79</sup> P. O. Lagaditis, P. E. Sues, J. F. Sonnenberg, K. Y. Wan, A. J. Lough, R. H. Morris *J. Am. Chem. Soc.* **2014**, *136*, 1367-1380.
- <sup>80</sup> S. L. Yu, W. Y. Shen, Y. Y. Li, Z. R. Dong, Y. Q. Xu, Q. Li.; J. N. Zhang, J. X. Gao *Adv. Synth. Catal.* **2012**, *354*, 818-822.
- <sup>81</sup> Y. Y. Li, S. L. Yu, X. F. Wu, J. L. Xiao, W. Y. Shen, Z. Dong, J. X. Gao *J. Am. Chem. Soc.* **2014**, *136*, 4031-4039.
- <sup>82</sup> M. Ranocchiari, A. Mezzetti *Organometallics* **2009**, *28*, 1286-1288.
- <sup>83</sup> R. Bigler, E. Otth, A. Mezzetti *Organometallics* **2014**, *33*, 4086-4099.
- <sup>84</sup> R. Bigler, A. Mezzetti *Org. Lett.* **2014**, *16*, 6460-6463.
- <sup>85</sup> R. Bigler, R. Huber, A. Mezzetti *Angew. Chem. Int. Ed.* **2015**, *54*, 5171-5174.
- <sup>86</sup> (a) R. Langer, G. Leituss, Y. Ben-David, D. Milstein *Angew. Chem. Int. Ed.* **2011**, *50*, 2120-2124; (b) R. Langer, M. A. Iron, L. Kostantinovski, Y. Diskin-Posner, G. Leituss, Y. Ben-David, D. Milstein, *Chem. Eur. J.* **2012**, *18*, 7196-7209.
- <sup>87</sup> R. Langer, M. A. Iron, L. Konstantinovski, Y. Diskin-Posner, G. Leituss, Y. Ben-David, D. Milstein *Chem.—Eur. J.* **2012**, *18*, 7196.
- <sup>88</sup> S. Enthaler, B. Hagemann, G. Erre, K. Junge, M. Beller *Chem.—Asian J.* **2006**, *1*, 598.
- <sup>89</sup> S. Enthaler, G. Erre, M. K. Tse, K. Junge, M. Beller *Tetrahedron Lett.* **2006**, *47*, 8095.
- <sup>90</sup> G. Wienhofer, F. A. Westerhaus, K. Junge, R. Ludwig, M. Beller *Chem.—Eur. J.* **2013**, *19*, 7701.
- <sup>91</sup> A. Naik, T. Maji, O. Reiser, *Chem. Commun.* **2010**, *46*, 4475-4477.
- <sup>92</sup> W. Reppe, H. Vetter, *Liebigs Ann. Chem.* **1953**, *582*, 133.
- <sup>93</sup> (a) H.-J. Knolker, J. Heber, C. H. Mahler, *Synlett* **1992**, 1002; (b) H.-J. Knolker, J. Heber, *Synlett* **1993**, 924; (c) H.-J. Knolker, E. Baum, R. Klaus, *Tetrahedron Lett.* **1995**, *36*, 7647.
- <sup>94</sup> (a) A. J. Pearson, R. A. Dubbert *J. Chem. Soc. Chem. Commun.* **1991**, 202; (b) A. J. Pearson, R. J. Shively, Jr., R. A. Dubbert, *Organometallics* **1992**, *11*, 4096; (c) A. J. Pearson, R. J. Shively, Jr., *Organometallics* **1994**, *13*, 578; (d) A. J. Pearson, A. Perosa, *Organometallics* **1995**, *14*, 5178; (e) A. J. Pearson, X. Yao, *Synlett* **1997**, 1281.
- <sup>95</sup> (a) H.-J. Knolker, E. Baum, H. Goesmann, R. Klaus, *Angew. Chem.* **1999**, *111*, 2196; *Angew. Chem. Int. Ed.* **1999**, *38*, 2064.
- <sup>96</sup> (a) C. P. Casey, H. Guan, *J. Am. Chem. Soc.* **2007**, *129*, 5816; For an highlight on this discovery: (b) R. M. Bullock, *Angew. Chem.* **2007**, *119*, 7504; *Angew. Chem. Int. Ed.* **2007**, *46*, 7360.
- <sup>97</sup> For the first preparation of Shvo complex: (a) Y. Blum, D. Czarkie, Y. Rahamim, Y. Shvo, *Organometallics* **1985**, *4*, 1459; (b) Y. Shvo, D. Czierkie, Y. Rahamin, D. F. Ghodosh, *J. Am. Chem. Soc.* **1986**, *108*, 7400; For reviews on the Shvo catalyst: (c) R. Prabhakaran, *Synlett* **2004**, 2048; (d) R. Karvembu, R. Prabhakaran, K. Natarajan, *Coord. Chem. Rev.* **2005**, *249*, 911; (e) B. L. Conley, M. K. Pennington-Boggio, E. Boz, T. J. Williams, *Chem. Rev.* **2010**, *110*, 2294.
- <sup>98</sup> X. Lu, R. Cheng, N. Turner, Q. Liu, M. Zhang, X. Sun *J. Org. Chem.* **2014**, *79*, 9355-9364.

- 
- <sup>99</sup> (a) S. Moulin, H. Dentel, A. Pagnoux-Ozherelyeva, S. Gaillard, A. Poater, L. Cavallo, J.-F. Lohier, J.-L. Renaud, *Chem. Eur. J.* **2013**, *19*, 17881-17890; (b) D. S. Mérel, M. Elie, J.-F. Lohier, S. Gaillard, J.-L. Renaud, *ChemCatChem* **2013**, *5*, 2939-2945; (c) A. Pagnoux-Ozherelyeva, N. Pannetier, M. D. Mbaye, S. Gaillard, J.-L. Renaud, *Angew. Chem.* **2012**, *124*, 5060-5064; *Angew. Chem. Int. Ed.* **2012**, *51*, 4976-4980; (d) J. P. Hopewell, J. E. D. Martins, T. C. Johnson, J. Godfrey, M. Wills, *Org. Biomol. Chem.* **2012**, *10*, 134-145; (e) T.-T. Thai, D. S. Mérel, A. Poater, S. Gaillard, J.-L. Renaud, *Chem. Eur. J.* **2015**, *21*, 7066-7070.
- <sup>100</sup> A. Berkessel, S. Reichau, A. von der Höh, N. Leconte, J.-M. Neudörfl, *Organometallics* **2011**, *30*, 3880-3887.
- <sup>101</sup> (a) S. Fleischer, S. Zhou, K. Junge, M. Beller, *Angew. Chem.* **2013**, *125*, 5224-5228; *Angew. Chem. Int. Ed.* **2013**, *52*, 5120-5124; (b) A. Tlili, J. Schranck, H. Neumann, M. Beller, *Chem. Eur. J.* **2012**, *18*, 15935-15939.
- <sup>102</sup> For a recent review on (cyclopentadienone)iron complexes, see: A. Quintard, J. Rodriguez, *Angew. Chem.* **2014**, *126*, 4124-4136; *Angew. Chem. Int. Ed.* **2014**, *53*, 4044-4055.
- <sup>103</sup> S. Fleischer, S. S. Zhou, K. Junge, M. Beller, *Angew. Chem.* **2013**, *125*, 5224; *Angew. Chem. Int. Ed.* **2013**, *52*, 5120.
- <sup>104</sup> A. Berkessel, S. Reichau, A. von der Höh, N. Leconte, J.-M. Neudörfl, *Organometallics* **2011**, *30*, 3880-3887.
- <sup>105</sup> J. P. Hopewell, J. E. D. Martins, T. C. Johnson, J. Godfrey, M. Wills, *Org. Biomol. Chem.* **2012**, *10*, 134-145.
- <sup>106</sup> S. Zhou, S. Fleischer, K. Junge, M. Beller, *Angew. Chem., Int. Ed.* **2011**, *50*, 5120.
- <sup>107</sup> S. Fleischer, S. Zhou, S. Werkmeister, K. Junge, M. Beller *Chem.—Eur. J.* **2013**, *19*, 4997.
- <sup>108</sup> S. Zhou, S. Fleischer, H. Jiao, K. Junge, M. Beller *Adv. Synth. Catal.* **2014**, *356*, 3451 – 3455.
- <sup>109</sup> S. Fleischer, S. Werkmeister, S. Zhou, K. Junge, M. Beller *Chem.—Eur. J.* **2012**, *18*, 9005.
- <sup>110</sup> A. Pagnoux-Ozherelyeva, N. Pannetier, M. D. Mbaye, S. Gaillard, J.-L. Renaud *Angew. Chem., Int. Ed.* **2012**, *51*, 4976.
- <sup>111</sup> T.-T. Thai, D. S. Merel, A. Poater, S. Gaillard, J.-L. Renaud *Chem. Eur. J.* **2015**, *21*, 7066 – 7070.
- <sup>112</sup> T. Yan, B. L. Feringa, K. Barta *Nat. Commun.* **2014** 5:5602 doi: 10.1038/ncomms6602.
- <sup>113</sup> H.-J. Pan, T. Wei Ng, Y. Zhao *Chem. Commun.*, **2015**, *51*, 11907-11910.
- <sup>114</sup> C. Federsel, A. Boddien, R. Jackstell, R. Jennerjahn, P. Dyson, R. Scopelliti, G. Laurenczy, M. Beller, *Angew. Chem. Int. Ed.* **2010**, *49*, 9777.
- <sup>115</sup> C. Ziebart, C. Federsel, P. Anbarasan, R. Jackstell, W. Baumann, A. Spannenberg, M. Beller *J. Am. Chem. Soc.* **2012**, *134*, 20701.
- <sup>116</sup> R. Langer, Y. Diskin-Posner, G. Leitus, L. J. W. Shimon, Y. Ben-David, D. Milstein, *Angew. Chem., Int. Ed.* **2011**, *50*, 9948.
- <sup>117</sup> F. Bertini, I. Mellone, A. Ienco, M. Peruzzini, L. Gonsalvi *ACS Catal.* **2015**, *5*, 1254-1265.
- <sup>118</sup> F. Zhu, L. Zhu-Ge, G. Yang, S. Zhou *ChemSusChem* **2015**, *8*, 609 – 612.
- <sup>119</sup> T. Zell, Y. Ben-David, D. Milstein, *Angew. Chem., Int. Ed.* **2014**, *53*, 4685.
- <sup>120</sup> S. Werkmeister, K. Junge, B. Wendt, E. Alberico, H. Jiao, W. Baumann, H. Junge, F. Gallou, M. Beller *Angew. Chem., Int. Ed.* **2014**, *53*, 8722.
- <sup>121</sup> S. Chakraborty, H. Dai, P. Bhattacharya, N. T. Fairweather, M. S. Gibson, J. A. Krause, H. Guan, *J. Am. Chem. Soc.* **2014**, *136*, 7869.
- <sup>122</sup> (a) D. Spasyuk, D. G. Gusev, *Organometallics* **2012**, *31*, 5239; (b) A. Acosta-Ramirez, M. Bertoli, D.

- 
- G. Gusev, M. Schlaf, *Green Chem.* **2012**, *14*, 1178.
- <sup>123</sup> N. Ségaud, J.-N. Rebilly, K. Sénéchal-David, R. Guillot, L. Billon, J.-P. Baltaze, J. Farjon, O. Reinaud, F. Banse, *Inorg. Chem.* **2013**, *52*, 691-700.
- <sup>124</sup> (a) M. Costas, K. Chen, L. Jr Que *Coord. Chem. Rev.* **2000**, *200-202*, 517-544; (b) L. Jr Que, W.B. Tolman *Nature* **2008**, *455*, 333-340; (c) A. C. Mayer, C. Bolm *Iron-catalyzed Oxidation Reactions. Oxidation of C-H and C = C bonds.* **2008**, 73-92, in: B. Plietker *Iron Catalysis in Organic Chemistry*, **2008**, Wiley, Weinheim.
- <sup>125</sup> M. Grau, G. J.P. Britovsek *Top Organomet Chem* **2015**, *50*, 145-172.
- <sup>126</sup> (a) M. S. Chen, M. C. White, *Science* **2007**, *318*, 783-787; (b) M. S. Chen, M. C. White, *Science* **2010**, *327*, 566-570.
- <sup>127</sup> S. E. Denmark, J. Fu, M. J. Lawler, S. Lee, E. Huntsman, E. J. J. Grabowski, *Org. Synth.* **2006**, *83*, 121-130.
- <sup>128</sup> (a) Classical preparation of NaBAR<sub>F</sub>: M. Brookhart, B. Grant, A. F. Volpe, *Organometallics* **1992**, *11*, 3920-3922; (b) Alternative preparation of NaBAR<sub>F</sub>: N. A. Yakelis, R. G. Bergman, *Organometallics* **2005**, *24*, 3579-3581; (c) Preparation of KBAR<sub>F</sub> and AgBAR<sub>F</sub>: E. Buschmann, J. S. Miller, K. Bowman-James, C. N. Miller, *Inorg. Synth.* **2002**, *33*, 83.
- <sup>129</sup> (a) R. Langer, G. Leitus, Y. Ben-David, D. Milstein, *Angew. Chem. Int. Ed.* **2011**, *50*, 2120-2124.
- <sup>130</sup> W. C. Still, M. Kahn, A. Mitra, *J. Org. Chem.* **1978**, *43*, 2923-2925.
- <sup>131</sup> A. Dömling, I. Ugi, *Angew. Chem. Int. Ed.* **2000**, *39*, 3168-3210.
- <sup>132</sup> F. E. Hahn, *Angew. Chem. Int. Ed.* **1993**, *32*, 650-665.
- <sup>133</sup> W. Kandatege; K. Alliston, *Journal of the American Chemical Society*, **1995**, *117*, 1220 - 1224.
- <sup>134</sup> P. Bertus, J. Szymoniak, *Chem. Commun.* **2001**, 1792-1793.
- <sup>135</sup> W. C. Still, M. Kahn, A. Mitra, *J. Org. Chem.* **1978**, *43*, 2923-2925.
- <sup>136</sup> (a) J. M. Grill, J. H. Reibenspies, S. A. Miller, *J. Organomet. Chem.* **2005**, *690*, 3009-3017; (b) M. Hatano, T. Asai, K. Ishihara, *Tetrahedron Lett.* **2008**, *49*, 379-382.
- <sup>137</sup> P. Gajewski, M. Renom-Carrasco, S. Vailati Facchini, L. Pignataro, L. Lefort, J. G. de Vries, R. Ferraccioli, A. Forni, U. Piarulli and C. Gennari, *Eur. J. Org. Chem.* **2015**, 1887-1893.
- <sup>138</sup> (a) B. Ye, N. Cramer, *Angew. Chem.* **2014**, *126*, 8030-8033; *Angew. Chem. Int. Ed.* **2014**, *53*, 7896-7899; (b) B. Ye, N. Cramer, *J. Am. Chem. Soc.* **2013**, *135*, 636-639.
- <sup>139</sup> Estimated price per gram upon purchase of 1 kg of (R)-BINOL from Reuter Chemischer Apparatebau KG.
- <sup>140</sup> (a) D. Kampen, C. Reisinger, B. List, *Top. Curr. Chem.* **2009**, *291*, 1-37; (b) M. Terada, *Chem. Commun.* **2008**, 4097-4112.
- <sup>141</sup> T. Ooi, M. Kameda, K. Maruoka, *J. Am. Chem. Soc.* **2003**, *125*, 5139-5151.
- <sup>142</sup> M. Ikunaka, K. Maruoka, Y. Okuda, T. Ooi, *Org. Process Res. Dev.* **2003**, *7*, 644.
- <sup>143</sup> T. Hameury, J. Guillemont, L. van Hijfte, V. Bellosta, J. Cossy *Org. Lett.* **2009**, *11*, 2397-2400.
- <sup>144</sup> P. Gajewski, M. Renom-Carrasco, S. Vailati Facchini, L. Pignataro, L. Lefort, J. G. de Vries, R. Ferraccioli, U. Piarulli and C. Gennari, *Eur. J. Org. Chem.* **2015**, 5526-5536.
- <sup>145</sup> T. Ooi, M. Kameda, K. Maruoka, *J. Am. Chem. Soc.* **2003**, *125*, 5139.
- <sup>146</sup> (a) G. A. Olah, S. C. Narang, L. D. Field, R. Karpeles, *J. Org. Chem.* **1981**, *46*, 2408; (b) P. R. Brooks, M. C. Wirtz, M. G. Vetelino, D. M. Rescek, G. F. Woodworth, B. P. Morgan, J. W. Coe, *J. Org. Chem.* **1999**, *64*, 9719-9721.
- <sup>147</sup> D. L. Comins, A. Dehghani, *Tetrahedron Letters* **1992**, *33*, 6299-6302.

- 
- <sup>148</sup> T. Ohe, N. Miyaoura, A. Suzuki, *J. Org. Chem.* **1993**, *58*, 2201-2208.
- <sup>149</sup> A. F. Littke, C. Dai, G. C. Fu, *J. Am. Chem. Soc.* **2000**, *122*, 4020-4028.
- <sup>150</sup> T. Watanabe, N. Miyaoura, A. Suzuki, *Synlett* 1992, 1992, 207-210.
- <sup>151</sup> R. A. Altman, S. Buchwald, *Nat. Protoc.* **2007**, *2*, 3115-3121.
- <sup>152</sup> T. Ohe, N. Miyaoura, A. Suzuki, *J. Org. Chem.* **1993**, *58*, 2201-2208.
- <sup>153</sup> C. J. O'Brien, E. A. B. Kantchev, C. Valente, N. Hadei, G. A. Chass, A. Lough, A. C. Hopkinson, M. G. Organ, *Chem. Eur. J.* **2006**, *12*, 4743-4748.
- <sup>154</sup> Hruszkewycz, D. P.; Balcells, D.; Guard, L. M.; Hazari, N.; Tilset, M. *J. Am. Chem. Soc.* **2014**, *136*, 7300-7316
- <sup>155</sup> Zhao, T.-L.; Li, Y.; Li, S.-M.; Zhou, Y.-G.; Sun, F.-Y.; Gao, L.-X.; Hana, F.-S. *Adv. Synth. Catal.* **2011**, *353*, 1543-1550
- <sup>156</sup> S. Moulin, H. Dentel, A. Pagnoux-Ozherelyeva, S. Gaillard, A. Poater, L. Cavallo, J.-F. Lohier, J.-L. Renaud *Chem. Eur. J.* **2013**, *19*, 17881 – 17890.
- <sup>157</sup> M. G. Coleman, A. N. Brown, B. A. Bolton, H. Guan, *Adv. Synth. Catal.* **2010**, *352*, 967-970.
- <sup>158</sup> X. Lu, Y. Zhang, N. Turner, M. Zhang, T. Li *Org. Biomol. Chem.*, **2014**, *12*, 4361-4371.
- <sup>159</sup> W. C. Still, M. Kahn, A. Mitra, *J. Org. Chem.* **1978**, *43*, 2923-2925.
- <sup>160</sup> T. Ooi, M. Kameda, K. Maruoka *J. Am. Chem. Soc.* **2003**, *17*, 5104.
- <sup>161</sup> L. Claisen, T. Ewan, *Annalen*, **1895**, *284*, 245.
- <sup>162</sup> A. Hosomi, H. Hayashida, Y. Tominaga *J. Org. Chem.* **1989**, *54*, 3254-3256.
- <sup>163</sup> Bruker, SMART, SAINT and SADABS, Bruker AXS Inc., Madison, Wisconsin, USA, **1997**.
- <sup>164</sup> G. M. Sheldrick, *Acta Crystallogr. Sect. A* **2008**, *64*, 112-122.
- <sup>165</sup> M. N. Burnett, C. K. Johnson, ORTEP-III: Oak Ridge Thermal Ellipsoid Plot Program for Crystal Structure Illustrations, Oak Ridge National Laboratory Report ORNL-6895, **1996**.
- <sup>166</sup> (a) S. L. Colletti, R. L. Halterman, *Organometallics* **1991**, *10*, 3438-3448; (b) S. L. Colletti, R. L. Halterman, *Organometallics* **1992**, *11*, 980-983.
- <sup>167</sup> A. G. Schafer, J. M. Wieting, T. J. Fisher, A. E. Mattson, *Angew. Chem. Int. Ed.* **2013**, *52*, 11321 – 11324.
- <sup>168</sup> R. Patchett, I. Magpantay, L. Saudan, C. Schotes, A. Mezzetti, F. Santoro, *Angew. Chem. Int. Ed.* **2013**, *52*, 10352-10355.
- <sup>169</sup> H. Yue, H. Huang, G. Bian, H. Zong, F. Li, L. Song, *Tetrahedron: Asymmetry* **2014**, *25*, 170-180.
- <sup>170</sup> Y. Li, S. Yu, X. Wu, J. Xiao, W. Shen, Z. Dong, J. Gao, *J. Am. Chem. Soc.* **2014**, *136*, 4031-4039.
- <sup>171</sup> Y.-S. Shih, R. Boobalan, C. Chen, G.-H. Lee, *Tetrahedron: Asymmetry* **2014**, *25*, 327-333.
- <sup>172</sup> J. Li, Y. Tang, Q. Wang, X. Li, L. Cun, X. Zhang, J. Zhu, L. Li, J. Deng, *J. Am. Chem. Soc.* **2012**, *134*, 18522-18525.
- <sup>173</sup> R. Soni, J.-M. Collinson, G. C. Clarkson, M. Wills, *Org. Lett.* **2011**, *13*, 4304-4307.
- <sup>174</sup> H. Mizoguchi, T. Uchida, T. Katsuki, *Angew. Chem.* **2014**, *126*, 3242-3246; *Angew. Chem. Int. Ed.* **2014**, *53*, 3178-3182.
- <sup>175</sup> A. Z. Gonzalez, J. G. Román, E. Gonzalez, J. Martinez, J. R. Medina, K. Matos, J. A. Soderquist, *J. Am. Chem. Soc.* **2008**, *130*, 9218-9219.
- <sup>176</sup> K. Matsumura, N. Arai, K. Hori, T. Saito, N. Sayo, T. Ohkuma, *J. Am. Chem. Soc.* **2011**, *133*, 10696-10699.
- <sup>177</sup> R. C. Samanta, S. De Sarkar, R. Fröhlich, S. Grimme, A. Studer *Chem. Sci.*, **2013**, *4*, 2177-2184.